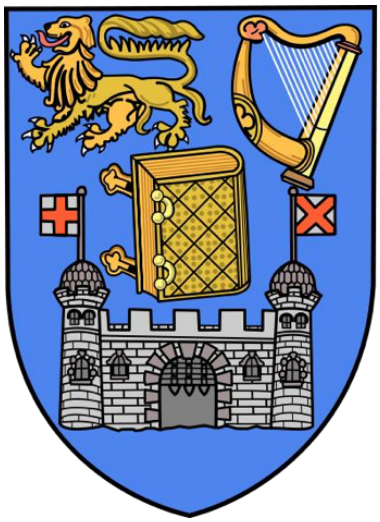
The antiviral potential of itaconate and its derivative 4-Octyl itaconate against RNA viruses



Thesis submitted to the University of Dublin

for the degree of Doctor of Philosophy

by

Hauke Johannes Weiß

Under supervision of:

Prof. Luke O'Neill

Inflammation Research Group - School of Biochemistry and Immunology – Trinity College Dublin

January 2023

Declaration

This thesis is submitted by the undersigned to the University of Dublin for the examination of Doctor of Philosophy. I declare that this thesis has not been submitted as an exercise for a degree at this or any other university and is entirely my own work with the exception of the following figures:

Figures 3.1 and 3.2:

This work was performed by Clarisse Salgado-Benvindo.

Figures 3.3, 3.4 and 3.7:

This work was performed in collaboration with Laurens Liesenborghs.

Figure 3.6:

This work was done in collaboration with Alexander Hooftman.

Figures 4.3, 4.4 and 4.6:

This work was done in collaboration with Pau Ribo Molina.

Figure 4.13:

This work was done by Leentje Persoons and Pau Ribo Molina.

Figure 4.16:

This work was done in collaboration with Yunan Zheng.

I agree to deposit this thesis in the University's open access institutional repository or allow the library to do so on my behalf, subject to Irish Copyright Legislation and Trinity College Library conditions of use and acknowledgement.

_____

Hauke Weiß

Acknowledgements

What a journey! It's pretty difficult to condense all my impression of these 3 or so years into a couple of pages in the acknowledgements section of this thesis, but I'll give it a try. The pint of Guinness I had during proofreading the thesis for the last time should help…

First of all I want to thank Luke. You have been an incredible mentor during my time in the lab, and every time I speak to one of my friends doing a PhD in other labs or other countries, it makes me appreciate the time I had in your lab more. I vividly remember our phone interview: Me standing beside a French motorway in the early morning on the way to a festival, struggling to understand anything with cars blasting past. When you offered me the job in spite of this slightly chaotic interview, I considered it a huge gamble on my end, as I have never stepped foot on Irish soil before, and I did not know a single person in the country. But I am glad I made the decision to join you. You gave me an incredible amount of freedom to explore what I was interested in, while still guiding me whenever I got stuck. It is an incredible achievement making your students look forward to a meeting with the supervisor, this is very rare amongst PhD students, trust me. No matter how good or bad the results, I always came out of our meetings feeling better than before. Also all of our generous nights out, and of course the epic trip to Poland were truly iconic. This has been an incredible part of my life.

To the lab: You're all amazing! I have never seen a lab with such a tight knit sense of community, and I don't think I'll ever see one. You guys kept me sane during this whole COVID mess, and I consider you all true ~~colleagues~~ friends. I hope I'll be able to stay in touch with you once I inevitably leave the lab. Thanks for all the banter in the lab, and the countless days and nights out. Tristram: Keep that positive energy up, despite only being 19 years old, there is a lot I can learn from you. (I'm a bit disappointed though that I didn't find any dick jokes in the thesis while proof reading, I had the laptop sitting open in the reading room long enough..) Alex, you were a great inspiration when you were in the lab, and still are, thanks for helping me out in my first couple of years. See you soon (in Poland I guess). Alessia I hope you'll find worthy prank competitor once I'm gone, keep that fuego alive. Shane, hang in there bud, I'm sure itaconate does.. something. Also thanks to the phenomenon that is Zibigniev, for his help in the lab and for hosting us (multiple times) in his home country. Emily and Juliana, it was an honour being part of the girl band – a politically correct Tschüss from me. I hope our lovebirds Christian and Maureen will continue to bless the lab with completely non-awkward interactions – All the best to you guys! Also a lot of thanks to Kathy for all your help, and for holding the lab together. I wasn't joking when I said this lab does not function without you. Anne and Eva, I also have to thank you for your help, and keeping us all grounded when shit gets a bit over the top. To the newbies, Fiona and Yukun, all the best for your LON lab experience.

Next I want to thank all my friends from the Freiburg crew: These past years were the ultimate challenge whether our friendship can stand the test of time – It does.

Not that I ever doubted that.. Especially Koko, Steffi, Chris and Semmo, you guys helped me get through the difficult time during the lockdowns, and I'm looking forward to our Mexico trip. And Maria, thanks for being my best friend for, like 20 years now? That's mad! You got me through so much in that time, more than you might think. Thank you!

I must also thank the Lübeck crew: Freddy, Luke, Steffen and Raphi. It was amazing finally having you here in Ireland last year. I can't wait to get together for the next Vatertag.

Lastly, I want to thank my parents, and also Thurid for all of your love and support. It is because of your guidance and work that I was able to achieve this. I know it wasn't always easy with me, you staid resilient when the teachers told you there is no chance I'll be able to go to a Gymnasium, let alone university. I hope this thesis has done you proud. And Thurid, you are the best sister one could wish for!

If I have forgotten anyone, I'm really sorry, it's pretty late.

Thanks to all of you lovely people!

Table of contents

Declaration **3**

Acknowledgements **5**

Table of contents **8**

List of Figures **12**

List of tables **14**

Abbreviations **15**

Abstract **22**

Chapter 1: Introduction **24**

1.1 General introduction **25**

1.1.1 Macrophages and innate immunity 25

1.1.2 Innate immune receptors 26

1.2 Innate antiviral responses and interferon signalling **29**

1.3 RNA viruses **33**

1.3.1 SARS-CoV-2 33

1.3.2 Influenza 37

1.4 CRM1 ..... **40**

1.4.1 CRM1 inhibition 42

1.4.2 CRM1 and Viruses 46

1.5 Metabolic reprogramming in macrophages **48**

1.5.1 Itaconate 49

1.5.2 Antiviral properties of Itaconate and its derivatives 58

1.6 Aims **61**

Chapter 2: Materials and Methods **62**

2.1 Materials 63
2.1.1 Buffers 63
2.1.2 Cell culture reagents 64
2.1.3 Mice 64
2.1.4 Hamsters 65
2.1.5 Cells 65
2.1.6 Viruses 70
2.1.7 Primers 71
2.1.8 Plasmids 72
2.1.9 Antibodies 72
2.1.10 Stimulants 73
2.1.11 Software 73
2.2 Methods 74
2.2.1 Assay for pseudo particle cell entry inhibition 74
2.2.2 Cytopathic effect (CPE) reduction assay 74
2.2.3 Virus titration 75
2.2.4 Western Blotting 75
2.2.5 Flow Cytometry 77
2.2.6 RT-qPCR 77
2.2.7 Confocal microscopy 78
2.2.8 Fusion assay 79
2.2.9 CRM1 activity assay 79
2.2.10 Quantitative profiling of 4-OI modified cysteinome in THP-1 cells 80
2.2.11 Cellular Fractionation 82
2.2.12 Co-immunoprecipitation 83
2.2.13 PBMC isolation 83

2.2.14 LDH release assay 84

2.2.15 Statistical analysis 84

Chapter 3: 4-OI is an antiviral agent in SARS-CoV-2 infection.....86

3.1 4-OI is antiviral against SARS-CoV-2 87

3.1.1 4-OI decreases SARS-CoV-2 induced cell death and restricts replication *in vitro* 87

3.1.2 4-OI decreases SARS-CoV-2 induced pathology and restricts replication *in vivo* 90

3.2 4-OI reduces ACE2 induced uptake of SARS-CoV-2 94

3.2.1 ACE2 expression is decreased with 4-OI *in vitro* 94

3.2.2 ACE2 expression is decreased with 4-OI *in vivo* 98

3.2.3 Exogenous itaconate increases ACE2 expression 98

3.2.4 4-OI is unable to counter overexpression of ACE2 in HEK cells 101

3.2.5 4-OI reduces ACE2 dependent uptake of spike expressing particles 103

3.3 Discussion 105

3.3.1 4-OI is antiviral in SARS-CoV-2 105

3.3.2 ACE2, 4-OI and interferons 106

3.3.4 4-OI versus itaconate in ACE2 expression 109

3.3.5 An alternative mechanism? 110

Chapter 4: 4-Octyl itaconate reduces IAV replication by targeting the nuclear export protein CRM1 113

4.1 4-OI is antiviral in Influenza 114

4.1.1 Itaconate and 4-OI are not antiviral in HMPV 114

4.1.2 Influenza replication is restricted by 4-OI but not by itaconate 116

4.1.3 4-OI does not impair IAV membrane fusion 118

4.1.4 4-OI does not interfere with tetraspanin expression 121

4.2 4-OI inhibits CRM1 activity 123
4.2.1 IAV NP is trapped in the nucleus after 4-OI treatment 123
4.2.2 CRM1 accumulates in the cytosol of 4-OI treated BMDMs 125
4.2.3 4-OI decreases CRM1 protein levels in lung epithelial cells 127
4.2.4 4-OI does not decrease CRM1 mRNA expression levels 130
4.3 4-OI induces global protein ubiquitination 132
4.4 4-OI shuts down CRM1 mediated nuclear export 134
4.4.1 p53 and p65 accumulate in the nucleus upon 4-OI treatment 134
4.4.2 4-OI dose-dependently decreases CRM1 activity 136
4.4.3 Endogenous itaconate does not affect CRM1 protein levels 137
4.4.4 Exogenous itaconate does not decrease CRM1 protein levels 140
4.5 4-OI inhibits CRM1 through dicarboxypropylation of C528 142
4.5.1 Toxicity of high dose 4-OI is partly through CRM1 inhibition 145
4.5.2 4-OI alters RanBP1 protein levels and subcellular location through CRM1 alkylation 148
4.6 Discussion 151
4.6.1 4-OI and Influenza 151
4.6.2 IAV replication is halted at the NP export stage 152
4.6.3 CRM1 inhibition – a possible mechanism? 153
4.6.4 Dicarboxypropylation of C528 by 4-OI inhibits CRM1 154
Chapter 5: General discussion 159
5.1 Itaconate derivatives as antivirals? 160
5.2 The price of CRM1 inhibition 163
5.3 Broadening the horizon 164
Chapter 6: References 167
Chapter 7: Publications 205

List of Figures

Figure 1.1: TLRs and their adaptors. 28

Figure 1.2: Innate antiviral sensors and type I IFN activation. 32

Figure 1.3: The life cycle of SARS-CoV-2. 36

Figure 1.4: The life cycle of IAV. 39

Figure 1.5: Mechanism of the nuclear exporter CRM1. 41

Figure 1.6: Structural model of CRM1. 44

Figure 1.7: Itaconate's position in the TCA cycle. 51

Figure 1.8: Chemical structures of itaconate and 4-OI 54

Figure 1.9: Itaconate exerts anti-inflammatory and anti-microbial function through a variety of pathways. 57

Figure 1.10: The antiviral effects of itaconate and its derivatives. 60

Figure 3.1: 4-OI reduces SARS-CoV-2 induced pathology. 88

Figure 3.2: 4-OI restricts replication of SARS-CoV-2. 90

Figure 3.3: 4-OI reduces SARS-CoV-2 induced pathology *in vivo*. 92

Figure 3.4: 4-OI restricts replication of SARS-CoV-2 *in vivo*. 93

Figure 3.5: 4-OI decreases ACE2 expression in Nuli-1 cells. 96

Figure 3.6: 4-OI decreases ACE2 expression in A549 cells. 97

Figure 3.7: 4-OI decreases ACE2 expression *in vivo*. 99

Figure 3.8: Itaconate might slightly increase expression of ACE2 in epithelial cells. 100

Figure 3.9: 4-OI does not reduce ACE2 expression in HEK-Blue™ hACE2 Cells. 102

Figure 3.10: 4-OI reduces ACE2 dependent viral uptake in Calu-3 cells. 104

Figure 3.11: 4-OI decreases ACE2 expression. 108

Figure 3.12: 4-OI might trap ACE2 in the nucleus. 112

Figure 4.1: 4-OI is not antiviral in hMPV. 115

Figure 4.2: 4-OI decreases IAV replication. 117

Figure 4.3: Replication kinetics of 4-OI decreasing IAV replication. 119

Figure 4.4: 4-OI does not decrease viral uptake. 120

Figure 4.5: 4-OI does not decrease tetraspanin expression. 122

Figure 4.6: 4-OI decreases cytosolic levels of NP after IAV infection. 124

Figure 4.7: 4-OI increases CRM1 protein levels in BMDMs. 126

Figure 4.8: 4-OI decreases CRM1 protein in NHBE cells. 128

Figure 4.9: 4-OI decreases CRM1 protein in Nuli-1 cells. 129

Figure 4.10: 4-OI slightly increases CRM1 mRNA expression. 131

Figure 4.11: 4-OI induces global protein ubiquitination. 133

Figure 4.12: 4-OI induces nuclear accumulation of CRM1 cargo proteins p53 and p65. 135

Figure 4.13: Impact of 4-OI on CRM1 dependent proteins. 138

Figure 4.14: Endogenous itaconate does not drive CRM1 degradation. 139

Figure 4.15: Exogenous itaconate does not affect CRM1 protein levels. 141

Figure 4.16 CRM1 is alkylated by 4-OI at C528 143

Figure 4.17: Deactivation of CRM1 by 4-OI-mediated C528 alkylation. 147

Figure 4.18: 4-OI reduces RanBP1 protein levels in a CRM1 dependent manner. 149

Figure 4.19: Proposed mechanism of 4-OI inhibiting IAV replication. 155

Figure 4.20: 4-OI binds CRM1 at C528, blocking cargo binding. 158

Figure 5.1: Two for the price of one. 162

List of tables

Table 1.1: List of viruses that use CRM1 as part of their replication cycle. 47

Table 1.2: Differences and similarities between itaconate, 4-OI and IRG1 in immunity 55

Table 2.1: List of Buffers used in this project 63

Table 2.2: List of primers used in this project 71

Table 2.3: List of antibodies used in western blotting and Confocal microscopy experiments 72

Table 2.4: List of stimulants and reagents used throughout the project 73

Table 2.5: Table 2: Composition of gels used for SDS PAGE 76

Abbreviations

4-OI	4-octyl itaconate
ACE2	Angiotensin-converting enzyme 2
ACOD1	Aconitate decarboxylase 1
AIM2	Absent in melanoma 2
AML	Acute myeloid leukemia
APC	Antigen presenting cell
ATF3	Activating transcription factor 3
ATP	Adenosine triphosphate
BEGM	Bronchial Epithelial Cell Growth Medium
BM	Bone marrow
BMDM	Bone marrow derived macrophage
BSA	Bovine serum albumin
CAC	Colitis-associated colorectal cancer
cAMP	Cyclic adenosine monophosphate
CD	Cluster of differentiation
cDNA	Complementary DNA
CHAPS	3-((3-cholamidopropyl) dimethylammonio)-1-propanesulfonate
CLR	C-type lectin receptor
COVID-19	Coronavirus disease 2019
CRE	cAMP response element
CREB	Cyclic AMP response element-binding protein
CRM1	Chromosomal Maintenance 1
cRNA	Complimentary RNA
CT	Cycle threshold
DAG	Diglyceride
DAPI	4′,6-diamidino-2-phenylindole
DC	Dendritic cell
DMEM	Dulbecco's Modified Eagle Medium

DMF	Dimethyl fumarate
DMI	Dimethyl itaconate
DMSO	Dimethyl sulfoxide
DNA	Deoxyribonucleic acid
dsRNA	Doublestranded RNA
ECL	Enhanced chemiluminescent
EDTA	Ethylenediaminetetraacetic acid
EMEM	Eagle's minimal essential medium
EPPS	3-[4-(2-Hydroxyethyl)piperazin-1-yl]propane-1-sulfonic acid
ER	Endoplasmic reticulum
FACS	Fluorescence-activated cell sorting
FCS	Fetal Calf Serum
FDA	U.S. Food and Drug Administration
FELASA	Federation of European Laboratory Animal Science Associations
FIV	Feline Immunodeficiency Virus
FSC	Forward Scatter
GDP	Guanosine diphosphate
GFP	Green fluorescent protein
GIMAP7	Guanosine triphosphatase IMAP family member 7
GPCR	G protein-coupled receptor
GTP	Guanosine triphosphate
HA	Hemagglutinin
HAE cells	Primary human airway epithelial cells
HEAT	**H**untingtin, **E**longation factor 3, protein phosphatase 2**A** (PP2A) and **T**OR1
HEK	Human embryonic kidney
HIF-1α	Hypoxia-inducible factors 1α
HIV	Human immunodeficiency virus
HMPV	Human metapneumovirus
HPRA	Health Products Regulatory Authority

HRMDS	Higher risk myelodysplastic syndrome
HRP	Horseradish peroxidase
HSV	Herpes simplex virus
IA-DTB	Iodoacetamide polyethyleneoxide desthiobiotin
IAV	Influenza A virus
ICL	isocitrate lyase
IDH	Isocitrate dehydrogenase
IFN	Interferon
IFNAR	IFN-α receptor
IFNGR	IFN-γ receptor
IFNLR	IFN-λ receptor
Ig	Immunoglobulin
IL	Interleukin
IL10RB	Interleukin 10 receptor, beta subunit
IMDM	Iscove's Modified Dulbecco's Medium
IP	Intraperitoneal
IP3	Inositol trisphosphate
IRF	Interferon regulatory factor
Irg1	Immunoresponsive gene 1
ISG	Interferon-stimulated gene
JAK	Janus kinase
KEAP1	Kelch-like ECH-associated protein 1
LC-MS/MS	Liquid Chromatography with tandem mass spectrometry
LDH	Lactate dehydrogenase
LFA-1	Lymphocyte function-associated antigen 1
LMB	Leptomycin B
LPS	Lipopolysaccharide
LUMC	Leiden University Medical Center
MAPK	Mitogen activated protein kinase
mCRC	Metastatic colorectal cancer
mCRPC	Metastatic castration resistant prostate cancer

MCT1	Monocarboxylate transporter 1
MDA5	Melanoma differentiation-associated protein
MDCK cells	Madin-Darby canine kidney cells
MDS	Myelodysplastic Syndrome
MeV	Measles morbillivirus
MFI	Mean fluorescent intensity
MM	Multiple myeloma
MOI	Multiplicity of infection
MPS	Mononuclear phagocyte system
mRNA	Messenger RNA
MS	Mass spectrometry
MS	Multiple Sclerosis
MTS assay	3-(4,5-dimethylthiazol-2-yl)-5-(3-carboxymethoxyphenyl)-2-(4-sulfophenyl)-2H-tetrazolium assay
NA	Neuraminidase
NADPH	Reduced nicotinamide adenine dinucleotide phosphate
NES	Nuclear export signal
NF-κB	Nuclear factor kappa-light-chain-enhancer of activated B cells
NHBE cells	Normal human bronchial epithelial cells
NK cell	Natural killer cell
NLRP3	NOD-, LRR- and pyrin domain-containing protein 3
NP	Nucleoprotein
NPC	Nuclear pore complex
NRF2	Nuclear factor erythroid 2-related factor 2
NSP	Non-structural protein
OGC	Oxoglutarate carrier
OXGR1	2-Oxoglutarate receptor 1
OXPHOS	Oxidative phosphorylation
PBS	Phosphate-buffered saline
PCR	Polymerase chain reaction
PFA	Paraformaldehyde

Pgk-1	Phosphoglycerate kinase 1
PIP2	Phosphatidylinositol 4,5-bisphosphate
PIV	Parainfluenza virus
PKA	Protein kinase A
PKB	Protein kinase B
PKC	Protein kinase C
PKI	Protein Kinase Inhibitor
PLC	Phospholipase C
PMA	Phorbol 12-myristate 13-acetate
PMSF	Phenylmethylsulphonyl fluoride
Poly (I:C)	Polyinosinic:polycytidylic acid
PPP	Pentose phosphate pathway
PRR	Pattern recognition receptor
PRRSV	Porcine reproductive and respiratory syndrome virus
PSG	Penicillin-Streptomycin-Glutamine
PTM	Post-translational modification
PVDV	Polyvinylidene difluoride
qPCR	Quantitative polymerase chain reaction
Rab11	Ras-related protein 11
RAN	Ras-related nuclear protein
RanBP1	RAN Binding Protein 1
RanGAP	Ran GTPase-activating protein
RdRP	RNA-dependent RNA polymerase
RIG-I	Retinoic acid-inducible gene I
RIPK1	Receptor-interacting protein kinase-1
RIPK2	Receptor-interacting protein kinase-2
RLR	RIG-I like receptor
RNA	Ribonucleic acid
ROS	Reactive oxygen species
RPMI	Roswell Park Memorial Institute Medium
RSV	Respiratory syncytial virus

RT	Room temperature
RT-qPCR	Reverse transcription quantitative polymerase chain reaction
SARS-CoV-2	Severe acute respiratory syndrome coronavirus 2
SCFA	Short-Chain Fatty Acid
SD	Standard deviation
SDH	Succinate dehydrogenase
SDS PAGE	Sodium dodecyl sulphate–polyacrylamide gel electrophoresis
SEM	Standard error of mean
SINE	Selective inhibitors of nuclear export
SSC	Side scatter
ssRNA	Single-stranded RNA
STAT	Signal transducer and activator of transcription protein
TAM	Tumour-associated macrophage
TBST	Tris-buffered saline tween
TCA cycle	Tricarboxylic acid cycle
TCD	Trinity College Dublin
$TCID_{50}$	Median Tissue Culture Infectious Dose
TEMED	Tetramethylethylenediamine
TF	Tissue factor
TGF-β	Transforming growth factor beta
TLR	Toll-like receptor
TMT	Tandem Mass Tag
TNF	Tumor necrosis factor
TPCK	L-(tosylamido-2-phenyl) ethyl chloromethyl ketone
UPS18	Ubiquitin specific peptidase 18
UV	Ultraviolet
VACV	Vaccinia Virus
vRNA	Viral RNA
vRNP	Viral ribonucleoprotein
vRNP	Influenza A viral ribonucleoprotein
WCL	Whole cell lysate

WNV	West Nile virus
WT	Wildtype
XPO1	Exportin 1

Abstract

Itaconate is a Krebs cycle derived metabolite which has been shown to have anti-inflammatory properties. This specially applies to derivatives of itaconate, notably the cell permeable analogue 4-octyl itaconate (4-OI) which has been extensively studied in models of inflammation. Itaconate and 4-OI have been shown to be antiviral against Zika virus, Influenza A virus (IAV) and Severe acute respiratory syndrome coronavirus 2 (SARS-CoV-2). Here itaconate and 4-OI have been examined as potential antiviral agents for IAV and SARS-CoV-2.

4-OI inhibited replication of both SARS-CoV-2 and IAV *in vitro* and *in vivo*. In lung epithelial cells, 4-OI potently blocked expression of the SARS-CoV-2 uptake receptor, Angiotensin-converting enzyme 2 (ACE2), reducing ACE2 dependent uptake. For IAV, 4-OI inhibited replication of the virus by restricting nuclear export of viral ribonucleoproteins (vRNPs), a key step in the IAV replication cycle. This nuclear retention was achieved by deactivation and subsequent degradation of Chromosomal Maintenance 1 protein (CRM1), also known as Exportin 1 (XPO1), a host cell protein exploited by IAV during replication. 4-OI-mediated deactivation of CRM1 resulted in accumulation of the IAV nucleoprotein (NP), the Rev protein of Feline Immunodeficiency Virus (FIV), as well as the natural CRM1 cargos RAN Binding Protein 1 (RanBP1), p53 and p65 in the nucleus of treated cells. Further mechanism of action studies revealed that, similar to known CRM1 inhibitors, 4-OI modified a key cysteine in the cargo binding pocket of CRM1 at position 528 through an alkylation reaction called 2,3-dicarboxypropylation. Subsequent studies in a cell line in which the cysteine at position 528 in CRM1 was substituted by a serine,

confirmed that modification of this residue was indeed the cause of the observed inhibitory effect induced by 4-OI on CRM1 function. Overall, this study demonstrates a mechanism through which 4-OI directly interferes with SARS-CoV-2 infection, and the replication cycle of CRM1-dependent viruses, which contributes to our understanding of the antiviral and anti-inflammatory properties of this multifaceted immuno-metabolite.

Chapter 1: Introduction

1.1 General introduction

The COVID-19 pandemic is the most dramatic to have struck the world since the 1918 Influenza pandemic. In times like these the need for potent antivirals becomes painfully obvious. In this study I have explored antiviral properties of 4-octyl-itaconate (4-OI), a derivative of the Krebs cycle-derived metabolite itaconate which has been shown to have immunomodulatory and anti-inflammatory properties. I have found that 4-OI restricts both Influenza A virus (IAV) and Severe acute respiratory syndrome coronavirus 2 (SARS-CoV-2) replication, expanding the knowledge of 4-OI and itaconate, and possibly indicating an anti-viral approach that could have the added benefit of supressing inflammation, a combination that could have clinical potential for severe Influenza and COVID-19.

1.1.1 Macrophages and innate immunity

The innate immune system relies on evolutionary established, genetically determined defence mechanisms that do not change or vary within a species during infection, unlike the adaptive immune system where genetic rearrangement leads to large diversity in antibody and T cell receptor repertoires. It provides an immediate response towards a detected pathogen and is active in almost every multicellular organism.

The innate immune system consists of multiple cell types and layers. Anatomical barriers such as the skin and mucosal layers protect the host from pathogens by physically separating them, while also providing protection through

secretion of antimicrobial peptides and enzymes [1]. Macrophages are front line cells in cellular innate immunity and were first described by Ilya Metchnikoff as early as 1882. They are mononuclear phagocytes of myeloid origin, that are present in almost every tissue, and as such are part of the mononuclear phagocyte system (MPS) [2]. The main function of macrophages is the clearance of microbes, cancer cells, cellular debris and other foreign components in a process called phagocytosis, in which the macrophage engulfs and digests its target. This process is facilitated by the production of reactive oxygen species (ROS) and digestive enzymes in the endosomes containing the target within the macrophage. Macrophages are thus a crucial component of the innate immune system, identifying their targets using a range of genetically determined pattern recognition receptors (PRRs). The first PRR to be identified was Toll-like receptor 4 (TLR4), a discovery awarded the Nobel Prize in Physiology or Medicine to Bruce A. Beutler and Jules A. Hoffmann in 2011 [3]. TLR4 was found to bind and respond to bacterial lipopolysaccharide (LPS) from gram negative bacteria [4].

1.1.2 Innate immune receptors

In the years after Hoffmann's and Beutler's discovery, the functions of many other TLRs were identified, each with another specific microbial ligand. TLR3 was found to bind double stranded ribonucleic acid (dsRNA), a hallmark of viral infection [5], TLR5 to bind bacterial flagellin [6], and TLR7 and 8 to recognize viral single stranded RNA (ssRNA) [7]. Shizuo Akira and colleagues found TLR2 and TLR6 to recognize gram positive bacteria by binding to lipid structures [8,9], and TLR9 was

shown to bind to bacterial DNA [10]. TLR10 binds triacylated lipopeptides [11], and is expressed in humans but not in mice. Conversely, mice express TLR11, which binds bacterial profilin and flagellin [12,13], TLR12, which binds profilin [12], and TLR13, which binds bacterial ribosomal RNA[14], which are all missing in humans. All TLRs bind their ligands upon dimerization with another copy of the same TLR, or, in some instances, with specific other TLRs. TLR2 for example was found to heterodimerize with TLR1 or TLR6 [15], while TLR11 dimerizes with TLR12 [16]. In figure 1.1, all currently known TLRs are displayed with their ligands and primary signalling adaptors. Besides TLRs, other PRRs were also discovered in the following years, most notably NOD like receptors (NLRs) [17], the first of which was discovered in 1999 [18], RIG-like receptors (RLRs) [19], first described in 2004 [20], and C-type lectin receptors (CLRs) [21], which, although being considered part of the immune system for a long time, were shown to bind microbial products in 2000 [22].

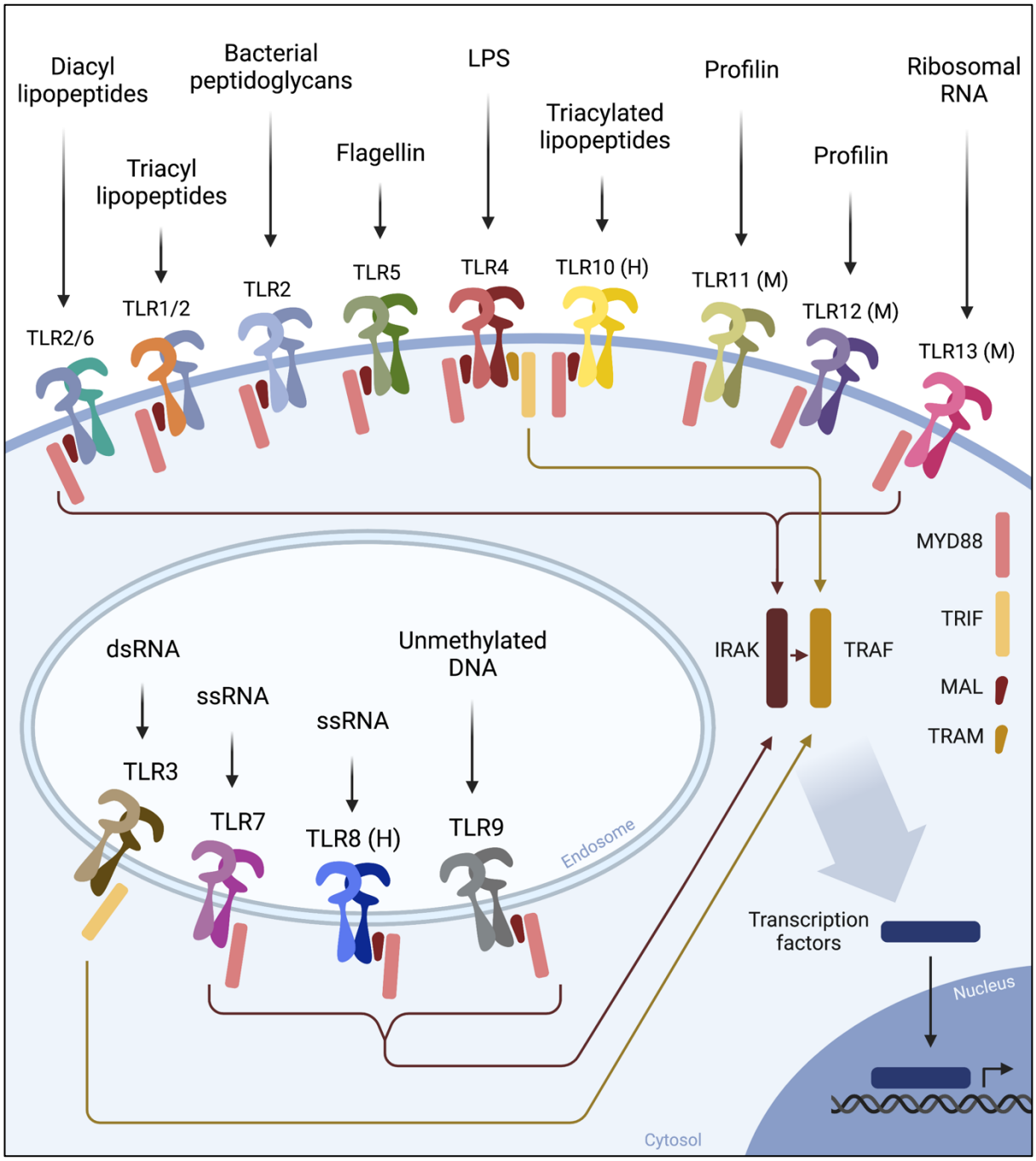


Figure 1.1: TLRs and their adaptors.

There are 13 known TLRs, 10 of which can be found in humans. They signal through MYD88, TRIF, or both, and can trigger a variety of inflammatory responses depending on the stimulus. (Figure taken from Weiss et al. 2022) [23].

1.2 Innate antiviral responses and interferon signalling

The immune system has co-evolved alongside viruses to provide protection from the ever changing threat of viral infection. Innate immune cells such as macrophages, dendritic cells (DCs), neutrophils, and natural killer (NK) cells provide the first line of protection until the adaptive immune response can take over. DCs are antigen presenting cells, whose main function it is to display parts of a pathogen on their surface other immune cells. A subset of DCs, plasmacytoid dendritic cells (pDCs) are of particular importance in innate antiviral immunity due to their high secretion of antiviral cytokines [24]. Neutrophils kill viruses through phagocytosis on the release of granules containing antiviral components [25], while NK cells can directly attack infected cells to limit the spread of the virus [26]. In addition to immune cells, cells of the epithelium in the first layer of defence are able to release antiviral cytokines as well [27].

Key to the human antiviral response are interferons (IFNs), cytokines that are produced by infected cells as a response to detection of viral components by PRRs such as the aforementioned TLRs and RLRs [28]. Other means of sensing viruses are the cytosolic deoxyribonucleic acid (DNA) sensors absent in melanoma 2 (AIM2) [29], cyclic GMP–AMP synthase (cGAS), or Gamma-interferon-inducible protein 16 (IFI16) [30], as well as various sensors of glycosylated viral proteins [31].

RNA viruses induce interferons mostly through TLR3 (double stranded RNA (dsRNA)), TLR7/8 (single-stranded RNA (ssRNA)), RIG-I (dsRNA) and melanoma differentiation-associated protein (MDA5) (dsRNA), however some RNA viruses activate other PRRs as well [31]. Additionally, sensing of mitochondrial nucleic acids

by PRRs in damaged or infected cells can trigger antiviral responses [32]. Activation of these PRRs leads to initiation of various signalling cascades, that result in activation of interferon regulatory factors (IRFs) [33]. IRFs are transcription factors, that induce expression of IFNs [34]. IFNs can also be induced by other transcription factors downstream of the above motioned antiviral PRRs, such as nuclear factor kappa-light-chain-enhancer of activated B cells (NFκB) [35], or activating transcription factor (ATF) and activator protein AP-1 [36].

The most prominent group of IFNs are the type I IFNs IFN-α and IFN-β. Once released, they activate nearby immune cells, primarily macrophages and NK cells by binding the IFN-α receptor (IFNAR), a receptor that is activated by all type I IFNs [37]. The IRFs mostly responsible for type I IFN expression are IRF3 [38] and IRF7 [39].

The type II IFN group only consists of only one cytokine, IFN-γ, that binds the IFN-γ receptor (IFNGR). Secreted by a large variety of cells, IFN-γ promotes differentiation of macrophages and T cells into type I immunity-promoting subtypes and reducing type II responses [40]. Type 1 immunity is directed against intracellular pathogens and is characterized by activation of cluster of differentiation 4^+ T helper lymphocytes ($CD4^+$ T_H1 cells) and cytotoxic $CD8^+$ T cells, while type 2 responses are involved in clearance of parasitic infections, involving T_H2 cells or eosinophiles [41].

The type III IFNs are four subtypes of four IFN-λ, that signal through the IFN-λ receptor (IFNLR1) and the interleukin 10 receptor, beta subunit (IL10RB) [42]. In their function similar to type I IFNs, type III IFNs mostly serve as an early defence line in the epithelium [43]. At the epithelial surface in the lung, both type I and type III IFNs protect from viral infection in the lower respiratory tract, while type III IFNs are particularly of importance in controlling infections in the upper respiratory tract [44].

Generally, in epithelial cells, type III IFNs respond early to viral infection, while type I IFNs enforce antiviral immunity if infection persists [45].

All interferons signal through the Janus kinases - signal transducer and activator of transcription protein (JAK-STAT) pathway and activation of the respective receptors leads to the expression of interferon-stimulated genes (ISGs) that initiate robust antiviral responses [46]. There are many ISGs. It is suggested that as much as 10% of the human genome might be regulated by IFNs [47]. Many components of the above described IFN signalling pathways, such as PRRs and signalling molecules, are ISGs themselves, and are induced to amplify viral sensing and IFN responses [48]. Other ISGs have direct antiviral properties and interfere with viral entry [49], translation [50], or egress [51]. ISG15 is an ISG with a broad spectrum of functions. As an extracellular cytokine, it can bind to the Lymphocyte function-associated antigen 1 (LFA-1) integrin receptor and amplify type II IFN production [52]. In the cell, it can covalently modify lysine residues in a process termed ISGylation [53], and regulate type I IFN production by preventing degradation of ubiquitin specific peptidase 18 (USP18), an IFNAR inhibitor [54]. Recently, ISG15 has also been shown to be involved in lipid metabolism, regulating the lipid profile during Vaccinia virus (VACV) infection [55].

Another ISG, ISG20, is a potent exonuclease able to degrade viral RNA [56]. Interestingly, some forms of the SARS-CoV-2 uptake receptor angiotensin-converting enzyme 2 (ACE2), have been described to be ISGs [57]. Measuring ISG expression is a standard way to draw conclusions about the presence of IFN signalling in a cell. The main mechanisms of virus sensing through PRRs are depicted in Figure 1.2.

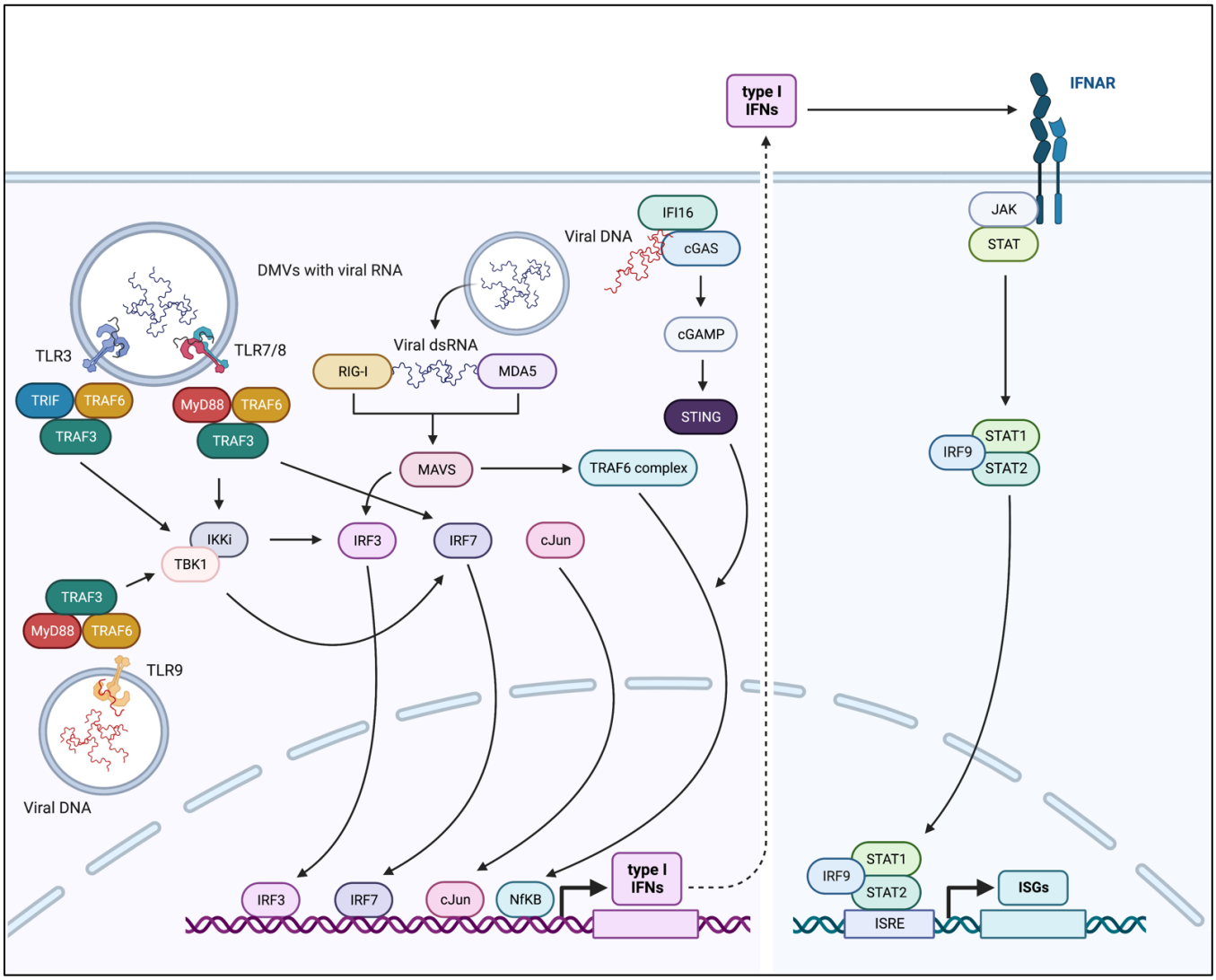


Figure 1.2: Innate antiviral sensors and type I IFN activation.

The main sensors of viral genome elements in innate immune cells are TLR3, TLR7/8, RIG-I, cGAS, and MDA5. Activation of these receptors leads to activation of various signalling cascades, resulting in activation of transcription factors for the type I IFNs IFN-α and IFN-β, such as IRFs, but also c-Jun or NFκB. Type I IFNs can signal in both an autocrine and a paracrine manner through binding IFNAR. Activation of this receptor ultimately leads to activation of the Jak/STAT pathway and expression of ISGs.

1.3 RNA viruses

While there are many commensal viruses, some viral infections can lead to disease and even death if untreated. The life cycle of a virus consists of multiple steps. First the virus attaches to, and enters the host cell and releases its genomic information. Within the cell, the viral genome is then amplified and new viral particles are assembled from it. These particles leave the cell to infect other hosts [58].

The genomic material of viruses can be made up of both single and double-stranded RNA or DNA molecules, each group utilizing distinct replication techniques. Most RNA viruses have a single-stranded RNA genome and can be further classified into negative-sense or positive-sense viruses. Due to its similarity to messenger RNA (mRNA), viral positive-sense RNA can be directly translated in the host cytosol, without the need for intermediates. Negative-sense RNA however needs to be transcribed into positive-sense RNA first [58].

1.3.1 SARS-CoV-2

SARS-CoV-2 is a positive-sense ssRNA virus, responsible for the COVID-19 pandemic. Infection with this highly pathogenic virus can lead to development of the disease, characterized by fever, cough, and in some cases pneumonia. In severe cases, COVID-19 can lead to dyspnea, hypoxia, respiratory failure and even death [59]. As of January 2023, more than 6,700,000 people have died from the disease [60].

SARS-CoV-2 mainly infects cells of the respiratory tract, however in severe cases other organs can be affected as well [61]. The entry receptor for this virus has been identified as ACE2 [62], a membrane bound enzyme mainly responsible for

lowering blood pressure by hydrolysis of angiotensin II [63]. ACE2 is a highly variable protein and multiple variations exist depending on age, gender or ethnicity. It is believed that these variations can impact the susceptibility of an individual to get infected with SARS-CoV-2 [64,65]. One isoform has been identified to be expressed as a result of IFN stimulation and viral infection [57], however, this truncated version was later found to be irrelevant for viral uptake as it lacks SARS-CoV-2 spike binding sites [66]. As some splice variants display no, or lower affinity to the spike than others, driving expression of low-affinity versions of ACE2 has been explored to potentially limit uptake of the virus [67].

Upon ACE2 binding, viral uptake is facilitated by the spike protein, one of the four structural proteins of SARS-CoV-2. Another host protein important for SARS-CoV-2 uptake is the serine protease transmembrane protease, serine 2 (TMPRSS2). TMPRSS2 cleaves the SARS-CoV-2 spike, which is required for full binding of the spike to ACE2 [68]. Viral uptake after ACE2 binding is also regulated by TMPRSS2 through further cleavage of the spike at the S2 site, after which the virus is taken up via the plasma membrane [69]. Second to this process, SARS-CoV-2 can also enter the cell through endocytosis, in a process termed the late entry pathway, which is independent of TMPRSS2 [70]. Both ACE2 and TMPRSS2 have been investigated as potential targets for antiviral therapy against COVID-19.

The other three viral proteins are the envelope, the membrane and the nucleocapsid proteins, which is bound to the viral RNA [71]. After being taken up through an endosome, the virus releases the RNA into the cytosol which then gives rise to the non-structural proteins (NSPs). The NSPs form the viral replication and transcription complex, facilitating the generation and release of new viral particles

through the endoplasmic reticulum (ER) and the Golgi [71]. Figure 1.3 summarizes the replication cycle of SARS-CoV-2.

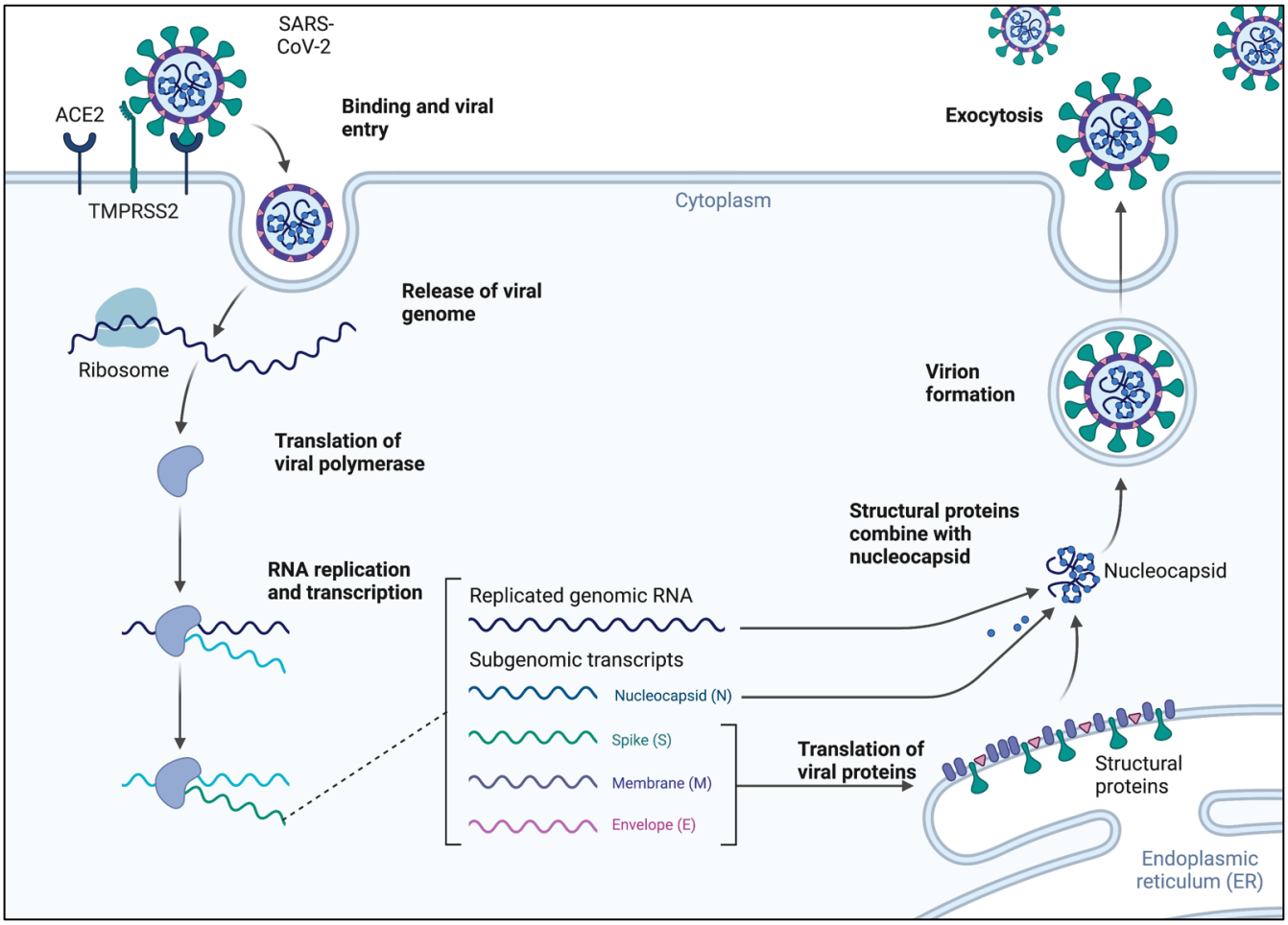


Figure 1.3: The life cycle of SARS-CoV-2.

The virus binds the entry receptor ACE2 on the host cell surface after priming of the spike by TMPRSS2, and is subsequently taken up through endocytosis. After release of the viral RNA from the acidified endosome, the viral RNA polymerase is expressed to start the replication process. The replicated RNA binds the nucleocapsid, and forms a new virion together with structural proteins, that are translated at the ER. The freshly replicated virus exits the cell via exocytosis.

1.3.2 Influenza

Influenza is another ssRNA virus. Unlike SARS-CoV-2 however, this virus has negative-sense RNA genome and thus a distinctly different replication cycle. There are four influenza species: Influenza A (IAV), B (IBV), C (ICV), and D (IDV) virus. Here I will cover IAV.

IAV entry into the cell is facilitated by the viral hemagglutinin (HA) protein present on the surface of the viral particle [72]. HA binds to sialic acid on the glycoproteins and glycolipids in the host cell membrane [73,74] in a complex process, that is still not fully understood and a definitive receptor for IAV remains unknown. Recently, tetraspanins have been proposed to assist viral entry into host cells [75]. Once the viral particle is internalized through endocytosis, the low pH of the endosome initiates fusion of the viral envelope with the endosomal membrane, releasing the viral genome into the cytoplasm, enveloped in the viral ribonucleoprotein (vRNP) [76]. The vRNP complex consists of the viral RNA (vRNA), the nucleoprotein (NP), and the viral polymerase [77,78].

Unlike for most respiratory RNA viruses, replication of the influenza genome occurs in the nucleus. To enter, IAV utilizes the host cell machinery used for nuclear import by hijacking the importin-α–importin-β nuclear import pathway [79]. Once inside the nucleus, RNA transcription is carried out by the viral polymerase. As the RNA genome is negative-sense, a complimentary copy (cRNA) needs to be generated first, which is then used as a template for production of new vRNA [80]. Viral mRNA for protein translation is transcribed directly from the vRNA before cRNA transcription. To allow for correct export and translation of viral RNA, the viral

polymerase “steals” the 5′ cap from host mRNA and attaches it to the viral mRNA in a process called cap snatching [81]. The translation of viral proteins is 100% dependent on the host translation machinery [80]. Freshly synthesized NP and polymerase proteins re-enter the nucleus to form a complex with newly transcribed vRNA to form new vRNPs [82,83], which are transported to the cytosol by the host Chromosomal maintenance 1 (CRM1) nuclear export pathway [84]. CRM1 is mostly located in the nuclear membrane, but has been shown to be dissociated from the nucleus when deactivated [85]. This deactivation is result of a cysteine modification in its substrate binding grove, and CRM1 inhibitors are being investigated as antivirals for viruses that depend on this export system for replication [86].

In the cytoplasm, the vRNP migrates to the plasma membrane for full assembly of the IAV particle, escorted by cellular Ras-related protein 11 (Rab11) [87]. The components of the viral envelope are transported to the plasma membrane by the host ER and combined with the vRNP when budding out of the cell [88,89]. The release of IAV is facilitated by neuraminidase (NA) in the viral membrane, which cleaves sialic acid residues on the cell surface, preventing binding of HA [90,91]. In figure 1.4 I summarize the life cycle of Influenza viruses.

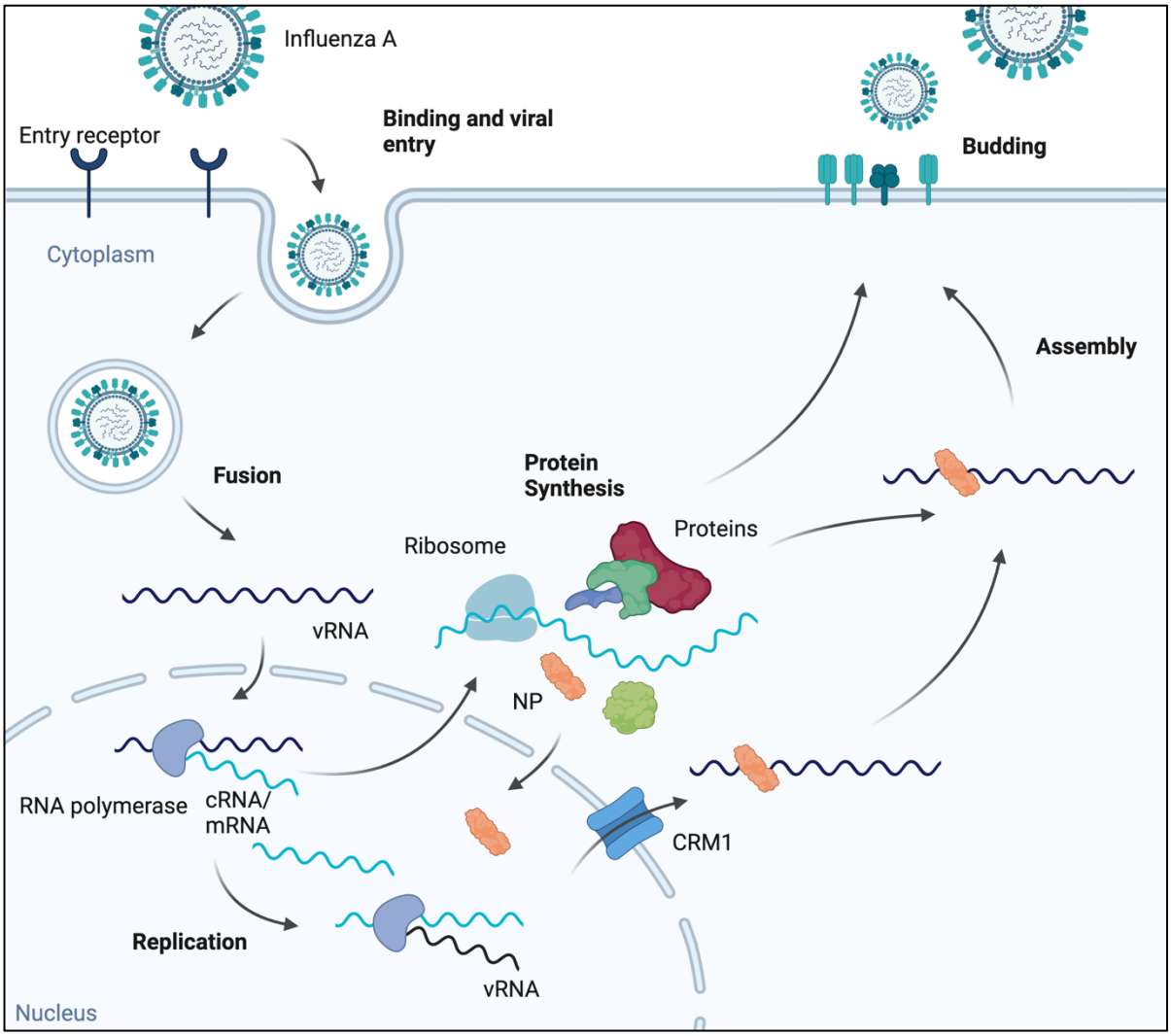


Figure 1.4: The life cycle of IAV.

Influenza enters the cell by binding to sialic acid on uptake receptors in tetraspanin rich regions. After the fusion, the vRNA is released into the cytosol and subsequently transported to the nucleus. Here, viral polymerases transcribe the vRNA into both cRNA, which is transcribed back into more vRNA for replication of the genome, and into mRNA. The replicated vRNA is transported out of the nucleus by the cellular transporter CRM1, forming the new RNP. The mRNA exits the nucleus and is translated by the host ribosome. The viral proteins than either enter the nucleus to assist with replication, stay in the cytosol for the RNP formation, or migrate to the cell membrane. Once assembled, the RNP buds out of the cell in a region expressing the viral surface proteins, thus creating a new virion.

1.4 CRM1

A crucial part of influenza replication involves the nuclear export protein CRM1, also known as exportin 1 (XPO1), which is a focus of this study. In the absence of viral infection however, this transporter is responsible for a number of biological processes. CRM1 transports a variety of proteins and RNA species from the nucleus across the nuclear membrane into the cytosol [92]. While smaller molecules can pass through the so called nuclear pore complex (NPC), larger molecules require an active transport mechanism to leave the nucleus [93]. CRM1 recognizes the nuclear export signal (NES) on its cargo proteins, prompting engagement of the cargo binding pocket of CRM1 with the target and export using Guanosine-5'-triphosphate (GTP) hydrolysis as a fuel source [94]. To this end CRM1 binds the active form of ras-related nuclear protein (RAN), RAN-GTP, in the nucleus. The complex is then bound by the co-factor Ran-specific binding protein 1 (RanBP1) and under GTP hydrolysis to guanosine diphosphate (GDP) by Ran GTPase-activating protein (RanGAP), shuttled through the NPC and subsequently disassembled [95]. This transport works along the GTP – GDP gradient, and as GTP is predominantly limited to the nucleus, it is unidirectional [96]. Once in the cytosol, RanGDP is recycled for another round of transport and free CRM1 shuttles back into the nucleus through the NPC [97]. Figure 1.5 depicts an overview over the CRM1 export cycle.

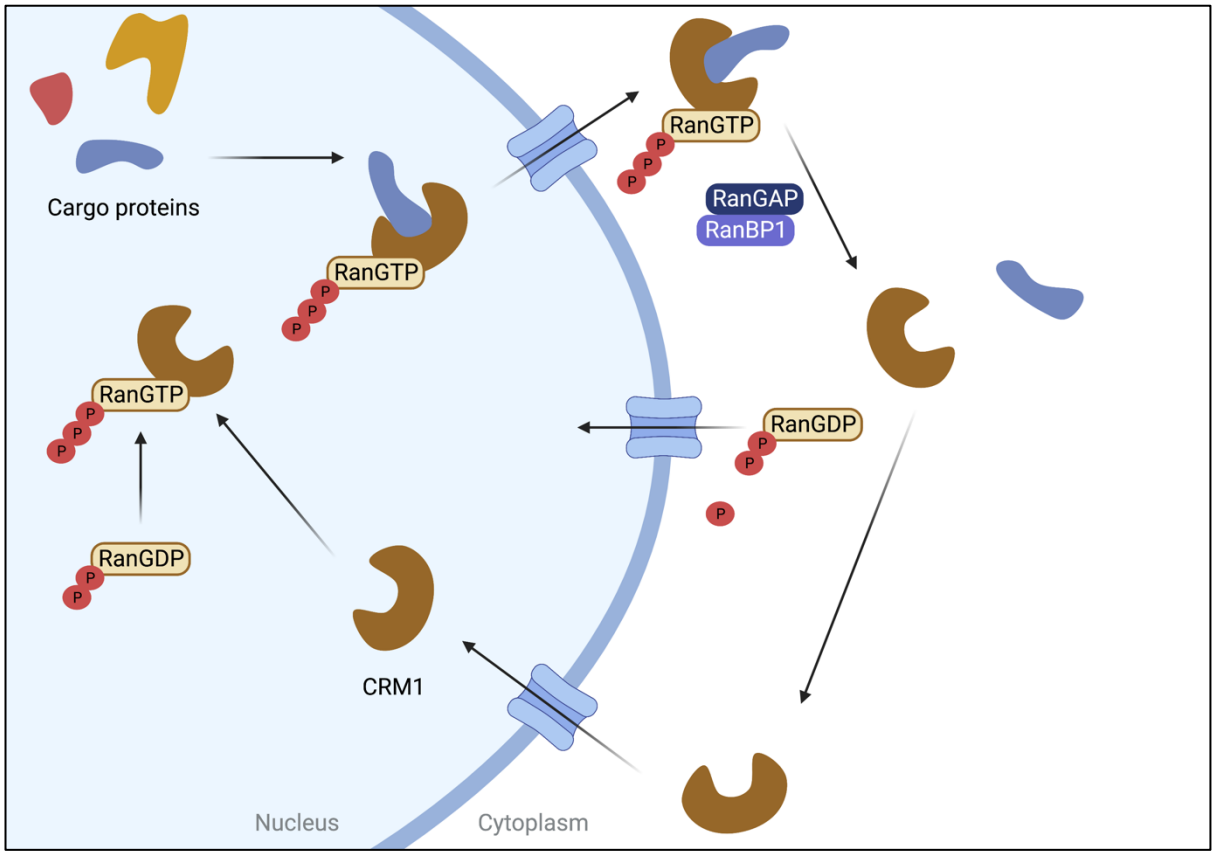


Figure 1.5: Mechanism of the nuclear exporter CRM1.

Upon binding of RanGTP, CRM1 is able to recognize the NES of its cargo proteins, carrying them to the cytoplasm though the nuclear pore complex. Here, the complex is disassembled under GTP hydrolysis and the cargo is released. This process is facilitated by the binding of RanGAP and RanBP1. RanGDP and CRM1 subsequently re-enter the nucleus to bind more cargo.

About 220 proteins are known to contain an NES, however it is estimated that over 1000 proteins depend on CRM1 for their subcellular localization [98]. Amongst the most studied CRM1 cargos are various members of tumour suppressor families, such as p53 [99]. These factors play an important role in maintaining stability of the genome and their presence in the nucleus are crucial for preventing cellular transformation [100]. For this reason, overexpression of CRM1 and subsequent increased export of these factors from the nucleus has been associated with various cancer types, including pancreatic, lung, gastric, and colorectal cancer [101–104], and targeting CRM1 has become a target in cancer therapy.

Interestingly, the products of multiple oncogenes are also transported by CRM1, suggesting that the pro-tumour effect of CRM1 is more complex than simply exclusion of anti-cancer factors from the nucleus [98,105]. Nevertheless, CRM1 inhibitors have shown promising results in treating malignancies, with one, KPT-330, also named Selinexor, already being U.S. Food and Drug Administration (FDA) approved and used to treat multiple myeloma (MM).

1.4.1 CRM1 inhibition

Most known CRM1 inhibitors follow a similar mechanism of action. The first specific CRM1 inhibitor to be discovered was leptomycin B (LMB), an antifungal metabolite isolated from *Streptomyces* [106]. After anti-tumour efficacy was confirmed [107], it was found that LMB binds and covalently modifies a cysteine residue in the cargo binding pocket of CRM1 in an alkylation reaction [108].

The CRM1 protein contains HEAT (acronym for **H**untingtin, **E**longation factor 3, protein phosphatase 2**A** (PP2A) and **T**OR1) repeats, formed by two linked antiparallel alpha helices each. The cargo binding pocket is formed by the A helices of the 11th and 12th HEAT repeat, which recognizes the NES motif on cargo proteins [109]. Cargo binding, together with RanGTP binding to the 9th HEAT loop induces an active state in CRM1, initiating the transport [110]. Cys528, the cysteine residue alkylated by LMB, is situated on HEAT repeat 11 in the cargo binding pocket, and its modification results in the pocket being unable to bind the NES on target proteins [108]. Figure 1.6 depicts a more detailed structured model of CRM1 and the position of Cys528 within the cargo binding cleft. All subsequent CRM1 inhibitors work through covalent or non-covalent modification of Cys528. After the discovery of LMBs properties, multiple small molecule inhibitors of CRM1 were developed. These so called selective inhibitors of nuclear export (SINEs) were designed to be more effective and specific than LMB, while targeting the same cysteine. KPT-330 was the most successful candidate out of a group of structurally related compounds and importantly, other than with LMB, the modification of Cys528 by SINEs is slowly reversible, making these molecules more suitable for drug development [111]. While having been shown to inhibit the replication of various viruses, the primary incentive for SINE development has been cancer therapy.

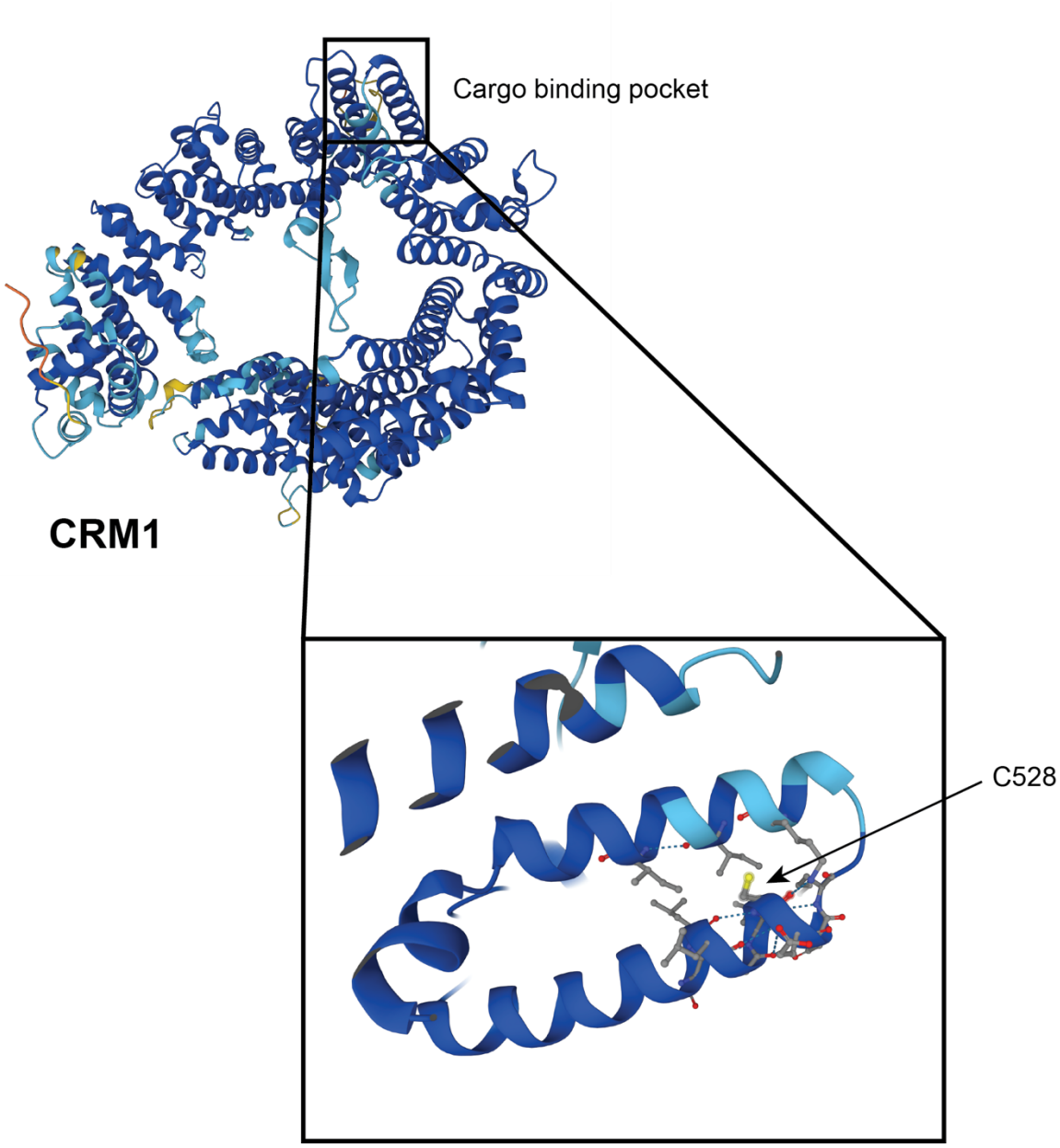


Figure 1.6: Structural model of CRM1.

CRM1 binds its cargo via its cargo binding pocket (highlighted), which is made up off of the 11th and 12th HEAT repeat. Situated within the cleft is Cys528 which is involved in binding of the cargo NES. Alkylation of this cysteine residue by LMB or SINEs effectively blocks cargo binding to the cleft and shuts down CRM1 mediated nuclear export. Predicted protein structure was generated using the AlphaFold Protein Structure Database.

Three SINEs have advanced to clinical trials. KPT-8602 was proposed as a less toxic alternative to KPT-330 [112], and is currently being trialled in relapsed/refractory MM, metastatic colorectal cancer (mCRC), metastatic castration resistant prostate cancer (mCRPC), higher risk myelodysplastic syndrome (HRMDS), acute myeloid leukemia (AML) and newly diagnosed intermediate/high-risk MDS (NCT02649790). The orally administered SL-801 recently completed a phase 1 clinical trial in solid tumours in 2022 (NCT02667873), however no results have been posted yet. A mid-trial report showed encouraging results for activity and safety in patients with advanced, poor prognosis tumours [113].

The by far best studied SINE however is KPT-330. While being approved by the FDA for use in MM in 2020, KPT-330 has been trialled in multiple other cancers. In solid tumours such as advanced de-differentiated liposarcoma (NCT02606461) [114], castration-resistant prostate cancer (NCT02215161) [115], or a mix of solid tumours (NCT01607905) [116] KPT-330 yielded mostly disappointing results, displaying strong adverse effects and low efficacy. In AML, KPT-330 showed more potential (NCT01607892) [117], especially in combination with other, conventional treatments (NCT02299518) [118], or (NCT02212561) [119]. As mentioned above, KPT-330 has been approved for use in multiple myeloma. Despite early trials showing only limited success (NCT01607892) [120], further trials were conducted using KPT-330 in combination treatments, leading to a successful phase 3 trial with a KPT-330/bortezomib/dexamethasone co-treatment showing high efficacy in the KPT-330 arm (NCT03110562) [121].

As CRM1 is ubiquitously expressed throughout the body, not just in cancer cells, treatment with CRM1 inhibitors can significantly impact cell biology in healthy

cells. This is why SINEs only play a role for drug development in certain cancers, where severe side effects are tolerable. Using SINEs as antivirals in humans, while potentially effective, has therefore not been extensively studied yet.

1.4.2 CRM1 and Viruses

As mentioned above in the case of IAV, CRM1 is hijacked by many viruses that enter the nucleus as part of their life cycle. This includes viruses that replicate in the nucleus, such as IAV itself [122] or human immunodeficiency virus (HIV) [123], but also viruses that only shuttle parts of their proteome to the nucleus, such as Respiratory syncytial virus (RSV) [124]. Inhibition of CRM1 by for example SINEs or LMB has been shown to inhibit replication of CRM1 dependent viruses both *in vivo* and *in vitro*. In influenza, CRM1 inhibition by the SINE KPT-335 has been shown to retain viral NP in the nucleus, thereby reducing viral replication [122]. LMB has been shown to be antiviral in HIV by reducing nuclear export of Rev [125], as well as in Rabies Virus [126], RSV [127] and others. Surprisingly, KPT-330 has not been extensively studied as an antiviral agent but antiviral potential can be assumed. Interestingly, CRM1 inhibition has also been shown to restrict SARS-Cov-2 replication, not only through possible nuclear retention of viral components containing an NES such as the nucleocapsid protein [128], the ORF3b protein [129], or the spike [130], but also by nuclear trapping of the SARS-Cov-2 uptake receptor ACE2 [131]. In the wake of this discovery, KPT-330 has also been trialled for use in SARS-CoV-2 in 2020 (NCT04349098) and (NCT04355676). Table 1.1 lists all viruses that have

been shown to depend on CRM1 for replication, and whether CRM1 inhibition slowed down replication.

Virus	CRM1 inhibitor used	Reference
Dengue	LMB	[132]
Hepatitis B (HBV)	KPT-335	[133]
HIV	KPT-185, LMB	[125,134]
HMCV	KPT-8602	[135]
HTLV-1	-	[136]
IAV	KPT-330, KPT-335, LMB	[137–139]
Rabies	LMB	[126]
RSV	LMB, KPT-335	[127,140]
SARS-CoV-2	KPT-330	[131]

Table 1.1: List of viruses that use CRM1 as part of their replication cycle.

1.5 Metabolic reprogramming in macrophages

This thesis discusses the macrophage metabolite itaconate and its possible anti-viral role in IAV and SARS-CoV-2 infections. Itaconate emerged as a dominant metabolite upregulated in M1 macrophages.

Upon activation, immune cells undergo distinct metabolic changes. Studying these changes has given rise to the emerging field of immunometabolism, reshaping our understanding of how metabolism is integrated into immunity. It has emerged that many metabolites and metabolic enzymes fulfil moonlighting roles as regulators of immune cell activity and polarization.

In addition to pathogen clearance by phagocytosis, macrophages can, depending on lineage and location, enhance (classically activated, or M1 macrophages) or decrease (alternatively activated, or M2 macrophages) inflammation by the release of specific cytokines and chemokines, and play an important role in overall tissue homeostasis [141]. M1 macrophages are induced by LPS or IFN-γ, and are chacterized by the realase of pro-inflammatory cytokines such as tumour necrosis factor-α (TNF-α), interleukin-1β (IL-1β), or IL-6 [142]. They arise in inflammatory settings and are involved in activation of surrounding immune cells and pathogen clearance through phagocytosis [142]. M2 macrophages are induced by cytokines such as IL-4, and have largely antiinflamatory properties through release of IL-10 and transforming growth factor beta (TGF-β), contributing to resolution and tissue repair [143].

In M1 macrophages, these metabolic changes are characterized by an interrupted tricarboxylic acid (TCA) cycle and subsequently reduced oxidative

phosphorylation (OXPHOS). The break in the TCA cycle is a result of repression of two key enzymes, succinate dehydrogenase (SDH) and isocitrate dehydrogenase (IDH), resulting in accumulation of their substrates succinate and citrate respectively [144,145]. Succinate in itself has been shown to boost production of the pro-inflammatory cytokine IL-1β through stabilization of Hypoxia-inducible factor 1α (HIF-1α) [144], and increase mitochondrial reactive oxygen species (ROS) in classically activated macrophages [146]. Accumulated citrate has been shown to boost fatty acid synthesis [147,148].

This metabolic shift means that activated macrophages need to generate energy through glycolysis [149], a process that is less effective, but faster in adenosine triphosphate (ATP) generation [150]. Interestingly this metabolic state resembles the Warburg Effect observed in cancer cells, where rapid proliferation and biomass generation are substantial [151]. In addition, glycolytic intermediates are also increasingly funnelled into the pentose phosphate pathway (PPP), resulting in increased generation of reduced nicotinamide adenine dinucleotide phosphate (NADPH), which is involved in the anti-oxidant response [152,153], and elevated nucleotide production for DNA and RNA synthesis [154].

1.5.1 Itaconate

Itaconate is a metabolite that has become increasingly studied in the field of immunometabolism in recent years. In classically activated macrophages, itaconate is one of the most highly upregulated metabolites, reaching millimolar concentrations and exerting striking immunomodulatory functionality. Despite being produced by

these inflammation-driving innate immune cells, itaconate has actually been found to be anti-inflammatory, acting as an important counterweight in macrophage mediated immune responses [155]. Generated from aconitate by the enzyme Aconitate Decarboxylase 1 (ACOD1), itaconate is able to interrupt the TCA cycle by inhibiting SDH and thereby reducing LPS induced generation of ROS and production of the pro-inflammatory cytokine IL-1β [156]. Expression of the *Acod1* gene, also named immunoresponsive gene 1 (*Irg1*), is mostly restricted to the myeloid lineage [148]. Figure 1.7 displays the TCA cycle and itaconate synthesis. Itaconate is readily exported from the mitochondrion into the cytosol by the oxoglutarate carrier (OGC).

Itaconate was identified as an activator of the anti-inflammatory transcription factor Nuclear factor erythroid 2-related factor 2 (NRF2) by inactivation of Kelch-like ECH-associated protein 1 (KEAP1) utilizing 4-OI as an itaconate mimic [155]. Endogenous itaconate might have a similar effect since NRF2 activation in response to LPS is restricted in IRG1-deficient macrophages [157], and exogenous itaconate was later confirmed to also activate NRF2 [158]. More recently, itaconate, as well as 4-OI have been shown to block activation of the NOD-, LRR- and pyrin domain-containing protein 3 (NLRP3) inflammasome [159], as well as phosphorylation of JAK1 [160]. Mechanistically, itaconate and 4-OI are able to alkylate cysteine residues on certain proteins, inducing a post-translational modification (PTM) called 2, 3-dicarboxypropylation, thereby modifying protein activity and stability [155].

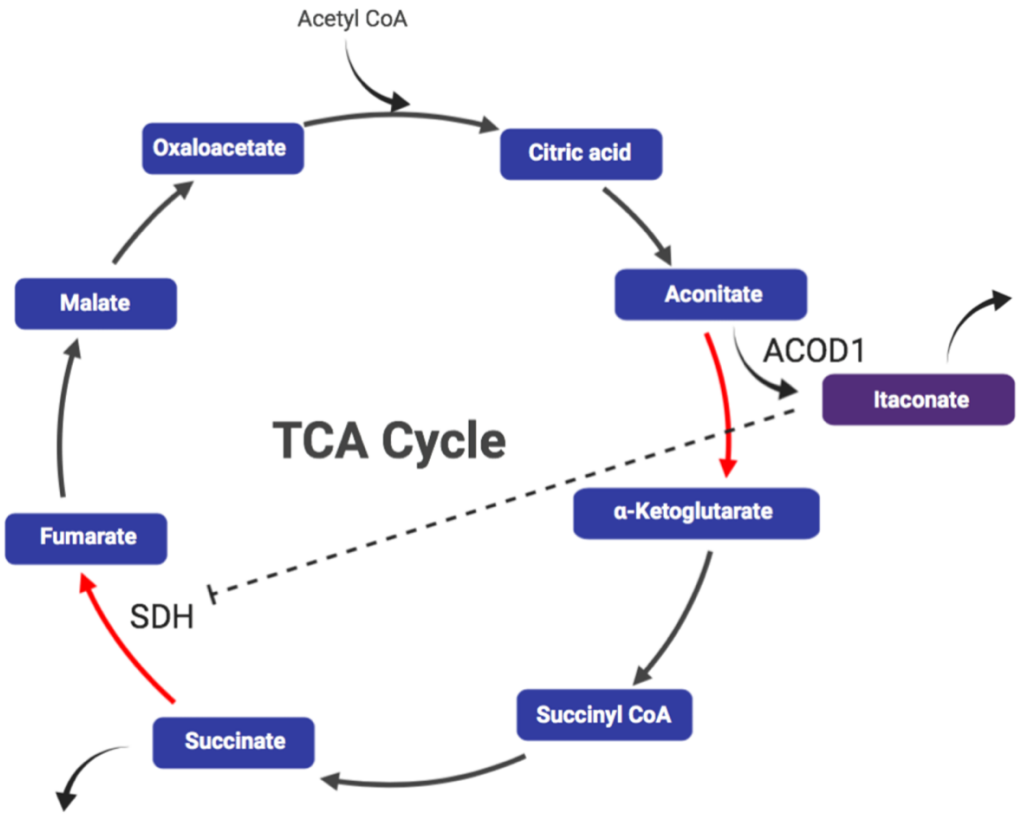


Figure 1.7: Itaconate's position in the TCA cycle.

In classically activated macrophages, itaconate is generated from aconitate by ACOD1, interrupting the TCA cycle at two points.

Additionally, itaconate is able to inhibit enzymes through competitive binding of an enzyme-binding pocket. Ten–Eleven Translocation-2 (TET2) for example is inhibited by both itaconate and 4-OI through this mechanism, regulating DNA methylation and decreasing induction of certain LPS induced genes [161].

Itaconate has been found to be exported from classically activated macrophages, suggesting the possibility of an extracellular messenger function. A receptor or plasma membrane transporter for itaconate however remains to be identified.

As a negatively charged, polar metabolite, itaconate has been proposed to be unable to spontaneously cross the cell membrane, prompting the design and use of cell-permeable itaconate derivatives such as dimethyl itaconate (DMI) [156], and synthesized 4-OI [155]. These derivatives share the electrophilic properties of itaconate and were thought to be, at least in part, metabolized into itaconate. It emerged that DMI is quickly degraded and in fact not converted to itaconate [162], and despite actually increasing extracellular itaconate [155], 4-OI might have additional effects that go beyond the properties of unmodified itaconate. Importantly, these derivatives are more electrophilic than the unmodified metabolite, possibly resulting in stronger interaction with binding partners [163], which is why often lower concentrations of these derivatives are need to achieve similar effects to those of unmodified itaconate. The structures of both itaconate and 4-OI are shown in figure 1.8.

In addition to these synthetically produced derivatives, naturally occurring derivatives of itaconate, mesaconate and citraconate have been recently identified in classically activated macrophages [164]. Both share itaconate's anti-inflammatory and

electrophilic properties to varying degrees, while only citraconate was revealed as an Irg1 inhibitor [165]. How these isomers are generated is now known, but it is possible that some of itaconate's properties are indirectly through generation of these metabolites.

A key difference has been found between 4-OI and itaconate. 4-OI blocks type I IFN production, while exogenous itaconate actually increases IFN-β production [166]. It is possible that observations of effects caused by extracellular itaconate might be influenced by receptor mediated signalling events as the possibility of an itaconate receptor exists. The role of endogenous itaconate in IFN-β production is still unclear. The above mentioned study showed decreased IFN production in *Irg1* knockout (KO) cells [166], while others were unable to confirm a link between IRG expression and IFN-β production [167]. Additionally, high doses of exogenous itaconate were in one instance able to decrease IFN expression in response to IAV infection [168].

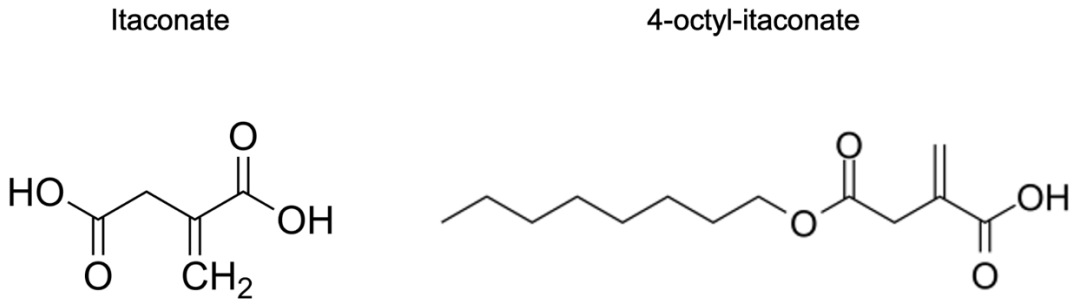


Figure 1.8: Chemical structures of itaconate and 4-OI

Similarly, observations that 4-OI can inhibit prostaglandin generation and release, which could not yet be confirmed for exogenous itaconate or IRG1 [169]. On the other hand, there is no evidence that 4-OI can inhibit SDH in the same fashion itaconate does, as 4-OI could not increase succinate levels and is generally unable to bind the succinate binding pocket of SDH [170]. Notably however, 4-OI causes a similar phenotype to SDH inhibition, possibly through an alternative mechanism [171]. Additionally, it is possible that IRG1 has itaconate independent functions, as it has recently been shown that IRG1 can itself directly bind to proteins such as guanosine triphosphatase IMAP family member 7 (GIMAP7), driving TNFα production [167]. Generally, there is also a possibility of IRG1 directly regulating gene expression, as TCA cycle enzymes have recently been shown to enter the nucleus, modulating gene expression through histone acetylation [172].

Key differences and similarities between itaconate, 4-OI and IRG1 dependent effects explored through *Irg1* KO cells are summarized in table 1.2.

Target	**Itaconate**	**4-OI**	***Irg1* KO**
NRF2 expression	↑	↑↑	↓
SDH activity	↓	**-**	↑
IFN-β production	↑ ↓	↓	↑ ↓
NLRP3 activity	↓	↓	↑
Jak1 phosphorylation	↓	↓	**-**
TET2 activation	↓	↓	↑
TFEB nuclear translocation	↑	↑	↓

Table 1.2: Differences and similarities between itaconate, 4-OI and IRG1 in immunity

Itaconate has been found to have antimicrobial properties long before its relevance in immunity became apparent. As early as 1977 a study found an antibacterial function of itaconate in *Pseudomonas indigofera* [173]. More recently, itaconate has been shown to restrict growth of *M. tuberculosis, Staphylococcus aureus, S. enterica, Legionella pneumophillia* and *Acinetobacter baumannii* [174]. Here, itaconate inhibits isocitrate lyase (ICL), a metabolic enzyme critical for microbial survival in low-glucose conditions [175]. Both itaconate and 4-OI have been shown to regulate lysosomal function through nuclear translocation of Transcription factor EB (TFEB), augmenting clearance of bacteria through phagocytosis [176].

A graphical overview of itaconate and its relevance in immunity are summarized in Figure 1.9. Overall, the implementation of the itaconate family into inflammatory processes is highly complex and requires further research.

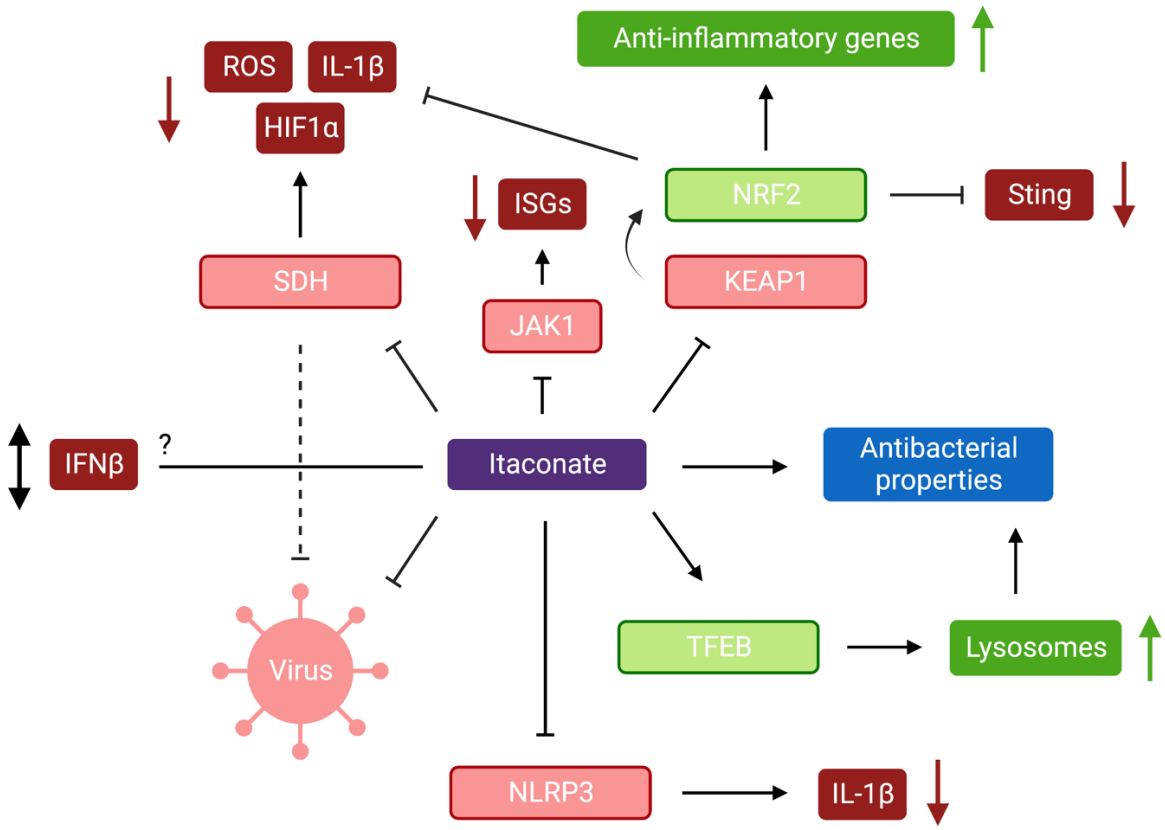


Figure 1.9: Itaconate exerts anti-inflammatory and anti-microbial function through a variety of pathways. Besides its antibacterial properties, one of the first immunologically relevant functions of itaconate discovered is the inhibition of SDH, reducing expression of proinflammatory mediators, production of ROS and release of IL-1β. In the cytosol, itaconate has been found to activate anti-inflammatory transcription factor NRF2 by releasing it from its inhibitor KEAP1. Furthermore itaconate can induce TFEB nuclear translocation and inhibit JAK1 phosphorylation as well as activation of the NLRP3 inflammasome. Itaconate has been shown to restrict replication of certain viruses, while its role in IFNβ production is still unclear. Anti-inflammatory factors are displayed in green, pro-inflammatory factors are displayed in red.

1.5.2 Antiviral properties of Itaconate and its derivatives

Both 4-OI and itaconate have been shown to have antiviral properties. In neurons, itaconate has been found to be upregulated after Zika virus infection. The virus induces signalling through receptor-interacting protein kinase-1 (RIPK1) and receptor-interacting protein kinase-2 (RIPK2), leading to an Interferon Regulatory Factor 1 (IRF1)-dependant upregulation of IRG1 and subsequent production of itaconate, which is then able to induce an antiviral metabolic state in Zika virus and also West Nile virus (WNV) infections. Here, IRG1 upregulation and itaconate have been shown to inhibit SDH followed by accumulation of succinate, and neuronal respiration, thereby restricting viral replication, with 4-OI directly restricting the virus [177].

In COVID-19, itaconate levels were found to be negatively correlated with disease severity [178]. Subsequently, 4-OI has been described to restrict SARS-CoV-2, Herpes Simplex Virus (HSV), and Vaccinia Virus (VACV) replication, a mechanism however remain to be explored [179]. A screen of other itaconate derivatives showed antiviral potential of itaconate-based compounds in IAV infection. Although no definitive mechanism was shown, it was suggested that the compounds might interfere with export of the viral NP [180]. More recently, anti-influenza properties of itaconate derivatives have been expanded to 4-OI, when Sohail et al. showed that both itaconate and 4-OI can reduce IAV replication [168].

Another virus whose replication is restricted by 4-OI is Porcine reproductive and respiratory syndrome virus (PRRSV). Here it was recently shown that 4-OI

interferes with attachment, replication, and release of the virus. Furthermore, 4-OI reduced inflammatory responses to the virus [181].

Taking into account the potential boost of IFN signalling observed by Swain et al., exogenous itaconate might additionally increase antiviral immunity in an IFN dependent manner [166]. Figure 1.10 summarizes the known antiviral properties that have been attributed to itaconate.

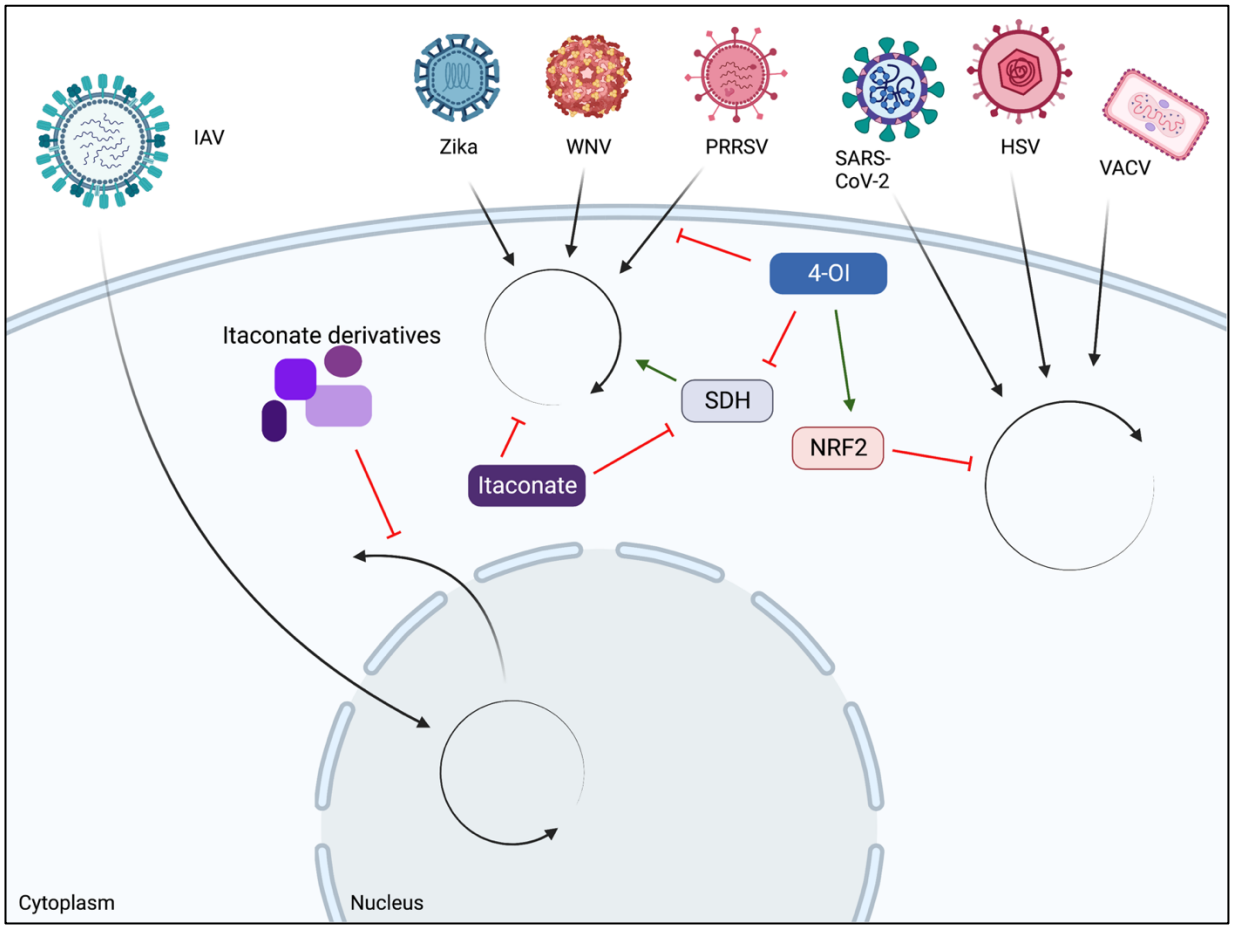


Figure 1.10: The antiviral effects of itaconate and its derivatives.

4-OI and number of Itaconate derivatives have been shown to restrict IAV replication, potentially through inhibition of its nuclear export. Itaconate restricts Zika Virus and WNV replication through SDH inhibition, as well as through creation of an "antiviral state". 4-OI inhibits an array of viruses, potentially through NRF2 activation, including SARS-CoV-2, HSV, and VACV. 4-OI also restricts replication of PRRSV.

1.6 Aims

Given the literature summarized above, itaconate and 4-OI have a high potential as antiviral agents. Combined with their anti-inflammatory properties, drugs derived from these molecules could reduce inflammation caused by viral infections, while simultaneously reducing viral loads, giving them a unique therapeutic angle.

In this project, I set out to explore itaconate and 4-OI in the context of IAV and SARS-CoV-2 infection. The specific aims are as follows:

- Confirm observed antiviral properties of 4-OI in IAV and SARS-CoV-2
- Explore possible broad, or virus-specific, antiviral mechanisms of the itaconate family
- Identify similarities or differences between 4-OI, exogenous itaconate and IRG1 in viral replication
- Explore the role of CRM1 as a target of 4-OI in its anti-viral effect.

This project improves our understanding of itaconate metabolism and might help in the quest for new antivirals agents.

Chapter 2: Materials and Methods

2.1 Materials

2.1.1 Buffers

The standard buffers used throughout this project are listed in table 2.1.

Buffer	Composition
Flow buffer	Sodium azide (0.1% w/v), Bovine serum albumin (BSA) (0.1% w/v), Fetal calf serum (FCS) (1.5% v/v), PBS
Fluorescence-activated cell sorting (FACS) buffer	Sodium azide (0.1%), BSA (0.1% w/v), FCS (1.5% v/v), PBS
Low stringency lysis buffer	HEPES pH 7.5 (50 mM), NaCl (100 mM), EDTA (1 mM), glycerol (10% v/v), nonident p40 (NP-40) (0.5% v/v), phenylmethylsulphonyl fluoride (PMSF) (1mM), aprotinin (11.5 µg/ml), leupeptin (1 µg/ml), sodium orthovanadate (1 mM)
Phosphate-buffered saline (PBS) (10X)	NaCl (1.45 M), NaH2PO4 (39 mM), NaH_2PO_4 (22.7 M)
Sample lysis buffer for western blot	Tris pH 6.8 (0.125 M), glycerol (10% v/v), SDS (0.02% w/v), DTT (5% w/v)
Sodium dodecyl sulphate–polyacrylamide gel electrophoresis (SDS PAGE) running buffer (10X)	Tris (25 mM), glycine (192 mM), SDS (0.1% w/v)
SDS PAGE transfer buffer (10X)	Tris (0.25 M), glycine (1.9 M), SDS (35 mM)
Tris-buffered saline tween (TBST) (10X)	Tris (12.11 g), NaCl (87.6 g), tween 20 (10 ml), distilled H2O to 1 L

Table 2.1: List of Buffers used in this project

2.1.2 Cell culture reagents

Tissue culture plastics were purchased from Thermo Fisher Scientific. Dulbecco's Modified Eagle Medium (DMEM), Roswell Park Memorial Institute Medium (RPMI), and plasticware were purchased from Thermo Fisher Scientific. Bronchial Epithelial Cell Growth Medium (BEGM) was from Lonza and FCS was purchased from Biosera unless stated otherwise. Penicillin-streptomycin, trypsin-EDTA and red cell lysis buffer were purchased from Sigma Aldrich unless stated otherwise. L929 supernatant was obtained by removing the supernatant from L929 cells at 60 - 70% confluency.

2.1.3 Mice

C57BL/6 mice were obtained from Harlan UK and were maintained under pathogen-free conditions. All mice were bred and maintained under specific pathogen free conditions under protocols in line with Irish and European Union regulations. Mice used for all experiments were littermates and matched for age. Animals were sacrificed by carbon dioxide asphyxiation and cells were harvested *post mortem*.

Use of animals received ethical approval by the universities' ethics committees in accordance with the personal licence approved by the Health Products Regulatory Authority (HPRA).

2.1.4 Hamsters

Wild-type Syrian hamsters (*Mesocricetus auratus*) were purchased from Janvier Laboratories. The animals were bred and housed under specific pathogen free conditions in individually ventilated Isocages (Techniplast). The hamsters were sacrificed by intraperitoneal administration of 500 µl Dolethal (200 mg/ml sodium pentobarbital, Vétoquinol).

Use of animals received ethical approval by the Ethical Committee of KU Leuven, following institutional guidelines approved by the Federation of European Laboratory Animal Science Associations (FELASA).

2.1.5 Cells

2.1.5.1 BMDMs

Bone marrow derived macrophages (BMDMs) are murine macrophages generated from bone marrow. Mice at the age of 7 to 16 weeks were sacrificed, hind legs were removed, and femur and tibia were cleaned off muscle tissue using scissors and tweezers. Both ends of femur and tibia were cut off, and using DMEM, the bone marrow was flushed out directly into a conical tube. Red blood cells were lysed in cell lysis buffer for 5 min and then resuspended in 30 ml DMEM containing 20% v/v L929 supernatant, 10% v/v FCS, 1% w/v penicillin and 100 U/ml streptomycin. The cells were then plated in non-tissue culture-coated 10 cm dishes at a volume of 10 ml per dish. for 7 days at 37°C, 5% CO^2. On day 7, the cells were harvested, re-plated at 0.5 x

10^6 cells/ml. The cells were lifted and harvested by adding cold PBS and then scraping off the attached cells.

2.1.5.2 L929 cells

L929 cells are a murine fibroblast cell line. These cells were cultured in complete DMEM supplemented with 10% v/v FCS and 100 U/ml penicillin/streptomycin in T175 flasks at 37°C, 5% CO^2. At 70% confluency, the supernatant was harvested to be used in BMDM differentiation.

2.1.5.3 A549 cells

A549 cells are human lung carcinoma epithelial cells. Cells were cultured in DMEM containing 10% v/v FCS and 100 U/ml penicillin/streptomycin in a T175 flask, 37°C, 5% CO^2. Cells were grown to 70% confluency before being split or plated out. To harvest cells, the medium was removed, and cells were washed in PBS. 10% Trypsin-EDTA in PBS was added, the flask was incubated for 5 minutes at 37°C, then the trypsin was deactivated in PBS containing 10% v/v FCS. For experiments, cells were plated at 0.25 x 10^6 cells/ml.

2.1.5.4 NuLi-1 cells

NuLi-1 cells are immortalized human bronchial epithelial cells. All plasticware used in experiments with NuLi-1 cells were pre-coated with collagen over night at 4°C on a shaker. After coating, the plastics were washed 3 times in PBS, before air-drying and sterilization for 1 h under ultraviolet (UV) light for 1 h at room temperature (RT). NuLi-1 cells were cultured in BEGM (BulletKit, Lonza) with all included supplements

added to the media in T75 flasks, 37°C, 5% CO^2. Cells were grown to 70% confluency before being split or plated out. To harvest cells, the medium was removed, and cells were washed in PBS. 10% v/v Trypsin-EDTA in PBS was added, the flask was incubated for 5 minutes at 37°C, then the trypsin was deactivated in PBS containing 10% v/v FCS. For experiments, cells were plated at 0.25 x 10^6 cells/ml.

2.1.5.5 NHBE cells

Normal human bronchial epithelial (NHBE) cells were cultured in BEGM (BulletKit, Lonza) with all included supplements added to the media in T75 flasks at 37°C, 5% CO^2. Cells were grown to 70% confluency before being split or plated out. To harvest cells, the medium was removed, and cells were washed in PBS. 10% Trypsin-Ethylenediaminetetraacetic acid (EDTA) in PBS was added, the flask was incubated for 5 minutes at 37°C, then the trypsin was deactivated in PBS containing 10% v/v FCS. For experiments, cells were plated at 0.25 x 10^6 cells/ml.

2.1.5.6 Jurkat cells

Jurkat cells are immortalized human T lymphocytes. These cells were cultured in full RPMI supplemented with 10% v/v FBS, 100 U/ml penicillin/streptomycin and 10 mM Hepes in a T75 flask at 37°C, 5% CO^2. For experiments, cells were plated at 0.5 x 10^6 cells/ml. Jurkat $XPO1^{C528S}$ cells are a gift from Dirk Daelemans and were generated as described before [182]. Jurkat $XPO1^{C528S}$ cells were cultured the same as WT cells. For experiments, cells were plated at 0.5 x 10^6 cells/ml.

2.1.5.7 THP-1 cells

THP-1 cells are a human leukaemia monocytic cell line, that can be differentiated into macrophage-like cells. THP-1 cells were cultured in RPMI, supplemented with 10% v/v FBS, 0.05 mM 2-mercaptoethanol (Gibco), and 100 U/ml penicillin/streptomycin at 37°C, 5% CO^2. For experiments, cells were plated in 6 well plates at 0.5 x 10^6 cells/ml.

2.1.5.8 MDCK cells

Madin-Darby canine kidney (MDCK) cells are immortalized canine kidney cells. The cells were cultured in Eagle's minimal essential medium (EMEM; Lonza) plus 10% FBS, 10mM Hepes, 1% w/v Sodium Bicarbonate, 1X Non-essential Amino Acid Solution, 100 U/ml Pen-Strep-Glut mixture (all Lonza) at 37°C, 5% CO^2. For experiments, cells were plated at 0.25 x 10^6 cells/ml.

2.1.5.9 Calu-3 cells

Calu-3 is a human lung adenocarcinoma cell line. Calu-3 cells were maintained in DMEM containing 10% FCS and 100 U/ml penicillin-streptomycin in a T175 flask, 37°C, 5% CO^2. Cells were grown to 70% confluency before being split or plated out. To harvest cells, the medium was removed, and cells were washed in PBS. 10% v/v Trypsin-EDTA in PBS was added, the flask was incubated for 5 minutes at 37^{o}C, then the trypsin was deactivated in PBS containing 10% v/v FCS. For experiments, cells were plated at 0.25 x 10^6 cells/ml.

2.1.5.10 Vero E6 cells

Vero E6 cells are epithelial-like kidney cells from the African green monkey. These cells were cultured in DMEM, supplemented with 8% v/v FCS (Bodinco), 2 mM L-glutamine, 100 IU/ml of penicillin, and 100 µg/ml of streptomycin (Sigma-Aldrich) at 37°C, 5% CO^2. For experiments, cells were plated at 5 x 10^4 cells/ml.

2.1.5.11 Vero-118 cells

Vero-118 cells are a sub-clone of Vero E6. The cells were cultured in Iscove's modified Dulbecco's medium (IMDM; Lonza) supplemented with 10% v/v FBS, 100 U/ml Pen-Strep-Glut mixture (Lonza) at 37°C, 5% CO^2. For experiments, cells were plated at 0.4 x 10^6 cells/ml.

2.1.5.12 Hela cells

Hela is an immortalized human cervical cancer cell line. Hela cells were cultured in DMEM supplemented with 10% v/v FCS and 20 µg/ml gentamicin at 37°C, 5% CO^2. For experiments, cells were plated at 0.5 x 10^6 cells/ml.

2.1.5.13 HAE cells

Primary human airway epithelial (HAE) cells were established at the Department of Pulmonology of the Leiden University Medical Center (LUMC) from tumour-free resected human bronchial tissue from patients undergoing resection surgery for lung cancer as previously described [183]. The cells were cultured in EMEM (Lonza) supplemented with 2% v/v FCS, and 25 mM HEPES (Lonza) at 37°C, 5% CO^2. For experiments, cells were plated at 0.25 x 10^6 cells/ml.

2.1.6 Viruses

Pandemic influenza A/H1N1 virus (isolate A/Netherlands/602/2009) and seasonal influenza A/NL/213/03 H3N2 virus (isolate A/Netherlands/213/2003) were generated as previously reported [184,185]. Recombinant influenza A/WSN/33 (H1N1) was generated as previously described [186]. SARS-CoV-2/Leiden-0002 (Genbank: MT510999.1) isolates were obtained from nasopharyngeal samples at the LUMC at the first wave of the pandemic.

2.1.7 Primers

Primers were designed in house and purchased from Eurofins Genomics.

Target	5′ – Primer	3′ – Primer
Ace2	GGTCTTCTGTCACCCGATTT	CATCCACCTCCACTTCTCTAA
Ace2 "relevant"	GTAACGGACCCAGGAAAT	CCATTGTCACCTTTGTGC
Isg20	AGGCTGTTGTGGCGTGAG	ATCGTTGCCCTCGCATCTTC
Rps13	TCACCGTTTGGCTCGATATT	GGCAGAGGCTGTAGATGATT
Crm1	GCACCTCTTGGACTGAATCG	AAGCGACAGCACAGACACAC
Ace2 (hamster)	GGGAACTGTCAAAGGGTACAG	CCCTTCCTACATCAGTCCTACT
Il-2 (hamster)	GTGCACCCACTTCAAGCTCTAA	AAGCTCCTGTAAGTCCAGCAGTAAC
Tnfa (hamster)	AGCTGGTTGTCTTTGAGAGACATG	GGAGTGGCTGAGCCATCGT
Ifng (hamster)	TTTCTCCATGCTGCTGTTGAA	GGCCATCCAGAGGAGCATAG
Il-6 (hamster)	GGTATGCTAAGGCACAGCACACT	CCTGAAAGCACTTGAAGAATTCC
E (SARS-CoV-2)	ACAGGTACGTTAATAGTTAATAGCGT	ATATTGCAGCAGTACGCACACA
RdRp (SARS-CoV-2)	GTGARATGGTCATGTGTGGCGG	CARATGTTAAASACACTATTAGCATA

Table 2.2: List of primers used in this project

2.1.8 Plasmids

Plasmid expressing Rev-GFP was generated and used as described before [187].

2.1.9 Antibodies

Target	Clone	Source
ACE2	5G3	Thermo Fisher
ACE2	polyclonal	Cell Signaling Technology
CRM1	D6V7N	Cell Signaling Technology
GAPDH	GA1R	Thermo Fisher
H3	D1H2	Cell Signaling Technology
Influenza A NP-FITC labelled	D67J	Life technologies
ISG15	22D2	Cell Signaling Technology
Lamin B1	119D5-F1	LifeSpan BioSciences
Mouse IgG (H+L)	Polyclonal	Jackson ImmunoResearch
Mouse IgG (H+L)-AF488 labelled	Polyclonal	Thermo Fisher
Mouse IgG2b-Alexa 594 labelled	Polyclonal	Thermo Fisher
Mouse immunoglobulins-HRP labelled	Polyclonal	Agilent technologies
IAV NP	D67J	Thermo Fisher
p53	polyclonal	Cell Signaling Technology
p65	D14E12	Cell Signaling Technology
Rabbit IgG (H+L)	Polyclonal	Jackson ImmunoResearch
STAT1	D1K9Y	Cell Signaling Technology
STAT1 (phospho)	58D6	Cell Signaling Technology
α-Tubulin	11H10	Cell Signaling Technology
β-actin	BA3R	Thermo Fisher

Table 2.3: List of antibodies used in western blotting and Confocal microscopy experiments

2.1.10 Stimulants

Stimulants and metabolites used in this project are listed in table 2. Itaconic acid was made to pH 7.4 before use.

Clone	Source
4-OI	R&D Systems and Merck
Actinomycin D	Merck
Itaconate	Merck
KPT-330	Selleck Chemicals
LPS	Enzo Life Sciences
Poly (I:C)	Invivogen
R848	Invivogen
IFN-α	Cell Signaling

Table 2.4: List of stimulants and reagents used throughout the project

2.1.11 Software

FlowJoTM v 10.7 (FlowJo) was used to analyse flow cytometry data. Graphpad Prism 8.0 (Graphpad) was used to format data and perform statistical analysis. Image Lab 6.1 (Bio-Rad) was used to analyse western blots. Biorender was used to create figures. Leica Application Suite X was used to analyse confocal microscopy images.

2.2 Methods

2.2.1 Assay for pseudo particle cell entry inhibition

Lentiviral pseudo particles expressing the SARS-CoV-2 spike and a firefly luciferase reporter gene were a gift from the Bowie lab and generated as previously described [188]. Calu-3 cells were seeded into a 96 well plate at 2.5 x 10^5 cells/ml, 125 µl per well and left to settle down over night. The cells were then treated with 4-OI or DMSO for 24 h, before removing the media and inoculating the cells with either spike bearing or control lentivirus for 48 h. The cells were then lysed in 50 µl passive lysis buffer (Promega) for 20 min at RT on a shaker. 20 µl the lysate was then transferred to a reading plate, mixed with 40 µl substrate solution and luciferase activity was measured on a luminometer immediately, using Ascent software (Thermo Fisher). The rate of ACE2 dependent viral uptake was assessed by comparing luciferase activity in cells infected with spike bearing vs non-spike bearing particles.

2.2.2 Cytopathic effect (CPE) reduction assay

Vero E6 cells were plated in 96-well clusters at a density of 5 × 10^3 cells/well in 100 µL. 24 h after seeding, the cells were incubated with indicated concentrations 4-OI for 1 hour. After that, half the cells were left uninfected or infected with SARS-CoV-2 at an MOI of 0.015. After three days, cell viability was measured by MTS assay using the CellTiter 96® AQueous MTS Reagent (Promega). MTS absorbance was measured at 495 nm with an EnVision multiplate reader (PerkinElmer).

2.2.3 Virus titration

Samples were titrated in quadruplicates in MDCK cells seeded in 96 well-plates. Cells were inoculated with 10-fold serial dilutions of the sample in serum-free cell culture EMEM medium with IAV A/H1N1, A/H3N2, or A/WSN/33 virus, in the presence or absence of 0.7 μg/ml TPCK trypsin (Merck, T1426), respectively. Three days post inoculation, supernatants of infected cell cultures were tested for agglutination using turkey erythrocytes, with observed hemagglutination in the presence of the virus in the supernatant. Endpoint infectious viral titre ($TCID_{50}$/ml) was calculated from quadruplicates for each individual sample using the Spearman-Karber method.

2.2.4 Western Blotting

For western blot analysis, cells were washed with PBS and lysed in sample lysis buffer. The lysate was then heated to 95^{o}C for 5 minutes to denature the proteins. Protein samples were stored at -20^{o}C until further use. The samples were resolved on 8 or 12 w/v % sodium dodecyl sulphate-polyacrylamide gel electrophoresis (SDS-PAGE) gels on the Bio-Rad Mini Protean III electrophoresis system, and run at 80 V for 15 min, and then 120 V for approximately 1:30 h. Proteins were transferred onto a methanol activated Polyvinylidene difluoride (PVDF) membrane using the BioRad wet transfer system. The transfer was run at 200 mA per box for 2 hours, or at 40 mA overnight. The compositions of the gels used are laid out in table 2.5.

Reagent	8% Resolving Gel	12% Resolving Gel	Stacking Gel
dH2O	3.5ml	2.5ml	2ml
30% Acrylamide Mix	2ml	3ml	0.5ml
Tris-HCl pH 6.8 [1M]	-	-	375µl
Tris-HCl pH 8.8 [1.5M]	1.9ml	1.9ml	-
10% SDS	75µl	75µl	30µl
10% APS	75µl	75µl	30µl
TEMED	3µl	3µl	3µl

Table 2.5: Table 2: Composition of gels used for SDS PAGE

After the transfer, membranes were blocked with 5% w/v milk and 0.1% v/v Tween-20 in TBS for 1 h at room temperature, washed, and incubated with the appropriate antibodies in 5% w/v BSA in TBS with 0.1% v/v Tween-20 overnight at 4°C. All primary antibody incubations were followed by incubation with secondary horseradish peroxidase (HRP)-conjugated antibody (Pierce) 1:2000, in 5% w/v milk and 0.1% v/v Tween-20 in TBS for 1 h, RT, and visualized using WesternBright enhanced chemiluminescent (ECL) Spray (Advansta) or FEMTO ECL (Thermo Fisher) on a ChemiDoc MP™ Imaging System (BioRad). Primary antibodies for western blotting and other antibodies used in this project are listed in table 2.3.

2.2.5 Flow Cytometry

After harvesting, cells were stained using 1:1000 Live/Dead Aqua viability dye (Thermo Fisher) in PBS for 10 min at RT prior to antibody staining. After washing, surface staining was performed in PBS + fluorescence labelled antibodies, for 30 min at 4°C. The surface staining cocktail also contained 1:300 anti-CD16/32 (Biozol) to block Fc-receptors. Surface staining was performed with the fluorophore-conjugated monoclonal antibodies anti-CD9 (eBioSN4 (SN4 C3-3A2)) and anti-CD81 (1D6-CD81) (Both Invitrogen). Cells were collected on LSR II and Fortessa flow cytometers (BD Biosciences) and analysed using FlowJo (TreeStar) software. As compensation controls, unstained cells, Live/Dead stained cells and fluorophore-coupled anti-rat beads (BD Biosciences) were used.

2.2.6 RT-qPCR

RNA extraction from cells was carried out using a RNA extraction kit (Applied Biosystems) according to the manufacturer's instructions. Isolated RNA was quantified using a NanoDrop 2000 spectrophotometer (Thermo Fisher), and RNA concentration was normalised to the lowest concentration across all samples with RNAse-free water. The RNA samples were converted into complementary DNA (cDNA) using the High-Capacity cDNA Reverse Transcription Kit (Applied Biosystems) according to manufacturer's instructions. Reverse transcription quantitative polymerase chain reaction (RT-qPCR) was performed in a 96 well qPCR plate by adding 4 µl cDNA to 6µl SYBR Green Master Mix (Applied Biosystems), and

run on a 7500 Fast Real-Time PCR machine (Applied Biosystems). A melt curve was generated for all primers which were run for the first time. Relative expression was calculated from the cycle threshold (CT) values for each sample and gene of interest. Primers were designed by us and purchased from Eurofins Genomics.

2.2.7 Confocal microscopy

For confocal microscopy, cells were plated on coverslips (collagen-coated for NuLi-1). After treatment, the coverslips were washed in PBS, and the cells were fixed in 2% PFA in PBS for 15 minutes at room temperature. The monolayer was again washed and either stored in PBS at 4°C overnight, or immediately permeabilized with 0.1 % v/v Triton X-100 made in PBS, for 15 min at room temperature. The cells were then blocked in 2% BSA in PBS for 45 min, and subsequently stained in PBS, 2% w/v BSA, containing 1:400 anti-CRM1, or anti-p65 (both Cell Signaling) for 1 h at room temperature. After another washing step in PBS, the cells were first incubated in PBS, 2% w/v BSA, containing 1:1000 Alexa Fluor 546 conjugated secondary antibody (Thermo Fisher) for 1 h, and then in PBS, 2% w/v BSA, containing 1:1000 4′,6-diamidino-2-phenylindole (DAPI) (Thermo Fisher). The coverslips were then first washed in PBS, then in dH_2O, and then adhered to glass slides with 2 - 3 µl ProLong™ Gold Antifade Mountant (Thermo Fisher) and stored horizontally at room temperature overnight in the dark. For storage up to several weeks, the slides were kept at 4°C. Pictures were taken on a Leica SP8 microscope (Leica Microsystems) and analysed by Leica Application Suite X.

2.2.8 Fusion assay

Vero118 cells were plated into 6 well plates on day 0 and transfected with either 0,2 µg/µl pCAGGs F HMPV NL/1/94, pCAGGs HA A/Neth/213/2003, or eGFP on day 1 using Xtremegene HP (Merck) in Optimem (Thermo Fisher) according to manufacturer's instructions. On day 2 the media was refreshed and the cells were treated with 4-OI if applicable. On day 3, the medium was replaced with IMDM (Stemcell technologies), containing 1% w/v Penicillin-Streptomycin-Glutamine (Gibco) containing 0.07% w/v trypsin (Gibco) for 1 h at 37°C, and subsequent incubated in PBS shock solution (PBS pH 5) for 10 min at RT. After washing in PBS the cells were again stored in normal IMDM (+ compound if applicable), and fixed in 80% acetone in PBS on day 4.

2.2.9 CRM1 activity assay

HeLa cells stably expressing the XPO1-dependent NLSSV40-AcGFP-NESPKI reporter were cultured as described previously [189]. To assess the CRM1-mediated nuclear export function, reporter cells were seeded at 8000 cells per well in 96-well tissue culture plates. The next day, cells were treated with a serial dilution of 4-OI or DMSO for 24 h, fixated and counterstained with DAPI. Fluorescence was imaged on an ArrayScan XTI High Content Reader (Thermo Fisher). Nuclear and cytoplasmic compartments were segmented and their average pixel intensities in the green channel were quantitated employing the HCS Studio software (Thermo Fisher). GraphPad Prism was used for dose-response curve fitting based on the percentage of

cells having a predominant nuclear localisation of the reporter construct. A ratio of nuclear to cytoplasmic signal equal or above 1.4 was considered predominantly nuclear. Representative images were taken by confocal microscopy on a Leica TCS SP5 confocal microscope (Leica Microsystems).

2.2.10 Quantitative profiling of 4-OI modified cysteinome in THP-1 cells

THP-1 cells were seeded into 6 cm petri dish (4 million per dish) in 5 ml media, and treated with DMSO, 125μM OI or 250 μM 4-OI, respectively, for 16 hours at 37°C, 5% CO^2. 10 dishes of cells were treated (4 dishes with DMSO, 3 dishes with 125 μM and 3 dishes with 250 μM 4-OI) in each replicate experiment for utilizing TMT-10plex isobaric label reagent. Cells were harvested and washed with PBS twice. Each cell pellet was lysed on ice with 100 μL of 0.5% v/v 3-((3-cholamidopropyl) dimethylammonio)-1-propanesulfonate (CHAPS) buffer containing 1x EDTA-free Pierce Halt™ protease inhibitor cocktail and 1x benzonase for 30 min. Lysate was collected by centrifugation (20,000 g, 15 min) at 4 ℃ to remove debris. Protein concentration was determined by BCA protein assay kit. Lysate (0.4 mg from each dish, 4mg/ml) was incubated with 500 μM of IA-DTB for 1 hour, followed by 5 mM DTT for 30 min, and 20 mM iodoacetamide for 30 min at RT in the dark. The resulting lysate was precipitated by 400 μL methanol, 100 μL chloroform, and 300 μL water. The precipitated protein was centrifuged at 4000 x g for 10 min at 4 ℃, washed twice with 500 μl methanol with sonicating briefly each time to break up the protein pellet. Washed protein pellet was resuspend in 200 μL of 0.2 M EPPS buffer (pH 8.5) with

brief sonication and digested with 8 µg of trypsin/Lys-C overnight at 37 ℃ shaking at 500 rpm. TMT-10plex reagents (0.8 mg in each reagent) were resuspended in dry acetonitrile, added to the digested samples, and incubated for 1 hr at room temperature with shaking at 500 rpm. Afterwards, the TMT labelling reaction was terminated by adding 50% v/v hydroxylamine (0.3% final concentration) to the mixture and incubate for 15 min. The labelled peptide samples were dried in speedvac. 600 µl of 50% streptavidin resin slurry was washed with 10 ml PBS three times. Dried peptides were resuspended in 1 ml PBS and pooled together to incubate with the streptavidin resin overnight at 4 ℃. Resin was washed three times each with PBS, followed by PBS containing 0.1% SDS, and water to remove non-specific binding peptides from the resin. Resin-bound peptides were eluted by incubating the resin with 500 µl of elution buffer (50% v/v acetonitrile + 0.1% w/v TFA) in a thermomixer shaking at 1000 rpm for 10 min. Resin was centrifuged to collect supernatant. Repeat elution with 200 µl of elution buffer and combined supernatant was dried in speedvac. The dried peptide was resuspended in 300 µL 0.1% w/v TFA and subjected to Pierce High pH Reversed-Phase Peptide Fractionation Kit following manufacturer's protocol.

Fractionated peptides were reconstituted in 20 µl 0.1% v/v formic acid. Samples were then analysed by LC-MS/MS on a Fusion Lumos mass spectrometry. Around 0.5 µg of total peptides from each fraction were analysed on an UltiMate 3000 nano-LC system (Thermo Fisher) coupled via a 25 cm C18 column (EASY-Spray, Thermo Fisher). Peptides were separated at a flow rate of 250 nl/min with a linear 110 min gradient from 2% to 35% solvent B (100% acetonitrile, 0.1% formic acid). Each sample was run for 120 min, including sample loading and column equilibrating

times. Data were acquired in data-dependent mode. MS1 spectra were measured with a resolution of 120,000, an automatic gain control target of 4 x 10^5, maximum injection time 50 ms, and a mass range from 300 to 1800 m/z. MS2 spectra were collected using top-speed mass spec method within 3 s of cycle time at a resolution of 50,000, an automatic gain control target of 8 x 10^5, an isolation window of 1.0 m/z and a normalized collision energy of 38.

All raw data were analysed with MaxQuant software version 1.6.15.0. Spectral searches were performed using 10plex TMT as the isobaric labels. Carbamidomethylation of cysteine residues was set as fixed modification, while oxidation of methionine residues, acetylation of protein N-term and IA-DTB on cysteine residues were set as variable modifications. Competition ratio was calculated by dividing the TMT reporter ion intensities from control channel (DMSO) by the 4-OI treated channel.

2.2.11 Cellular Fractionation

Cells were harvested and 10 % of the cell suspension was isolated as total faction and processed as in the Western Blotting protocol. To separate nuclear and cytoplasmic fractions of harvested cells, NP-40 cell lysis buffer (Invitrogen) was used according to manufacturer's instructions. The lysates were assayed by Western Blotting together with the Total fraction.

2.2.12 Co-immunoprecipitation

Nuli-1 cells were seeded in 10 cm dishes the day prior to treatment. The following day, cells were treated as required. Following treatment, cells were washed with 3 ml PBS before lysis in 500 µL low stringency lysis buffer on ice. Plates were scraped with a cell scraper and lysate transferred into microcentrifuge tubes. Tubes were agitated at 1100 rpm at 4°C for 15 mins before being centrifuged at 21380 x g for 10 mins at 4°C. 50 µl of resulting supernatant was mixed with 50 µl sample lysis buffer and treated as the whole cell lysate (WCL) sample. 4 µg anti-CRM1 antibody or the equivalent concentration of rabbit IgG antibody, and 40 µl A/G PLUS agarose beads were added to the remaining supernatant, which was subsequently incubated at 4°C in a ferris wheel mixer for 3 hrs. IP samples were subsequently centrifuged at 400 x g for 2 mins at 4°C, supernatant was removed, and the beads washed three times with 1 ml low stringency lysis buffer. The immune complexes were eluted by addition of 40 µl sample lysis buffer, boiled at 95°C for 5 mins and analysed by SDS-PAGE.

2.2.13 PBMC isolation

10 ml human blood was diluted 1:1 in PBS and layered over 10 ml lymphoprep (Stemcell Technologies) using a Pasteur pipette in a 50 ml tube. The tube was then centrifuged at 400 x g for 30 mins with the brake off, after which the upper plasma layer was discarded. The cells at the plasma-density gradient medium interface were retained, and 20 ml PBS was added to this in a new 50 ml tube. The tube was centrifuged for 8 mins at 300 x g and the supernatant was removed and discarded.

The remaining pellet of mononuclear cells was resuspended, counted and plated at 1 x 10^6 cells/ml in RPMI supplemented with 10% v/v FCS and 100 U/ml penicillin/streptomycin at 37°C, 5% CO^2.

2.2.14 LDH release assay

The CytoTox 96 Non-Radioactive Cytotoxicity Assay (Promega) was used to quantify lactate dehydrogenase (LDH) release from cells as a measure of cell death in Jurkat WT and $XPO1^{C528S}$ cells following 4-OI treatment. Freshly harvested supernatants were used in this assay. 50 µl of each supernatant was added to 50 µl CytoTox 96 Reagent and incubated at RT in the dark for 30 mins. 50 µl acetic acid was added to stop the reaction, and absorbance at 492 nm was measured using a FLUOstar OPTIMA plate reader (BMG LabTech). As a positive control for maximum LDH release, 100 µl total lysis solution was added to untreated cells 30 mins before harvesting. Medium alone was also used to correct for background absorbance.

2.2.15 Statistical analysis

Details of all statistical analyses performed can be found in the figure legends. p-values were determined using unpaired Student's t-test for pairwise comparison of variables and one-way ANOVA for multiple comparison of variables. Differences were considered statistically significant when $p<0,05$ (*$p<0,05$, **$p<0,01$, ***$p<0,001$, ****$p<0,0001$). Data are shown as mean ± SEM unless otherwise stated. Sample sizes were determined based on previous experiments using similar methodologies. All

depicted data points are biological replicates taken from distinct samples with n = the number of animals or the number of independent experiments with cell lines. Statistics were calculated using GraphPad Prism 9 software.

Chapter 3: 4-OI is an antiviral agent in SARS-CoV-2 infection

3.1 4-OI is antiviral against SARS-CoV-2

3.1.1 4-OI decreases SARS-CoV-2 induced cell death and restricts replication *in vitro*

Itaconate and its cell permeable derivative 4-OI have been shown to exhibit antiviral properties in various studies. In light of the ongoing COVID-19 pandemic, I sought to investigate potential antiviral properties of these molecules in context of a SARS-CoV-2 infection. Since Trinity College Dublin (TCD) was at the time (March 2020) unable to work on SARS-CoV-2, I established a collaboration with Dr. Martijn van Hemert from Leiden University Medical Center, an expert in coronavirus research who had all tools available from the start of the pandemic. Experiments using the live virus were conducted in his lab, with me acting in an advisory role using my background in metabolism.

First, cell viability was assessed in VeroE6 cells infected with SARS-CoV-2. Here, the virus caused over 60 % cell death, while pre-treatment with 4-OI was able to fully prevent any cytotoxicity induced by the virus from concentrations as low as 50 μM (Fig. 3.1 A). It is noteworthy that higher concentrations of 4-OI resulted in viability levels above 100 %, which can possibly be explained by increased proliferation. Itaconate however was not able to prevent SARS-CoV-2 induced toxicity before becoming toxic itself (Fig. 3.1 B). Next, overall toxicity of 4-OI was evaluated in human airway epithelial (HAE) cells. Concentrations of up to 150 μM imposed no toxicity in these cells when treated for up to 72 h (Fig. 3.1 C).

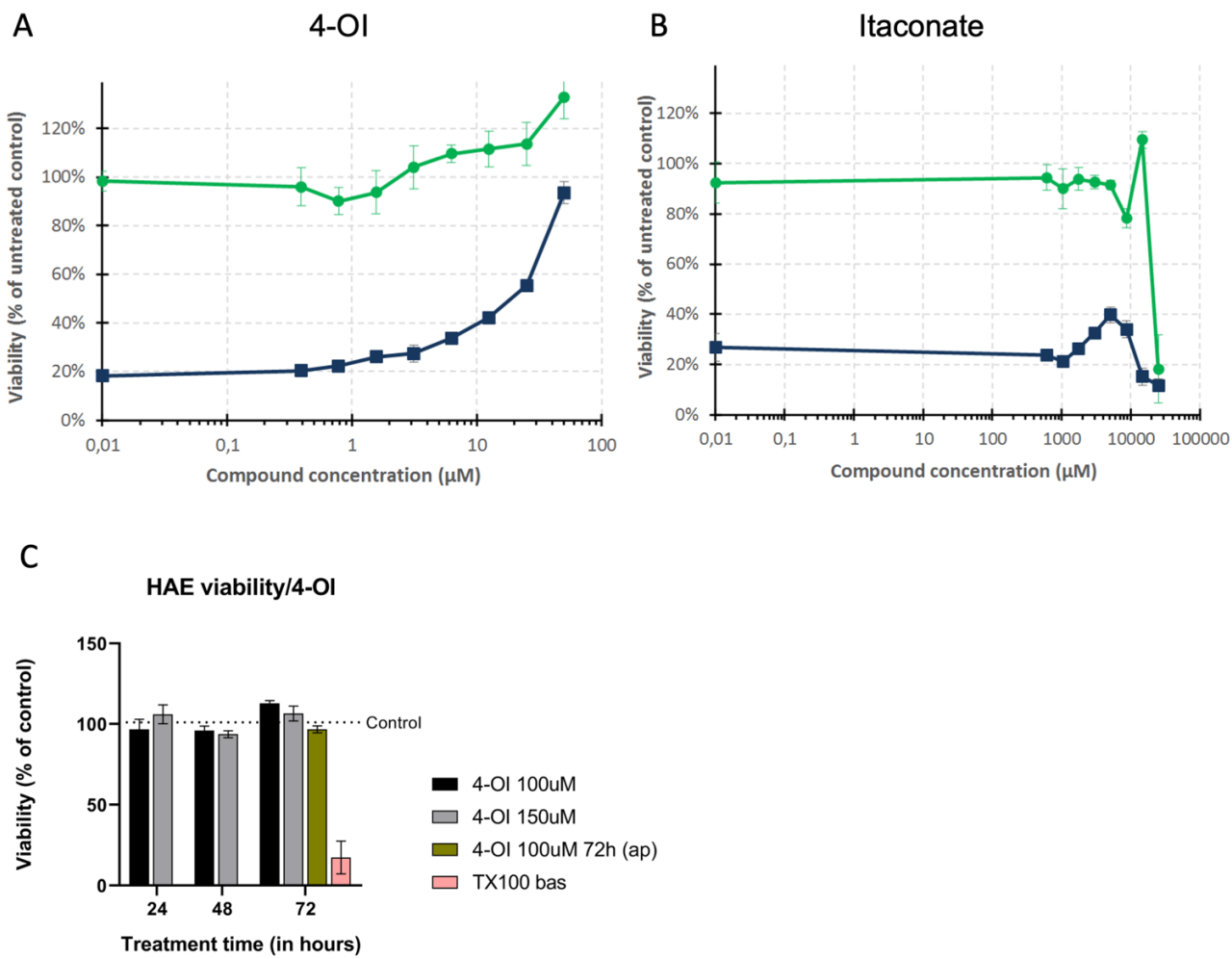


Figure 3.1: 4-OI reduces SARS-CoV-2 induced pathology.

(A - B) CPE reduction assay of cells infected with SARS-CoV-2. Vero E6 cells (1x10^4 cells) were treated with indicated concentrations of 4-OI (A), or itaconate (B) for 2 h, and subsequently infected with SARS-CoV-2 at an MOI of 0.015 (blue line) or left uninfected (green line). Cell viability was determined by MTS cell viability assay 72 h post-infection. **(C)** HAE cells (1x10^4 cells) were treated with 100 or 150 µM 4OI, TX100 bas or vehicle for indicated timepoints. Cells viability was assessed by MTS cell viability assay. Data in A and B are representative of 3 individual experiments and depicted as mean ± SD for n=3. Data in C are mean ± SEM for n=3 Experiments were carried out by Clarisse Salgado-Benvindo.

Whether this reduction in cell death could also be explained by reduced viral replication as previously described for other viruses for the itaconate metabolite family [177], was next investigated. Indeed, increasing concentrations of 4-OI were able to significantly reduce levels of viral RNA-dependent RNA polymerase (RdRP) and envelope (E) mRNA detected in infected cells in both cell lysate and supernatant of Calu-3 cells (Fig. 3.2 A), which was reflected by reduced levels of shed viable virus, as indicated by plaque assay (Fig. 3.2 B). The observation of this antiviral effect was subsequently confirmed in HAE cells, where viral titres were decreased in cells pre-treated with 4-OI (Fig 3.2 C). These results were subsequently confirmed by Olagnier et al., shortly after, proposing 4-OI induced activation of NRF2 to be the mechanism of the antiviral effect observed [179].

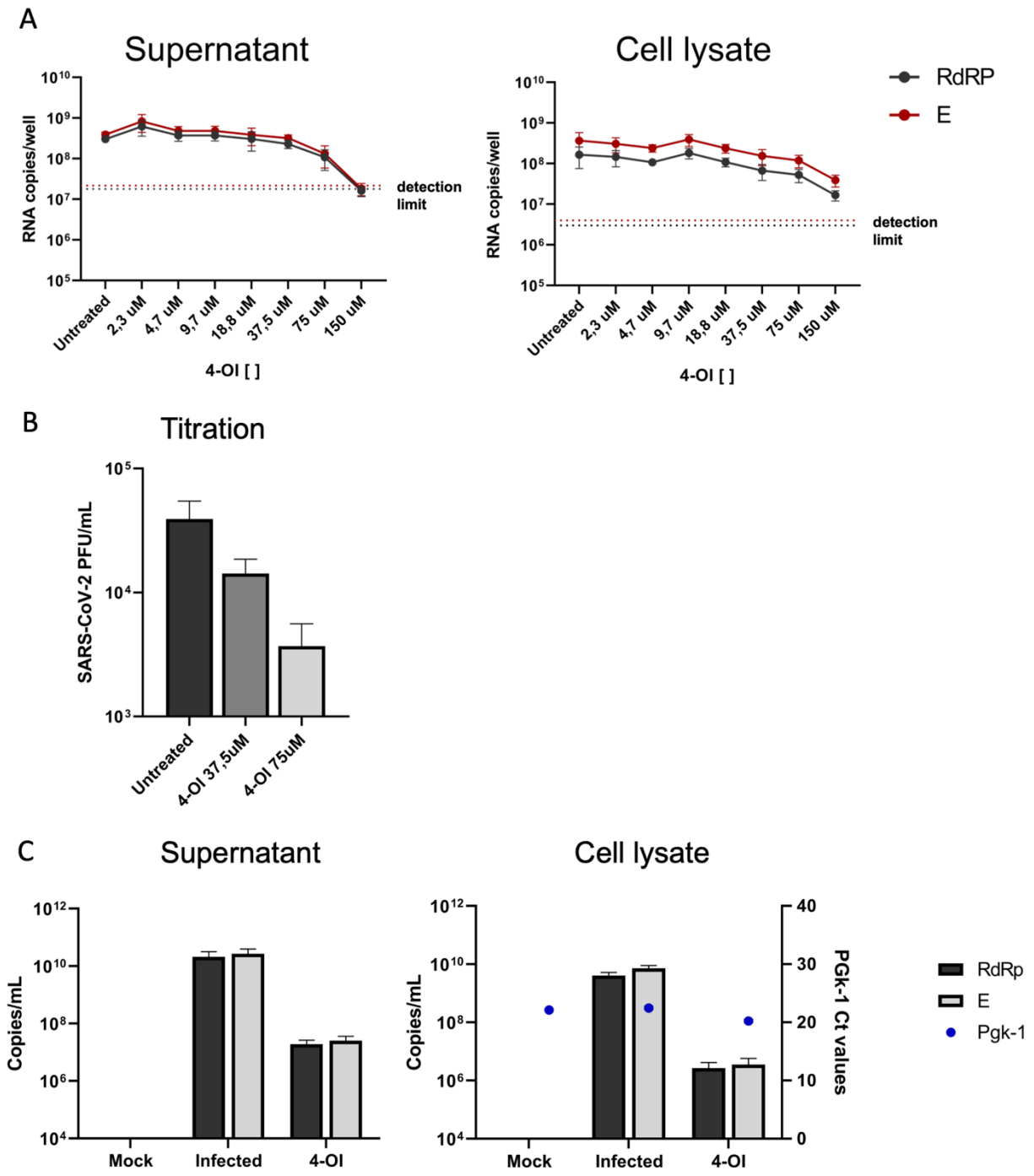


Figure 3.2: 4-OI restricts replication of SARS-CoV-2.

(A) Calu-3 cells (4 x 10^4 cells) were treated with indicated concentrations of 4-OI 4 h prior to infection with SARS-CoV-2. Levels of viral RNA in cell lysate and supernatant were assessed by qPCR 16 h post inoculation. **(B)** Plaque assay analysis of Calu-3 cells (4 x 10^4 cells) treated with either 4-OI or vehicle at indicated concentrations 4 h before infection with SARS-CoV-2. Depicted are bar graphs representing the amount of infectious particles detected in the supernatant 16 h post inoculation. **(C)** (4 x 10^4 cells) HAE cells were treated with either 150 µM 4-OI or vehicle 40 h before, and 2 h after infection with SARS-CoV-2. Presence of viral RNA in cell lysate and supernatant was assessed by qPCR 72 h post inoculation, in addition to expression of host Pgk-1 in the cell lysate. Data are mean ± SD for n=3. Experiments were carried out by Clarisse Salgado-Benvindo.

3.1.2 4-OI decreases SARS-CoV-2 induced pathology and restricts replication *in vivo*

Whether this protective effect would translate *in vivo* was investigated next. Still unable to perform meaningful experiments with the live virus in TCD, I started a collaboration with Hendrik Jan Thibaut at KU Leuven. He had a hamster model of SARS-CoV-2 infection running and shipped us samples from the animals after trialling 4-OI in his system.

Hamsters were IP injected with 50 mg/kg 4-OI prior to infection with SARS-CoV-2 and both viral titres and pathology were assessed four days post infection. In the lung of these animals, 4-OI was able to reduce SARS-CoV-2-induced pathology. Lung histology scores of 4-OI treated animals remained below those of uninfected animals (Fig. 3.3 A). In the lung, expression of selected pro-inflammatory cytokines was also assessed. As seen in figure 3.3 B, 4-OI significantly reduced expression of SARS-CoV-2 induced IL-2 and TNF-α, while reductions in IL-6 and IFN-ɣ were not significant but noticeable.

Viral titres were also measured in infected animals. Again, as in the *in vitro* experiments, 4-OI was able to reduce viral titres. Lungs harvested from animals that were treated with 4-OI contained less virus than animals that were left untreated (Fig. 3.4). Overall therefore, 4-OI can restrict SARS-CoV-2 replication, which was not only manifested in decreased viral replication, but also in reduced virus-induced inflammation and pathology.

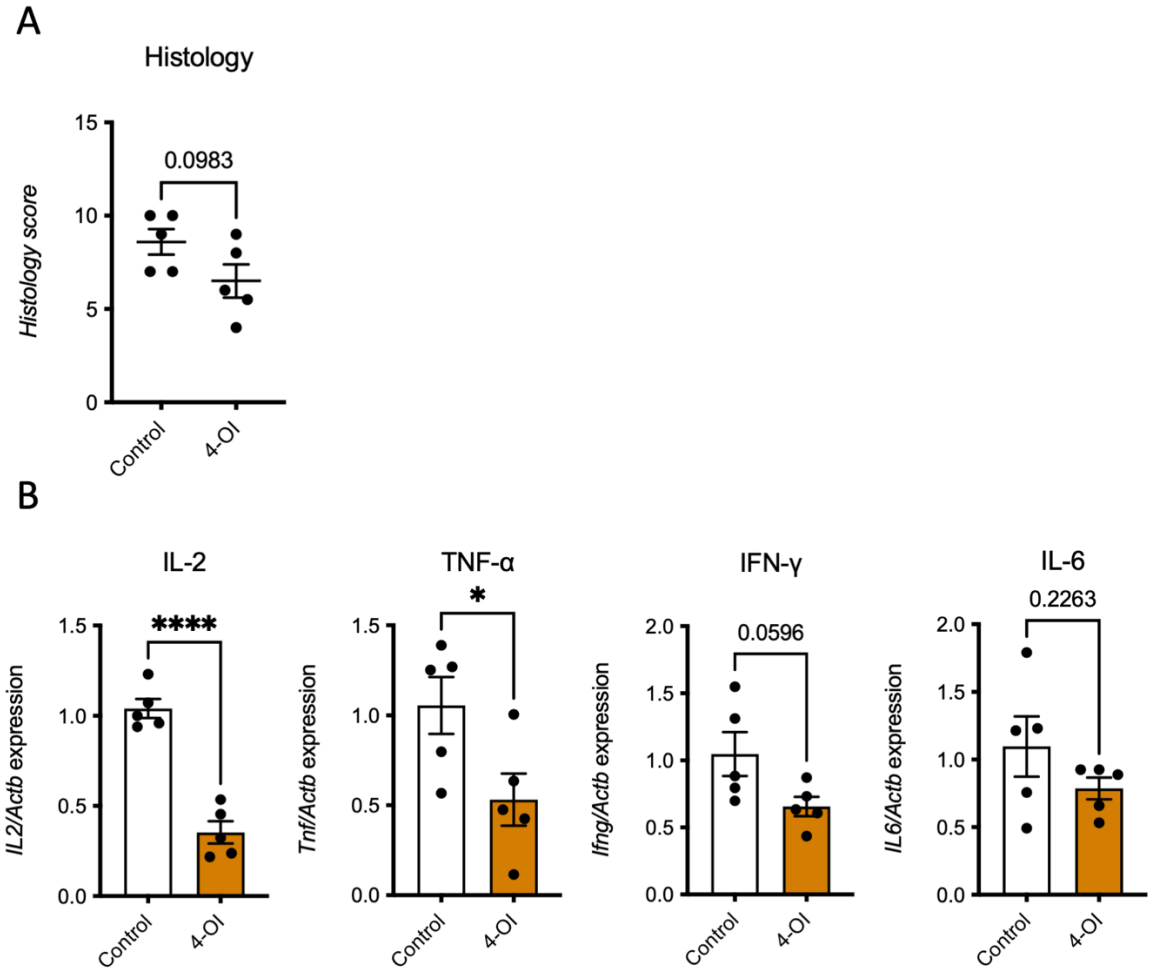


Figure 3.3: 4-OI reduces SARS-CoV-2 induced pathology *in vivo*.

(A) Hamsters were IP injected daily with either 50mg/kg 4-OI or vehicle, starting 2 days prior to intranasal infection (or starting on the day of infection) with SARS-CoV-2 at a $TCDI_{50}$ of 2 x 10^6. On day 4, the hamsters were sacrificed and lung pathology was assessed by histology scoring. **(B)** qPCR analysis of lung samples from the hamsters in (A). Depicted is the expression of various pro-inflammatory cytokines. The experiment was carried out once. Data are mean ± SD for n=5. *p<0.05, ****p<0.0001, as calculated using an unpaired student's t-test. Animal work and histology scoring was done by Laurens Liesenborghs, qPCR and data analysis by me.

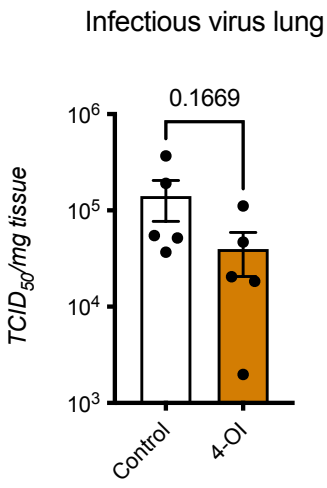


Figure 3.4: 4-OI restricts replication of SARS-CoV-2 *in vivo*.

Hamsters were IP injected daily with either 50mg/kg 4-OI or vehicle, starting 2 days prior to intranasal infection with SARS-CoV-2 at a $TCDI_{50}$ of 2 x 10^6. The hamsters were sacrificed on day 4 and viral load in the lungs was assessed by plaque assay. The experiment was carried out once. Data are mean ± SD for n=5. P value was calculated using an unpaired student's t-test. Animal work and plaque assay were done by Laurens Liesenborghs.

3.2 4-OI reduces ACE2 induced uptake of SARS-CoV-2

3.2.1 ACE2 expression is decreased with 4-OI *in vitro*

The uptake receptor for SARS-CoV-2, ACE2, is at least partly induced by interferon signalling [57], despite some variants potentially not being relevant for viral uptake [190]. As 4-OI can potently block IFN responses [191], whether 4-OI can impact expression levels of ACE2 through this pathway was next explored, expanding the search for a mechanism of the antiviral effect observed.

To verify the IFN dependency of ACE2 expression, an antibody to block IFNAR was used before treating Nuli-1 cells with TLR3 agonist Poly (I:C) and TLR7/8 agonist R848. Indeed, Poly (I:C) induced expression of ACE2 alongside ISG20, which could at least in part be attenuated by blocking IFNAR (Fig. 3.5A). Residual induction of ACE2 could be due to other transcription factors downstream of TLR3, such as IRF3 and NF-κB. Pre-treatment with 4-OI decreased Poly (I:C) induced expression of both ISG20 and ACE2, while R848 did not induce either (Fig. 3.5B). Western Blotting was then used to investigate whether these changes in expression resulted in altered protein levels and signalling. As shown in figure 3.5 C, Poly (I:C) induced phosphorylation of STAT1 (lane 3 compared to 1, third panel), which was blocked with 4-OI (lane 4). Both ISG15 (second panel) and ACE2 (top panel) were increased in expression (lane 3 compared to 1), which was blocked by 4-OI (lane 4). Interestingly, ACE2 protein levels were also increased after R848 treatment (lane 5), with 4-OI blocking induction here as well (lane 6). Also, basal ACE2 expression levels were slightly decreased as well with 4-OI (lane 2 compared to 1). As it later emerged that only particular transcript variants of ACE2 might be responsible for viral uptake [192], the expression for that

particular variant was also determined. Primers used in previous panels would pick up all isoforms of ACE2, potentially including variants that are incapable of binding the SARS-CoV-2 spike.

As shown in figure 3.5 D, the expression pattern of the "relevant" variant matched the previous data, with Poly (I:C) induced expression ACE2 being blocked by 4-OI. The commonly used lung epithelial cell line A549 was next examined. As A549 cells have reduced expression of TLR3, the receptor for Poly (I:C), and TLR7/8 are not expressed at all [193], the cells were co-treated with IFN-α to induce TLR3 expression and increase Poly (I:C) mediated responses. As shown in figure 3.6 A, again, Poly (I:C) was able to induce ACE2 expression, which was blocked by 4-OI. ACE2 induction however was much lower than in Nuli-1 cells.

To asses ACE2 protein levels, IFN-α in combination with Poly (I:C) treatment was again used. In figure 3.6 B, IFN-α on its own induced some STAT1 phosphorylation (panel 3, lane 3) compared to non-stimulated (lane 1), and could be slightly reduced by 4-OI treatment (lane 4). As expected, Poly (I:C) treatment induced strong phosphorylation of STAT1 (lane 5), which was potently blocked by 4-OI (lane 6). Expression of ISG15 was increased after IFN-α treatment (second panel, lane 3), and combined treatment of IFN-α and Poly(I:C) (lane 5), compared to unstimulated cells (lane 1). Treatment with 4-OI after stimulation (lanes 4 and 6) potently reduced ISG15 expression. ACE2 expression (top panel) followed the same pattern, although basal expression (lane 1) could already be reduced slightly by 4-OI (lane 2). Again, IFN-α (lane 3), and the combination of IFN-α and Poly(I:C) (lane 5) increased ACE2 expression, with the latter being more potent. 4-OI reduced expression of induced ACE2 (lanes 4 and 6).

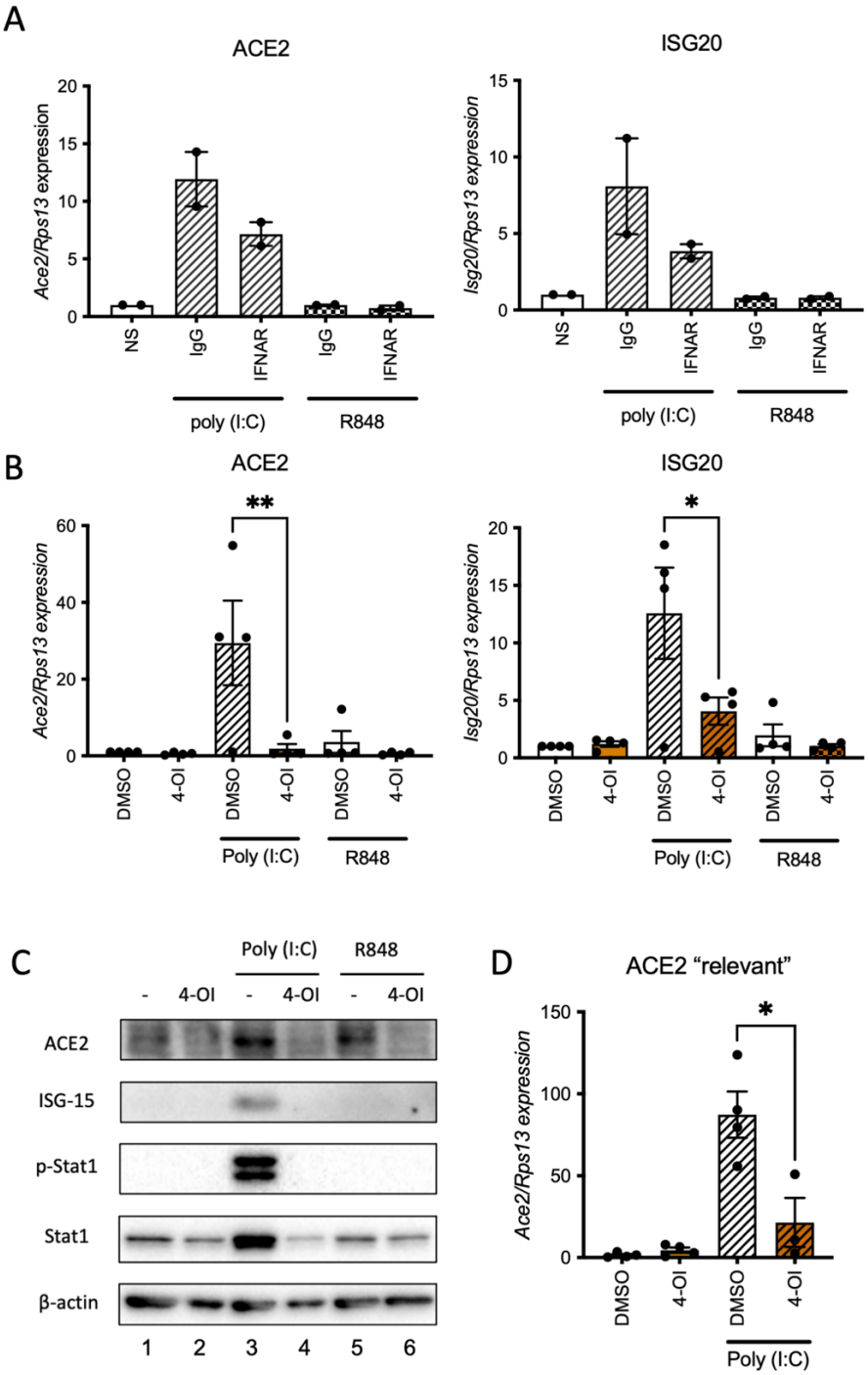


Figure 3.5: 4-OI decreases ACE2 expression in Nuli-1 cells.

(A) qPCR analysis of NuLi-1 cells (2.5 x 10^5 cells) pre-treated with IFNAR blocking antibodies or IgG for 1 h, followed by 20 µg/ml Poly (I:C) or 10 µg/ml R848. **(B-C)** NuLi-1 cells (2.5 x 10^5 cells) were pre-treated with 250 µM 4-OI or vehicle for 3 h, followed by either 20 µg/ml Poly (I:C) or 10 µg/ml R848 for 16 h. qPCR results of expression changes in ISG20 and ACE2 are shown in B, western blotting of proteins harvested from these cells are shown in C. **(D)** NuLi-1 cells (2.5 x 10^5 cells) were pre-treated with 250 µM 4-OI or vehicle for 3 h, followed by 20 µg/ml Poly (I:C) for 16 h. Depicted is qPCR analysis of the uptake-relevant splice variant of ACE2. Data are mean ± SEM for n=4 (B and D) or N=2 (A) *p<0.05, **p<0.01, as calculated using a one-way ANOVA followed by Sidak's multiple comparisons test. Blots are representative of 3 individual experiments. Some replicates of the qPCR experiments were done in collaboration with Alexander Hooftman.

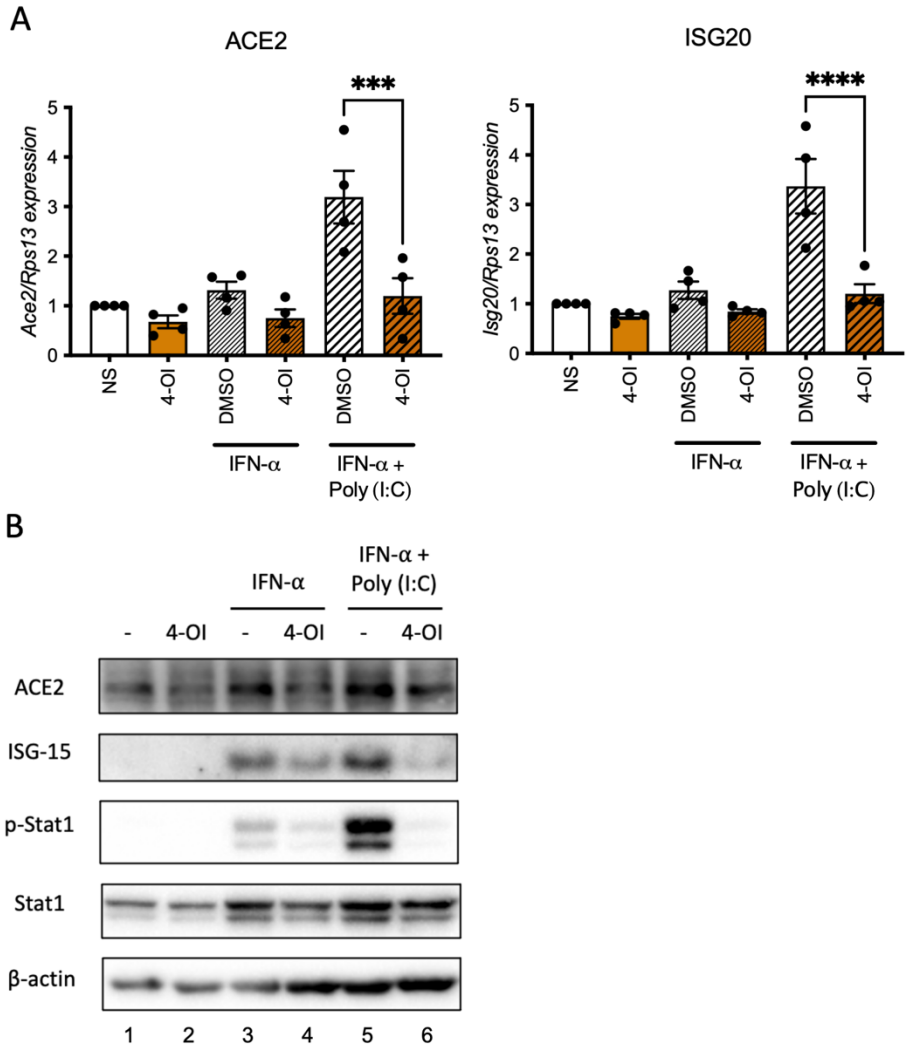


Figure 3.6: 4-OI decreases ACE2 expression in A549 cells.

(A-B) A549 cells (2.5 x 10^5 cells) were pre-treated with 250 µM 4-OI or vehicle for 3 h, followed by either 10 ng/ml IFN-α, or 10 ng/ml IFN-α + 20 µg/ml Poly I:C for 16 h. qPCR results of expression changes in ISG20 and ACE2 are shown in A, western blotting of proteins harvested from these cells are shown in B. Data are mean ± SEM for n=4. ***p<0.001, ****p<0.0001 as calculated using a one-way ANOVA followed by Sidak's multiple comparisons test. Blots are representative of 3 individual experiments.

3.2.2 ACE2 expression is decreased with 4-OI *in vivo*

Whether a decrease of ACE2 expression could also be observed in vivo was next examined. This part was again done in collaboration with Hendrik Jan Thibaut, who kindly isolated and shipped samples from his SARS-CoV-2 hamster model. RNA was isolated from the lungs of infected hamsters that were either treated with 4-OI or vehicle compound. Figure 3.7 shows that animals that were treated with 4-OI had an about 50 % reduction in ACE2 expression, reflecting the results obtained *in vitro*.

3.2.3 Exogenous itaconate increases ACE2 expression

Being a derivative of itaconate, 4-OI is used predominantly to mimic intracellular itaconate. Endogenous itaconate however cannot be assessed easily as cells that express ACE2 do not produce itaconate. For that reason exogenous itaconate was tested.

Interestingly, experiments using itaconic acid instead of 4-OI yielded different results. In contrast to 4-OI, itaconic acid increased basal protein levels of both ISG15 (top panel) and ACE2 (middle panel) in A549 cells (lane 2 compared with 1) (Fig. 3.8 A). As shown in figure 3.8 B, in Nuli-1 cells, itaconate slightly boosted Poly (I:C) induced ACE2 expression (top panel, lane 4 compared to 3). Examining mRNA expression in figure 3.8 C, itaconate was able to increase Poly (I:C) induced ACE2 expression as well. This would be in line with recent discoveries of unmodified itaconate being able to induce IFNAR dependent signalling events [166]. Itaconate itself was therefore unlikely to be antiviral here.

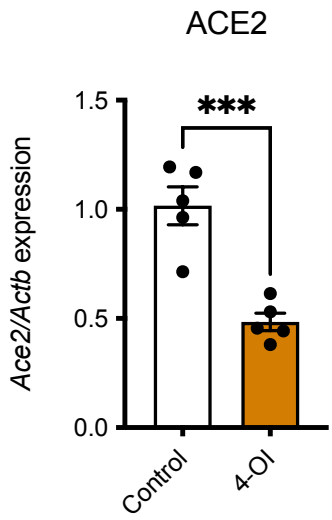


Figure 3.7: 4-OI decreases ACE2 expression *in vivo*.

Hamsters were IP injected daily with either 50mg/kg 4OI or vehicle, starting on the day of infection with SARS-CoV-2 at a $TCDI_{50}$ of 2×10^6. On day 4, the hamsters were sacrificed and ACE2 expression in the lung was assessed by qPCR. This experiment was carried out once. Data are mean ± SD for n=5. ***p<0.001 as calculated using unpaired Student's t-test. Animal work and histology scoring was done by Laurens Liesenborghs, qPCR and data analysis by me.

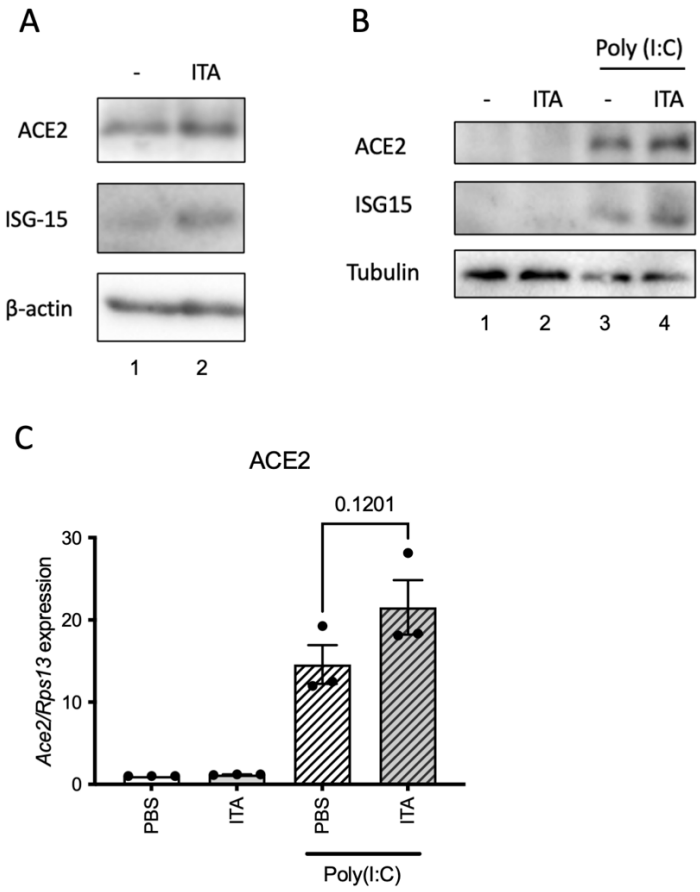


Figure 3.8: Itaconate might slightly increase expression of ACE2 in epithelial cells.

(A) A549 cells (2.5 x 10^5 cells) were pre-treated with either 10 mM itaconic acid or vehicle for 3 h, before being treated with 10 ng/ml IFN-α or being left untreated. **(B)** Nuli-1 cells (2.5 x 10^5 cells) were treated with 15 mM itaconate or vehicle for 3 h prior to treatment with 20 µg/ml Poly (I:C) for 18 h. **(C)** qPCR analysis of NuLi-1 cells (2.5 x 10^5 cells) pre-treated with either 10 mM itaconic acid or vehicle for 3 h, before being treated with 20 µg/ml Poly (I:C) or being left untreated. qPCR data are mean ± SEM for n=3. P value was calculated using a one-way ANOVA followed by Sidak's multiple comparisons test. Blots are representative of 2 individual experiments.

3.2.4 4-OI is unable to counter overexpression of ACE2 in HEK cells

The next step was to investigate whether the observed reduction of ACE2 expression with 4-OI translated into a decreased uptake of the virus and if this could contribute to the mechanism of the antiviral effect observed for SARS-CoV-2. A model using a pseudo particle expressing the spike protein from SARS-CoV-2 on its surface was used. These pseudo particles express a firefly luciferase reporter gene, so successful uptake of the particle could be determined by luciferase assay. The cells used in previous experiments, A549 and Nuli-1, however did not express sufficient levels of basal ACE2 to be potently infected with the particle. ACE2-overexpressing HEK cells were tested first. As somewhat expected, treatment of these HEK-Blue™ hACE2 cells with Poly(I:C) did not induce ACE2 expression (Fig. 3.9 A, top panel, lane 1 compared to 4). Furthermore, 4-OI did not decrease ACE2 protein levels (lane 1 compared to 2 and 3, and lane 4 compared to 5 and 6). As shown in figure 3.9 B, ACE2 mRNA levels were also assessed in these cells, reflecting the Western Blotting results as Poly (I:C) did not induce increased expression of ACE2, and 4-OI was unable to reduce expression, suggesting that 4-OI interferes with the natural induction pathway of this receptor rather than blocking it on the RNA or protein level. Assessing uptake in these cells would make little sense if reduction of ACE2 is considered as a mechanism.

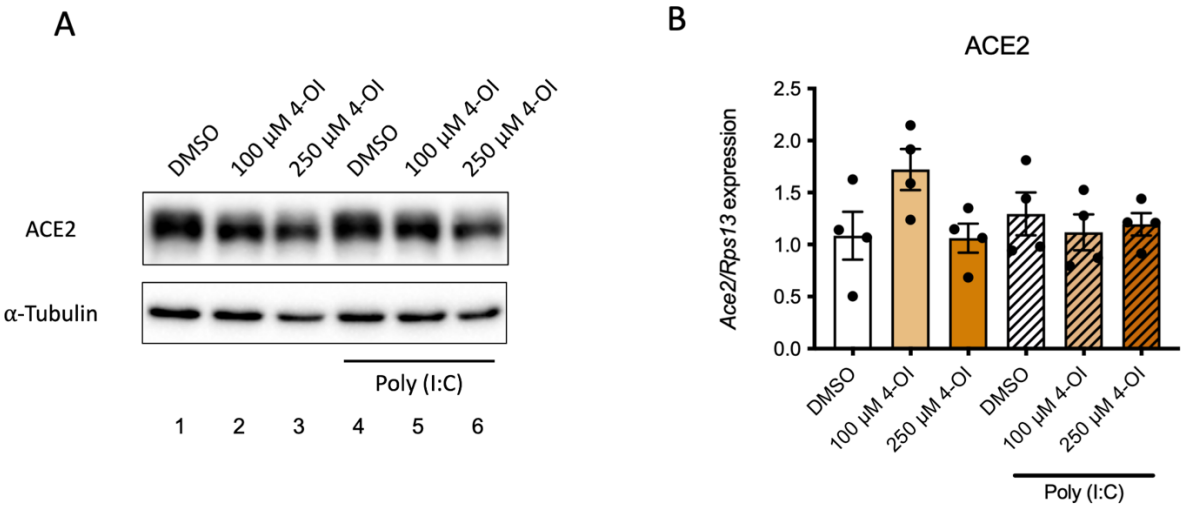


Figure 3.9: 4-OI does not reduce ACE2 expression in HEK-Blue™ hACE2 Cells.

(A-B) HEK-Blue™ hACE2 cells (2.5 x 10^5 cells) were treated with indicated concentrations of 4-OI or DMSO for 3 h prior to treatment with 20 µg/ml Poly (I:C) for 16 h. ACE2 protein levels were assessed by western blotting (A) and mRNA expression by qPCR (B). Blots are representative of 2 individual experiments. Data are mean ± SEM for n=4.

3.2.5 4-OI reduces ACE2 dependent uptake of spike expressing particles

Calu-3 cells, another bronchial epithelial cell line that we used earlier to demonstrate the antiviral capacity of 4-OI in this virus, were therefore tested in the uptake assay. These cells express sufficient levels of ACE2 to facilitate uptake of both the live virus as well as the spike-bearing pseudo particle.

As shown in figure 3.10 A, qPCR analysis revealed that unlike in A549 and Nuli-1 cells, Poly (I:C) was not able to induce ACE2 expression. 4-OI was however able to decrease basal levels of ACE2 mRNA. ACE2 protein levels in these cells reflected these results (Fig. 3.10 B). Poly (I:C) was not able to increase ACE2 expression (upper panel, lane 1 vs lane 4), while 4-OI reduced ACE2 protein levels in absence (lanes 2 and 3 compared to 1), or presence of Poly (I:C) (lanes 5 and 6 compared to 4).

Given these results, an uptake assay in these cells was preferred, comparing the uptake of the spike bearing particle to uptake of a particle without spike to determine an uptake rate and rule out non-ACE2 dependent uptake. Pre-treatment with 4-OI did result in decreased uptake of the particle (Fig. 3.10 C), suggesting that reduced ACE2 expression could be part of the antiviral mechanism of 4-OI in SARS-CoV-2.

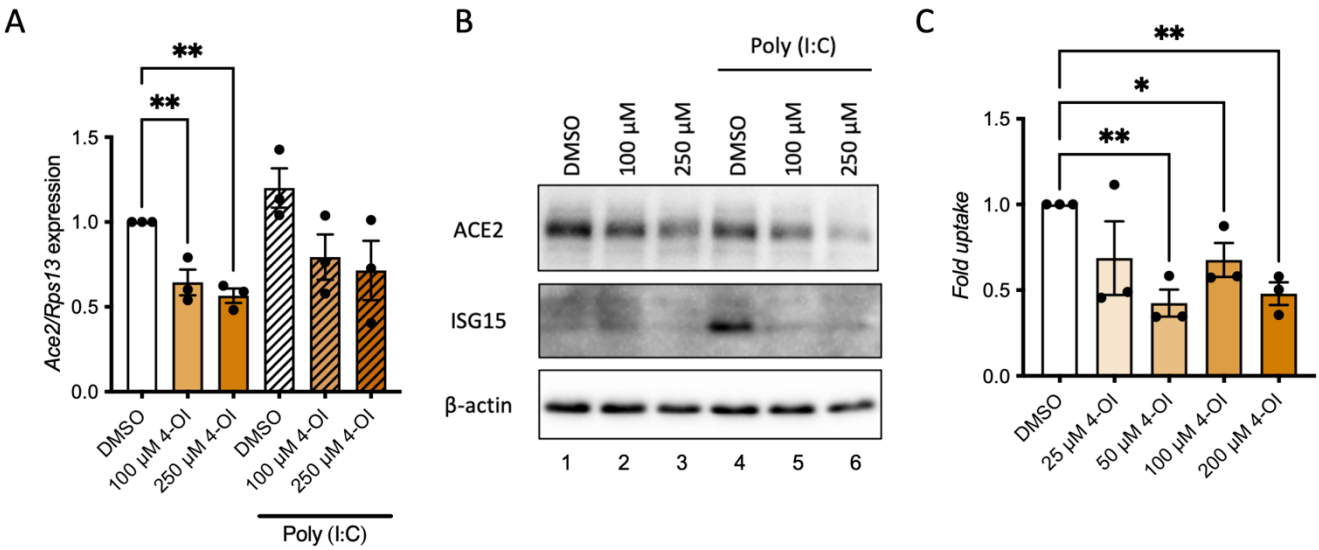


Figure 3.10: 4-OI reduces ACE2 dependent viral uptake in Calu-3 cells.

(A-B) Calu-3 cells (1.5 x 10^5 cells) were pre-treated with 100 or 250 µM 4-OI or vehicle for 3 h, before being treated with 1 µg/ml Poly I:C or being left untreated. qPCR results of expression changes in ISG20 and ACE2 are shown in A, western blotting of proteins harvested from these cells are shown in B. **(C)** Calu-3 cells (2.5 x 10^4 cells) were treated with indicated concentrations of 4-OI for 24 h, and inoculated with spike expressing lentivirus for 48 h. Viral uptake was determined by luciferase assay and spike dependent uptake was calculated comparing uptake of spike-, vs. non-spike-bearing particle. Data was normalized to uptake ratio after DMSO treatment. Data are mean ± SEM for n=3. *p<0.05, **p<0.01, as calculated using a one-way ANOVA followed by Sidak's multiple comparisons test. Blots are representative of 3 individual experiments.

3.3 Discussion

The devastating effect the COVID-19 pandemic had on the world needs no introduction. The outbreak significantly increased and sped up our efforts to examine a role for itaconate and its derivatives in COVID-19. The antiviral potential of itaconate in SARS-CoV-2 was first tested with collaborators, followed by an investigation into possible mechanisms, with a focus on ACE2.

3.3.1 4-OI is antiviral in SARS-CoV-2

At the beginning of the pandemic we began collaborating with the lab of Martijn van Hemert at Leiden University Medical Center with whom we uncovered antiviral properties of 4-OI in SARS-CoV-2 infections. The results that have been observed agreed with publications suggesting antiviral properties of itaconate derivatives [177,180,194]. The results of our collaborators were confirmed after by Olagnier et al., expanding the antiviral effect to more viruses and suggesting an NRF2 dependent mechanism [179]. Importantly, itaconate itself did not show any effects, highlighting the differences between 4-OI and itaconate in some models. We were also able to expand the observations *in vivo* using hamster models of SARS-CoV-2 infection to confirm the antiviral and anti-inflammatory potential of this metabolite, blocking both infection and inflammation at the same time, collaborating with the lab of Hendrik Jan Thibaut, who conducted the animal work.

It is this "dual effect" approach that makes the itaconate family such interesting candidates for use in infectious diseases. I will explore this potential in more detail in chapter 5.

3.3.2 ACE2, 4-OI and interferons

Mechanistically, I was building on previous data from our lab, implementing 4-OI into IFN signalling. Itaconate and its derivatives had been shown to alkylate and deactivate JAK1, a crucial part of the IFNAR signalling pathway, effectively blocking the induction of IFN-induced genes [160]. Since, at the time, expression of the receptor for SARS-CoV-2 uptake, ACE2 was proposed to be IFN dependent [57], and 4-OI blocked IFN signalling, I hypothesized that 4-OI might reduce viral uptake. This concept is illustrated in figure 3.11, although different variants of ACE2 exist, not all of which can bind the virus. In particular IFN-induced variants did not seem to contribute to SARS-CoV-2 uptake, as they are often truncated, lacking the spike binding domain [192]. Interestingly, this splice variant was induced by Poly (I:C) as well, despite originally being described as not being IFN dependent. A reduction in expression of the "relevant" form was however also shown, as well as basal levels of ACE2, and importantly, 4-OI actually caused reduced ACE2 dependent viral uptake.

Here, a previously suggested link between Nrf2 and the antiviral function of 4-OI could also be a possibility, as Nrf2 deficiency had previously been associated with overexpression of ACE2 [195]. This possibility has indeed already been suggested elsewhere [196].

The impact on basal ACE2 expression by 4-OI is difficult to discuss, as many factors play into the regulation of ACE2. One factor that has been shown to upregulate ACE2 is Hepatocyte Nuclear Factor 1α (HNF-1α) [197], however this research was conducted before the pandemic and involvement in viral uptake is unknown. More recently, STAT3 was found to be a transcription factor upregulating ACE2 expression, and as STAT3 inhibition resulted in reduced SARS-CoV-2 uptake, it can be assumed that the variant induced by STAT3 is fully functional [198]. As JAK1 is involved in STAT3 mediated signalling [199], and 4-OI can inhibit JAK1 [160], this might be a potential mechanism through which 4-OI can regulate expression of uptake relevant ACE2 splice variants and SARS-CoV-2 uptake itself. Furthermore, TLR3 activation can induce production of IL-6, which can activate STAT3 through IL-6R in an autocrine manner [200], possibly explaining induction of the "relevant" variant of ACE2 observed with Poly (I:C). These possibilities are summarized in figure 3.11.

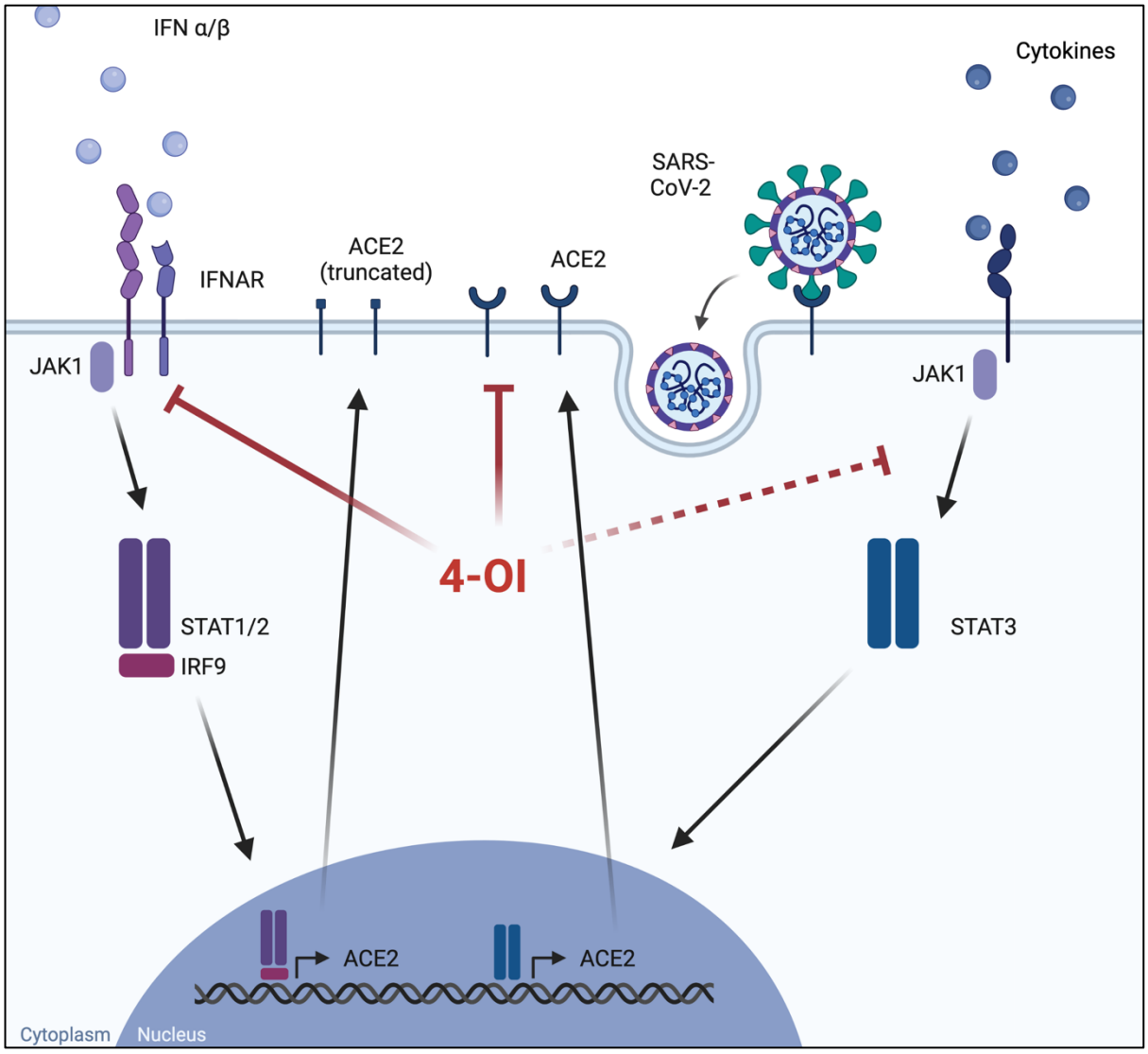


Figure 3.11: 4-OI decreases ACE2 expression.

Internalization of SARS-CoV-2 relies on the expression of its uptake receptor ACE2. The data in this thesis suggests 4-OI can inhibit IFNAR dependent induction of truncated ACE2 by inhibiting JAK1, while also reducing basal ACE2 expression IFN independent. Additionally, 4-OI can possibly inhibit STAT3 induced expression of functional ACE2 through JAK1 inhibition. This reduction of surface ACE2 expression could lead to reduced uptake of the virus.

3.3.4 4-OI versus itaconate in ACE2 expression

Interesting in this regard is also the divergence between 4-OI and exogenous itaconate. While unmodified itaconate had been shown to suppress replication of Zika virus [177], this was not the case for SARS-CoV-2. It is however noteworthy that as itaconate production is restricted to myeloid cells, assessment of the role of endogenous itaconate proved difficult in SARS-CoV-2 infection models. An antiviral function of exogenous itaconate in SARS-CoV-2 could also not be confirmed. Considering my hypothesis on uptake reduction this is not surprising, as itaconate did not decrease, but if anything increased expression of ACE2. Mechanistically, this could be partly explained by the diverging functions of itaconate and 4-OI in IFN signalling. While 4-OI clearly inhibits expression of [201], as well as responses to type I IFNs [160], the function of itaconate in this regard is debated.

While itaconate has been shown to also decrease IFN mediated responses [168], it has also been shown to boost type I IFN mediated signalling events, which could explain increased expression of ISGs, such as certain ACE2 splice variants, as shown in this work. Similarly controversial is where this divergence might stem from. 4-OI was originally generated as a tool to study endogenous itaconate, as exogenous itaconate was deemed chemically unfit to spontaneously cross the cell membrane. While it has since been shown that itaconate does in fact cross the cell membrane in some instances [166], it is still unknown how the transport is facilitated. As it may require active transport through transporters, itaconate uptake could be highly cell-type specific. I have not confirmed whether exogenous itaconate is actually taken up in the epithelial cell types used in this work. Another explanation for differences

between itaconate and 4-OI is receptor mediated signalling. Metabolites have been shown to bind receptors on the cell surface, such as GPR91 (succinate) [202], GPR81 (lactate) [203], or GPR43 (SCFA) [204], and it is likely that itaconate binds one or multiple receptors as well. Due to the structural similarity to succinate, GPR91 would be a suitable candidate. In fact, preliminary data from our lab has shown that itaconate can induce similar signalling events as those found downstream of GPR91 such as cyclic AMP response element-binding protein (CREB) phosphorylation [205]. As 4-OI readily diffuses through the cell membrane, it might be less prone to receptor binding.

On the other hand, 4-OI and itaconate might also have different functions intracellularly, as it has been debated whether 4-OI actually does get converted into itaconate upon entry, or if it gets metabolized differently [161,166]. Additionally, itaconate derivatives such as 4-OI have been found to be more electrophilic than itaconate itself and therefore are more cysteine reactive than the unmodified metabolite [166]. While 4-OI is still an important tool to study itaconate, the above factors may explain some of the differences we have observed between itaconate and 4-OI in regard to their role in ACE2 expression and as an antiviral in general. Overall however, since itaconate can induce type I IFNs, it should have an antiviral effect.

3.3.5 An alternative mechanism?

Recent data from our lab has opened up room for speculation on a secondary mechanism through which 4-OI could be antiviral in SARS-CoV-2, tying it into the data from the next chapter of this work. 4-OI can inactivate the nuclear exporter CRM1, trapping cargos such as IAV NP, p65 and p53 in the nucleus. Another natural

cargo of CRM1 is ACE2, and CRM1 inhibitors such as KPT-330 have been shown to be antiviral in SARS-CoV-2 by trapping ACE2 in the nucleus, thereby reducing surface level expression of the receptor and ultimately reducing uptake of the virus [131]. Preliminary data (not shown in this thesis) suggests that, as with KPT-330, 4-OI treatment leads to ACE2 accumulation in the nucleus. While it does not explain downregulation of ACE2 expression by 4-OI, it could explain disturbed surface expression of ACE2 and reduced viral uptake with 4-OI. More experiments will be conducted to explore this hypothesis. The concept is visualized in figure 3.12.

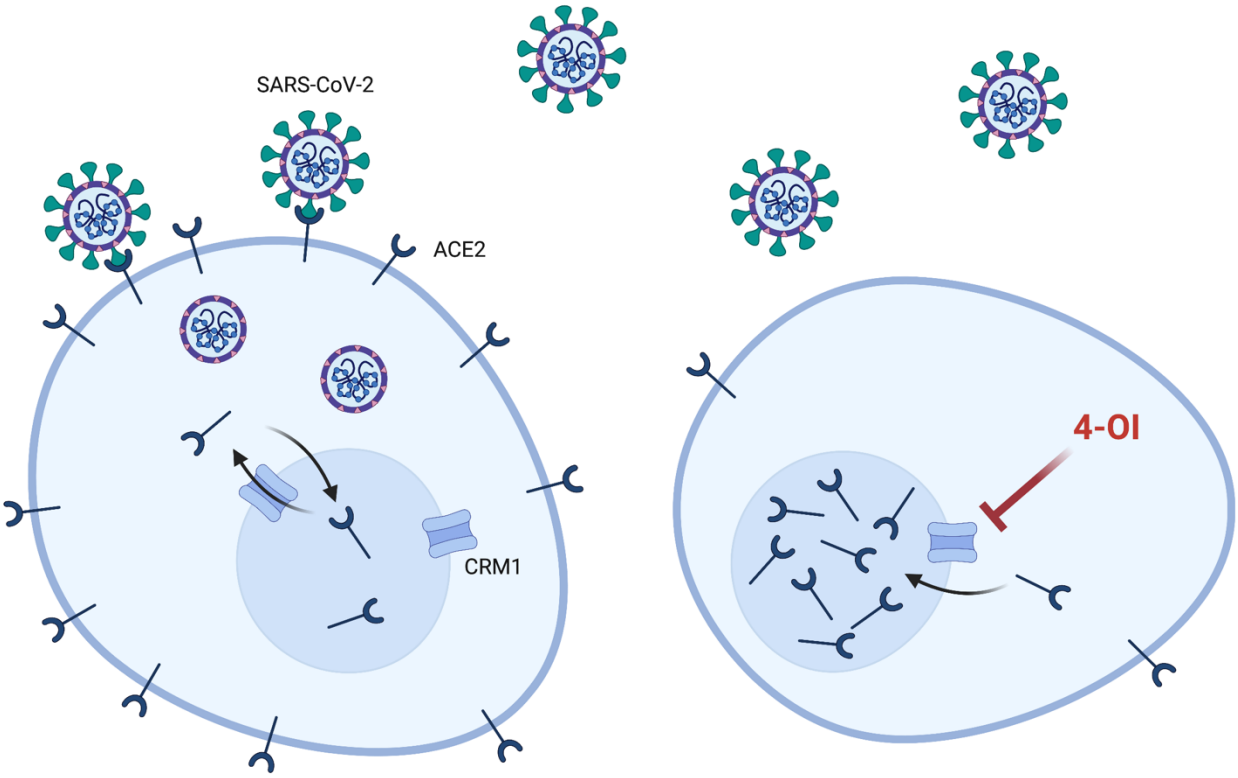


Figure 3.12: 4-OI might trap ACE2 in the nucleus.
Alternative hypothesis on how 4-OI could restrict uptake of SARS-CoV-2. Inhibition of the nuclear exporter CRM1 has been shown to retain ACE2 in the nucleus, thereby limiting availability of the receptor on the cell surface for SARS-CoV-2.

Chapter 4: 4-Octyl itaconate reduces IAV replication by targeting the nuclear export protein CRM1

4.1 4-OI is antiviral in Influenza

4.1.1 Itaconate and 4-OI are not antiviral in HMPV

Inhibition of ACE2 might be an important part of the anti-viral effect of 4-OI. The results from Olagnier et al. proposed NRF2 activation as another aspect through which 4-OI exerts its antiviral properties [179], painting 4-OI as a broad antiviral agent. Of course inhibition of ACE2 would not account for antiviral effects in viruses other than SARS-CoV-2, which is why I next set out to identify more viruses that could be inhibited by 4-OI, and potentially identify a mechanism. This project started out as a collaboration between me and Pau Ribo Molina at Erasmus MC Rotterdam in the lab of Bernadette van den Hoogen.

Another respiratory RNA virus was next assessed, human metapneumovirus (HMPV). Neither 4-OI, nor itaconate treatment resulted in decreased viral load after hMPV infection with in A549 cells (Fig. 4.1 A) or Vero118 cells (Fig. 4.1 B) in the timeframe from 2 h until 72 h post infection. A single, preliminary experiment (not shown) was conducted on respiratory syncytial virus (RSV), measles morbillivirus (MeV), herpes simplex virus (HSV), or parainfluenza virus (PIV) in A549 cells 48 h post infection. None of the results indicated an antiviral potential of 4-OI in any of the above viruses, despite published antiviral effects of 4-OI in HSV [179].

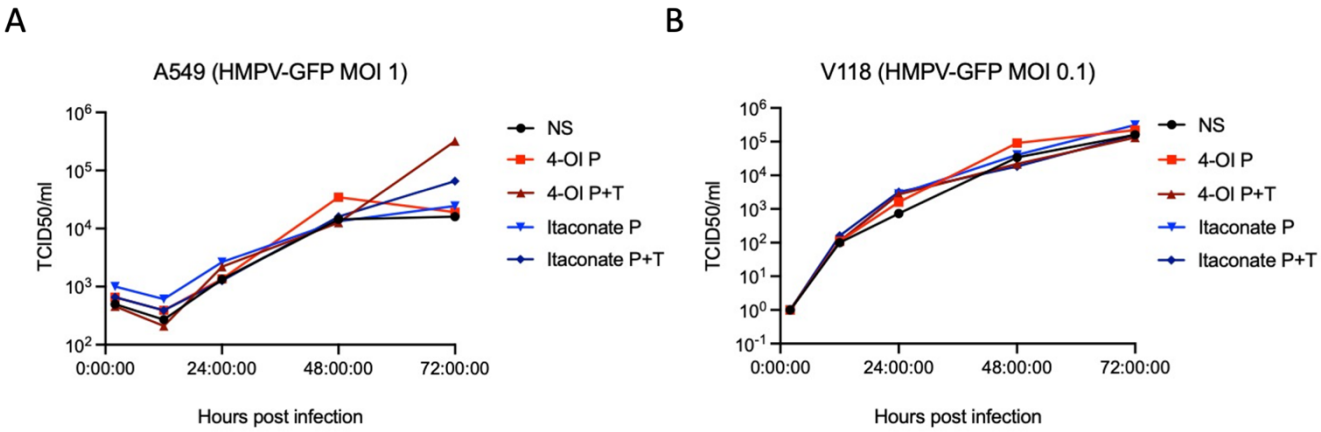


Figure 4.1: 4-OI is not antiviral in hMPV.

(A-B) A549 (A) and Vero118 (B) cells (2.5 x 10^5 cells) were treated with 10 mM itaconic acid or 100 μM 4-OI for 48 h, inoculated with hMPV for 2 h, and then either treated again with 10 mM itaconic acid or 100 μM 4-OI or left untreated (NS). P indicates pre-treatment condition, while P+T indicates pre- plus post-treatment conditions. Plaque assay was performed to determine the viral concentration in the supernatant at the indicated timepoints. Data are representative of 3 individual experiments.

4.1.2 Influenza replication is restricted by 4-OI but not by itaconate

In yet another respiratory virus, IAV, however, a combination of pre-treatment, and post-infection treatment with 4-OI resulted in decreased viral titre of the WSN/33 strain in MDCK cells when treated with 100 μM, but not 10 μM 4-OI, as indicated by qPCR of the supernatant collected from the cells (Fig. 4.2 A). Plaque assay of the same supernatant showed a non-significant decrease in viral titres with 10 μM 4-OI, and a significant decrease in viral load with 100 μM 4-OI (Fig. 4.2 B). Itaconate had no effect on viral load in either assay at 1 or 10 mM (Fig. 4.2 A-B). To assess the effect in more detail, a dose response was carried out with 4-OI in both MDCK and A549 cells. As shown in figure 4.2 C, in MDCKs the antiviral effect became evident from concentrations as low as 6.25 μM, whereas in A549s concentrations above 100 μM were required to achieve antiviral potency (Fig. 4.2 D). The concentrations used were not toxic in the respective cell types (Fig. 4.2 C-D, grey line).

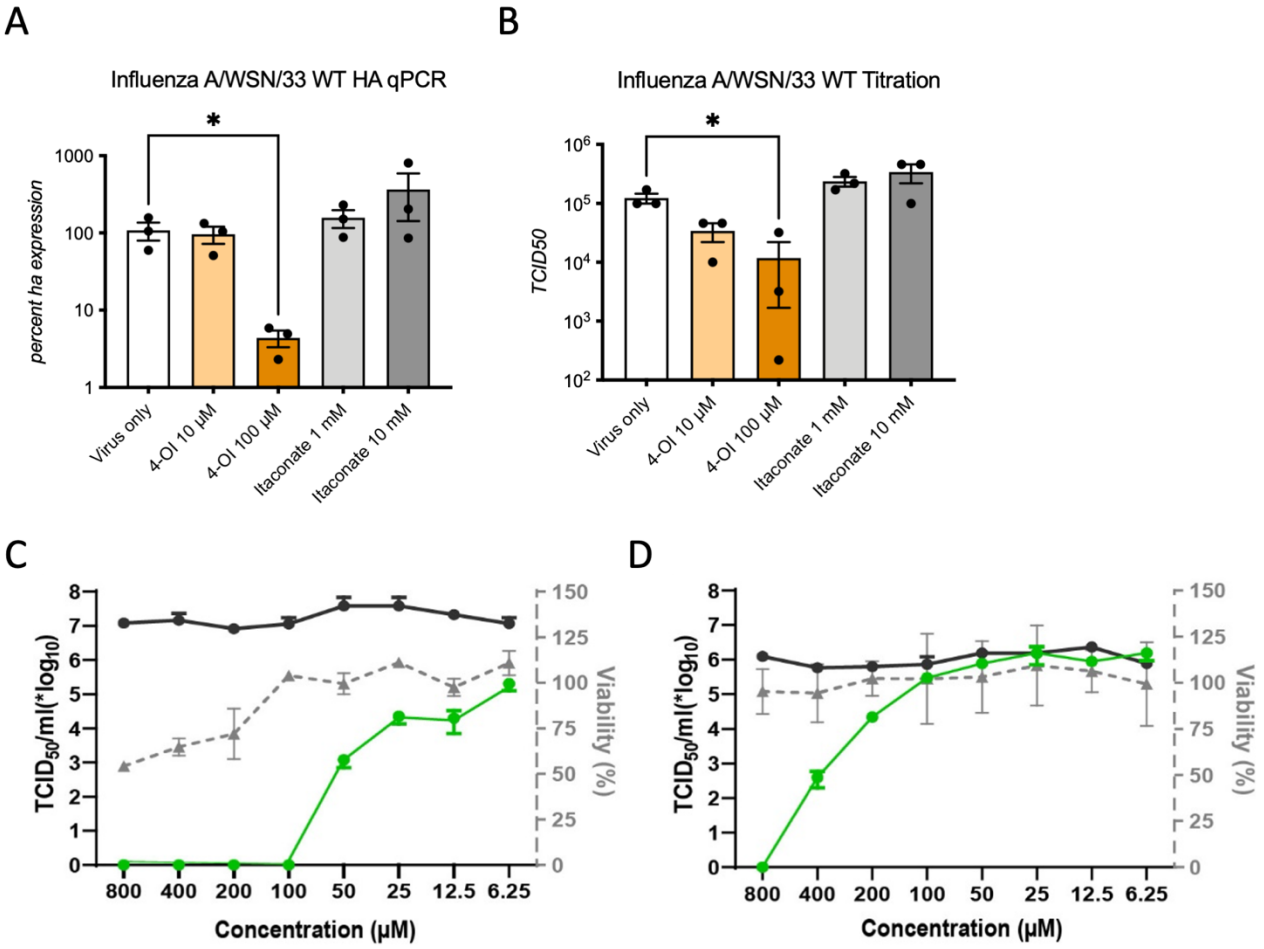


Figure 4.2: 4-OI decreases IAV replication.

(A-B) MDCK cells (2 x 10^5 cells) were treated with itaconic acid or 4-OI for 48 h, inoculated with IAV for 2 h, and treated again with 10 mM itaconic acid or 100 µM 4-OI for 48 h. qPCR (A) and titration (B) were performed with the supernatant. **(C-D)** Dose-dependent effect of 4-OI (green line) compared to DMSO (black line) on virus titres (left Y axis) at 48 h post inoculation in MDCK (B, MOI 0.01) (2. x 10^5 cells) and A549 (C, MOI 0.1) cells (2.5 x 10^5 cells), with corresponding Live/Dead staining of 4-OI treated cells normalized to DMSO measured using flow cytometry (grey dotted line, Right Y-axis). Data are mean ± SEM for n=3. *$p<0.05$, as calculated using a one-way ANOVA followed by Sidak's multiple comparisons test. This work was done in collaboration with Pau Ribo Molina.

Next, the replication kinetics of IAV WSN/33 in A549 and MDCK cells were investigated. In both cell lines 4-OI, but not itaconate had a profound impact on viral replication, resulting in decreased viral titers in most timepoints sampled. The reduction was noticably stronger in MDCK cells (Fig. 4.3 A) compared to A549 cells (Fig. 4.3 B) which is not surprising given they responded better to 4-OI in previous experiments. As IAV WSN/33 is a lab adapted Influenza A H1N1 strain isolated in 1933 [206], other, more recently circulating IAV strains were investigated, namely IAV A/NL/602/09 H1N1, and the A/NL/213/03 H3N2 strains, that circulated in the Netherlands in 2009 and 2003 respectively. Figure 4.3 C-D shows that, again, replication was slowed down with a combination of pre- and post-treatment of 100 μM 4-OI from as early as 8 h post infection, but not with itaconate.

4.1.3 4-OI does not impair IAV membrane fusion

To examine the antiviral mechanism, features that distinguish Influenza from other RNA viruses were assessed, first focussing on viral entry. A fusion assay was performed to assess whether this process was affected by 4-OI (Fig. 4.4). The cells used in the assay express a viral fusion protein on their surface. A low PH thereby triggers fusion of the cellular membranes, resulting in visible dark cell clusters indicated by red arrows. No changes in fusion capacity of the HMPV F protein (middle row) or IAV HA protein (right row) after 4-OI treatment were shown. Vero118 cells transfected with plasmids expressing the respective fusion protein fused regardless of treatment, suggesting 4-OI does not impair fusion of the virus with the host cellular membrane.

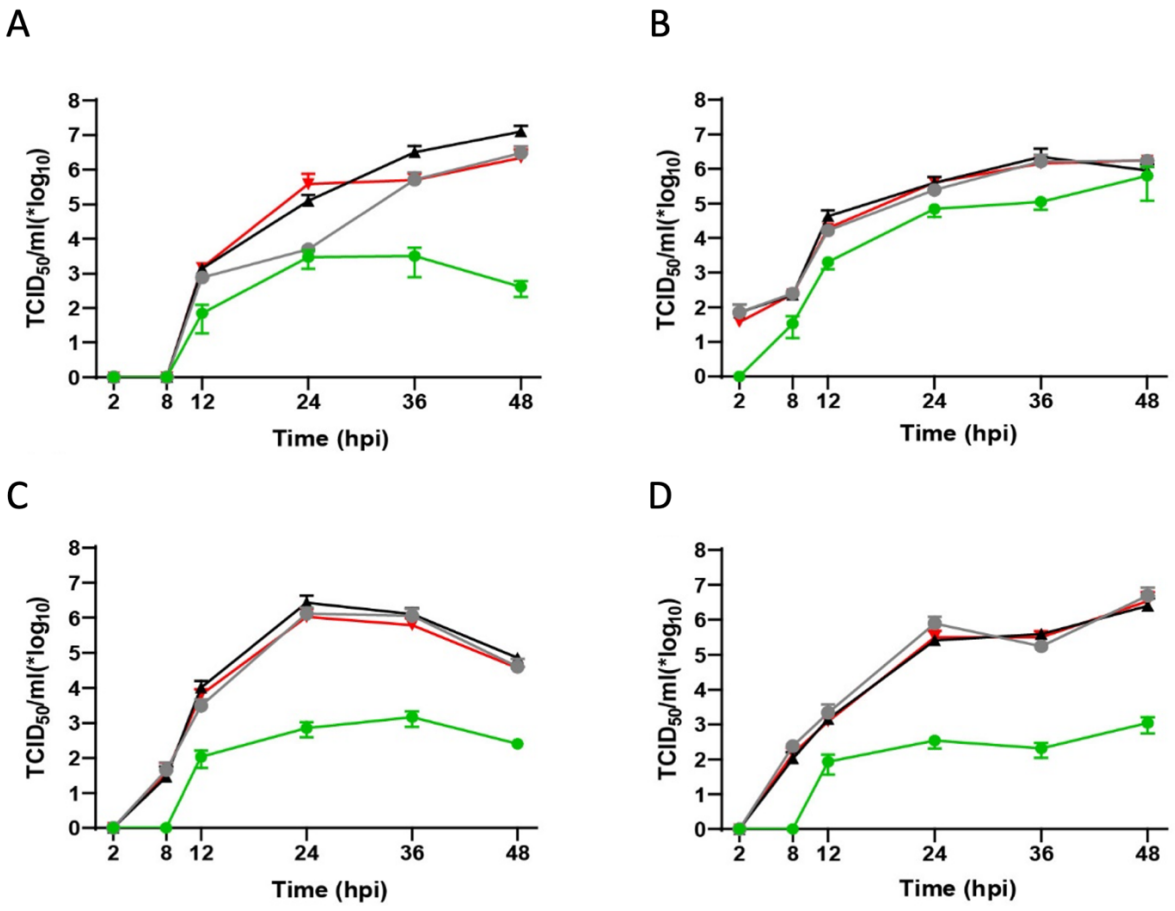


Figure 4.3: Replication kinetics of 4-OI decreasing IAV replication.

(A-B) Replication kinetics of IAV A/WSN/33 in MDCK (A, MOI 0.01) and A549 cells (2.5 x 10^5 cells) (B, MOI 0.1), treated with 100 µM 4-OI (green), DMSO (grey) or 10 mM Itaconate (black), or left untreated (red) for 48 h. (**C-D)** Replication kinetics of IAV A/NL/602/09 H1N1 (C, MOI 0.01) and A/NL/213/03 H3N2 (D, MOI 0.01) in MDCK cells (2.5 x 10^5 cells), treated with 100 µM 4-OI (green), DMSO (grey) or Itaconate 10 mM (black), or left untreated (red) for 48 h. All kinetics are representative of 3 independent experiments and are depicted as mean ± SD for n=3. Replication kinetics were done in collaboration with Pau Ribo Molina.

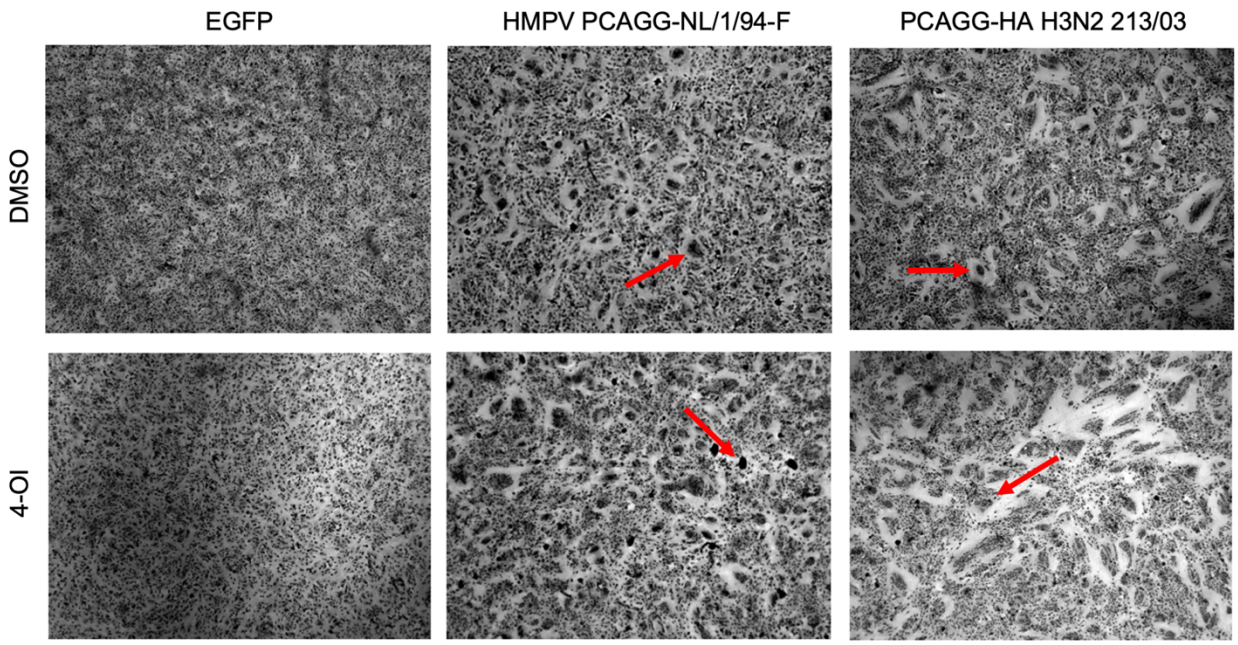


Figure 4.4: 4-OI does not decrease viral uptake.

Vero118 cells (1.2 x 10^6) were transfected with either 0.2 µg/µl eGFP, pCAGGs F HMPV NL/1/94, pCAGGs HA A/Neth/213/2003, or left untreated. After 24 h, the cells were treated with either 100 µM 4-OI or vehicle for 48 h, before initiating fusion at pH 5.0. DNA was stained using Giemsa solution. Red arrows indicate the clusters formed by cells fusing together. The fusion assay was performed once only. This experiment was performed by Pau Ribo Molina

4.1.4 4-OI does not interfere with tetraspanin expression

As IAV uptake takes place in tetraspanin-rich regions on the cell surface [75], whether expression of the tetraspanins CD9 and CD81 was regulated by 4-OI treatment was assessed next using flow cytometry. Gating on live, single BMDMs (Fig. 4.5 A) no decrease in either CD81 (Fig. 4.5 B), or CD9 (Fig. 4.5 C) expression was found after 4-OI treatment. Expression of CD9 was actually slightly increased in context of 4-OI treatment.

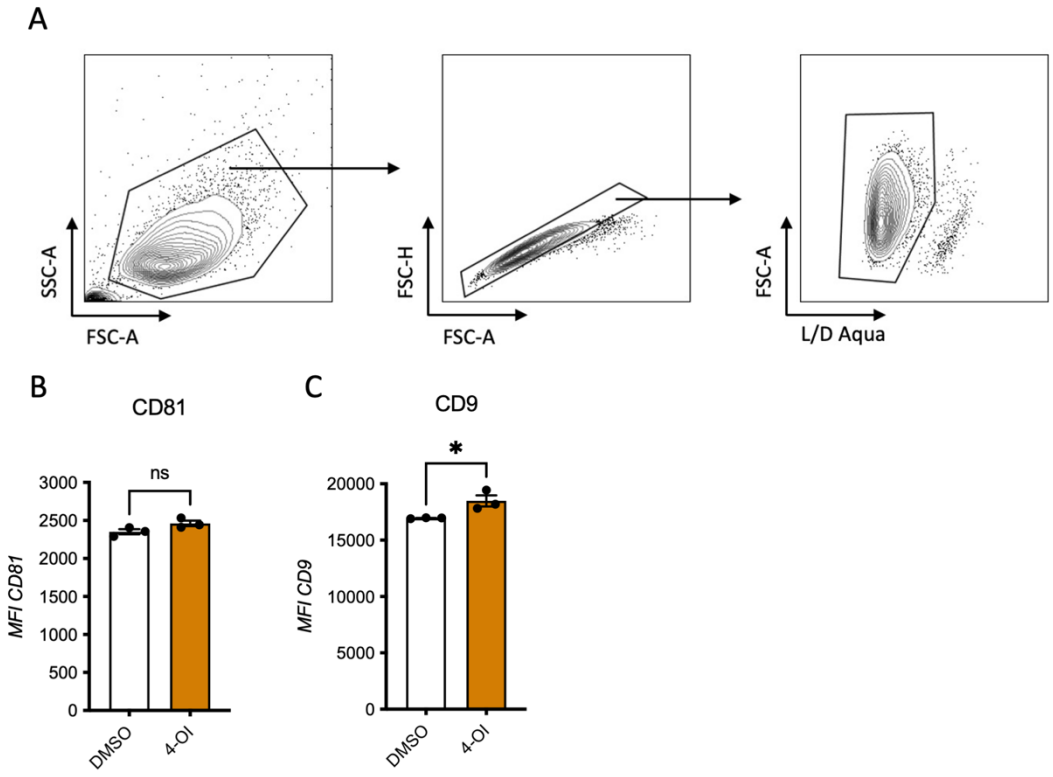


Figure 4.5: 4-OI does not decrease tetraspanin expression.

(A-C) A549s (2.5 x 10^5) were treated with 100 μM 4-OI or vehicle for 24 h and flow cytometry was performed. A depicts the gating strategy used to identify the live cell population. Live cells were identified as Live/Dead Aqua (L/D Aqua) negative. **(B-C)** Bar graphs showing the mean fluorescent intensity (MFI) of CD81 (B) and CD9 (C) expression. Data are mean ± SD for n=3. *$p<0.05$ as calculated using unpaired Student's t-test. Data is representative of 3 individual experiments.

4.2 4-OI inhibits CRM1 activity

4.2.1 IAV NP is trapped in the nucleus after 4-OI treatment

The viral protein NP, which shuttles viral RNA out of the nucleus after replication of the viral RNA genome was examined next in figure 4.6. In cells infected with IAV, NP was detected in the cytoplasm after 48, but not after 16 h (Fig. 4.6 A, middle row, 2nd panel, lanes 3 and 4). When treated with 4-OI, the levels of NP in the cytoplasm were decreased 48 h post infection (middle row, 2nd panel, lane 6). In the nucleus, NP was also accumulated 48 h after infection (bottom row, 2nd panel, lane 4), but 4-OI treatment did not block this accumulation here (lane 6).

Itaconate treatment did not alter levels of NP after IAV infection in either the nucleus (bottom row, 2nd panel, lane 8), or the cytoplasm (middle row, 2nd panel, lane 8). Total NP was decreased with 4-OI (top row, top panel lane 6 vs 4) in line with the expected decreased viral load, but not with itaconate (lane 8). Confocal microscopy confirmed this observation. While initially located in the nucleus shortly after IAV infection (Fig. 4.6 B, top left), NP could also be detected in the cytosol after 48 h (top right). When treated with 4-OI, NP is mostly in the nucleus 16 h after infection (middle left), it was however also still confined to the nucleus after 48 h (middle right). Again, itaconate treatment did not alter sub-cellular distribution of NP 16, or 48 h after IAV infection compared to untreated, IAV infected cells (bottom row compared to top row). Thus, 4-OI treatment appeared to be interfering with the nuclear export of NP. In host cells, export of NP is facilitated by the nuclear exporter CRM1. CRM1 protein levels were decreased after 4-OI treatment (Fig. 4.6 A, top row, top panel, lane 6 vs 1).

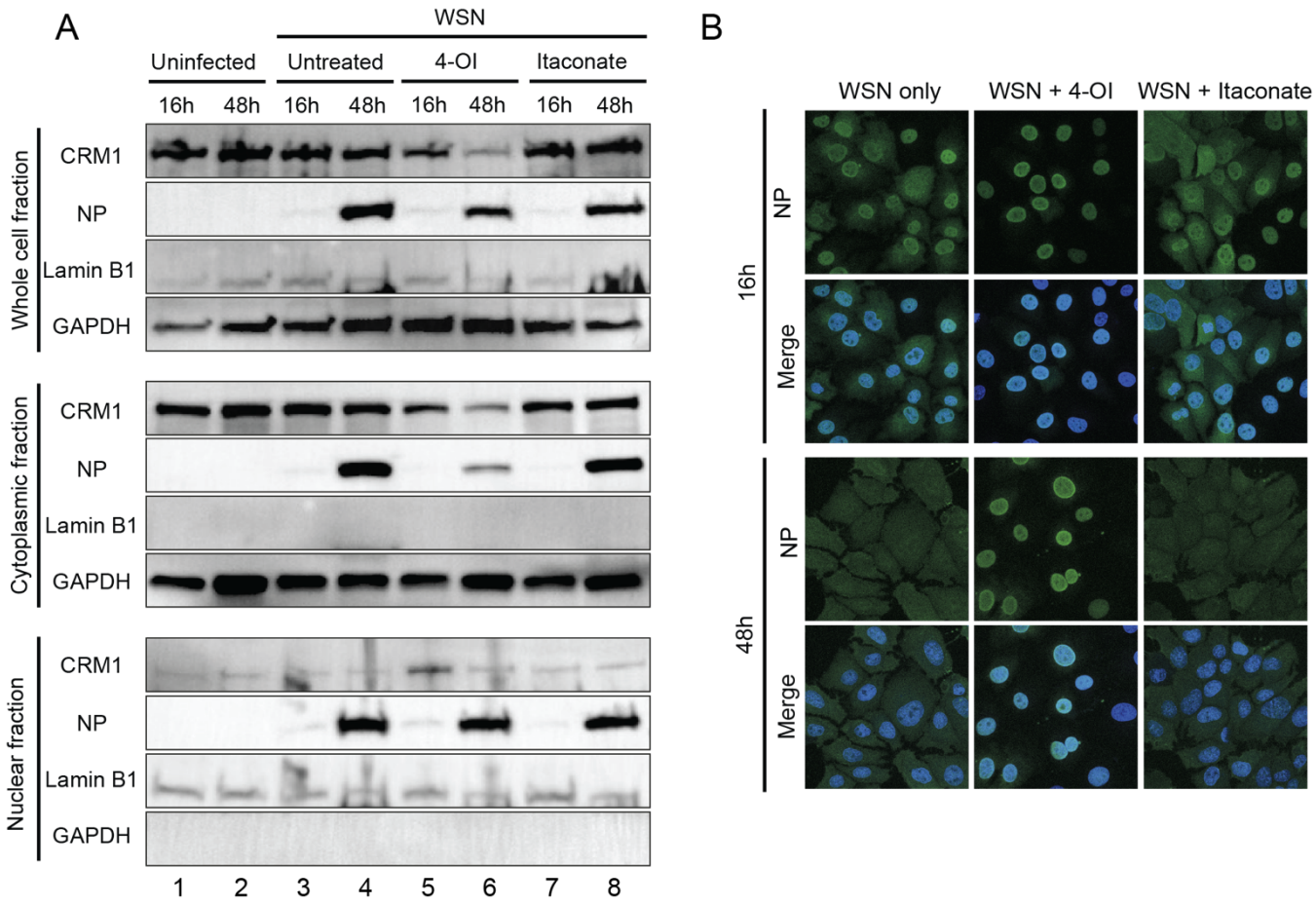


Figure 4.6: 4-OI decreases cytosolic levels of NP after IAV infection.

(A) MDCK cells (2.5 x 10^5 cells) were treated with 10 mM itaconic acid, 100 μM 4-OI or vehicle for 48 h, inoculated with IAV for 2 h, and treated again with 10 mM itaconic acid, 100 μM 4-OI or vehicle for either 16 h or 48 h. The cells were then harvested and fractionated into cytosolic and nuclear and total faction. Western blotting was performed with each fraction. **(B)** Confocal microscopy was performed with cells treated as in A. Blots and confocal images are representative of 3 independent experiments. This experiment was performed by Pau Ribo Molina.

4.2.2 CRM1 accumulates in the cytosol of 4-OI treated BMDMs

In some instances, CRM1 has to be shown to dissociate from the nuclear membrane and accumulate in the cytosol upon inactivation [207].

BMDMs were treated with 4-OI to assess the subcellular location of CRM1 before and after treatment. As shown in figure 4.7 A, when treated with 4-OI, an accumulation of CRM1 in the cytosol in BMDMs after 24, and 48 h was detected (top middle panel, lanes 3 and 4), but not 8 h (lane 2) compared to non-treated cells (lane 1). In the nucleus, CRM1 levels were decreased after 24 h (top left panel, lane 3), but not after 8, or 48 h (lanes 2 and 4). Total CRM1 levels were increased after 24 and 48 h of 4-OI treatment (top right panel, lanes 3 and 4) compared to 8 h treatment or non-treated cells (lanes 1 and 2). Densitometry was performed to quantify the increase in CRM1 expression after 4-OI treatment, revealing a roughly fourfold increase after 48 h post treatment (Fig. 4.7 B). Confocal microscopy confirmed this observation, as CRM1 could not be detected in the cytosol of untreated cells (Fig. 4.7 C, left panels), but could be seen accumulated in the cytosol of BMDMs after 4-OI treatment (right panels).

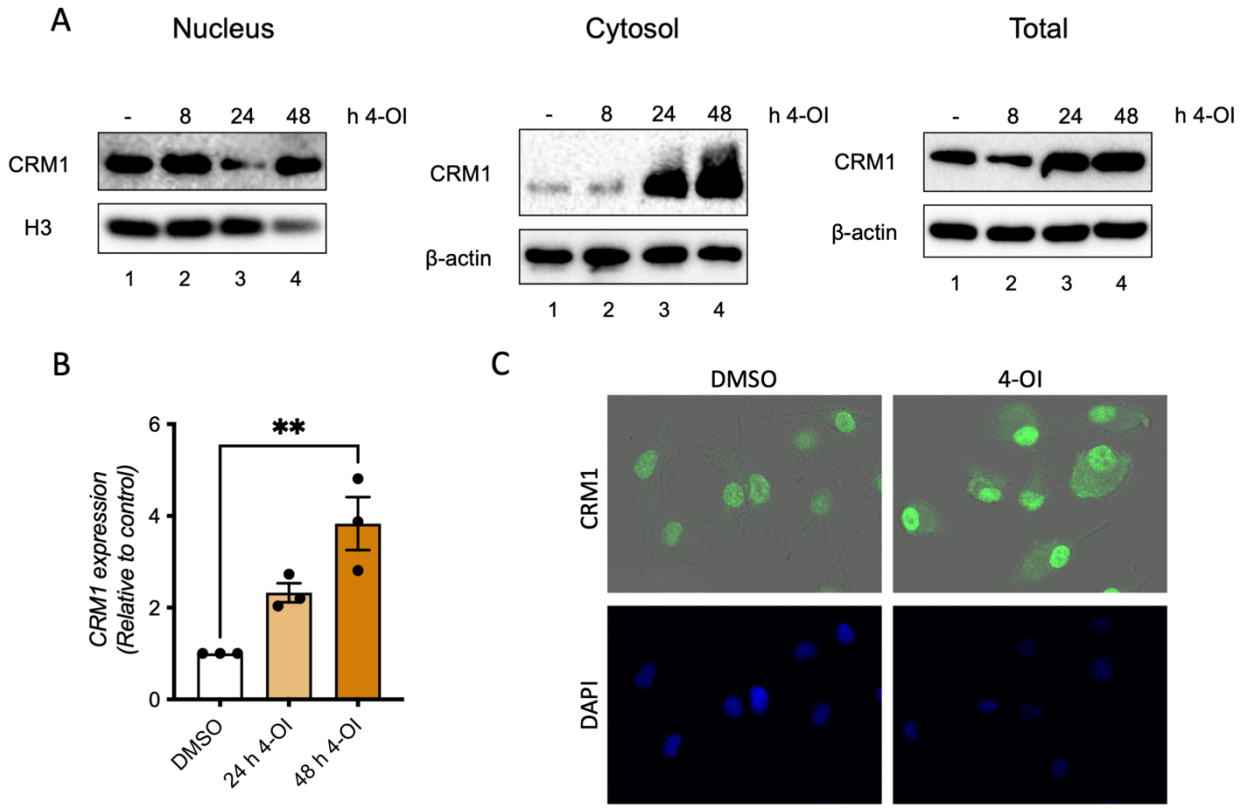


Figure 4.7: 4-OI increases CRM1 protein levels in BMDMs.

(A) BMDMs (5 x 10^5 cells) were treated with 250 μM 4-OI or vehicle for indicated timepoints. Harvested cells were then fractionated into cytosolic and nuclear faction and analysed by western blotting. **(B**) Quantification of densitometry of blots from A. **(C)** (2.5 x 10^5 cells) BMDMs were treated with 250 μM 4-OI or vehicle for 24 h and visualized by confocal microscopy. Data are mean ± SD. **p<0.01, as calculated using a one-way ANOVA followed by Sidak's multiple comparisons test. Blots are representative of 3, and confocal images are representative of 2 independent experiments.

4.2.3 4-OI decreases CRM1 protein levels in lung epithelial cells

As macrophages are not a very relevant cell type for influenza infections and most CRM1 related research has been done in other cell types, epithelial cells were examined next. In NHBE primary lung epithelial cells, a strong decrease in CRM1 protein levels was observed after 24 and 48 h of 4-OI treatment (Fig. 4.8 A lanes 2 and 3) compared to untreated cells (lane 1). Densitometry on these blots was performed to quantify the 4-OI induced decrease of CRM1 protein levels for the 24 h timepoint (Fig. 4.8 B). As shown in figure 4.8 C. confocal microscopy confirmed this data and revealed this decrease to be mainly due to decreased levels in the nucleus (top left panel compared to top right panel).

This reduction in CRM1 protein levels was even stronger in Nuli-1 cells. Here, CRM1 protein levels were again decreased after 24 h (Fig. 4.9 A lane 3), but not after 6 h of 4-OI treatment (lane 2). Densitometry revealed a 80 % reduction in CRM1 protein in cells that had been incubated with 4-OI (Fig. 4.9 B). Furthermore, confocal microscopy confirmed decreased CRM1 levels after 4-OI treatment (Fig. 4.9 C, top right panel compared to top left panel).

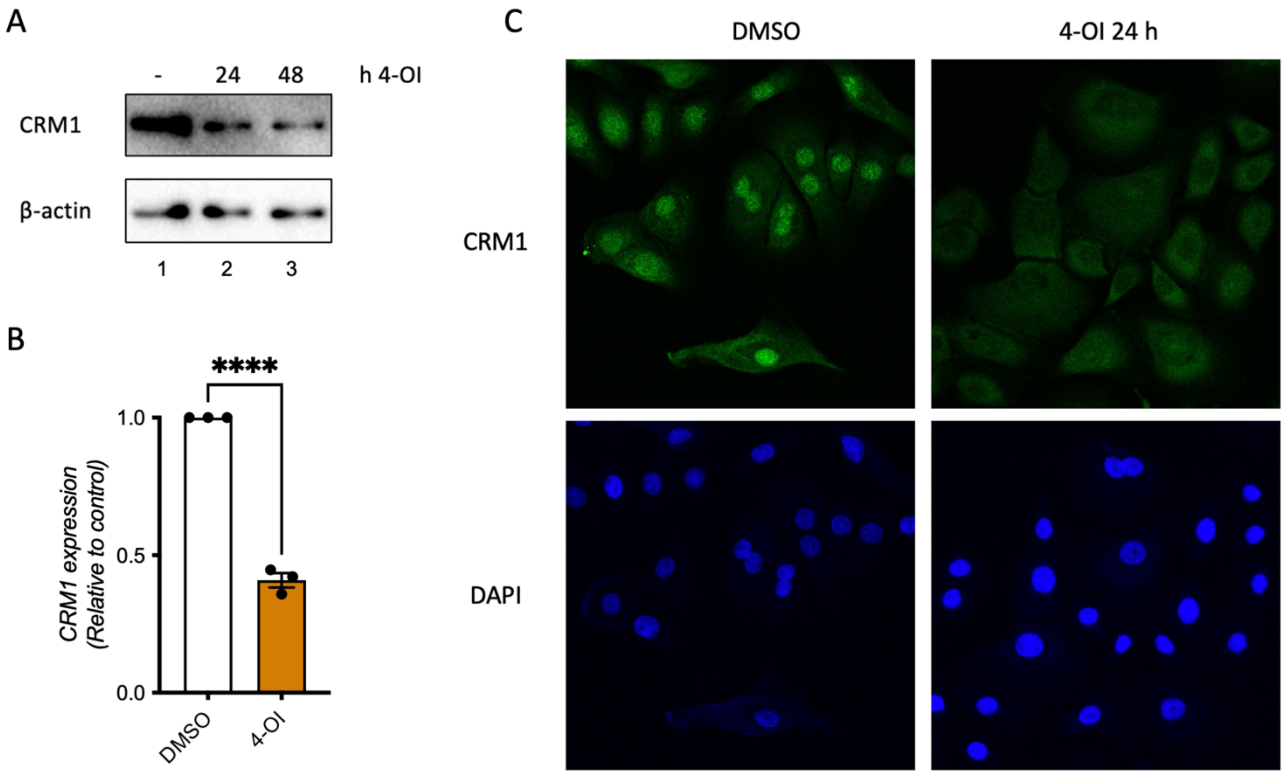


Figure 4.8: 4-OI decreases CRM1 protein in NHBE cells.

(A) NHBE cells (2.5 x 10^5 cells) were treated with 100 μM 4-OI or vehicle for indicated timepoints. Harvested cells were fractionated into nuclear and cytosolic fractions and analysed by western blotting. **(B)** Quantification of densitometry of blots from A at timepoint 24 h. **(C)** Depicted are NHBE cells (1.25 x 10^5 cells), treated with 100 μM 4-OI or vehicle for 24 h and visualized by confocal microscopy. Data are mean ± SD for n=3. ****$p<0.0001$ as calculated using unpaired Student's t-test. Confocal images are representative of 3 independent experiments.

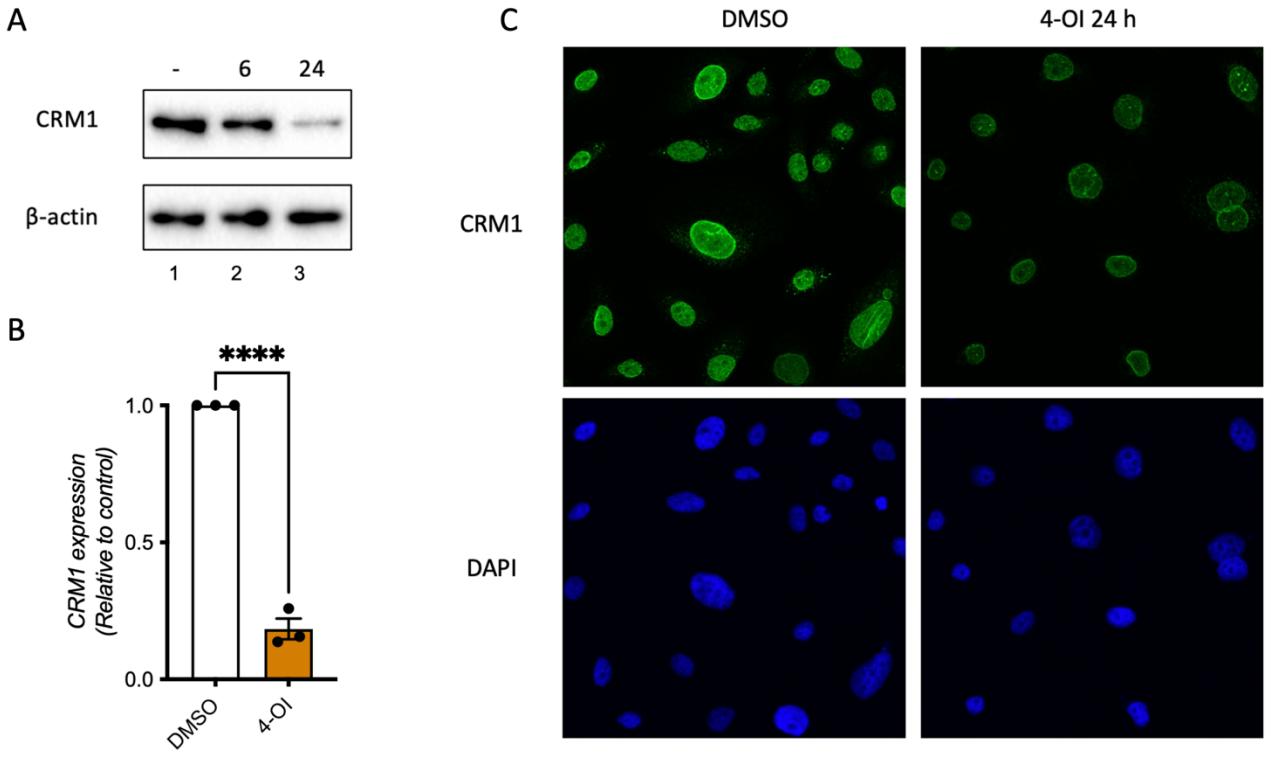


Figure 4.9: 4-OI decreases CRM1 protein in Nuli-1 cells.

(A) Nuli-1 cells (2.5 x 10^5 cells) were treated with 100 µM 4-OI or vehicle for indicated timepoints. Harvested cells were fractionated into nuclear and cytosolic fractions and analysed by western blotting. **(B)** Quantification of densitometry of blots from A at timepoint 24 h. **(C)** (1.25 x 10^5 cells) Depicted are NHBE cells, treated with 100 µM 4-OI or vehicle for 24 h and visualized by confocal microscopy. Data are mean ± SEM for n=3. ****$p<0.0001$ as calculated using unpaired Student's t-test. Confocal images are representative of 3 independent experiments.

4.2.4 4-OI does not decrease CRM1 mRNA expression levels

To investigate whether CRM1 expression is affected at the transcriptional level, CRM1 mRNA levels were assessed in the above cell types in figure 4.10. Decreased CRM1 levels in NHBE cells were not due to decreased expression, as CRM1 mRNA was slightly increased after 24 h of both 100 μM and 250 μM 4-OI treatment in NHBE cells (Fig. 4.10 A). In NuLi-1 cells, 24 h of 4-OI treatment also increased mRNA expression levels of CRM1 at both 100 μM and 250 μM (Fig. 4.10 B). These results suggest 4-OI mediated modulation of CRM1 at the translational or protein level.

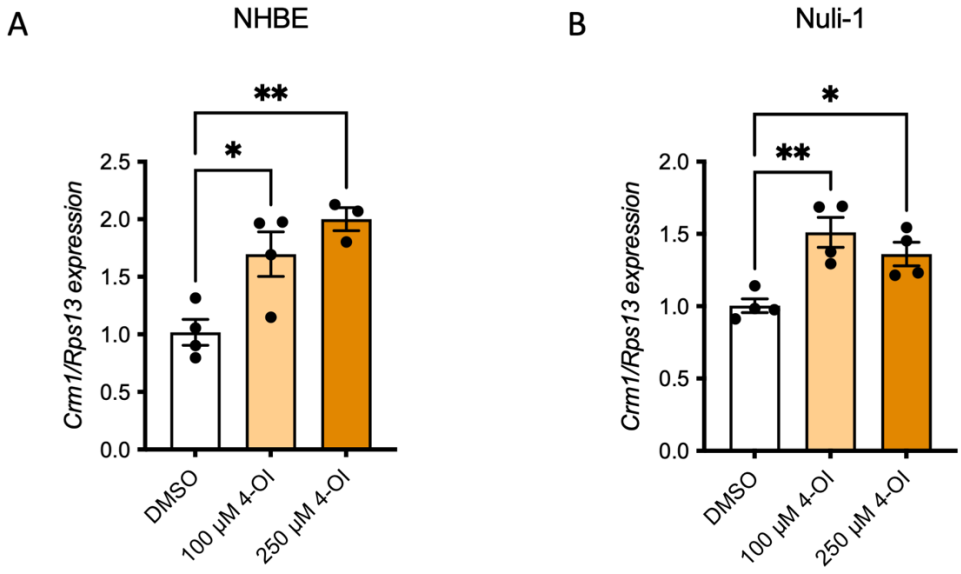


Figure 4.10: 4-OI slightly increases CRM1 mRNA expression.

(A) qPCR analysis of NHBE cells treated with 4-OI or vehicle for 24 h. (**B)** qPCR analysis of NuLi-1 cells treated with 4-OI or vehicle for 24 h. Data are mean ± SEM for n=4 (Except for (A), right data set, which is n=3). *p<0.05, **p<0.01, as calculated using a one-way ANOVA followed by Sidak's multiple comparisons test.

4.3 4-OI induces global protein ubiquitination

With CRM1 and other dicarboxypropylation targets of 4-OI and itaconate such as KEAP1 [155], being diminished upon treatment, the question could be raised how these proteins are degraded. Controlled protein recycling is achieved through ubiquitination, a biochemical process that attaches one or multiple ubiquitin proteins to the target, leading to degradation via the proteasome [208]. We aimed to assess whether ubiquitination could be responsible for diminished protein levels after dicarboxypropylation of CRM1 and other targets.

Data from our lab suggest up to 16,000 cysteines to be potentially modified by 4-OI, and if a significant portion of these targets are ubiquitinated, it can be assumed that this should lead to a noticeable shift in global ubiquitin levels. Indeed, blotting for ubiquitin on whole-cell lysate revealed increased ubiquitination globally after 4-OI treatment (lane 2), but not after treatment with KPT-330 (lane 3), which only specifically targets CRM1 (Fig. 4.11 A). CRM1 ubiquitination was next assessed in figure 4.11 B. Ubiquitination of CRM1 however wasn't detected in samples treated with 4-OI (lane 2), or KPT-330 (lane 3) compared to untreated (lane 1). Despite an upregulation of global ubiquitination upon 4-OI treatment ubiquitination of CRM1 specifically could not be detected.

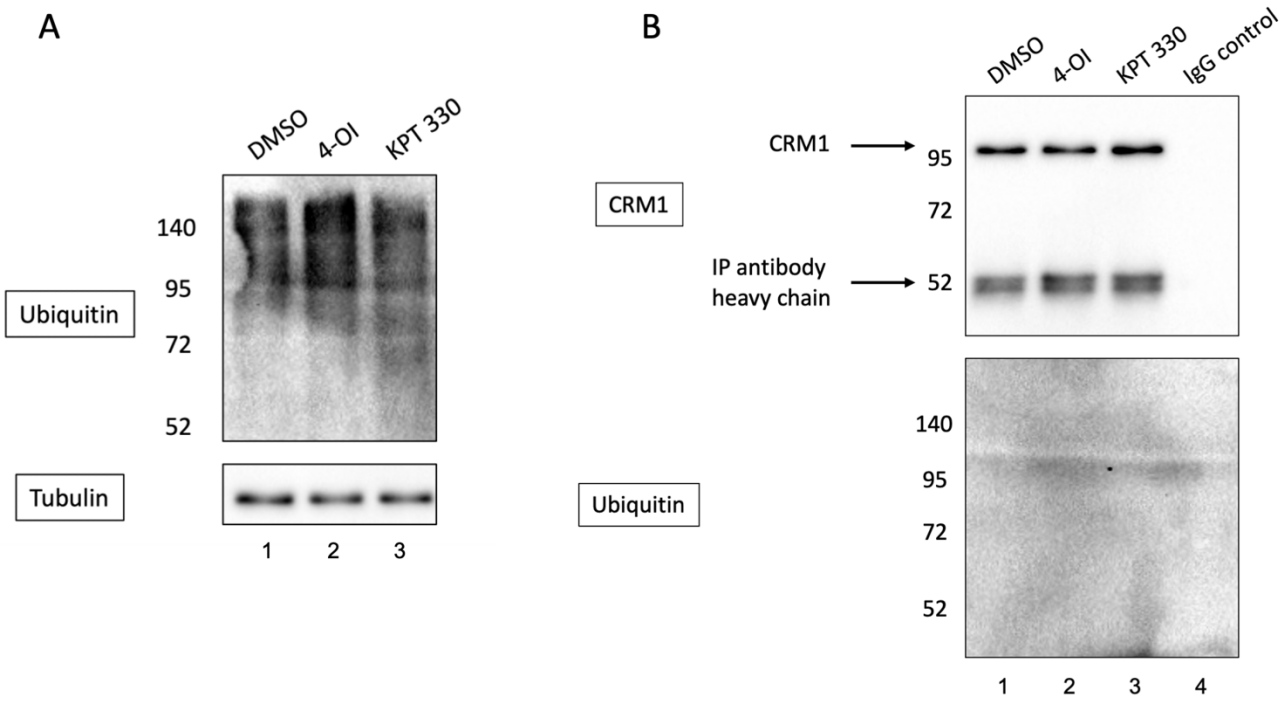


Figure 4.11: 4-OI induces global protein ubiquitination.

(A) Nuli-1 cells (5 x 10^5 cells) were treated with 100 µM 4-OI, 100 nM KPT-330, or DMSO control for 24 h and global protein ubiquitination was assessed by western blotting. **(B)** Nuli-1 cells (5 x 10^5 cells) were treated with 100 µM 4-OI, 100 nM KPT330, or DMSO control for 24 h. CRM1 was pulled down via immunoprecipitation, and ubiquitination was assessed by western blotting. Data are representative of 3 individual experiments.

4.4 4-OI shuts down CRM1 mediated nuclear export

4.4.1 p53 and p65 accumulate in the nucleus upon 4-OI treatment

A decrease in CRM1 expression has been associated with the nuclear accumulation of its natural cargo proteins p65 and p53 [102,209]. In NHBE cells, p53 and p65 were found to be accumulated in the nucleus after 4-OI treatment, (Fig. 12 A, lane 2, left panel) compared to non-treated cells (lane 1, left panel). In the cytosol, these proteins were decreased after 4-OI treatment (lane 2, right panel) compared to the non-treated control (lane 1, right panel), further suggesting impaired CRM1 activity. As shown in figure 4.12 B, the shift of subcellular location of p65 from the cytosol to the nucleus after 4-OI treatment was confirmed by confocal microscopy (Fig. 4.12 C, top left panel compared to top right panel). In Nuli-1 cells, again, 4-OI treatment resulted in accumulated p53 in the nucleus (left panel, lane 2 compared with 1). In the cytosol, levels of p53 were unchanged after 4-OI treatment (right panel). p65 localized from the cytosol to the nucleus after 4-OI treatment (Fig. 4.12 D, top left panel compared to top right panel).

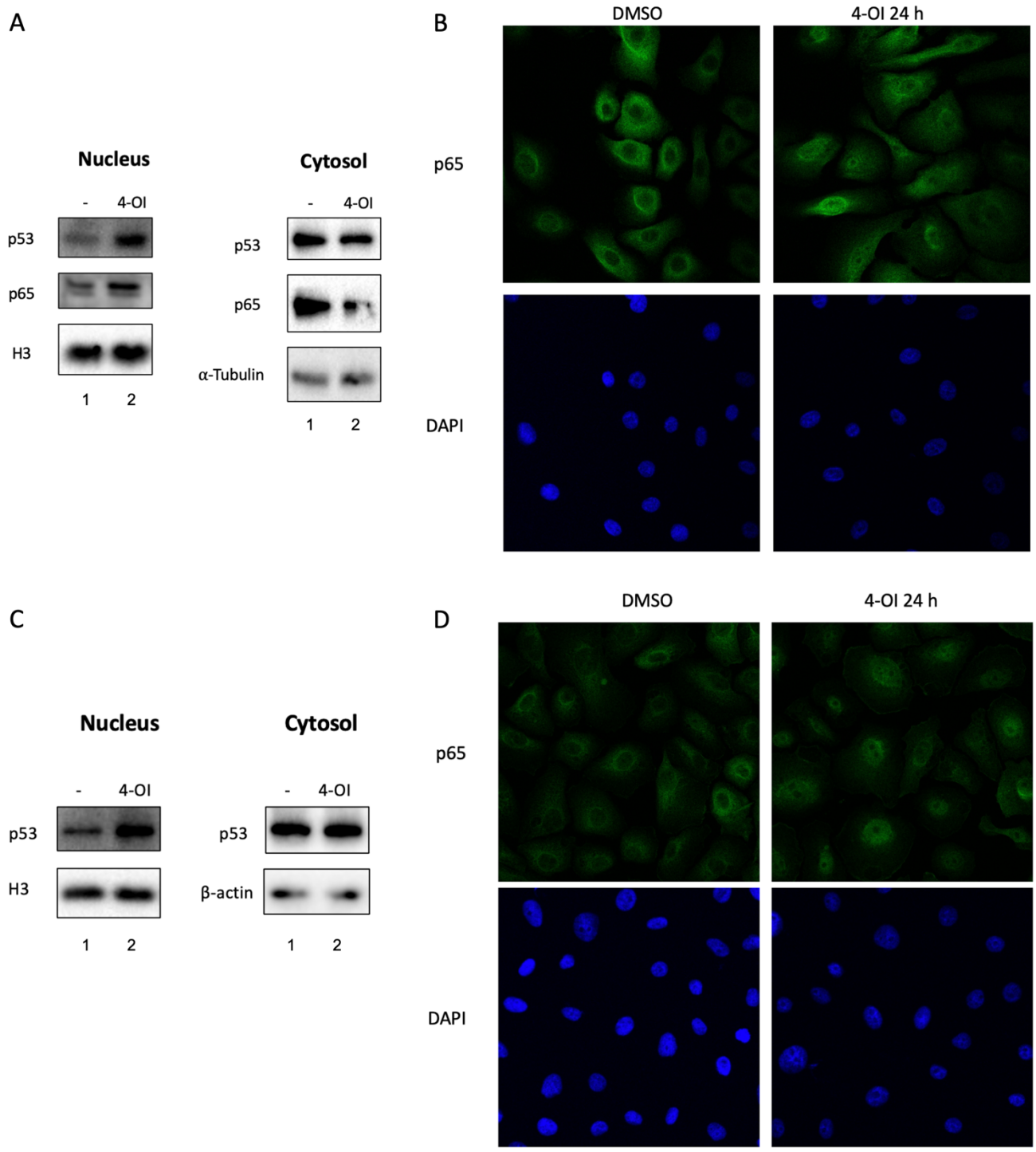


Figure 4.12: 4-OI induces nuclear accumulation of CRM1 cargo proteins p53 and p65.

(A) Western blot analysis of nuclear and cytosolic fractions from NHBE cells (2.5 x 10^5 cells) treated with 100 µM 4-OI or vehicle for 24 h. **(B)** Depicted are NHBE cells (2.5 x 10^5 cells), treated with 100 µM 4-OI or vehicle for 24 h and visualized by confocal microscopy. **(C)** Western blot analysis of nuclear and cytosolic fractions from NuLi-1 cells (1.25 x 10^5 cells) treated with 100 µM 4-OI or vehicle for 6 h. **(D)** Depicted are NuLi-1 cells (1.25 x 10^5 cells), treated with 100 µM 4-OI or vehicle for 24 h and visualized by confocal microscopy. Blots and confocal images are representative of 3 (NHBE) or 2 (Nuli-1) independent experiments.

4.4.2 4-OI dose-dependently decreases CRM1 activity

To further investigate the effect of 4-OI on CRM1 activity, I organized a collaboration with Dr. Dirk Daelemans, an expert in CRM1 research at KU Leuven. To study SINEs, he developed assays to specifically measure CRM1 activity. In his lab, a CRM1-dependent GFP cargo assay was employed to visualise and quantify the effectivity of 4-OI as an inhibitor of CRM1 activity. To this end, Hela cells stably expressing a GFP containing the CRM1-dependent NES from Protein Kinase Inhibitor (PKI) were used. This GFP reporter protein shuttles between the nucleus and the cytoplasm and accumulates in the nucleus upon inactivation of CRM1 [210]. The Hela cells were treated with varying concentrations of 4-OI for 24 hours, and the subcellular location of the reporter protein was assessed. Confocal microscopy demonstrated that 4-OI treatment caused accumulation of the reporter protein in the nucleus, as shown for 250 µM (Fig. 4.13 A). Quantification of the ratio of nuclear to cytoplasmic GFP upon treatment with a range of 4-OI, revealed a dose dependent increase of nuclear reporter protein upon 4-OI treatment (Fig. 4.13 B). As translocation of this reporter protein depends on CRM1 activity, these results confirm that 4-OI indeed targets the activity of CRM1.

To support that 4-OI inhibits the nuclear export mediated by CRM1, the effect on the nucleus to cytoplasm translocation of the Rev protein of Feline Immunodeficiency Virus (FIV) was used. The export of FIV Rev is mediated through its NES and is suggested to bind to CRM1 [211]. Previously reported for HIV, Rev shuttles to the cytoplasm in a CRM1 dependent manner upon actinomycin D treatment, while Rev remains mainly in the nucleus in the presence of an CRM1

inhibitor [212,213]. Here, in FIV Rev-GFP transfected Vero cells, Rev-GFP was predominantly found in the nucleus. Figure 4.13 C shows that upon actinomycin D treatment of Vero cells transfected with Rev-GFP, a proportion of the Rev-GFP protein shuttles to the cytoplasm in the presence of DMSO(2nd panel from left compared to left). This was not the case after co-treatment with 100 μM 4-OI (right panel) or 100 nM KPT-330 (2nd panel from right), upon which Rev-GFP remained in the nucleus. These results confirm that 4-OI has a direct effect on CRM1-mediated transport of viral proteins from the nucleus to the cytoplasm.

4.4.3 Endogenous itaconate does not affect CRM1 protein levels

Earlier 4-OI, but not exogenous itaconate were shown to be antiviral in IAV, with 4-OI targeting CRM1. A role for IRG1 in CRM1 inhibition was next tested. To induce expression of IRG1 and production of itaconate, THP-1 cells were differentiated into a macrophage-like phenotype and subsequently treated with increasing concentrations of LPS. While IRG1 was induced, LPS was not able to decrease CRM1 protein expression (Fig. 4.14 A, lane 1 compared to lanes 2 – 6). The same was true in PBMCs, where LPS treatment, despite inducing IRG1, did not result in altered CRM1 protein levels either (Fig. 4.14 B lane 1 compared to lanes 2 – 6). We therefore conclude that endogenous itaconate is unlikely affect CRM1 expression.

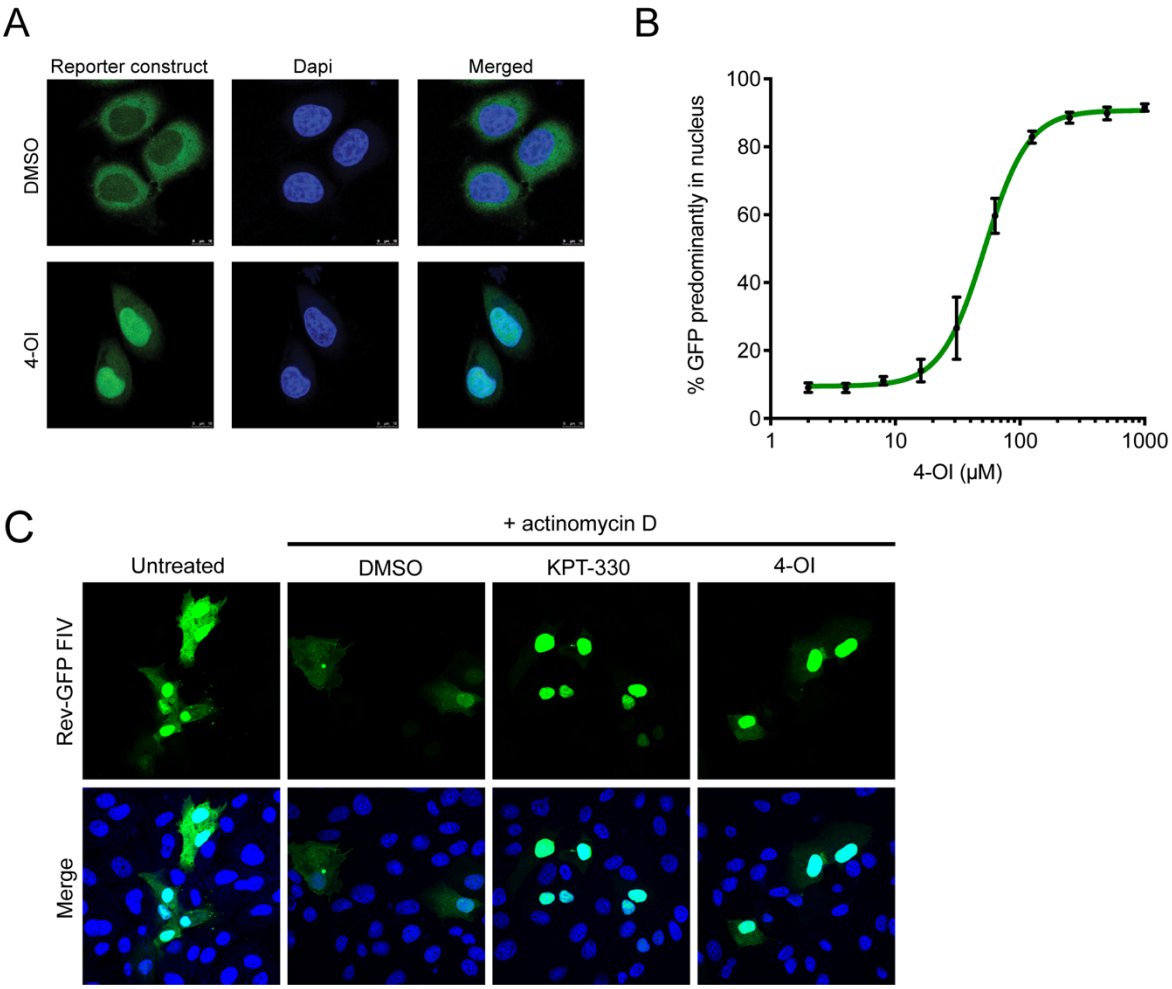


Figure 4.13: Impact of 4-OI on CRM1 dependent proteins.

(A) The effect of treatment with 4-OI in a reporter HeLa cell line stably expressing a CRM1-dependent GFP reporter protein. Cells (8 x 10^3) were treated with 100 μM 4-OI or DMSO for 24 h, and the subcellular location was assessed by confocal microscopy. Confocal images are representative of 2 independent experiments. (**B)** Quantification of results from panel A. Cells were treated with indicated concentrations of 4-OI for 24 h and the percentage of cells with a predominantly nuclear localization of the GFP reporter protein was assessed. The experiment was conducted three times, and results are depicted as mean ± SD. (**C)** Confocal microscopy image of Vero-118 cells (1.25 x 10^5) transfected with FIV Rev-GFP (green). Cells were left untreated, or treated with actinomycin D simultaneously to DMSO, 100 μM 4-OI or 100 nM KPT-330. Merge images include nuclear staining with Hoechst (blue). Confocal images are representative of 3 individual experiments. The uptake assay was performed by Leentje Persoons, the confocal images of Rev by Pau Ribo Molina.

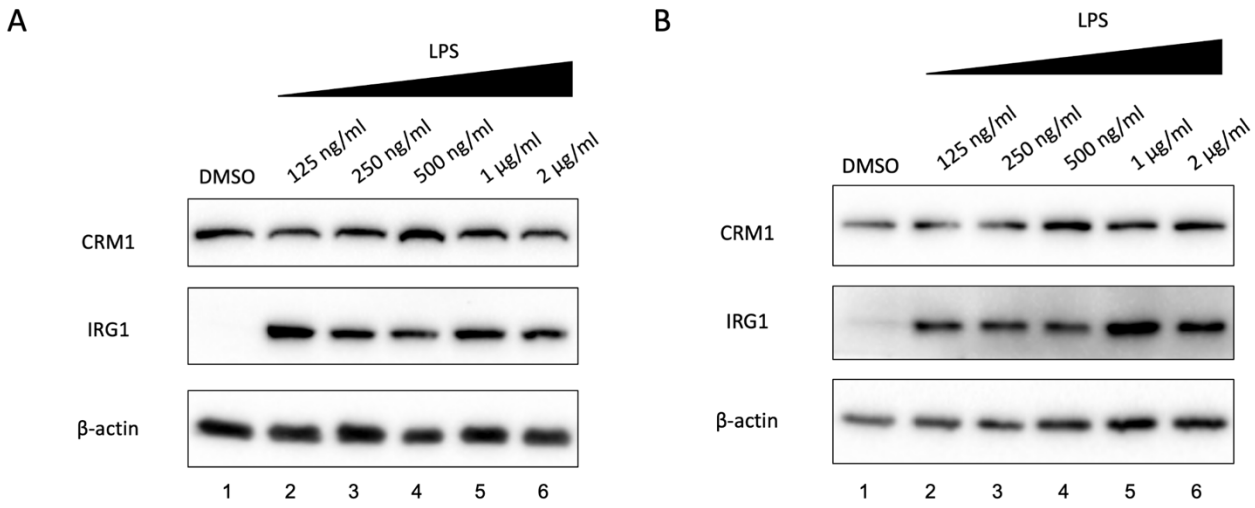


Figure 4.14: Endogenous itaconate does not drive CRM1 degradation.

(A) THP-1 cells (5 x 10^5 cells) were differentiated using 100 ng/ml PMA for 72 h, and subsequently treated with increasing concentrations of LPS for 48 h. IRG1 and CRM1 protein levels were evaluated by Western Blotting. **(B)** PBMCs (5 x 10^5 cells) were treated with increasing concentrations of LPS for 48 h. IRG1 and CRM1 protein levels were evaluated by Western Blotting. Blots are representative of 3 (THP-1) or 2 individual experiments (PBMC).

4.4.4 Exogenous itaconate does not decrease CRM1 protein levels

Next, exogenous itaconate was tested on CRM1 expression. To this end, Nuli-1 cells were treated with increasing concentrations of itaconic acid, as well as the CRM1 inhibitor KPT-330 as a control. While KPT-330 potently decreased CRM1 expression (Fig. 4.15 A, top panel, lane 6 compared to lane 1), exogenous itaconate did not (lanes 2 – 5 compared to lane 1) since the loading control (bottom panel) also showed a decrease. Blots were therefore quantified by densitometry in figure 4.15 B and concentrations above 10 mM considered toxic. In BMDMs, itaconate treatment did not result in altered expression of CRM1 either (Fig. 4.15 C, top panel). I thus conclude that there is unlikely to be a role for unmodified itaconate in CRM1 regulation, which is consistent with earlier findings that 4-OI but not itaconate restricted nuclear export of NP, and ultimately IAV replication.

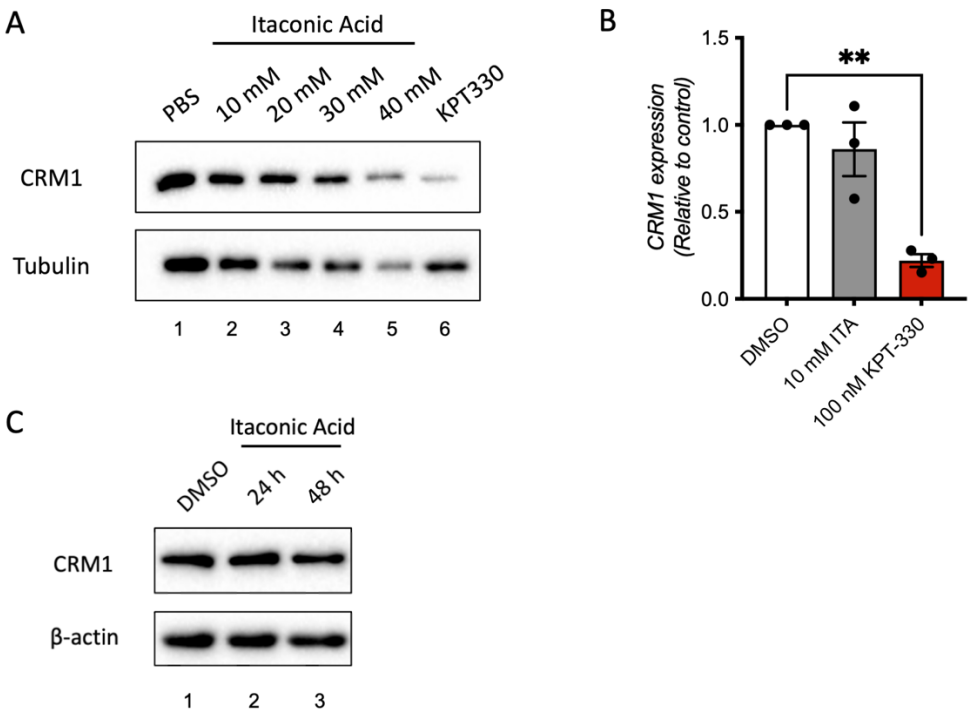


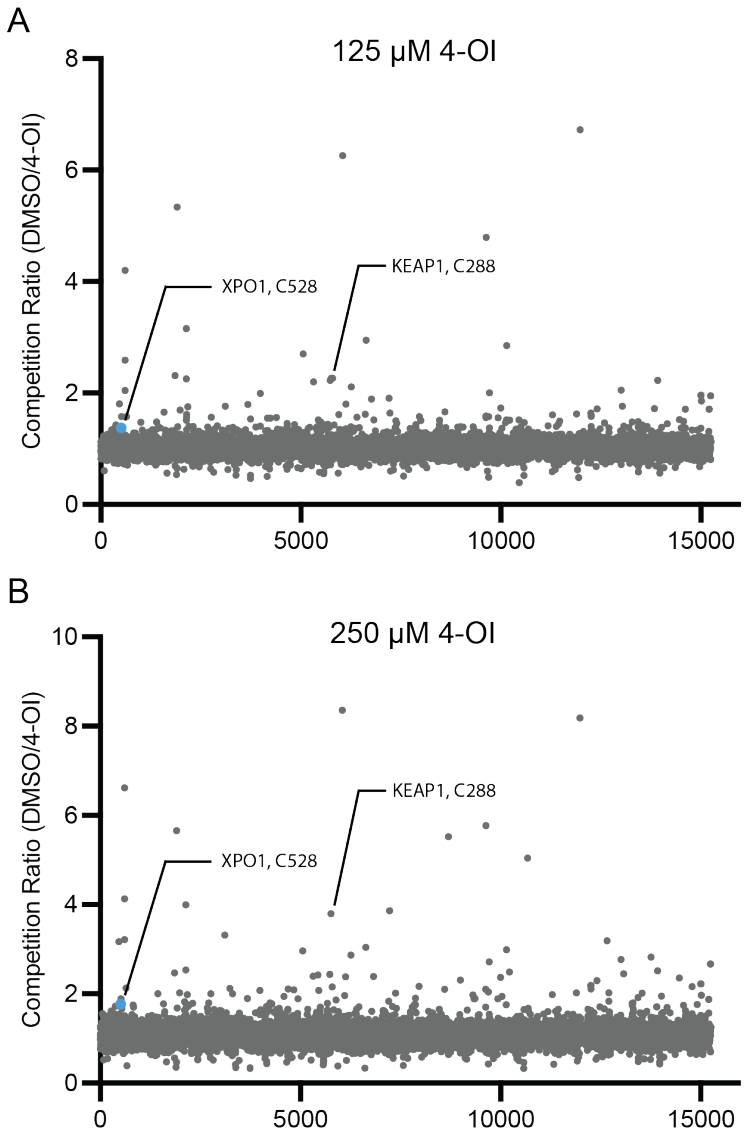
Figure 4.15: Exogenous itaconate does not affect CRM1 protein levels.

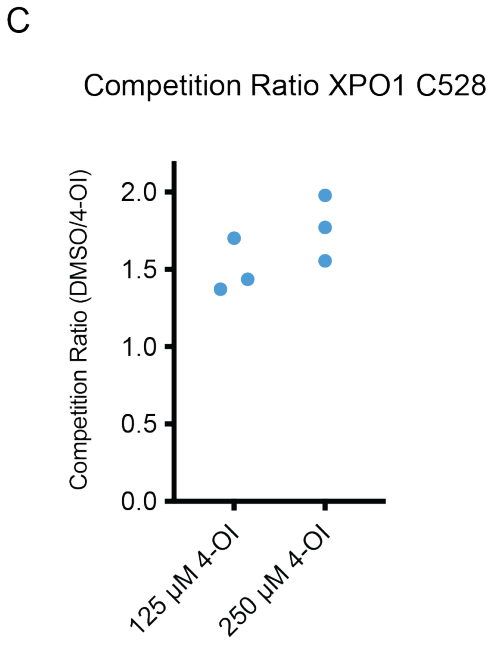
(A) Nuli-1 cells (2.5 x 10^5 cells) were treated with indicated concentrations of itaconic acid, 100 nM KPT330 or vehicle for indicated timepoints. Harvested cells were analysed by western blotting. **(A)** Quantification of blots from (B). **(C)** BMDMs (5 x 10^5 cells) were treated with 10 mM itaconate for 24 or 48 h. CRM1 levels were assessed by western blotting. Blots are representative of 3 individual experiments.

4.5 4-OI inhibits CRM1 through dicarboxypropylation of C528

Itaconate and its derivatives are known to be cysteine modifiers through a process called 2,3-dicarboxypropylation [155,214], an alkylation reaction. CRM1 has recently been suggested as a potential target for 2,3-dicarboxypropylation by itaconate [214], and CRM1 inhibitors such as LMB or KPT-330, specifically act through alkylation of a key cysteine 528 inside the hydrophobic cargo binding pocket of CRM1 [111,215,216]. To investigate whether CRM1 is indeed modified in this way by 4-OI, Liquid Chromatography with tandem mass spectrometry (LC-MS/MS) was performed on 4-OI treated THP-1 cells by a collaborator at Abbvie and 2,3-dicarboxypropylation of cysteine residues throughout the proteome was assessed by IA-DTB-based competitive cysteine profiling. While Abbvie provided the dataset, I conducted a full analysis of the data to assess CRM1 modification.

The well described 2,3-dicarboxypropylation target KEAP1 [155] was identified in this screen, while CRM1 was also detected as a target in the top 1 % of hits (Fig. 4.16 A - C). CRM1 was found to be modified in 6 positions: C34, 119, C164, C528, C723, and C1070, with C528 as the most significant hit (Fig. 4.16 D).





D

Cysteine position within **XPO1**	Competition Ratio **125 µM 4-OI**	Competition Ratio **250 µM 4-OI**
34	1.247473613	1.156489
119	1.951985261	1.738458
164	1.872828072	1.707449
528	1.702464095	1.979669
723	1.688483896	1.581661
1070	1.273189382	1.318805

Figure 4.16 CRM1 is alkylated by 4-OI at C528

(A – B) Mass spectrometry screening of 2,3-dicarboxypropilated cysteine residues in THP1 cells (4 x 10^6 cells) treated with 4-OI. Cells were treated with 125 µM (A), or 250 µM 4-OI (B) and IA-DTB-based competitive cysteine profiling was performed to identify 2,3-dicarboxypropylated cysteine residues on target proteins. Highlighted are C288 on Keap1, as well as C528 on CRM1. **(C)** Competition ratio values of C528 on CRM1 (n=3). **(D)** Raw competition ratio values of all detected modified cysteines within CRM1. Mass spectrometry data is representative of 3 independent experiments. Mass spectrometry was performed by Yunan Zheng, data analysis by me.

To demonstrate that the inhibitory effect of 4-OI on CRM1 activity is through the observed 2,3-dicarboxypropylation of C528, a mutant Jurkat cell line specifically designed to study the specificity of CRM1 inhibitors was employed. These mutant Jurkat XPO1^{C528S} cells contain a serine instead of cysteine at position 528 (C528S) of the CRM1 protein. This substitution leaves the protein functionally intact, but renders it resistant to modification by CRM1 inhibitors at this position [182].

Hence, a decrease in CRM1 expression levels, or reduction of CRM1 facilitated nuclear export, upon 4-OI treatment should not occur in these mutant cells. Upon treatment with 4-OI, as well as with KPT-330, of both wild type Jurkat cells and Jurkat XPO1^{C528S} cells, CRM1 expression levels were only significantly reduced in the wild type cells with 4-OI (Fig. 4.17 A, lane 2) and KPT-330 (lane 3), but not in the XPO1^{C528S} cells (lanes 5 and 6). The blots in figure 4.16 A were quantified by densitometry in figure 4.17 B. These results confirm that the C528S substitution in CRM1 indeed resulted in protection from both KPT-330 and 4-OI-mediated CRM1 degradation. In addition, the CRM1 cargo proteins p53 and p65 were accumulated in the nucleus of 4-OI treated (Fig. 4.17 C lane 2) compared to DMSO treated (lane 1) wild type Jurkat cells, but not the mutant XPO1^{C528S} Jurkat cells (lane 4 compared to lane 3), further confirming that 4-OI targets CRM1 through modification of this cysteine. Cytoplasmic and whole-cell fraction expression levels of p53 and p65 were unchanged (lanes 7 – 18). Nuclear accumulation of p53 and p65 in WT vs XPO1^{C528S} cells was quantified by densitometry in figures 4.17 D and E.

4.5.1 Toxicity of high dose 4-OI is partly through CRM1 inhibition

Inactivation of CRM1 has major implications for cell biology beyond inhibition of viral replication of viruses hijacking CRM1 as part of their life cycle. Vital cellular functions can be shut down when CRM1 is fully inactive for prolonged time periods [217]. At higher concentrations, some toxicity using 4-OI was observed, so whether some of that toxicity stems from CRM1 inhibition was assessed. To this end, WT Jurkat and Jurkat XPO1^{C528S} cells were treated with increasing concentrations of 4-OI and a toxic concentration of KPT-330, and LDH release was assessed after 24 h as a measure of cell death As shown in figure 4.17 F, in WT cells, 4-OI dose dependently increased LDH release, reaching 20 % at 250 µM, while 300 nM KPT-330 lead to 50 % LDH release. In XPO1^{C528S} cells however, while higher basally, LDH release did not increase significantly with 4-OI or KPT-330. These data suggest that CRM1 inhibition by C528 dicarboxypropylation is at least partly responsible for 4-OI induced cell death and might explain some of 4-OI's toxicity.

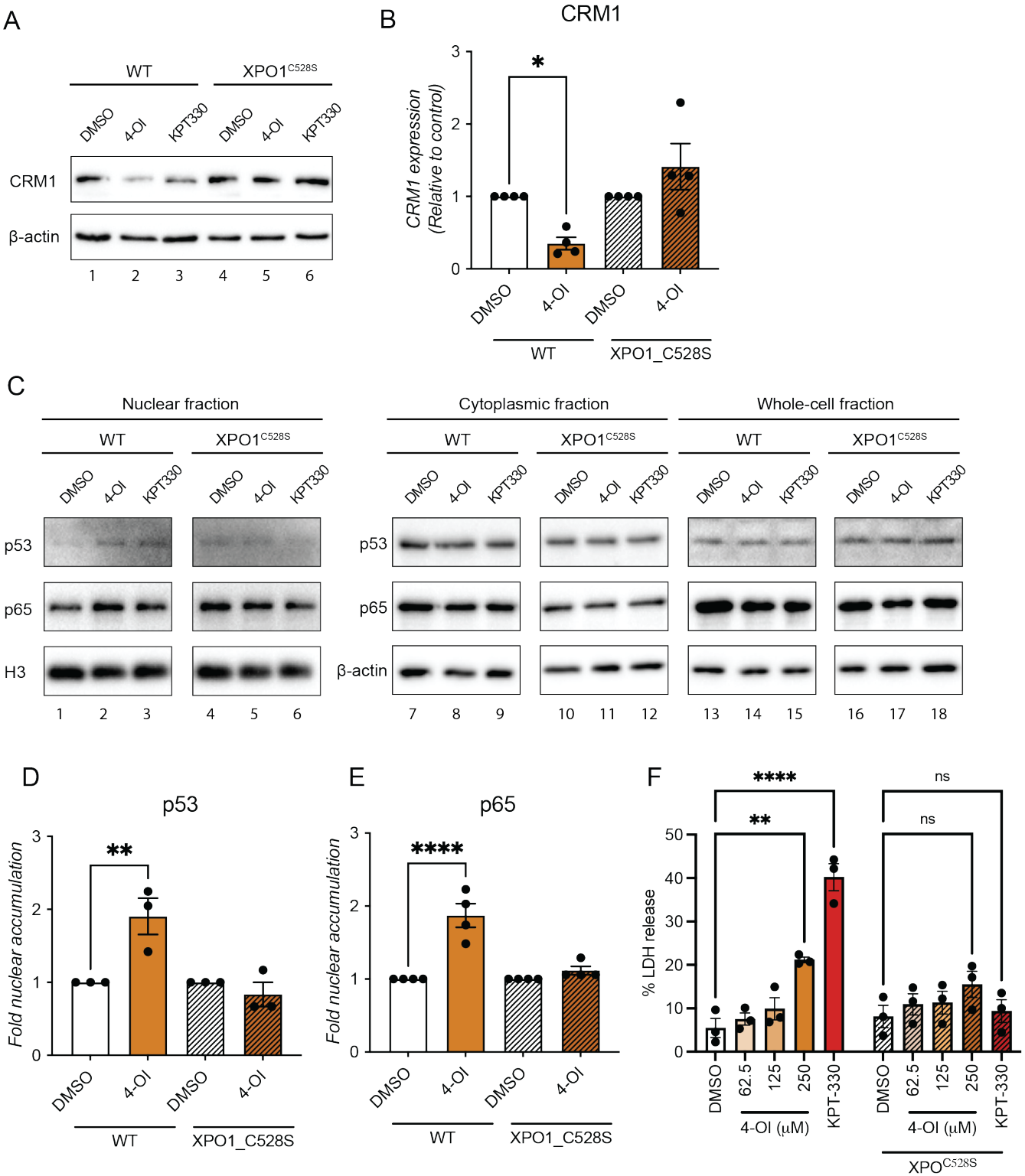

A
WT
XPO1C528S
DMSO
4-OI
KPT330
CRM1
β-actin
1 2 3 4 5 6
B
CRM1
CRM1 expression (Relative to control)
*
WT
XPO1_C528S
C
Nuclear fraction
Cytoplasmic fraction
Whole-cell fraction
p53
p65
H3
β-actin
1 2 3 4 5 6 7 8 9 10 11 12 13 14 15 16 17 18
D
p53
Fold nuclear accumulation
**
E
p65
****
F
% LDH release
****
**
ns
ns
62.5
125
250
KPT-330
4-OI (μM)
XPOC528S

Figure 4.17: Deactivation of CRM1 by 4-OI-mediated C528 alkylation.

(A) CRM1 protein expression levels in Jurkat and Jurkat XPO1^{C528S} cells. The cells (5 x 10^5 cells) were treated with either DMSO, 250 μM 4-OI or 25 nM KPT-330 for 24 h. CRM1 protein expression levels were assessed by western blotting and β-actin was used as loading control. Blots are representative of 4 individual experiments. **(B)** Densitometry of blots shown in A. Protein levels have been normalized relative to the untreated control of the respective cell line. **(C)** Expression levels of p65 and p53 protein in nucleus, cytoplasm and whole cell fractions of Jurkat and Jurkat XPO1^{C528S} cells (5 x 10^5 cells) upon 4-OI treatment. The cells were treated with DMSO, 250 μM 4-OI or 100 nM KPT330 for 2 h and nuclear-cytoplasmic fractionation was performed. H3 was used as loading control for nuclear fractions and β-actin for cytoplasmic and whole-cell fractions. Blots are representative of 4 (p65, CRM1), or 3 individual experiments (p53). (**D-E)** Densitometry of blots shown in C. Protein levels have been normalized relative to the untreated control of the respective cell line. **(F)** LDH release was measured in Jurkat and Jurkat XPO1^{C528S} cells (5 x 10^5 cells) treated with indicated concentrations of 4-OI or 300 nM KPT330 for 24 h. Data is representative of 3 individual experiments. Data are mean ± SD for n=4 (B, E), mean ± SD for n=3 (D), and mean ± SEM for n=3 (F), and. *p<0.05, **p<0.01, ****p<0.0001 as calculated using a one-way ANOVA followed by Sidak's multiple comparisons test.

4.5.2 4-OI alters RanBP1 protein levels and subcellular location through CRM1 alkylation

CRM1 binds to various co-factors to facilitate nuclear export. One of these factors, RanBP1, associates with CRM1 and assists in releasing the cargo from the exporter once outside the nucleus [218]. In that sense, RanBP1 itself is a cargo of CRM1 and has been found to be accumulated in the nucleus upon CRM1 inhibition [219]. Upon 24 h treatment with both 4-OI and KPT-330, RanBP1 protein levels were decreased in WT Jurkat cells (Fig. 4.18 A, lanes 2 and 3 compared to 1). As RanBP1 does not come up in the mass spec screen used to identify CRM1 as a binding target of 4-OI, we can assume that RanBP1 is not directly dicarboxypropylated by 4-OI. In XPO1^{C528S} cells however, RanBP1 protein levels are unchanged after 4-OI (lane 5) or KPT-330 (lane 6) treatment, suggesting the RanBP1 downregulation to be indirectly caused by the 4-OI facilitated degradation of CRM1. Basal RanBP1 levels in XPO1^{C528S} cells (lane 4) were slightly lower than in WT cells (lane 1). These results were quantified by densitometry in figure 4.17 B.

Examining the subcellular localisation of RanBP1, we were able to show its localisation to the nucleus upon treatment with 4-OI similarly to the other CRM1 cargos p53 and p65 in WT (Fig. 18 C lane 2), but not XPO1^{C528S} (lane 5) cells. RanBP1 protein levels in cytosolic and total fractions remained unchanged (lanes 7 – 18). Quantification of the nuclear accumulation of RanBP1 after 4-OI treatment can be found in figure 4.17 D.

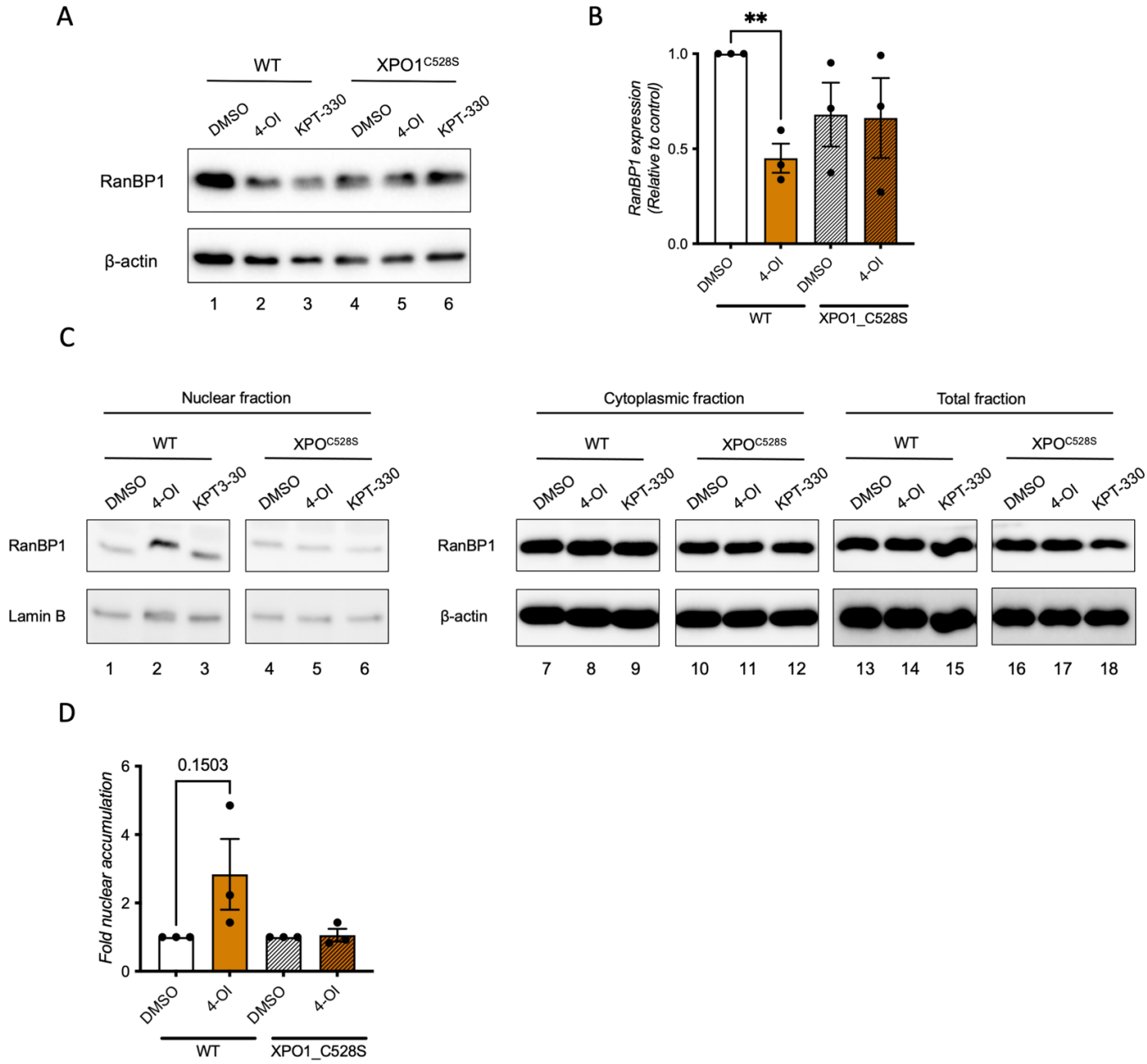


Figure 4.18: 4-OI reduces RanBP1 protein levels in a CRM1 dependent manner.

(A) RanBP1 protein expression levels in Jurkat and Jurkat XPO1^{C528S} cells. The cells (5 x 10^5 cells) were treated with either DMSO, 250 μM 4-OI or 25 nM KPT-330 for 24 h. RanBP1 protein expression levels were assessed by western blotting. Blots are representative of 4 individual experiments. (**B)** Densitometry of blots shown in C. Protein levels have been normalized relative to the untreated control of the respective cell line. **C.** Expression levels of RanBP1 protein in nucleus, cytoplasm and whole cell fractions of Jurkat and Jurkat XPO1^{C528S} cells upon 4-OI treatment. The cells (5 x 10^5 cells) were treated with DMSO, 250 μM 4-OI or 100 nM KPT330 for 2 h and nuclear-cytoplasmic fractionation was performed. Blots are representative of 3 individual experiments. (**D)** Densitometry of blots shown in C. Protein levels have been normalized relative to the untreated control of the respective cell line. Data are mean ± SD for n=3. **p<0.01 as calculated using a one-way ANOVA followed by Sidak's multiple comparisons test.

Overall, these data indicate that the antiviral effect of 4-OI against IAV is based on targeting the C528 on CRM1, affecting the nuclear export of the NP of IAV, as well as other CRM1-dependent cargos, such as FIV Rev, RanBP1, p53 and p65.

4.6 Discussion

4.6.1 4-OI and Influenza

Results from SARS-CoV-2 prompted an examination of 4-OI in other RNA viruses. Despite suggested broad antiviral effects of 4-OI, a screening attempt in 6 different RNA viruses yielded only reduced replication after 4-OI treatment in one virus – IAV. This is surprising given some of the viruses tested had since been shown to be restricted in replication by 4-OI, such as HSV [179], or HMPV (unpublished, seen at a conference). For some of the viruses tested we only performed the experiments once, which is why the data is not shown in this thesis, so maybe with optimization different results could have been achieved. For HMPV however, our data clearly disagrees with observations from other labs, as replication was monitored closely with both 4-OI and itaconate. In contrast, reduced replication in IAV with 4-OI was robust, and could be observed across multiple cell types and virus strains. Importantly, itaconate failed to mirror results achieved with 4-OI once again. As HMPV does not depend on CRM1 for its replication, these negative results actually support the hypothesis that the antiviral effect of 4-OI is through suppression of CRM1 activity.

After conducting experiments on IAV replication, a paper from the Frank Pessler group came out confirming our observations [168]. In this work, Sohail et al. extensively discuss the impact 4-OI and other members of the itaconate family have on IAV replication and IFN responses towards the virus. Interestingly, they found itaconate to restrict IAV replication, however to a much lower degree that 4-OI. In that

regard, our results diverge as we did not observe an antiviral effect using the unmodified metabolite.

As I got negative results from the screens on viruses besides IAV, I speculated on a more virus specific effect, prompting an investigation into features that distinguish IAV from the other viruses examined.

A definitive receptor for IAV is not known, however viral entry into cells is known to occur in tetraspanin-high regions on the cell surface and via binding to sialic acids [75]. Tetraspanins are expressed on the surface of the cell and are mainly involved in membrane protein organisation [220]. Two tetraspanins, CD9 and CD81 have been especially associated with IAV entry [221]. When assessing surface expression of CD9 and CD81 however, No changes were observed with 4-OI. Additionally, an HA fusion assay didn't reveal any changes in fusion of the viral particles with the membrane. Viral uptake is therefore unlikely to be affected by 4-OI.

4.6.2 IAV replication is halted at the NP export stage

First evidence for a mechanism came in the form of a subcellular localization assay of IAV NP, which proved to be accumulated with 4-OI in the nucleus. In fact, this had been observed already in a previous work with other itaconate derivatives, but not with itaconate or 4-OI itself [180]. Replication of Influenza occurs in the nucleus and import and export of viral RNA and proteins depend on the transport machinery of the host. The above mentioned study screened for potential antiviral molecules, and was able to narrow a selection of 20,000 compounds down to a few itaconate derivatives that show potential as antivirals against influenza [180]. While

none of these molecules were 4-OI or itaconate itself, the paper suggested the mechanism to be potentially dependent on the inhibition of export of viral RNA from the nucleus. This specific step in the IAV replication cycle was therefore examined. The viral protein NP is associated with the viral RNA, making up the vRNP. When investigating the subcellular location of the vRNP after 4-OI treatment, it was confined to the nucleus even 48 h post inoculation, while untreated cells were full of vRNP in both nucleus and cytoplasm. This result suggests that while the nuclear import and replication of the vRNP are intact, its export to the cytoplasm is inhibited.

4.6.3 CRM1 inhibition – a possible mechanism?

The cellular transporter relevant for vRNP export, CRM1, is a target for antiviral drug discovery, and CRM1 inhibitors are known to slow down influenza replication [86,222,223]. Interestingly, the mode of action of many CRM1 inhibitors is the alkylation of a specific cysteine residue, C528 [224], similar to the dicarboxypropylation induced by itaconate and 4-OI. In a 2020 publication by Chu Wang, a screen was conducted using a bioorthogonal probe, itaconate-alkyne (ITalk), to highlight proteins that could potentially be modified by itaconate. CRM1 came up in this screen as a potential target for members of the itaconate family [214].

As this modification has been shown to release inactivated CRM1 from the nucleus to the cytosol [85], the subcellular distribution of CRM1 and its targets was investigated. Indeed, 4-OI lead to CRM1 accumulation in the cytosol, while export targets of CRM1, such as p53, p65 or RanBP1 were accumulated in the nucleus. Assays specifically designed to measure and quantify CRM1 activity conducted by the group

of Dirk Daelemans, an expert in the field of CRM1 research supported our results by showing a dose dependent decrease of CRM1 activity with 4-OI. The concept of inhibition of IAV replication through deactivation of CRM1 is shown in figure 4.19.

4.6.4 Dicarboxypropylation of C528 by 4-OI inhibits CRM1

The modification of C528 by 4-OI was demonstrated by conducting iodoacetamide-desthiobiotin (IA-DTB)-based competitive cysteine profiling. Both 4-OI and the clinically approved CRM inhibitor KPT-330 did not only deactivate, but also degrade CRM1, as protein levels were decreased while mRNA levels were slightly increased in epithelial cells. Intriguingly however, the opposite was observed with 4-OI in BMDMs. Here, 4-OI actually increased CRM1 protein levels. It is not clear from our results whether this is a human-mouse, or an epithelial-myeloid cell difference. C528 however is conserved between the species and KPT-330 had been shown to inhibit nuclear export in human and mouse cells alike [139]. It can therefore be assumed that 4-OI targets CRM1 in BMDMs as well, but alkylation in these cells does not seem to lead to degradation. The increase might in fact be an indication of the non-functionality of modified CRM1 in BMDMs, as the cell might try to compensate for the loss of export function. This is mirrored by an increase of CRM1 mRNA with 4-OI in human epithelial cells, which had previously also been described for KPT-330 [225].

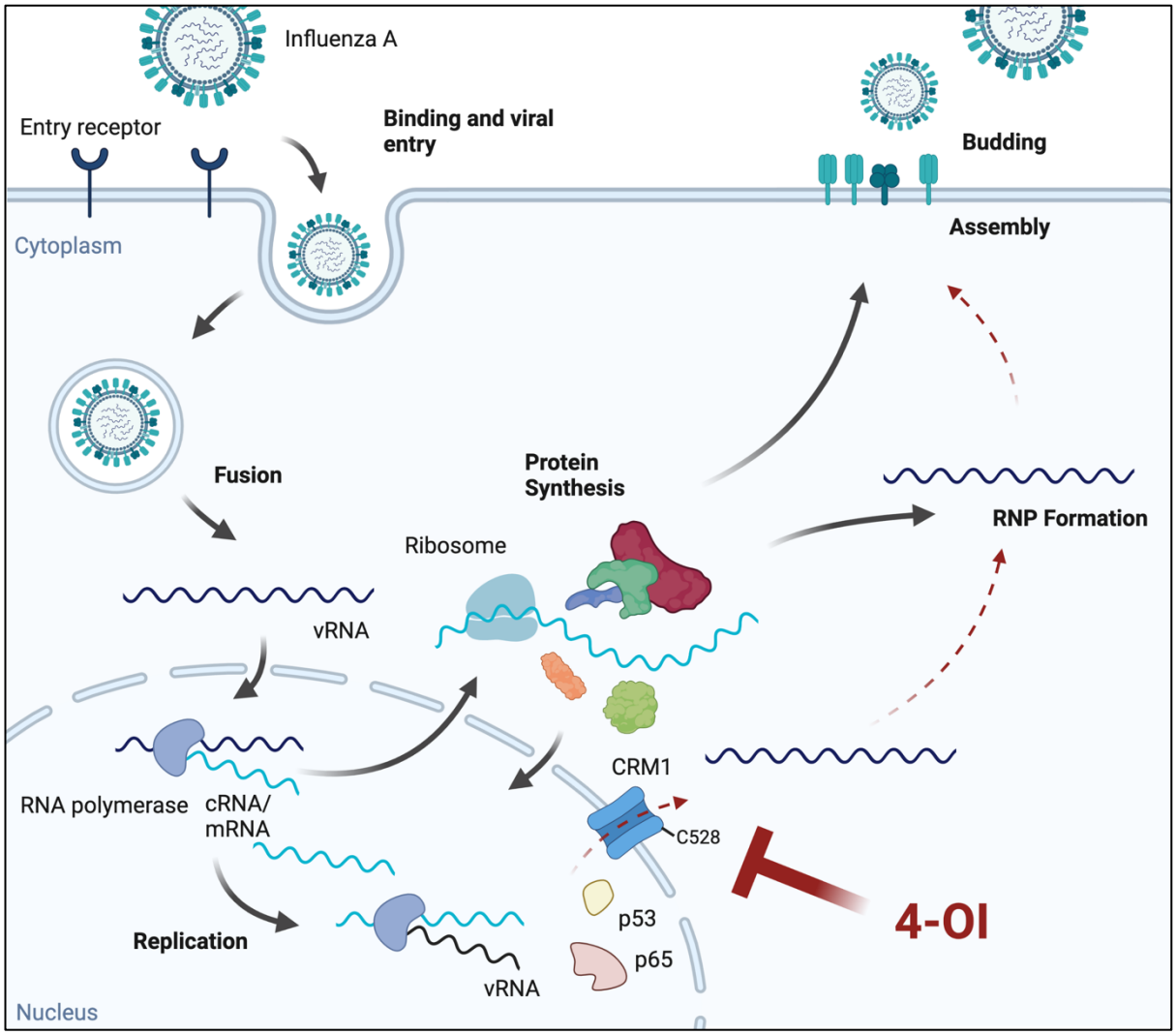


Figure 4.19: Proposed mechanism of 4-OI inhibiting IAV replication.

4-OI was shown to potently inhibit nuclear protein export by the transporter CRM1. Exporting RNA into the cytosol after replication in the nucleus is a crucial step in the life cycle of IAV. Inhibition of this step interferes drastically with the assembly of new viral particles and thus slows down viral replication.

The degradation of CRM1 with 4-OI in epithelial cells is likely to be through the proteasome, as alkylation of C528 in CRM1 had been shown to lead to CRM1 degradation through this pathway [225]. As poly-ubiquitination is a crucial part of the degradation machinery [226], whether dicarboxypropylaltion might lead to ubiquitination of the target protein and thus degradation was considered. While 4-OI did actually increase global ubiquitination events, a direct ubiquitination of CRM1 as a result of 4-OI treatment could not be confirmed. The degradation mechanism thus remains subject to speculation.

Deactivation of CRM1 appeared to occur through the above mentioned alkylation of C528 since in the Jurkat XPO1^{C528S} cell line, CRM1 degradation and retention of nuclear export cargos did not occur with 4-OI. Additionally, these cells were protected from cytotoxic effects induced by high concentrations of 4-OI that could potentially be caused by prolonged inhibition of CRM1. As cytotoxic concentrations were above concentrations needed to retain NP in the nucleus, cytotoxicity however can be ruled out as an explanation for the antiviral effect of 4-OI.

While ideal for studying the cysteine modification induced by 4-OI, these cells were not well suited to study the effect on IAV replication as IAV cannot replicate in these cells. Therefore, the 4-OI-mediated alkylation of CRM1 was assessed once again using cellular cargos of CRM1, demonstrating modification of C528 to be crucial for the 4-OI mediated inactivation of CRM1. CRM1 is modified by 4-OI in additional positions that were not directly assessed, however the lack of an effect by 4-OI observed in the knock-in cells point towards C528 being the relevant position. Figure 4.20 highlights the position CRM1 is modified in by 4-OI.

We were unable to investigate the potential antiviral role of endogenous itaconate in this context, as itaconate production is restricted to cells of the myeloid lineage. Exogenous itaconate had once again no effect on viral replication, neither did it decrease CRM1 activity. As discussed above, this could be attributed to inability of itaconate to enter the cell, or simply to a 4-OI specific effect due to increased electrophilicity.

Overall, I have demonstrated 4-OI to be an antiviral agent against IAV, revealing inhibition of CRM1 and subsequent interruption of the viral life cycle at the nuclear export stage as a likely mechanism of action.

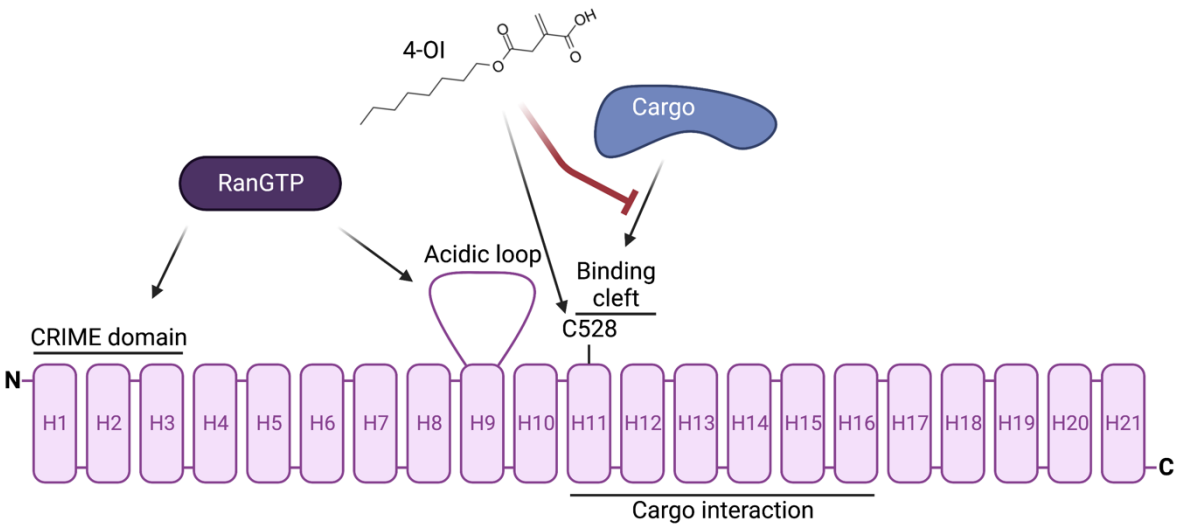


Figure 4.20: 4-OI binds CRM1 at C528, blocking cargo binding.

CRM1 consists of 21 HEAT domains. The CRIME domain in HEAT 1 – 3 , and the acidic loop in HEAT 9 bind RanGTP. HEAT 11 – 16 interact with cargo proteins, while the cargo binding cleft consists of HEAT 11 and 12. 4-OI binds the cargo binding cleft at C528 in HEAT 11, blocking association of the cargo with CRM1. This figure was modified after figure 1 in Ferreira et al., 2020. [227]

Chapter 5: General discussion

5.1 Itaconate derivatives as antivirals?

This work explored the antiviral potential of 4-OI. The mechanisms uncovered here have implications for the understanding of how members of the itaconate family shape cell biology. The key finding is the inhibition of CRM1, but while this was explored mainly from an antiviral perspective, there are also other areas that become of interest now that this particular effect has been revealed. Itaconate derivatives have been developed as potential drugs, making 4-OI not only a tool compound, but also a proto-drug.

Since CRM1 function is involved in the replication cycle of many different viruses, the mechanism proposed here might explain antiviral effects of 4-OI described for other viruses besides IAV. In fact, all viruses sensitive to 4-OI treatment as reported by Olagnier et al. have been described to depend on CRM1 in some capacity for their replication [131,179,228–230]. This indicates that 4-OI could have an effect against viruses that depend on CRM1-mediated cargo export from the nucleus [179]. Another example of well-characterized CRM1-mediated nuclear export has been described for FIV and HIV [231]. 4-OI or derivatives based on it could have activity against HIV. As proof of principle, translocation of the Rev protein of FIV from the nucleus to the cytoplasm upon treatment with actinomycin D was impaired in the presence of 4-OI in a similar manner as described in previous studies for HIV Rev protein [213]. In addition to host CRM1, it is also possible that 4-OI modifies viral proteins, potentially affecting viral replication.

Itaconate derivatives as potential antiviral drugs might have a key advantage over many conventional therapeutics. Besides restricting viral replication, itaconate

derivatives, such as 4-OI have well described anti-inflammatory properties. As it has been described previously by Sohail et al., 4-OI can reduce IFN mediated inflammatory responses without allowing the IAV burden to increase despite the decreased antiviral response of the immune system [232]. Additionally, unpublished work from our lab has shown that 4-OI can reduce blood clotting by blocking expression and release of tissue factor (TF), a hallmark of COVID-19, while simultaneously being able to restrict replication of SARS-CoV-2. This "double edged sword" could potentially be useful especially in more severe infections, where reduction of inflammatory responses is crucial for patient survival. While influenza is usually a relatively mild infection for most people, the intense flu season in the winter of 22/23 has shown how heavy of a burden this virus can lay on the healthcare system, and how severe disease caused by this virus can be at times, especially with other respiratory viruses like RSV and SARS-CoV-2 circulating as well. Given my results, this potential of course applies to SARS-CoV-2 as well. I have summarized factors through which 4-OI can be potentially beneficial in a viral infection in figure 5.1. The potential of itaconate derivatives in infectious diseases targeting both the pathogen and the host immune system alike was explored in more detail in a recent publication by McGettrick et al. [233].

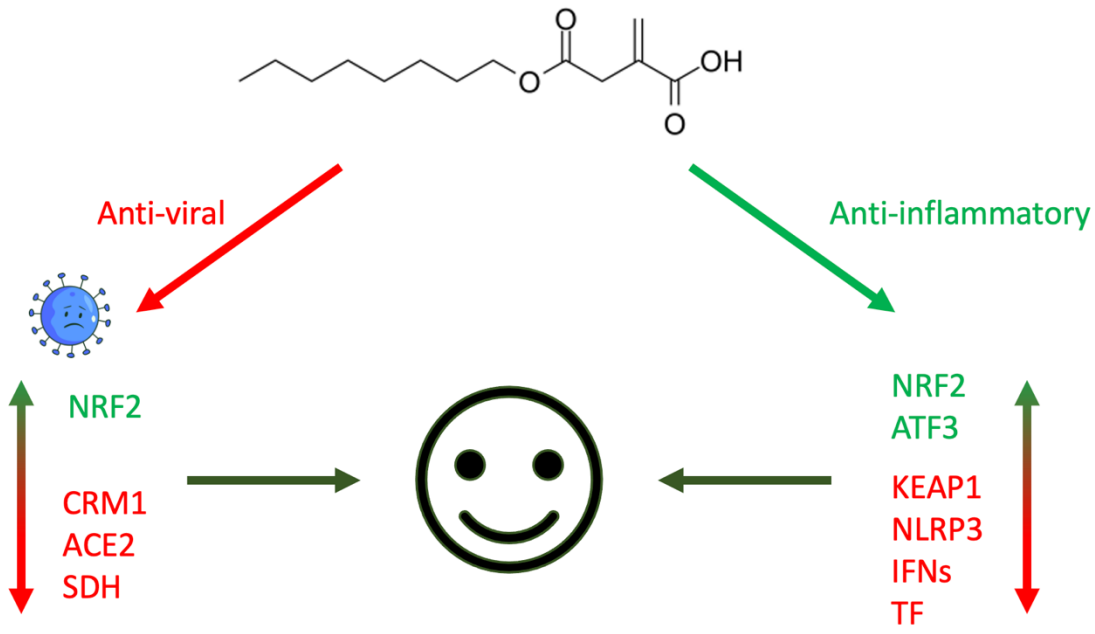


Figure 5.1: Two for the price of one.

4-OI has the unique potential to resolve virus based diseases by being anti-inflammatory and antiviral at the same time. Antiviral factors include the upregulation of NRF2, as well as the downregulation of SDH, and the in this work revealed targets CRM1 and ACE2. On the other hand, 4-OI has been shown to restrict virus induced inflammation by activating NRF2 and ATF3, while restricting KEAP1, NLRP3, IFNs, or TF.

5.2 The price of CRM1 inhibition

In general, CRM1 inhibitors have come up as potential antivirals multiple times. Most recently, the clinically approved CRM1 inhibitor KPT-330 had been trialled in SARS-CoV-2 after its antiviral potential in this virus was found [130]. While successful, most CRM1 inhibitors have fallen short of being seriously considered as an actual antiviral drug. The reason for this cautiousness is the severe side effects a prolonged inhibition of CRM1 can have. In the case of KPT-330, these can include severe nausea, vomiting, diarrhoea, loss of appetite, or weight loss [234]. An important factor in the severity of these effects is the mode of modification of C528 in CRM1. The first described CRM1 inhibitor LMB irreversibly modifies the structures of the binding groove, making it highly cytotoxic [235], while modern SINEs are reversible inhibitors [86]. Dicarboxypropylation by itaconate and 4-OI is irreversible, calling for a more careful application of this molecule group in potential patients if ever considered for clinical use [155]. If used as an antiviral, itaconate derivatives may be most useful for more severe viral infections and under close supervision, as CRM1 mediated side effects could not be excluded. With the added benefit of being an anti-inflammatory agent through a separate mechanism however, itaconate derivatives have an advantage over convectional CRM1 inhibitors for use in infectious diseases. More carefully designed itaconate based drugs that have a fast turnover could be used to specifically target only individual replication rounds to drive down replication while having a minimal impact on cellular function.

5.3 Broadening the horizon

The finding that nuclear translocation of cellular cargos of CRM1, p65 and p53 were as much affected by 4-OI treatment as the above-mentioned viral components, implies that itaconate and its derivatives can alter multiple processes in cells. The subcellular equilibrium of proteins is delicate and can cause major irregularities when disturbed. One of these irregularities is cancer, many of whose forms are characterized by an overexpression or hyperactivity of CRM1 [101,236,237]. For this reason SINEs have primarily been studied as anti-cancer agents [116,227,238], with KPT-330 being approved for treatment of multiple myeloma by the FDA [239]. Decreasing CRM1 overexpression in cancer cells allows for CRM1 dependent anti-tumour factors to accumulate in the nucleus, slowing down cancerous growth. One of these factors, p53, was highlighted as a cargo in our study and shown to locate to the nucleus upon 4-OI treatment, while the generally anti-inflammatory profile of itaconate and 4-OI might argue against the consideration of this molecule group as anti-cancer agents. In the literature, there is mixed data on the role of itaconate in cancer. Dimethyl itaconate for instance was able to protect from colitis-associated colorectal cancer (CAC), which was however mostly attributed to reduced inflammation in the tumour microenvironment, which is beneficial in this specific cancer [240]. More recently, 4-OI was found to be able to restrict the formation of metastasis in ovarian cancer *in vivo* [241].

Unmodified itaconate on the other hand had mostly been associated with tumour progression. Itaconate levels correlated with bad prognoses in a variety of peritoneal tumours [242]. Additionally, Irg1 was found to be upregulated in tumour-

associated macrophages (TAMs) [242], crucial facilitators of tumour growth, invasion, and metastasis [243]. Conversely, Irg1 was found to be upregulated in cells isolated from patients with ovarian cancer, and acted as a proto-oncogene role in glioma, leading to poor prognosis [244]. Recently, itaconate released from Myeloid-derived suppressor cells (MDSCs) has been shown to suppresses $CD8^+$ T-cell effector function and promotes tumour growth [245].

Once again, a common theme throughout this thesis emerges: The divergence between itaconate and 4-OI. In cancer, it seems clear that IRG1 and itaconate have cancer promoting properties, while its more electrophilic derivatives seem to be able to restrict tumour progression in some instances. Considering 4-OI as potential proto-drug in cancer however, pro-tumour effects of itaconate need to be taken into consideration. Application would only make sense in tumours that arise from overexpression of CRM1. As this is a common enough feature in many cancers, there is room for 4-OI to be studied more intensely in tumour biology, and the data we are presenting here opens the door for the itaconate family to be explored from this angle as well.

Cysteine modifiers have been suggested as both anti-cancer, and ant-viral drug candidates for more than 20 years [246], with Selinexor of course being an example of successful implementation. With the clinical approval of Dimethyl fumarate (DMF) for use in relapsing Multiple Sclerosis (MS) in 2013, a lot of doors were opened for cysteine modifiers in general, and metabolite derivatives specifically to be considered for drug development. Today, multiple companies are working on itaconate derivatives as potential drugs, despite having a broad range of effects. Identification

of a specific target (like for example CRM1), paired with a broad anti-inflammatory profile might be desirable for some pathologies.

In conclusion, we hope the discoveries presented in this work may not only expand the knowledge on the many functions of the members of the itaconate family, but also inspire fellow scientists to consider itaconate and other metabolites with a broad interactive spectrum as a starting point to design novel therapeutics for viral and inflammatory diseases, as well as in oncology.

Chapter 6: References

1. Marshall, J.S.; Warrington, R.; Watson, W.; Kim, H.L. An introduction to immunology and immunopathology. *Allergy, Asthma Clin. Immunol.* **2018**, *14*, 49, doi:10.1186/s13223-018-0278-1.
2. van Furth, R.; Cohn, Z.A.; Hirsch, J.G.; Humphrey, J.H.; Spector, W.G.; Langevoort, H.L. The mononuclear phagocyte system: a new classification of macrophages, monocytes, and their precursor cells. *Bull. World Health Organ.* **1972**, *46*, 845–52.
3. Jennings, B.H. Drosophila – a versatile model in biology & medicine. *Mater. Today* **2011**, *14*, 190–195, doi:10.1016/S1369-7021(11)70113-4.
4. Poltorak, A.; He, X.; Smirnova, I.; Liu, M.-Y.; Huffel, C. Van; Du, X.; Birdwell, D.; Alejos, E.; Silva, M.; Galanos, C.; et al. Defective LPS Signaling in C3H/HeJ and C57BL/10ScCr Mice: Mutations in Tlr4 Gene. *Science* **1998**, *282*, 2085–2088, doi:10.1126/science.282.5396.2085.
5. Alexopoulou, L.; Holt, A.C.; Medzhitov, R.; Flavell, R.A. Recognition of double-stranded RNA and activation of NF-κB by Toll-like receptor 3. *Nature* **2001**, *413*, 732–738, doi:10.1038/35099560.
6. Hayashi, F.; Smith, K.D.; Ozinsky, A.; Hawn, T.R.; Yi, E.C.; Goodlett, D.R.; Eng, J.K.; Akira, S.; Underhill, D.M.; Aderem, A. The innate immune response to bacterial flagellin is mediated by Toll-like receptor 5. *Nature* **2001**, *410*, 1099–1103, doi:10.1038/35074106.
7. Heil, F.; Hemmi, H.; Hochrein, H.; Ampenberger, F.; Kirschning, C.; Akira, S.; Lipford, G.; Wagner, H.; Bauer, S. Species-Specific Recognition of Single-Stranded RNA via Toll-like Receptor 7 and 8. *Science* **2004**, *303*, 1526–1529, doi:10.1126/science.1093620.

8. Takeuchi, O.; Hoshino, K.; Kawai, T.; Sanjo, H.; Takada, H.; Ogawa, T.; Takeda, K.; Akira, S. Differential Roles of TLR2 and TLR4 in Recognition of Gram-Negative and Gram-Positive Bacterial Cell Wall Components. *Immunity* **1999**, *11*, 443–451, doi:10.1016/S1074-7613(00)80119-3.

9. Takeuchi, O.; Kawai, T.; Mühlradt, P.F.; Morr, M.; Radolf, J.D.; Zychlinsky, A.; Takeda, K.; Akira, S. Discrimination of bacterial lipoproteins by Toll-like receptor 6. *Int. Immunol.* **2001**, *13*, 933–940, doi:10.1093/intimm/13.7.933.

10. Hemmi, H.; Takeuchi, O.; Kawai, T.; Kaisho, T.; Sato, S.; Sanjo, H.; Matsumoto, M.; Hoshino, K.; Wagner, H.; Takeda, K.; et al. A Toll-like receptor recognizes bacterial DNA. *Nature* **2000**, *408*, 740–745, doi:10.1038/35047123.

11. Guan, Y.; Ranoa, D.R.E.; Jiang, S.; Mutha, S.K.; Li, X.; Baudry, J.; Tapping, R.I. Human TLRs 10 and 1 Share Common Mechanisms of Innate Immune Sensing but Not Signaling. *J. Immunol.* **2010**, *184*, 5094–5103, doi:10.4049/jimmunol.0901888.

12. Yarovinsky, F.; Zhang, D.; Andersen, J.F.; Bannenberg, G.L.; Serhan, C.N.; Hayden, M.S.; Hieny, S.; Sutterwala, F.S.; Flavell, R.A.; Ghosh, S.; et al. TLR11 activation of dendritic cells by a protozoan profilin-like protein. *Science* **2005**, *308*, 1626–9, doi:10.1126/science.1109893.

13. Hatai, H.; Lepelley, A.; Zeng, W.; Hayden, M.S.; Ghosh, S. Toll-Like Receptor 11 (TLR11) Interacts with Flagellin and Profilin through Disparate Mechanisms. *PLoS One* **2016**, *11*, e0148987, doi:10.1371/journal.pone.0148987.

14. Oldenburg, M.; Krüger, A.; Ferstl, R.; Kaufmann, A.; Nees, G.; Sigmund, A.; Bathke, B.; Lauterbach, H.; Suter, M.; Dreher, S.; et al. TLR13 Recognizes Bacterial 23 S rRNA Devoid of Erythromycin Resistance–Forming Modification.

Science **2012**, *337*, 1111–1115, doi:10.1126/science.1220363.

15. Jin, M.S.; Kim, S.E.; Heo, J.Y.; Lee, M.E.; Kim, H.M.; Paik, S.-G.; Lee, H.; Lee, J.-O. Crystal Structure of the TLR1-TLR2 Heterodimer Induced by Binding of a Tri-Acylated Lipopeptide. *Cell* **2007**, *130*, 1071–1082, doi:10.1016/j.cell.2007.09.008.
16. Andrade, W.A.; Souza, M. do C.; Ramos-Martinez, E.; Nagpal, K.; Dutra, M.S.; Melo, M.B.; Bartholomeu, D.C.; Ghosh, S.; Golenbock, D.T.; Gazzinelli, R.T. Combined Action of Nucleic Acid-Sensing Toll-like Receptors and TLR11/TLR12 Heterodimers Imparts Resistance to Toxoplasma gondii in Mice. *Cell Host Microbe* **2013**, *13*, 42–53, doi:10.1016/j.chom.2012.12.003.
17. Rosenstiel, P.; Till, A.; Schreiber, S. NOD-like receptors and human diseases. *Microbes Infect.* **2007**, *9*, 648–657, doi:10.1016/j.micinf.2007.01.015.
18. Inohara, N.; Koseki, T.; del Peso, L.; Hu, Y.; Yee, C.; Chen, S.; Carrio, R.; Merino, J.; Liu, D.; Ni, J.; et al. Nod1, an Apaf-1-like Activator of Caspase-9 and Nuclear Factor-κB. *J. Biol. Chem.* **1999**, *274*, 14560–14567, doi:10.1074/jbc.274.21.14560.
19. Rehwinkel, J.; Gack, M.U. RIG-I-like receptors: their regulation and roles in RNA sensing. *Nat. Rev. Immunol.* **2020**, *20*, 537–551, doi:10.1038/s41577-020-0288-3.
20. Yoneyama, M.; Kikuchi, M.; Natsukawa, T.; Shinobu, N.; Imaizumi, T.; Miyagishi, M.; Taira, K.; Akira, S.; Fujita, T. The RNA helicase RIG-I has an essential function in double-stranded RNA-induced innate antiviral responses. *Nat. Immunol.* **2004**, *5*, 730–737, doi:10.1038/ni1087.
21. Kutikhin, A.; Yuzhalin, A. C-type lectin receptors and RIG-I-like receptors: new points on the oncogenomics map. *Cancer Manag. Res.* **2012**, 39,

doi:10.2147/CMAR.S28983.

22. Neth, O.; Jack, D.L.; Dodds, A.W.; Holzel, H.; Klein, N.J.; Turner, M.W. Mannose-Binding Lectin Binds to a Range of Clinically Relevant Microorganisms and Promotes Complement Deposition. *Infect. Immun.* **2000**, *68*, 688–693, doi:10.1128/IAI.68.2.688-693.2000.

23. Weiss, H.J.; O'Neill, L.A.J. Of Flies and Men—The Discovery of TLRs. *Cells* **2022**, *11*, 3127, doi:10.3390/cells11193127.

24. Ye, Y.; Gaugler, B.; Mohty, M.; Malard, F. Plasmacytoid dendritic cell biology and its role in immune-mediated diseases. *Clin. Transl. Immunol.* **2020**, *9*, doi:10.1002/cti2.1139.

25. Ma, Y.; Zhang, Y.; Zhu, L. Role of neutrophils in acute viral infection. *Immunity, Inflamm. Dis.* **2021**, *9*, 1186–1196, doi:10.1002/iid3.500.

26. Vivier, E.; Tomasello, E.; Baratin, M.; Walzer, T.; Ugolini, S. Functions of natural killer cells. *Nat. Immunol.* **2008**, *9*, 503–510, doi:10.1038/ni1582.

27. Miura, T.A. Respiratory Epithelial Cells as Master Communicators during Viral Infections. *Curr. Clin. Microbiol. Reports* **2019**, *6*, 10–17, doi:10.1007/s40588-019-0111-8.

28. Weber, F. Antiviral Innate Immunity: Introduction. In *Encyclopedia of Virology*; Elsevier, 2021; pp. 577–583.

29. Kumari, P.; Russo, A.J.; Shivcharan, S.; Rathinam, V.A. AIM2 in health and disease: Inflammasome and beyond. *Immunol. Rev.* **2020**, *297*, 83–95, doi:10.1111/imr.12903.

30. Unterholzner, L.; Keating, S.E.; Baran, M.; Horan, K.A.; Jensen, S.B.; Sharma, S.; Sirois, C.M.; Jin, T.; Latz, E.; Xiao, T.S.; et al. IFI16 is an innate immune sensor

for intracellular DNA. *Nat. Immunol.* **2010**, *11*, 997–1004, doi:10.1038/ni.1932.

31. Carty, M.; Guy, C.; Bowie, A.G. Detection of Viral Infections by Innate Immunity. *Biochem. Pharmacol.* **2021**, *183*, 114316, doi:10.1016/j.bcp.2020.114316.
32. Chowdhury, A.; Witte, S.; Aich, A. Role of Mitochondrial Nucleic Acid Sensing Pathways in Health and Patho-Physiology. *Front. Cell Dev. Biol.* **2022**, *10*, doi:10.3389/fcell.2022.796066.
33. Wu, J.; Chen, Z.J. Innate Immune Sensing and Signaling of Cytosolic Nucleic Acids. *Annu. Rev. Immunol.* **2014**, *32*, 461–488, doi:10.1146/annurev-immunol-032713-120156.
34. Fujita, T.; Sakakibara, J.; Sudo, Y.; Miyamoto, M.; Kimura, Y.; Taniguchi, T. Evidence for a nuclear factor(s), IRF-1, mediating induction and silencing properties to human IFN-beta gene regulatory elements. *EMBO J.* **1988**, *7*, 3397–3405, doi:10.1002/j.1460-2075.1988.tb03213.x.
35. Jiang, Z.; Mak, T.W.; Sen, G.; Li, X. Toll-like receptor 3-mediated activation of NF-κB and IRF3 diverges at Toll-IL-1 receptor domain-containing adapter inducing IFN-β. *Proc. Natl. Acad. Sci.* **2004**, *101*, 3533–3538, doi:10.1073/pnas.0308496101.
36. Samten, B.; Townsend, J.C.; Weis, S.E.; Bhoumik, A.; Klucar, P.; Shams, H.; Barnes, P.F. CREB, ATF, and AP-1 Transcription Factors Regulate IFN-γ Secretion by Human T Cells in Response to Mycobacterial Antigen. *J. Immunol.* **2008**, *181*, 2056–2064, doi:10.4049/jimmunol.181.3.2056.
37. Weerd, N.A.; Nguyen, T. The interferons and their receptors—distribution and regulation. *Immunol. Cell Biol.* **2012**, *90*, 483–491, doi:10.1038/icb.2012.9.
38. Sharma, S. Triggering the Interferon Antiviral Response Through an IKK-

Related Pathway. *Science (80-.).* **2003**, *300*, 1148–1151, doi:10.1126/science.1081315.

39. Honda, K.; Yanai, H.; Negishi, H.; Asagiri, M.; Sato, M.; Mizutani, T.; Shimada, N.; Ohba, Y.; Takaoka, A.; Yoshida, N.; et al. IRF-7 is the master regulator of type-I interferon-dependent immune responses. *Nature* **2005**, *434*, 772–777, doi:10.1038/nature03464.

40. Schoenborn, J.R.; Wilson, C.B. Regulation of Interferon-γ During Innate and Adaptive Immune Responses. In; 2007; pp. 41–101.

41. Annunziato, F.; Romagnani, C.; Romagnani, S. The 3 major types of innate and adaptive cell-mediated effector immunity. *J. Allergy Clin. Immunol.* **2015**, *135*, 626–635, doi:10.1016/j.jaci.2014.11.001.

42. Bartlett, N.W.; Buttigieg, K.; Kotenko, S. V; Smith, G.L. Murine interferon lambdas (type III interferons) exhibit potent antiviral activity in vivo in a poxvirus infection model. *J. Gen. Virol.* **2005**, *86*, 1589–1596, doi:10.1099/vir.0.80904-0.

43. Kotenko, S. V; Durbin, J.E. Contribution of type III interferons to antiviral immunity: location, location, location. *J. Biol. Chem.* **2017**, *292*, 7295–7303, doi:10.1074/jbc.R117.777102.

44. Ye, L.; Schnepf, D.; Staeheli, P. Interferon-λ orchestrates innate and adaptive mucosal immune responses. *Nat. Rev. Immunol.* **2019**, *19*, 614–625, doi:10.1038/s41577-019-0182-z.

45. Galani, I.E.; Triantafyllia, V.; Eleminiadou, E.-E.; Koltsida, O.; Stavropoulos, A.; Manioudaki, M.; Thanos, D.; Doyle, S.E.; Kotenko, S. V.; Thanopoulou, K.; et al. Interferon-λ Mediates Non-redundant Front-Line Antiviral Protection against

Influenza Virus Infection without Compromising Host Fitness. *Immunity* **2017**, *46*, 875-890.e6, doi:10.1016/j.immuni.2017.04.025.

46. Kotenko, S. V; Langer, J.A. Full house: 12 receptors for 27 cytokines. *Int. Immunopharmacol.* **2004**, *4*, 593–608, doi:10.1016/j.intimp.2004.01.003.

47. Shaw, A.E.; Hughes, J.; Gu, Q.; Behdenna, A.; Singer, J.B.; Dennis, T.; Orton, R.J.; Varela, M.; Gifford, R.J.; Wilson, S.J.; et al. Fundamental properties of the mammalian innate immune system revealed by multispecies comparison of type I interferon responses. *PLOS Biol.* **2017**, *15*, e2004086, doi:10.1371/journal.pbio.2004086.

48. Schneider, W.M.; Chevillotte, M.D.; Rice, C.M. Interferon-Stimulated Genes: A Complex Web of Host Defenses. *Annu. Rev. Immunol.* **2014**, *32*, 513–545, doi:10.1146/annurev-immunol-032713-120231.

49. Gao, S.; von der Malsburg, A.; Paeschke, S.; Behlke, J.; Haller, O.; Kochs, G.; Daumke, O. Structural basis of oligomerization in the stalk region of dynamin-like MxA. *Nature* **2010**, *465*, 502–506, doi:10.1038/nature08972.

50. Munir, M.; Berg, M. The multiple faces of proteinkinase R in antiviral defense. *Virulence* **2013**, *4*, 85–89, doi:10.4161/viru.23134.

51. Sarasin-Filipowicz, M.; Oakeley, E.J.; Duong, F.H.T.; Christen, V.; Terracciano, L.; Filipowicz, W.; Heim, M.H. Interferon signaling and treatment outcome in chronic hepatitis C. *Proc. Natl. Acad. Sci.* **2008**, *105*, 7034–7039, doi:10.1073/pnas.0707882105.

52. Swaim, C.D.; Scott, A.F.; Canadeo, L.A.; Huibregtse, J.M. Extracellular ISG15 Signals Cytokine Secretion through the LFA-1 Integrin Receptor. *Mol. Cell* **2017**, *68*, 581-590.e5, doi:10.1016/j.molcel.2017.10.003.

53. Loeb, K.R.; Haas, A.L. The interferon-inducible 15-kDa ubiquitin homolog conjugates to intracellular proteins. *J. Biol. Chem.* **1992**, *267*, 7806–7813, doi:10.1016/S0021-9258(18)42585-9.

54. Zhang, X.; Bogunovic, D.; Payelle-Brogard, B.; Francois-Newton, V.; Speer, S.D.; Yuan, C.; Volpi, S.; Li, Z.; Sanal, O.; Mansouri, D.; et al. Human intracellular ISG15 prevents interferon-α/β over-amplification and auto-inflammation. *Nature* **2015**, *517*, 89–93, doi:10.1038/nature13801.

55. Albert, M.; Vázquez, J.; Falcón-Pérez, J.M.; Balboa, M.A.; Liesa, M.; Balsinde, J.; Guerra, S. ISG15 Is a Novel Regulator of Lipid Metabolism during Vaccinia Virus Infection. *Microbiol. Spectr.* **2022**, *10*, doi:10.1128/spectrum.03893-22.

56. Leong, C.R.; Funami, K.; Oshiumi, H.; Mengao, D.; Takaki, H.; Matsumoto, M.; Aly, H.H.; Watashi, K.; Chayama, K.; Seya, T. Interferon-stimulated gene of 20 kDa protein (ISG20) degrades RNA of hepatitis B virus to impede the replication of HBV in vitro and in vivo. *Oncotarget* **2016**, *7*, 68179–68193, doi:10.18632/oncotarget.11907.

57. Ziegler, C.G.K.; Allon, S.J.; Nyquist, S.K.; Mbano, I.M.; Miao, V.N.; Tzouanas, C.N.; Cao, Y.; Yousif, A.S.; Bals, J.; Hauser, B.M.; et al. SARS-CoV-2 Receptor ACE2 Is an Interferon-Stimulated Gene in Human Airway Epithelial Cells and Is Detected in Specific Cell Subsets across Tissues. *Cell* **2020**, *181*, 1016-1035.e19, doi:10.1016/j.cell.2020.04.035.

58. Actor, J.K. Basic Virology. In *Elsevier's Integrated Review Immunology and Microbiology*; Elsevier, 2012; pp. 121–128.

59. Grant, M.C.; Geoghegan, L.; Arbyn, M.; Mohammed, Z.; McGuinness, L.; Clarke, E.L.; Wade, R.G. The prevalence of symptoms in 24,410 adults infected

by the novel coronavirus (SARS-CoV-2; COVID-19): A systematic review and meta-analysis of 148 studies from 9 countries. *PLoS One* **2020**, *15*, e0234765, doi:10.1371/journal.pone.0234765.

60. COVID-19 Dashboard by the Center for Systems Science and Engineering (CSSE) at Johns Hopkins University (JHU).

61. Gupta, A.; Madhavan, M. V.; Sehgal, K.; Nair, N.; Mahajan, S.; Sehrawat, T.S.; Bikdeli, B.; Ahluwalia, N.; Ausiello, J.C.; Wan, E.Y.; et al. Extrapulmonary manifestations of COVID-19. *Nat. Med.* **2020**, *26*, 1017–1032, doi:10.1038/s41591-020-0968-3.

62. Zhou, P.; Yang, X.-L.; Wang, X.-G.; Hu, B.; Zhang, L.; Zhang, W.; Si, H.-R.; Zhu, Y.; Li, B.; Huang, C.-L.; et al. A pneumonia outbreak associated with a new coronavirus of probable bat origin. *Nature* **2020**, *579*, 270–273, doi:10.1038/s41586-020-2012-7.

63. Wang, W.; McKinnie, S.M.K.; Farhan, M.; Paul, M.; McDonald, T.; McLean, B.; Llorens-Cortes, C.; Hazra, S.; Murray, A.G.; Vederas, J.C.; et al. Angiotensin-Converting Enzyme 2 Metabolizes and Partially Inactivates Pyr-Apelin-13 and Apelin-17. *Hypertension* **2016**, *68*, 365–377, doi:10.1161/HYPERTENSIONAHA.115.06892.

64. Vadgama, N.; Kreymerman, A.; Campbell, J.; Shamardina, O.; Brugger, C.; Research Consortium, G.E.; Deaconescu, A.M.; Lee, R.T.; Penkett, C.J.; Gifford, C.A.; et al. SARS-CoV-2 Susceptibility and ACE2 Gene Variations Within Diverse Ethnic Backgrounds. *Front. Genet.* **2022**, *13*, doi:10.3389/fgene.2022.888025.

65. Novelli, A.; Biancolella, M.; Borgiani, P.; Cocciadiferro, D.; Colona, V.L.;

D'Apice, M.R.; Rogliani, P.; Zaffina, S.; Leonardis, F.; Campana, A.; et al. Analysis of ACE2 genetic variants in 131 Italian SARS-CoV-2-positive patients. *Hum. Genomics* **2020**, *14*, 29, doi:10.1186/s40246-020-00279-z.

66. Blume, C.; Jackson, C.L.; Spalluto, C.M.; Legebeke, J.; Nazlamova, L.; Conforti, F.; Perotin, J.-M.; Frank, M.; Butler, J.; Crispin, M.; et al. A novel ACE2 isoform is expressed in human respiratory epithelia and is upregulated in response to interferons and RNA respiratory virus infection. *Nat. Genet.* **2021**, *53*, 205–214, doi:10.1038/s41588-020-00759-x.

67. Rehman, S. ur; Tabish, M. Alternative splicing of ACE2 possibly generates variants that may limit the entry of SARS-CoV-2: a potential therapeutic approach using SSOs. *Clin. Sci.* **2020**, *134*, 1143–1150, doi:10.1042/CS20200419.

68. Benton, D.J.; Wrobel, A.G.; Xu, P.; Roustan, C.; Martin, S.R.; Rosenthal, P.B.; Skehel, J.J.; Gamblin, S.J. Receptor binding and priming of the spike protein of SARS-CoV-2 for membrane fusion. *Nature* **2020**, *588*, 327–330, doi:10.1038/s41586-020-2772-0.

69. Takeda, M. Proteolytic activation of SARS-CoV-2 spike protein. *Microbiol. Immunol.* **2022**, *66*, 15–23, doi:10.1111/1348-0421.12945.

70. Ou, X.; Liu, Y.; Lei, X.; Li, P.; Mi, D.; Ren, L.; Guo, L.; Guo, R.; Chen, T.; Hu, J.; et al. Characterization of spike glycoprotein of SARS-CoV-2 on virus entry and its immune cross-reactivity with SARS-CoV. *Nat. Commun.* **2020**, *11*, 1620, doi:10.1038/s41467-020-15562-9.

71. V'kovski, P.; Kratzel, A.; Steiner, S.; Stalder, H.; Thiel, V. Coronavirus biology and replication: implications for SARS-CoV-2. *Nat. Rev. Microbiol.* **2021**, *19*, 155–170, doi:10.1038/s41579-020-00468-6.

72. Luo, M. Influenza Virus Entry. In; 2012; pp. 201–221.

73. Gottschalk, A. The viruses. In *Viruses*; 1959; pp. 51–61.

74. Weis, W.; Brown, J.H.; Cusack, S.; Paulson, J.C.; Skehel, J.J.; Wiley, D.C. Structure of the influenza virus haemagglutinin complexed with its receptor, sialic acid. *Nature* **1988**, *333*, 426–431, doi:10.1038/333426a0.

75. Earnest, J.T.; Hantak, M.P.; Park, J.-E.; Gallagher, T. Coronavirus and Influenza Virus Proteolytic Priming Takes Place in Tetraspanin-Enriched Membrane Microdomains. *J. Virol.* **2015**, *89*, 6093–6104, doi:10.1128/JVI.00543-15.

76. White, J.M.; Whittaker, G.R. Fusion of Enveloped Viruses in Endosomes. *Traffic* **2016**, *17*, 593–614, doi:10.1111/tra.12389.

77. Arranz, R.; Coloma, R.; Chichon, F.J.; Conesa, J.J.; Carrascosa, J.L.; Valpuesta, J.M.; Ortin, J.; Martin-Benito, J. The Structure of Native Influenza Virion Ribonucleoproteins. *Science (80-.).* **2012**, *338*, 1634–1637, doi:10.1126/science.1228172.

78. Pflug, A.; Guilligay, D.; Reich, S.; Cusack, S. Structure of influenza A polymerase bound to the viral RNA promoter. *Nature* **2014**, *516*, 355–360, doi:10.1038/nature14008.

79. Gabriel, G.; Klingel, K.; Otte, A.; Thiele, S.; Hudjetz, B.; Arman-Kalcek, G.; Sauter, M.; Shmidt, T.; Rother, F.; Baumgarte, S.; et al. Differential use of importin-α isoforms governs cell tropism and host adaptation of influenza virus. *Nat. Commun.* **2011**, *2*, 156, doi:10.1038/ncomms1158.

80. Fodor, E. The RNA polymerase of influenza A virus: mechanisms of viral transcription and replication. *Acta Virol.* **2013**, *57*, 113–122, doi:10.4149/av_2013_02_113.

81. Guilligay, D.; Tarendeau, F.; Resa-Infante, P.; Coloma, R.; Crepin, T.; Sehr, P.; Lewis, J.; Ruigrok, R.W.H.; Ortin, J.; Hart, D.J.; et al. The structural basis for cap binding by influenza virus polymerase subunit PB2. *Nat. Struct. Mol. Biol.* **2008**, *15*, 500–506, doi:10.1038/nsmb.1421.

82. Cros, J.F.; García-Sastre, A.; Palese, P. An Unconventional NLS is Critical for the Nuclear Import of the Influenza A Virus Nucleoprotein and Ribonucleoprotein. *Traffic* **2005**, *6*, 205–213, doi:10.1111/j.1600-0854.2005.00263.x.

83. Huet, S.; Avilov, S. V.; Ferbitz, L.; Daigle, N.; Cusack, S.; Ellenberg, J. Nuclear Import and Assembly of Influenza A Virus RNA Polymerase Studied in Live Cells by Fluorescence Cross-Correlation Spectroscopy. *J. Virol.* **2010**, *84*, 1254–1264, doi:10.1128/JVI.01533-09.

84. Huang, S.; Chen, J.; Chen, Q.; Wang, H.; Yao, Y.; Chen, J.; Chen, Z. A Second CRM1-Dependent Nuclear Export Signal in the Influenza A Virus NS2 Protein Contributes to the Nuclear Export of Viral Ribonucleoproteins. *J. Virol.* **2013**, *87*, 767–778, doi:10.1128/JVI.06519-11.

85. Rahmani, K.; Dean, D.A. Leptomycin B alters the subcellular distribution of CRM1 (Exportin 1). *Biochem. Biophys. Res. Commun.* **2017**, *488*, 253–258, doi:10.1016/j.bbrc.2017.04.042.

86. Mathew, C.; Ghildyal, R. CRM1 Inhibitors for Antiviral Therapy. *Front. Microbiol.* **2017**, *8*, doi:10.3389/fmicb.2017.01171.

87. Amorim, M.J.; Bruce, E.A.; Read, E.K.C.; Foeglein, A.; Mahen, R.; Stuart, A.D.; Digard, P. A Rab11- and Microtubule-Dependent Mechanism for Cytoplasmic Transport of Influenza A Virus Viral RNA. *J. Virol.* **2011**, *85*, 4143–4156, doi:10.1128/JVI.02606-10.

88. Daniels, R.; Kurowski, B.; Johnson, A.E.; Hebert, D.N. N-Linked Glycans Direct the Cotranslational Folding Pathway of Influenza Hemagglutinin. *Mol. Cell* **2003**, *11*, 79–90, doi:10.1016/S1097-2765(02)00821-3.

89. Rossman, J.S.; Lamb, R.A. Influenza virus assembly and budding. *Virology* **2011**, *411*, 229–236, doi:10.1016/j.virol.2010.12.003.

90. BURNET, F.M.; MCCREA, J.F.; ANDERSON, S.G. Mucin as Substrate of Enzyme Action by Viruses of the Mumps Influenza Group. *Nature* **1947**, *160*, 404–405, doi:10.1038/160404b0.

91. Palese, P.; Compans, R.W. Inhibition of Influenza Virus Replication in Tissue Culture by 2-deoxy-2,3-dehydro-N-trifluoroacetylneuraminic acid (FANA): Mechanism of Action. *J. Gen. Virol.* **1976**, *33*, 159–163, doi:10.1099/0022-1317-33-1-159.

92. Azizian, N.G.; Li, Y. XPO1-dependent nuclear export as a target for cancer therapy. *J. Hematol. Oncol.* **2020**, *13*, 61, doi:10.1186/s13045-020-00903-4.

93. Wente, S.R.; Rout, M.P. The Nuclear Pore Complex and Nuclear Transport. *Cold Spring Harb. Perspect. Biol.* **2010**, *2*, a000562–a000562, doi:10.1101/cshperspect.a000562.

94. Becskei, A.; Mattaj, I.W. The strategy for coupling the RanGTP gradient to nuclear protein export. *Proc. Natl. Acad. Sci.* **2003**, *100*, 1717–1722, doi:10.1073/pnas.252766999.

95. Bischoff, F.R.; Krebber, H.; Kempf, T.; Hermes, I.; Ponstingl, H. Human RanGTPase-activating protein RanGAP1 is a homologue of yeast Rna1p involved in mRNA processing and transport. *Proc. Natl. Acad. Sci.* **1995**, *92*, 1749–1753, doi:10.1073/pnas.92.5.1749.

96. Nachury, M. V.; Weis, K. The direction of transport through the nuclear pore can be inverted. *Proc. Natl. Acad. Sci.* **1999**, *96*, 9622–9627, doi:10.1073/pnas.96.17.9622.

97. Camus, V.; Stamatoullas, A.; Mareschal, S.; Viailly, P.-J.; Sarafan-Vasseur, N.; Bohers, E.; Dubois, S.; Picquenot, J.M.; Ruminy, P.; Maingonnat, C.; et al. Detection and prognostic value of recurrent exportin 1 mutations in tumor and cell-free circulating DNA of patients with classical Hodgkin lymphoma. *Haematologica* **2016**, *101*, 1094–1101, doi:10.3324/haematol.2016.145102.

98. Fu, S.-C.; Huang, H.-C.; Horton, P.; Juan, H.-F. ValidNESs: a database of validated leucine-rich nuclear export signals. *Nucleic Acids Res.* **2013**, *41*, D338–D343, doi:10.1093/nar/gks936.

99. Azmi, A.S.; Mohammad, R.M. Targeting Cancer at the Nuclear Pore. *J. Clin. Oncol.* **2016**, *34*, 4180–4182, doi:10.1200/JCO.2016.67.5637.

100. Bourdon, J.-C.; Surget, S.; Khoury, M.P. Uncovering the role of p53 splice variants in human malignancy: a clinical perspective. *Onco. Targets. Ther.* **2013**, 57, doi:10.2147/OTT.S53876.

101. Saulino, D.M.; Younes, P.S.; Bailey, J.M.; Younes, M. CRM1/XPO1 expression in pancreatic adenocarcinoma correlates with survivin expression and the proliferative activity. *Oncotarget* **2018**, *9*, 21289–21295, doi:10.18632/oncotarget.25088.

102. Subhash, V.V.; Yeo, M.S.; Wang, L.; Tan, S.H.; Wong, F.Y.; Thuya, W.L.; Tan, W.L.; Peethala, P.C.; Soe, M.Y.; Tan, D.S.P.; et al. Anti-tumor efficacy of Selinexor (KPT-330) in gastric cancer is dependent on nuclear accumulation of p53 tumor suppressor. *Sci. Rep.* **2018**, *8*, 12248, doi:10.1038/s41598-018-30686-1.

103. Aladhraei, M.; Kassem Al-Thobhani, A.; Poungvarin, N.; Suwannalert, P. Association of XPO1 Overexpression with NF-κB and Ki67 in Colorectal Cancer. *Asian Pacific J. Cancer Prev.* **2019**, *20*, 3747–3754, doi:10.31557/APJCP.2019.20.12.3747.

104. Gupta, A.; Saltarski, J.M.; White, M.A.; Scaglioni, P.P.; Gerber, D.E. Therapeutic Targeting of Nuclear Export Inhibition in Lung Cancer. *J. Thorac. Oncol.* **2017**, *12*, 1446–1450, doi:10.1016/j.jtho.2017.06.013.

105. Taagepera, S.; McDonald, D.; Loeb, J.E.; Whitaker, L.L.; McElroy, A.K.; Wang, J.Y.J.; Hope, T.J. Nuclear-cytoplasmic shuttling of C-ABL tyrosine kinase. *Proc. Natl. Acad. Sci.* **1998**, *95*, 7457–7462, doi:10.1073/pnas.95.13.7457.

106. HAMAMOTO, T.; UOZUMI, T.; BEPPU, T. Leptomycins A and B, new antifungal antibiotics. III. Mode of action of leptomycin B on Schizosaccharomyces pombe. *J. Antibiot. (Tokyo).* **1985**, *38*, 1573–1580, doi:10.7164/antibiotics.38.1573.

107. KOMIYAMA, K.; OKADA, K.; TOMISAKA, S.; UMEZAWA, I.; HAMAMOTO, T.; BEPPU, T. Antitumor activity of leptomycin B. *J. Antibiot. (Tokyo).* **1985**, *38*, 427–429, doi:10.7164/antibiotics.38.427.

108. Kudo, N.; Matsumori, N.; Taoka, H.; Fujiwara, D.; Schreiner, E.P.; Wolff, B.; Yoshida, M.; Horinouchi, S. Leptomycin B inactivates CRM1/exportin 1 by covalent modification at a cysteine residue in the central conserved region. *Proc. Natl. Acad. Sci. U. S. A.* **1999**, *96*, 9112–7, doi:10.1073/pnas.96.16.9112.

109. Güttler, T.; Madl, T.; Neumann, P.; Deichsel, D.; Corsini, L.; Monecke, T.; Ficner, R.; Sattler, M.; Görlich, D. NES consensus redefined by structures of PKI-type and Rev-type nuclear export signals bound to CRM1. *Nat. Struct. Mol. Biol.* **2010**,

17, 1367–1376, doi:10.1038/nsmb.1931.

110. Koyama, M.; Matsuura, Y. An allosteric mechanism to displace nuclear export cargo from CRM1 and RanGTP by RanBP1. *EMBO J.* **2010**, *29*, 2002–2013, doi:10.1038/emboj.2010.89.

111. Sun, Q.; Carrasco, Y.P.; Hu, Y.; Guo, X.; Mirzaei, H.; MacMillan, J.; Chook, Y.M. Nuclear export inhibition through covalent conjugation and hydrolysis of Leptomycin B by CRM1. *Proc. Natl. Acad. Sci. U. S. A.* **2013**, *110*, 1303–1308, doi:10.1073/pnas.1217203110.

112. Etchin, J.; Berezovskaya, A.; Conway, A.S.; Galinsky, I.A.; Stone, R.M.; Baloglu, E.; Senapedis, W.; Landesman, Y.; Kauffman, M.; Shacham, S.; et al. KPT-8602, a second-generation inhibitor of XPO1-mediated nuclear export, is well tolerated and highly active against AML blasts and leukemia-initiating cells. *Leukemia* **2017**, *31*, 143–150, doi:10.1038/leu.2016.145.

113. Wang, J.S.; Barve, M.A.; Chiorean, E.G.; LoRusso, P.; Courtney, K.D.; Qi, D.; Bullington, J.; Sardone, M.; Chen, J.; Brooks, C.; et al. 564P Updated results of a phase I study of Felezonexor (SL-801), a novel XPO-1 reversible inhibitor, in patients with relapsed/refractory solid tumours. *Ann. Oncol.* **2020**, *31*, S485–S486, doi:10.1016/j.annonc.2020.08.678.

114. Gounder, M.M.; Somaiah, N.; Attia, S.; Chawla, S.P.; Villalobos, V.M.; Chmielowski, B.; Burgess, M.A.; Schwartz, G.K.; Riedel, R.F.; von Mehren, M.; et al. Phase 2 results of selinexor in advanced de-differentiated (DDLS) liposarcoma (SEAL) study: A phase 2/3, randomized, double blind, placebo controlled cross-over study. *J. Clin. Oncol.* **2018**, *36*, 11512–11512, doi:10.1200/JCO.2018.36.15_suppl.11512.

115. Wei, X.X.; Siegel, A.P.; Aggarwal, R.; Lin, A.M.; Friedlander, T.W.; Fong, L.; Kim, W.; Louttit, M.; Chang, E.; Zhang, L.; et al. A Phase II Trial of Selinexor, an Oral Selective Inhibitor of Nuclear Export Compound, in Abiraterone- and/or Enzalutamide-Refractory Metastatic Castration-Resistant Prostate Cancer. *Oncologist* **2018**, *23*, 656-e64, doi:10.1634/theoncologist.2017-0624.

116. Abdul Razak, A.R.; Mau-Soerensen, M.; Gabrail, N.Y.; Gerecitano, J.F.; Shields, A.F.; Unger, T.J.; Saint-Martin, J.R.; Carlson, R.; Landesman, Y.; McCauley, D.; et al. First-in-Class, First-in-Human Phase I Study of Selinexor, a Selective Inhibitor of Nuclear Export, in Patients With Advanced Solid Tumors. *J. Clin. Oncol.* **2016**, *34*, 4142–4150, doi:10.1200/JCO.2015.65.3949.

117. Garzon, R.; Savona, M.; Baz, R.; Andreeff, M.; Gabrail, N.; Gutierrez, M.; Savoie, L.; Mau-Sorensen, P.M.; Wagner-Johnston, N.; Yee, K.; et al. A phase 1 clinical trial of single-agent selinexor in acute myeloid leukemia. *Blood* **2017**, *129*, 3165–3174, doi:10.1182/blood-2016-11-750158.

118. Bhatnagar, B.; Walker, A.R.; Mims, A.S.; Vasu, S.; Klisovic, R.B.; Behbehani, G.; Blachly, J.S.; Larkin, K.T.M.; Long, M.; Zhao, Q.; et al. Phase 1 study of selinexor plus mitoxantrone, etoposide, and cytarabine in acute myeloid leukemia. *J. Clin. Oncol.* **2018**, *36*, 7048–7048, doi:10.1200/JCO.2018.36.15_suppl.7048.

119. Alexander, T.B.; Lacayo, N.J.; Choi, J.K.; Ribeiro, R.C.; Pui, C.-H.; Rubnitz, J.E. Phase I Study of Selinexor, a Selective Inhibitor of Nuclear Export, in Combination With Fludarabine and Cytarabine, in Pediatric Relapsed or Refractory Acute Leukemia. *J. Clin. Oncol.* **2016**, *34*, 4094–4101, doi:10.1200/JCO.2016.67.5066.

120. Chen, C.; Siegel, D.; Gutierrez, M.; Jacoby, M.; Hofmeister, C.C.; Gabrail, N.;

Baz, R.; Mau-Sorensen, M.; Berdeja, J.G.; Savona, M.; et al. Safety and efficacy of selinexor in relapsed or refractory multiple myeloma and Waldenstrom macroglobulinemia. *Blood* **2018**, *131*, 855–863, doi:10.1182/blood-2017-08-797886.

121. Grosicki, S.; Simonova, M.; Spicka, I.; Pour, L.; Kriachok, I.; Gavriatopoulou, M.; Pylypenko, H.; Auner, H.W.; Leleu, X.; Doronin, V.; et al. Once-per-week selinexor, bortezomib, and dexamethasone versus twice-per-week bortezomib and dexamethasone in patients with multiple myeloma (BOSTON): a randomised, open-label, phase 3 trial. *Lancet* **2020**, *396*, 1563–1573, doi:10.1016/S0140-6736(20)32292-3.

122. Perwitasari, O.; Johnson, S.; Yan, X.; Howerth, E.; Shacham, S.; Landesman, Y.; Baloglu, E.; McCauley, D.; Tamir, S.; Tompkins, S.M.; et al. Verdinexor, a Novel Selective Inhibitor of Nuclear Export, Reduces Influenza A Virus Replication In Vitro and In Vivo. *J. Virol.* **2014**, *88*, 10228–10243, doi:10.1128/jvi.01774-14.

123. Booth, D.S.; Cheng, Y.; Frankel, A.D. The export receptor Crm1 forms a dimer to promote nuclear export of HIV RNA. *Elife* **2014**, *3*, doi:10.7554/eLife.04121.

124. Mathew, C.; Tamir, S.; Tripp, R.A.; Ghildyal, R. Reversible disruption of XPO1-mediated nuclear export inhibits respiratory syncytial virus (RSV) replication. *Sci. Rep.* **2021**, *11*, 19223, doi:10.1038/s41598-021-98767-2.

125. Wolff, B.; Sanglier, J.-J.; Wang, Y. Leptomycin B is an inhibitor of nuclear export: inhibition of nucleo-cytoplasmic translocation of the human immunodeficiency virus type 1 (HIV-1) Rev protein and Rev-dependent mRNA. *Chem. Biol.* **1997**, *4*, 139–147, doi:10.1016/S1074-5521(97)90257-X.

126. Pasdeloup, D.; Poisson, N.; Raux, H.; Gaudin, Y.; Ruigrok, R.W.H.; Blondel, D.

Nucleocytoplasmic shuttling of the rabies virus P protein requires a nuclear localization signal and a CRM1-dependent nuclear export signal. *Virology* **2005**, *334*, 284–293, doi:10.1016/j.virol.2005.02.005.

127. Ghildyal, R.; Ho, A.; Dias, M.; Soegiyono, L.; Bardin, P.G.; Tran, K.C.; Teng, M.N.; Jans, D.A. The Respiratory Syncytial Virus Matrix Protein Possesses a Crm1-Mediated Nuclear Export Mechanism. *J. Virol.* **2009**, *83*, 5353–5362, doi:10.1128/JVI.02374-08.
128. You, J.-H.; Reed, M.L.; Hiscox, J.A. Trafficking motifs in the SARS-coronavirus nucleocapsid protein. *Biochem. Biophys. Res. Commun.* **2007**, *358*, 1015–1020, doi:10.1016/j.bbrc.2007.05.036.
129. Freundt, E.C.; Yu, L.; Park, E.; Lenardo, M.J.; Xu, X.-N. Molecular Determinants for Subcellular Localization of the Severe Acute Respiratory Syndrome Coronavirus Open Reading Frame 3b Protein. *J. Virol.* **2009**, *83*, 6631–6640, doi:10.1128/JVI.00367-09.
130. Uddin, M.H.; Zonder, J.A.; Azmi, A.S. Exportin 1 inhibition as antiviral therapy. *Drug Discov. Today* **2020**, *25*, 1775–1781, doi:10.1016/j.drudis.2020.06.014.
131. Kashyap, T.; Murray, J.; Walker, C.J.; Chang, H.; Tamir, S.; Hou, B.; Shacham, S.; Kauffman, M.G.; Tripp, R.A.; Landesman, Y. Selinexor, a novel selective inhibitor of nuclear export, reduces SARS-CoV-2 infection and protects the respiratory system in vivo. *Antiviral Res.* **2021**, *192*, 105115, doi:10.1016/j.antiviral.2021.105115.
132. Rawlinson, S.M.; Pryor, M.J.; Wright, P.J.; Jans, D.A. CRM1-mediated Nuclear Export of Dengue Virus RNA Polymerase NS5 Modulates Interleukin-8 Induction and Virus Production. *J. Biol. Chem.* **2009**, *284*, 15589–15597,

doi:10.1074/jbc.M808271200.

133. Su, P.-Y.; Yen, S.-C.B.; Yang, C.-C.; Chang, C.-H.; Lin, W.-C.; Shih, C. Hepatitis B virus virion secretion is a CRM1-spike-mediated late event. *J. Biomed. Sci.* **2022**, *29*, 44, doi:10.1186/s12929-022-00827-w.

134. Boons, E.; Vanstreels, E.; Jacquemyn, M.; Nogueira, T.C.; Neggers, J.E.; Vercruysse, T.; van den Oord, J.; Tamir, S.; Shacham, S.; Landesman, Y.; et al. Human Exportin-1 is a Target for Combined Therapy of HIV and AIDS Related Lymphoma. *EBioMedicine* **2015**, *2*, 1102–1113, doi:10.1016/j.ebiom.2015.07.041.

135. Liao, Y.; Ke, X.; Deng, T.; Qin, Q. The Second-Generation XPO1 Inhibitor Eltanexor Inhibits Human Cytomegalovirus (HCMV) Replication and Promotes Type I Interferon Response. *Front. Microbiol.* **2021**, *12*, doi:10.3389/fmicb.2021.675112.

136. Nakano, K.; Watanabe, T. HTLV-1 Rex Tunes the Cellular Environment Favorable for Viral Replication. *Viruses* **2016**, *8*, 58, doi:10.3390/v8030058.

137. Elton, D.; Simpson-Holley, M.; Archer, K.; Medcalf, L.; Hallam, R.; McCauley, J.; Digard, P. Interaction of the Influenza Virus Nucleoprotein with the Cellular CRM1-Mediated Nuclear Export Pathway. *J. Virol.* **2001**, *75*, 408–419, doi:10.1128/JVI.75.1.408-419.2001.

138. Jorquera, P.A.; Mathew, C.; Pickens, J.; Williams, C.; Luczo, J.M.; Tamir, S.; Ghildyal, R.; Tripp, R.A. Verdinexor (KPT-335), a Selective Inhibitor of Nuclear Export, Reduces Respiratory Syncytial Virus Replication In Vitro. *J. Virol.* **2019**, *93*, doi:10.1128/JVI.01684-18.

139. Wu, M.; Gui, H.; Feng, Z.; Xu, H.; Li, G.; Li, M.; Chen, T.; Wu, Y.; Huang, J.; Bai, Z.; et al. KPT-330, a potent and selective CRM1 inhibitor, exhibits anti-

inflammation effects and protection against sepsis. *Biochem. Biophys. Res. Commun.* **2018**, *503*, 1773–1779, doi:10.1016/j.bbrc.2018.07.112.

140. Pickens, J.; Tripp, R. Verdinexor Targeting of CRM1 is a Promising Therapeutic Approach against RSV and Influenza Viruses. *Viruses* **2018**, *10*, 48, doi:10.3390/v10010048.

141. Gordon, S. Alternative activation of macrophages. *Nat. Rev. Immunol.* 2003, *3*, 23–35.

142. Yao, Y.; Xu, X.-H.; Jin, L. Macrophage Polarization in Physiological and Pathological Pregnancy. *Front. Immunol.* **2019**, *10*, doi:10.3389/fimmu.2019.00792.

143. Murray, P.J. Macrophage Polarization. *Annu. Rev. Physiol.* **2017**, *79*, 541–566, doi:10.1146/annurev-physiol-022516-034339.

144. Tannahill, G.M.; Curtis, A.M.; Adamik, J.; Palsson-McDermott, E.M.; McGettrick, A.F.; Goel, G.; Frezza, C.; Bernard, N.J.; Kelly, B.; Foley, N.H.; et al. Succinate is an inflammatory signal that induces IL-1β through HIF-1α. *Nature* **2013**, *496*, 238–242, doi:10.1038/nature11986.

145. Jha, A.K.; Huang, S.C.-C.; Sergushichev, A.; Lampropoulou, V.; Ivanova, Y.; Loginicheva, E.; Chmielewski, K.; Stewart, K.M.; Ashall, J.; Everts, B.; et al. Network Integration of Parallel Metabolic and Transcriptional Data Reveals Metabolic Modules that Regulate Macrophage Polarization. *Immunity* **2015**, *42*, 419–430, doi:10.1016/j.immuni.2015.02.005.

146. Mills, E.L.; Kelly, B.; Logan, A.; Costa, A.S.H.; Varma, M.; Bryant, C.E.; Tourlomousis, P.; Däbritz, J.H.M.; Gottlieb, E.; Latorre, I.; et al. Succinate Dehydrogenase Supports Metabolic Repurposing of Mitochondria to Drive

Inflammatory Macrophages. *Cell* **2016**, *167*, 457-470.e13, doi:10.1016/j.cell.2016.08.064.

147. Everts, B.; Amiel, E.; Huang, S.C.-C.; Smith, A.M.; Chang, C.-H.; Lam, W.Y.; Redmann, V.; Freitas, T.C.; Blagih, J.; van der Windt, G.J.W.; et al. TLR-driven early glycolytic reprogramming via the kinases TBK1-IKKε supports the anabolic demands of dendritic cell activation. *Nat. Immunol.* **2014**, *15*, 323–32, doi:10.1038/ni.2833.
148. Michelucci, A.; Cordes, T.; Ghelfi, J.; Pailot, A.; Reiling, N.; Goldmann, O.; Binz, T.; Wegner, A.; Tallam, A.; Rausell, A.; et al. Immune-responsive gene 1 protein links metabolism to immunity by catalyzing itaconic acid production. *Proc. Natl. Acad. Sci.* **2013**, *110*, 7820–7825, doi:10.1073/pnas.1218599110.
149. Freemerman, A.J.; Johnson, A.R.; Sacks, G.N.; Milner, J.J.; Kirk, E.L.; Troester, M.A.; Macintyre, A.N.; Goraksha-Hicks, P.; Rathmell, J.C.; Makowski, L. Metabolic reprogramming of macrophages: glucose transporter 1 (GLUT1)-mediated glucose metabolism drives a proinflammatory phenotype. *J. Biol. Chem.* **2014**, *289*, 7884–96, doi:10.1074/jbc.M113.522037.
150. Vazquez, A.; Liu, J.; Zhou, Y.; Oltvai, Z.N. Catabolic efficiency of aerobic glycolysis: The Warburg effect revisited. *BMC Syst. Biol.* **2010**, *4*, 58, doi:10.1186/1752-0509-4-58.
151. Warburg, O. On the origin of cancer cells. *Science* **1956**, *123*, 309–14, doi:10.1126/science.123.3191.309.
152. Horecker, B.L. The Pentose Phosphate Pathway. *J. Biol. Chem.* **2002**, *277*, 47965–47971, doi:10.1074/jbc.X200007200.
153. Murphy, M.P. Mitochondrial Thiols in Antioxidant Protection and Redox

Signaling: Distinct Roles for Glutathionylation and Other Thiol Modifications. *Antioxid. Redox Signal.* **2012**, *16*, 476–495, doi:10.1089/ars.2011.4289.

154. Wamelink, M.M.C.; Struys, E.A.; Jakobs, C. The biochemistry, metabolism and inherited defects of the pentose phosphate pathway: A review. *J. Inherit. Metab. Dis.* **2008**, *31*, 703–717, doi:10.1007/s10545-008-1015-6.

155. Mills, E.L.; Ryan, D.G.; Prag, H.A.; Dikovskaya, D.; Menon, D.; Zaslona, Z.; Jedrychowski, M.P.; Costa, A.S.H.; Higgins, M.; Hams, E.; et al. Itaconate is an anti-inflammatory metabolite that activates Nrf2 via alkylation of KEAP1. *Nature* **2018**, *556*, 113–117, doi:10.1038/nature25986.

156. Lampropoulou, V.; Sergushichev, A.; Bambouskova, M.; Nair, S.; Vincent, E.E.; Loginicheva, E.; Cervantes-Barragan, L.; Ma, X.; Huang, S.C.-C.; Griss, T.; et al. Itaconate Links Inhibition of Succinate Dehydrogenase with Macrophage Metabolic Remodeling and Regulation of Inflammation. *Cell Metab.* **2016**, *24*, 158–166, doi:10.1016/j.cmet.2016.06.004.

157. Fan, K.; Zan, X.; Zhi, Y.; Yang, Y.; Hu, K.; Zhang, X.; Zhang, X.; Zhao, S.; Chen, K.; Gong, X.; et al. Immune response gene 1 deficiency impairs Nrf2 activation and aggravates liver fibrosis in mice. *Biochem. Biophys. Res. Commun.* **2022**, *607*, 103–109, doi:10.1016/j.bbrc.2022.03.110.

158. Cordes, T.; Lucas, A.; Divakaruni, A.S.; Murphy, A.N.; Cabrales, P.; Metallo, C.M. Itaconate modulates tricarboxylic acid and redox metabolism to mitigate reperfusion injury. *Mol. Metab.* **2020**, *32*, 122–135, doi:10.1016/j.molmet.2019.11.019.

159. Hooftman, A.; Angiari, S.; Hester, S.; Corcoran, S.E.; Runtsch, M.C.; Ling, C.; Ruzek, M.C.; Slivka, P.F.; McGettrick, A.F.; Banahan, K.; et al. The

Immunomodulatory Metabolite Itaconate Modifies NLRP3 and Inhibits Inflammasome Activation. *Cell Metab.* **2020**, *32*, 468-478.e7, doi:10.1016/j.cmet.2020.07.016.

160. Runtsch, M.C.; Angiari, S.; Hooftman, A.; Wadhwa, R.; Zhang, Y.; Zheng, Y.; Spina, J.S.; Ruzek, M.C.; Argiriadi, M.A.; McGettrick, A.F.; et al. Itaconate and itaconate derivatives target JAK1 to suppress alternative activation of macrophages. *Cell Metab.* **2022**, *34*, 487-501.e8, doi:10.1016/j.cmet.2022.02.002.
161. Chen, L.-L.; Morcelle, C.; Cheng, Z.-L.; Chen, X.; Xu, Y.; Gao, Y.; Song, J.; Li, Z.; Smith, M.D.; Shi, M.; et al. Itaconate inhibits TET DNA dioxygenases to dampen inflammatory responses. *Nat. Cell Biol.* **2022**, *24*, 353–363, doi:10.1038/s41556-022-00853-8.
162. ElAzzouny, M.; Tom, C.T.M.B.; Evans, C.R.; Olson, L.L.; Tanga, M.J.; Gallagher, K.A.; Martin, B.R.; Burant, C.F. Dimethyl Itaconate Is Not Metabolized into Itaconate Intracellularly. *J. Biol. Chem.* **2017**, *292*, 4766–4769, doi:10.1074/jbc.C117.775270.
163. Bambouskova, M.; Gorvel, L.; Lampropoulou, V.; Sergushichev, A.; Loginicheva, E.; Johnson, K.; Korenfeld, D.; Mathyer, M.E.; Kim, H.; Huang, L.-H.; et al. Electrophilic properties of itaconate and derivatives regulate the IκBζ–ATF3 inflammatory axis. *Nature* **2018**, *556*, 501–504, doi:10.1038/s41586-018-0052-z.
164. Winterhoff, M.; Chen, F.; Sahini, N.; Ebensen, T.; Kuhn, M.; Kaever, V.; Bähre, H.; Pessler, F. Establishment, Validation, and Initial Application of a Sensitive LC-MS/MS Assay for Quantification of the Naturally Occurring Isomers Itaconate, Mesaconate, and Citraconate. *Metabolites* **2021**, *11*, 270,

doi:10.3390/metabo11050270.

165. Chen, F.; Elgaher, W.A.M.; Winterhoff, M.; Büssow, K.; Waqas, F.H.; Graner, E.; Pires-Afonso, Y.; Casares Perez, L.; de la Vega, L.; Sahini, N.; et al. Citraconate inhibits ACOD1 (IRG1) catalysis, reduces interferon responses and oxidative stress, and modulates inflammation and cell metabolism. *Nat. Metab.* **2022**, *4*, 534–546, doi:10.1038/s42255-022-00577-x.

166. Swain, A.; Bambouskova, M.; Kim, H.; Andhey, P.S.; Duncan, D.; Auclair, K.; Chubukov, V.; Simons, D.M.; Roddy, T.P.; Stewart, K.M.; et al. Comparative evaluation of itaconate and its derivatives reveals divergent inflammasome and type I interferon regulation in macrophages. *Nat. Metab.* **2020**, *2*, 594–602, doi:10.1038/s42255-020-0210-0.

167. Wu, R.; Liu, J.; Wang, N.; Zeng, L.; Yu, C.; Chen, F.; Wang, H.; Billiar, T.R.; Jiang, J.; Tang, D.; et al. Aconitate decarboxylase 1 is a mediator of polymicrobial sepsis. *Sci. Transl. Med.* **2022**, *14*, doi:10.1126/scitranslmed.abo2028.

168. Sohail, A.; Iqbal, A.A.; Sahini, N.; Chen, F.; Tantawy, M.; Waqas, F.; Winterhoff, M.; Ebensen, T.; Schultz, K.; Geffers, R.; et al. Itaconate and derivatives reduce interferon responses and inflammation in influenza A virus infection. *PLOS Pathog.* **2022**, *18*, e1010219, doi:10.1371/journal.ppat.1010219.

169. Diskin, C.; Zotta, A.; Corcoran, S.E.; Tyrrell, V.J.; Zaslona, Z.; O'Donnell, V.B.; O'Neill, L.A.J. 4-Octyl-Itaconate and Dimethyl Fumarate Inhibit COX2 Expression and Prostaglandin Production in Macrophages. *J. Immunol.* **2021**, *207*, 2561–2569, doi:10.4049/jimmunol.2100488.

170. Day, E.A.; O'Neill, L.A.J. Protein targeting by the itaconate family in immunity and inflammation. *Biochem. J.* **2022**, *479*, 2499–2510, doi:10.1042/BCJ20220364.

171. Minton, K. Neuronal itaconate restricts viral infection. *Nat. Rev. Immunol.* **2019**, *19*, 67, doi:10.1038/s41577-019-0121-z.

172. Li, W.; Long, Q.; Wu, H.; Zhou, Y.; Duan, L.; Yuan, H.; Ding, Y.; Huang, Y.; Wu, Y.; Huang, J.; et al. Nuclear localization of mitochondrial TCA cycle enzymes modulates pluripotency via histone acetylation. *Nat. Commun.* **2022**, *13*, 7414, doi:10.1038/s41467-022-35199-0.

173. McFadden, B.A.; Purohit, S. Itaconate, an isocitrate lyase-directed inhibitor in Pseudomonas indigofera. *J. Bacteriol.* **1977**, *131*, 136–144, doi:10.1128/jb.131.1.136-144.1977.

174. Naujoks, J.; Tabeling, C.; Dill, B.D.; Hoffmann, C.; Brown, A.S.; Kunze, M.; Kempa, S.; Peter, A.; Mollenkopf, H.-J.; Dorhoi, A.; et al. IFNs Modify the Proteome of Legionella-Containing Vacuoles and Restrict Infection Via IRG1-Derived Itaconic Acid. *PLOS Pathog.* **2016**, *12*, e1005408, doi:10.1371/journal.ppat.1005408.

175. McFadden, B.A.; Williams, J.O.; Roche, T.E. Mechanism of action of isocitrate lyase from Pseudomonas indigofera. *Biochemistry* **1971**, *10*, 1384–1390, doi:10.1021/bi00784a017.

176. Schuster, E.-M.; Epple, M.W.; Glaser, K.M.; Mihlan, M.; Lucht, K.; Zimmermann, J.A.; Bremser, A.; Polyzou, A.; Obier, N.; Cabezas-Wallscheid, N.; et al. TFEB induces mitochondrial itaconate synthesis to suppress bacterial growth in macrophages. *Nat. Metab.* **2022**, *4*, 856–866, doi:10.1038/s42255-022-00605-w.

177. Daniels, B.P.; Kofman, S.B.; Smith, J.R.; Norris, G.T.; Snyder, A.G.; Kolb, J.P.; Gao, X.; Locasale, J.W.; Martinez, J.; Gale, M.; et al. The Nucleotide Sensor ZBP1

and Kinase RIPK3 Induce the Enzyme IRG1 to Promote an Antiviral Metabolic State in Neurons. *Immunity* **2019**, doi:10.1016/j.immuni.2018.11.017.

178. Song, J.-W.; Lam, S.M.; Fan, X.; Cao, W.-J.; Wang, S.-Y.; Tian, H.; Chua, G.H.; Zhang, C.; Meng, F.-P.; Xu, Z.; et al. Omics-Driven Systems Interrogation of Metabolic Dysregulation in COVID-19 Pathogenesis. *Cell Metab.* **2020**, *32*, 188-202.e5, doi:10.1016/j.cmet.2020.06.016.

179. Olagnier, D.; Farahani, E.; Thyrsted, J.; Blay-Cadanet, J.; Herengt, A.; Idorn, M.; Hait, A.; Hernaez, B.; Knudsen, A.; Iversen, M.B.; et al. SARS-CoV2-mediated suppression of NRF2-signaling reveals potent antiviral and anti-inflammatory activity of 4-octyl-itaconate and dimethyl fumarate. *Nat. Commun.* **2020**, *11*, 4938, doi:10.1038/s41467-020-18764-3.

180. Sethy, B.; Hsieh, C.F.; Lin, T.J.; Hu, P.Y.; Chen, Y.L.; Lin, C.Y.; Tseng, S.N.; Horng, J.T.; Hsieh, P.W. Design, Synthesis, and Biological Evaluation of Itaconic Acid Derivatives as Potential Anti-Influenza Agents. *J. Med. Chem.* **2019**, *62*, 2390–2403, doi:10.1021/acs.jmedchem.8b01683.

181. Pang, Y.; Wang, Y.; Li, C.; Liu, J.; Duan, C.; Zhou, Y.; Fang, L.; Xiao, S. Itaconate derivative 4-OI inhibits PRRSV proliferation and associated inflammatory response. *Virology* **2022**, *577*, 84–90, doi:10.1016/j.virol.2022.10.007.

182. Neggers, J.E.; Vercruysse, T.; Jacquemyn, M.; Vanstreels, E.; Baloglu, E.; Shacham, S.; Crochiere, M.; Landesman, Y.; Daelemans, D. Identifying Drug-Target Selectivity of Small-Molecule CRM1/XPO1 Inhibitors by CRISPR/Cas9 Genome Editing. *Chem. Biol.* **2015**, *22*, 107–116, doi:10.1016/j.chembiol.2014.11.015.

183. Schrumpf, J.A.; Ninaber, D.K.; van der Does, A.M.; Hiemstra, P.S. TGF-β1

Impairs Vitamin D-Induced and Constitutive Airway Epithelial Host Defense Mechanisms. *J. Innate Immun.* **2020**, *12*, 74–89, doi:10.1159/000497415.

184. Schrauwen, E.J.A.; Herfst, S.; Chutinimitkul, S.; Bestebroer, T.M.; Rimmelzwaan, G.F.; Osterhaus, A.D.M.E.; Kuiken, T.; Fouchier, R.A.M. Possible increased pathogenicity of pandemic (H1N1) 2009 influenza virus upon reassortment. *Emerg. Infect. Dis.* **2011**, *17*, 200–208, doi:10.3201/eid1702.101268.
185. Munster, V.J.; Wit, E. De; Brand, J.M. a Van Den; Herfst, S.; Schrauwen, E.J. a; Bestebroer, T.M.; Vijver, D. Van De; Boucher, C. a; Koopmans, M.; Rimmelzwaan, G.F.; et al. Virus in Ferrets. **2009**, *503*, 481–483.
186. De Wit, E.; Spronken, M.I.J.; Bestebroer, T.M.; Rimmelzwaan, G.F.; Osterhaus, A.D.M.E.; Fouchier, R.A.M. Efficient generation and growth of influenza virus A/PR/8/34 from eight cDNA fragments. *Virus Res.* **2004**, *103*, 155–161, doi:10.1016/j.virusres.2004.02.028.
187. Stauber, R.; Gaitanaris, G.A.; Pavlakis, G.N. Analysis of Trafficking of Rev and Transdominant Rev Proteins in Living Cells Using Green Fluorescent Protein Fusions: Transdominant Rev Blocks the Export of Rev from the Nucleus to the Cytoplasm1. *Virology* **1995**, *213*, 439–449, doi:10.1006/viro.1995.0016.
188. Singh, S.; O'Reilly, S.; Gewaid, H.; Bowie, A.G.; Gautier, V.; Worrall, D.M. Reactive Centre Loop Mutagenesis of SerpinB3 to Target TMPRSS2 and Furin: Inhibition of SARS-CoV-2 Cell Entry and Replication. *Int. J. Mol. Sci.* **2022**, *23*, 12522, doi:10.3390/ijms232012522.
189. Vercruysse, T.; De Bie, J.; Neggers, J.E.; Jacquemyn, M.; Vanstreels, E.; Schmid-Burgk, J.L.; Hornung, V.; Baloglu, E.; Landesman, Y.; Senapedis, W.; et al. The Second-Generation Exportin-1 Inhibitor KPT-8602 Demonstrates Potent

Activity against Acute Lymphoblastic Leukemia. *Clin. Cancer Res.* **2017**, *23*, 2528–2541, doi:10.1158/1078-0432.CCR-16-1580.

190. Ng, K.W.; Attig, J.; Bolland, W.; Young, G.R.; Major, J.; Wrobel, A.G.; Gamblin, S.; Wack, A.; Kassiotis, G. Tissue-specific and interferon-inducible expression of nonfunctional ACE2 through endogenous retroelement co-option. *Nat. Genet.* **2020**, *52*, 1294–1302, doi:10.1038/s41588-020-00732-8.

191. Gunderstofte, C.; Iversen, M.B.; Peri, S.; Thielke, A.; Balachandran, S.; Holm, C.K.; Olagnier, D. Nrf2 Negatively Regulates Type I Interferon Responses and Increases Susceptibility to Herpes Genital Infection in Mice. *Front. Immunol.* **2019**, *10*, doi:10.3389/fimmu.2019.02101.

192. Onabajo, O.O.; Banday, A.R.; Stanifer, M.L.; Yan, W.; Obajemu, A.; Santer, D.M.; Florez-Vargas, O.; Piontkivska, H.; Vargas, J.M.; Ring, T.J.; et al. Interferons and viruses induce a novel truncated ACE2 isoform and not the full-length SARS-CoV-2 receptor. *Nat. Genet.* **2020**, *52*, 1283–1293, doi:10.1038/s41588-020-00731-9.

193. Tissari, J.; Sirén, J.; Meri, S.; Julkunen, I.; Matikainen, S. IFN-α Enhances TLR3-Mediated Antiviral Cytokine Expression in Human Endothelial and Epithelial Cells by Up-Regulating TLR3 Expression. *J. Immunol.* **2005**, *174*, 4289–4294, doi:10.4049/jimmunol.174.7.4289.

194. Cho, H.; Proll, S.C.; Szretter, K.J.; Katze, M.G.; Gale, M.; Diamond, M.S. Differential innate immune response programs in neuronal subtypes determine susceptibility to infection in the brain by positive-stranded RNA viruses. *Nat. Med.* **2013**, *19*, 458–464, doi:10.1038/nm.3108.

195. Zhao, S.; Ghosh, A.; Lo, C.-S.; Chenier, I.; Scholey, J.W.; Filep, J.G.; Ingelfinger,

J.R.; Zhang, S.-L.; Chan, J.S.D. Nrf2 Deficiency Upregulates Intrarenal Angiotensin-Converting Enzyme-2 and Angiotensin 1-7 Receptor Expression and Attenuates Hypertension and Nephropathy in Diabetic Mice. *Endocrinology* **2018**, *159*, 836–852, doi:10.1210/en.2017-00752.

196. Cuadrado, A.; Pajares, M.; Benito, C.; Jiménez-Villegas, J.; Escoll, M.; Fernández-Ginés, R.; Garcia Yagüe, A.J.; Lastra, D.; Manda, G.; Rojo, A.I.; et al. Can Activation of NRF2 Be a Strategy against COVID-19? *Trends Pharmacol. Sci.* **2020**, *41*, 598–610, doi:10.1016/j.tips.2020.07.003.

197. Senkel, S.; Lucas, B.; Klein-Hitpass, L.; Ryffel, G.U. Identification of target genes of the transcription factor HNF1β and HNF1α in a human embryonic kidney cell line. *Biochim. Biophys. Acta - Gene Struct. Expr.* **2005**, *1731*, 179–190, doi:10.1016/j.bbaexp.2005.10.003.

198. Liang, L.; Wang, D.; Yu, H.; Wang, J.; Zhang, H.; Sun, B.; Yang, F.; Wang, Z.; Xie, D.; Feng, R.; et al. Transcriptional regulation and small compound targeting of ACE2 in lung epithelial cells. *Acta Pharmacol. Sin.* **2022**, *43*, 2895–2904, doi:10.1038/s41401-022-00906-6.

199. Shien, K.; Papadimitrakopoulou, V.A.; Ruder, D.; Behrens, C.; Shen, L.; Kalhor, N.; Song, J.; Lee, J.J.; Wang, J.; Tang, X.; et al. JAK1/STAT3 Activation through a Proinflammatory Cytokine Pathway Leads to Resistance to Molecularly Targeted Therapy in Non–Small Cell Lung Cancer. *Mol. Cancer Ther.* **2017**, *16*, 2234–2245, doi:10.1158/1535-7163.MCT-17-0148.

200. Melkamu, T.; Kita, H.; O'Grady, S.M. TLR3 activation evokes IL-6 secretion, autocrine regulation of Stat3 signaling and TLR2 expression in human bronchial epithelial cells. *J. Cell Commun. Signal.* **2013**, *7*, 109–118, doi:10.1007/s12079-012-

0185-z.

201. Ryan, D.G.; Knatko, E. V.; Casey, A.M.; Hukelmann, J.L.; Dayalan Naidu, S.; Brenes, A.J.; Ekkunagul, T.; Baker, C.; Higgins, M.; Tronci, L.; et al. Nrf2 activation reprograms macrophage intermediary metabolism and suppresses the type I interferon response. *iScience* **2022**, *25*, 103827, doi:10.1016/j.isci.2022.103827.

202. He, W.; Miao, F.J.-P.; Lin, D.C.-H.; Schwandner, R.T.; Wang, Z.; Gao, J.; Chen, J.-L.; Tian, H.; Ling, L. Citric acid cycle intermediates as ligands for orphan G-protein-coupled receptors. *Nature* **2004**, *429*, 188–193, doi:10.1038/nature02488.

203. Morland, C.; Lauritzen, K.H.; Puchades, M.; Holm-Hansen, S.; Andersson, K.; Gjedde, A.; Attramadal, H.; Storm-Mathisen, J.; Bergersen, L.H. The lactate receptor, G-protein-coupled receptor 81/hydroxycarboxylic acid receptor 1: Expression and action in brain. *J. Neurosci. Res.* **2015**, *93*, 1045–1055, doi:10.1002/jnr.23593.

204. Tan, J.K.; McKenzie, C.; Mariño, E.; Macia, L.; Mackay, C.R. Metabolite-Sensing G Protein–Coupled Receptors—Facilitators of Diet-Related Immune Regulation. *Annu. Rev. Immunol.* **2017**, *35*, 371–402, doi:10.1146/annurev-immunol-051116-052235.

205. Keiran, N.; Ceperuelo-Mallafré, V.; Calvo, E.; Hernández-Alvarez, M.I.; Ejarque, M.; Núñez-Roa, C.; Horrillo, D.; Maymó-Masip, E.; Rodríguez, M.M.; Fradera, R.; et al. SUCNR1 controls an anti-inflammatory program in macrophages to regulate the metabolic response to obesity. *Nat. Immunol.* **2019**, *20*, 581–592, doi:10.1038/s41590-019-0372-7.

206. Dittmann, J.; Stertz, S.; Grimm, D.; Steel, J.; García-Sastre, A.; Haller, O.; Kochs,

G. Influenza A Virus Strains Differ in Sensitivity to the Antiviral Action of Mx-GTPase. *J. Virol.* **2008**, *82*, 3624–3631, doi:10.1128/JVI.01753-07.

207. Girirajan, S.; Campbell, C.; Eichler, E. Leptomycin B Alters the Subcellular Distribution of CRM1 (Exportin 1). *Physiol. Behav.* **2011**, *176*, 139–148, doi:10.1016/j.bbrc.2017.04.042.Leptomycin.

208. Callis, J. The Ubiquitination Machinery of the Ubiquitin System. *Arab. B.* **2014**, *12*, e0174, doi:10.1199/tab.0174.

209. Zerfaoui, M.; Errami, Y.; Naura, A.S.; Suzuki, Y.; Kim, H.; Ju, J.; Liu, T.; Hans, C.P.; Kim, J.G.; Abd Elmageed, Z.Y.; et al. Poly(ADP-Ribose) Polymerase-1 Is a Determining Factor in Crm1-Mediated Nuclear Export and Retention of p65 NF-κB upon TLR4 Stimulation. *J. Immunol.* **2010**, *185*, 1894–1902, doi:10.4049/jimmunol.1000646.

210. Van Neck, T.; Pannecouque, C.; Vanstreels, E.; Stevens, M.; Dehaen, W.; Daelemans, D. Inhibition of the CRM1-mediated nucleocytoplasmic transport by N-azolylacrylates: Structure–activity relationship and mechanism of action. *Bioorg. Med. Chem.* **2008**, *16*, 9487–9497, doi:10.1016/j.bmc.2008.09.051.

211. Behrens, R.T.; Aligeti, M.; Pocock, G.M.; Higgins, C.A.; Sherer, N.M. Nuclear Export Signal Masking Regulates HIV-1 Rev Trafficking and Viral RNA Nuclear Export. *J. Virol.* **2017**, *91*, doi:10.1128/JVI.02107-16.

212. Otero, G.C.; Harris, M.E.; Donello, J.E.; Hope, T.J. Leptomycin B Inhibits Equine Infectious Anemia Virus Rev and Feline Immunodeficiency Virus Rev Function but Not the Function of the Hepatitis B Virus Posttranscriptional Regulatory Element. *J. Virol.* **1998**, *72*, 7593–7597, doi:10.1128/jvi.72.9.7593-7597.1998.

213. Lee, C.H.; Chang, S.C.; Wu, C.H.H.; Chang, M.F. A Novel Chromosome Region

Maintenance 1-independent Nuclear Export Signal of the Large Form of Hepatitis Delta Antigen That Is Required for the Viral Assembly. *J. Biol. Chem.* **2001**, *276*, 8142–8148, doi:10.1074/jbc.M004477200.

214. Qin, W.; Zhang, Y.; Tang, H.; Liu, D.; Chen, Y.; Liu, Y.; Wang, C. Chemoproteomic Profiling of Itaconation by Bioorthogonal Probes in Inflammatory Macrophages. *J. Am. Chem. Soc.* **2020**, *142*, 10894–10898, doi:10.1021/jacs.9b11962.

215. Daelemans, D.; Afonina, E.; Nilsson, J.; Werner, G.; Kjems, J.; De Clercq, E.; Pavlakis, G.N.; Vandamme, A.-M. A synthetic HIV-1 Rev inhibitor interfering with the CRM1-mediated nuclear export. *Proc. Natl. Acad. Sci.* **2002**, *99*, 14440–14445, doi:10.1073/pnas.212285299.

216. Kudo, N.; Matsumor, i N.; Taoka, H.; Fujiwara, D.; Schreiner, E.; Wolff, B.; Yoshida, M.; Horinouchi, S. Leptomycin B inactivates CRM1 ¯exportin 1 by covalent modification at a cysteine residue in the. *Proc Natl Acad Sci USA* **1999**, *96*, 9112–9117.

217. Neupane, K.; Wahab, A.; Masood, A.; Faraz, T.; Bahram, S.; Ehsan, H.; Hannan, A.; Anwer, F. Profile and Management of Toxicity of Selinexor and Belantamab Mafodotin for the Treatment of Triple Class Refractory Multiple Myeloma. *J. Blood Med.* **2021**, *Volume 12*, 529–550, doi:10.2147/JBM.S317966.

218. Li, Y.; Zhou, J.; Min, S.; Zhang, Y.; Zhang, Y.; Zhou, Q.; Shen, X.; Jia, D.; Han, J.; Sun, Q. Distinct RanBP1 nuclear export and cargo dissociation mechanisms between fungi and animals. *Elife* **2019**, *8*, doi:10.7554/eLife.41331.

219. Azmi, A.S.; Khan, H.Y.; Muqbil, I.; Aboukameel, A.; Neggers, J.E.; Daelemans, D.; Mahipal, A.; Dyson, G.; Kamgar, M.; Al-Hallak, M.N.; et al. Preclinical

Assessment with Clinical Validation of Selinexor with Gemcitabine and Nab-Paclitaxel for the Treatment of Pancreatic Ductal Adenocarcinoma. *Clin. Cancer Res.* **2020**, *26*, 1338–1348, doi:10.1158/1078-0432.CCR-19-1728.

220. Termini, C.M.; Gillette, J.M. Tetraspanins Function as Regulators of Cellular Signaling. *Front. Cell Dev. Biol.* **2017**, *5*, doi:10.3389/fcell.2017.00034.

221. Thali, M. Tetraspanin functions during HIV-1 and influenza virus replication. *Biochem. Soc. Trans.* **2011**, *39*, 529–531, doi:10.1042/BST0390529.

222. Watanabe, K.; Takizawa, N.; Katoh, M.; Hoshida, K.; Kobayashi, N.; Nagata, K. Inhibition of nuclear export of ribonucleoprotein complexes of influenza virus by leptomycin B. *Virus Res.* **2001**, *77*, 31–42, doi:10.1016/S0168-1702(01)00263-5.

223. Chutiwitoonchai, N.; Mano, T.; Kakisaka, M.; Sato, H.; Kondoh, Y.; Osada, H.; Kotani, O.; Yokoyama, M.; Sato, H.; Aida, Y. Inhibition of CRM1-mediated nuclear export of influenza A nucleoprotein and nuclear export protein as a novel target for antiviral drug development. *Virology* **2017**, *507*, 32–39, doi:10.1016/j.virol.2017.04.001.

224. Neggers, J.E.; Vanstreels, E.; Baloglu, E.; Shacham, S.; Landesman, Y.; Daelemans, D. Heterozygous mutation of cysteine528 in XPO1 is sufficient for resistance to selective inhibitors of nuclear export. *Oncotarget* **2016**, *7*, 68842–68850, doi:10.18632/oncotarget.11995.

225. Turner, J.G.; Dawson, J.; Emmons, M.F.; Cubitt, C.L.; Kauffman, M.; Shacham, S.; Hazlehurst, L.A.; Sullivan, D.M. CRM1 inhibition sensitizes drug resistant human myeloma cells to topoisomerase II and proteasome inhibitors both in vitro and ex vivo. *J. Cancer* **2013**, *4*, 614–625, doi:10.7150/jca.7080.

226. Park, J.; Cho, J.; Song, E.J. Ubiquitin–proteasome system (UPS) as a target for

anticancer treatment. *Arch. Pharm. Res.* **2020**, *43*, 1144–1161, doi:10.1007/s12272-020-01281-8.

227. Ferreira, B.I.; Cautain, B.; Grenho, I.; Link, W. Small Molecule Inhibitors of CRM1. *Front. Pharmacol.* **2020**, *11*, doi:10.3389/fphar.2020.00625.

228. Williams, P.; Verhagen, J.; Elliott, G. Characterization of a CRM1-Dependent Nuclear Export Signal in the C Terminus of Herpes Simplex Virus Type 1 Tegument Protein UL47. *J. Virol.* **2008**, *82*, 10946–10952, doi:10.1128/JVI.01403-08.

229. Ślęzak, K.; Michalik, M.; Kowalczyk, A.; Rokita, H. YY1 is recruited to the cytoplasm of vaccinia virus-infected human macrophages by the Crm1 system. *Virus Res.* **2004**, *102*, 177–184, doi:10.1016/j.virusres.2004.01.028.

230. Zhao, Z.; Tao, M.; Han, W.; Fan, Z.; Imran, M.; Cao, S.; Ye, J. Nuclear localization of Zika virus NS5 contributes to suppression of type I interferon production and response. *J. Gen. Virol.* **2021**, *102*, doi:10.1099/jgv.0.001376.

231. Elinav, H.; Wu, Y.; Coskun, A.; Hryckiewicz, K.; Kemler, I.; Hu, Y.; Rogers, H.; Hao, B.; Ben Mamoun, C.; Poeschla, E.; et al. Human CRM1 Augments Production of Infectious Human and Feline Immunodeficiency Viruses from Murine Cells. *J. Virol.* **2012**, *86*, 12053–12068, doi:10.1128/jvi.01970-12.

232. Sohail, A.; Iqbal, A.A.; Sahini, N.; Chen, F.; Tantawy, M.; Waqas, F.; Winterhoff, M.; Ebensen, T.; Schultz, K.; Geffers, R.; et al. *Itaconate and derivatives reduce interferon responses and inflammation in influenza A virus infection*; 2022; Vol. 18; ISBN 1111111111.

233. McGettrick, A.F.; O'Neill, L.A. Two for the price of one: itaconate and its derivatives as an anti-infective and anti-inflammatory immunometabolite. *Curr.*

Opin. Immunol. **2023**, *80*, 102268, doi:10.1016/j.coi.2022.102268.

234. Gavriatopoulou, M.; Chari, A.; Chen, C.; Bahlis, N.; Vogl, D.T.; Jakubowiak, A.; Dingli, D.; Cornell, R.F.; Hofmeister, C.C.; Siegel, D.; et al. Integrated safety profile of selinexor in multiple myeloma: experience from 437 patients enrolled in clinical trials. *Leukemia* **2020**, *34*, 2430–2440, doi:10.1038/s41375-020-0756-6.

235. Kudo, N.; Wolff, B.; Sekimoto, T.; Schreiner, E.P.; Yoneda, Y.; Yanagida, M.; Horinouchi, S.; Yoshida, M. Leptomycin B Inhibition of Signal-Mediated Nuclear Export by Direct Binding to CRM1. *Exp. Cell Res.* **1998**, *242*, 540–547, doi:10.1006/excr.1998.4136.

236. Yue, L.; Sun, Z.; Yao, Y.; Shen, Z.; Wang, H.; Liu, X.; Zhou, F.; Xiang, J.; Yao, R.; Niu, H. CRM1, a novel independent prognostic factor overexpressed in invasive breast carcinoma of poor prognosis. *Oncol. Lett.* **2018**, doi:10.3892/ol.2018.8316.

237. Chen, Y.; Camacho, S.C.; Silvers, T.R.; Razak, A.R.A.; Gabrail, N.Y.; Gerecitano, J.F.; Kalir, E.; Pereira, E.; Evans, B.R.; Ramus, S.J.; et al. Inhibition of the Nuclear Export Receptor XPO1 as a Therapeutic Target for Platinum-Resistant Ovarian Cancer. *Clin. Cancer Res.* **2017**, *23*, 1552–1563, doi:10.1158/1078-0432.CCR-16-1333.

238. Dickmanns, A.; Monecke, T.; Ficner, R. Structural Basis of Targeting the Exportin CRM1 in Cancer. *Cells* **2015**, *4*, 538–568, doi:10.3390/cells4030538.

239. XPO1 Inhibitor Approved for Multiple Myeloma. *Cancer Discov.* **2019**, *9*, 1150–1151, doi:10.1158/2159-8290.CD-NB2019-085.

240. Wang, Q.; Li, X.L.; Mei, Y.; Ye, J.-C.; Fan, W.; Cheng, G.-H.; Zeng, M.-S.; Feng, G.-K. The anti-inflammatory drug dimethyl itaconate protects against colitis-associated colorectal cancer. *J. Mol. Med.* **2020**, *98*, 1457–1466,

doi:10.1007/s00109-020-01963-2.

241. Zhan, Z.; Wang, Z.; Bao, Y.; Liu, W.; Hong, L. OI inhibits development of ovarian cancer by blocking crosstalk between cancer cells and macrophages via HIF-1α pathway. *Biochem. Biophys. Res. Commun.* **2022**, *606*, 142–148, doi:10.1016/j.bbrc.2022.03.106.

242. Weiss, J.M.; Davies, L.C.; Karwan, M.; Ileva, L.; Ozaki, M.K.; Cheng, R.Y.S.; Ridnour, L.A.; Annunziata, C.M.; Wink, D.A.; McVicar, D.W. Itaconic acid mediates crosstalk between macrophage metabolism and peritoneal tumors. *J. Clin. Invest.* **2018**, *128*, 3794–3805, doi:10.1172/JCI99169.

243. Noy, R.; Pollard, J.W. Tumor-Associated Macrophages: From Mechanisms to Therapy. *Immunity* **2014**, *41*, 49–61, doi:10.1016/j.immuni.2014.06.010.

244. Basit, F.; Mathan, T.; Sancho, D.; de Vries, I.J.M. Human Dendritic Cell Subsets Undergo Distinct Metabolic Reprogramming for Immune Response. *Front. Immunol.* **2018**, *9*, doi:10.3389/fimmu.2018.02489.

245. Zhao, H.; Teng, D.; Yang, L.; Xu, X.; Chen, J.; Jiang, T.; Feng, A.Y.; Zhang, Y.; Frederick, D.T.; Gu, L.; et al. Myeloid-derived itaconate suppresses cytotoxic CD8+ T cells and promotes tumour growth. *Nat. Metab.* **2022**, *4*, 1660–1673, doi:10.1038/s42255-022-00676-9.

246. Casini, A.; Scozzafava, A.; Supuran, C.T. Cysteine-modifying agents: a possible approach for effective anticancer and antiviral drugs. *Environ. Health Perspect.* **2002**, *110*, 801–806, doi:10.1289/ehp.02110s5801.

Chapter 7: Publications

metabolites

MDPI

Review

Metabolite Transporters as Regulators of Immunity

Hauke J. Weiss * and Stefano Angiari

School of Biochemistry and Immunology, Trinity Biomedical Sciences Institute, Trinity College Dublin, Dublin 2, Ireland; angiaris@tcd.ie

* Correspondence: weissh@tcd.ie

Received: 4 September 2020; Accepted: 16 October 2020; Published: 19 October 2020



Abstract: In the past decade, the rise of immunometabolism has fundamentally reshaped the face of immunology. As the functions and properties of many (immuno)metabolites have now been well described, their exchange among cells and their environment have only recently sparked the interest of immunologists. While many metabolites bind specific receptors to induce signaling cascades, some are actively exchanged between cells to communicate, or induce metabolic reprograming. In this review, we give an overview about how active metabolite transport impacts immune cell function and shapes immunological responses. We present some examples of how specific transporters feed into metabolic pathways and initiate intracellular signaling events in immune cells. In particular, we focus on the role of metabolite transporters in the activation and effector functions of T cells and macrophages, as prototype adaptive and innate immune cell populations.

Keywords: cell metabolism; immunity; metabolite transporter; solute carrier; T cells; macrophages

1. Metabolites and Their Transporters: Key Players in Immunity

Active metabolite transport is key for the survival of every cell. In immune cells, availability of extracellular metabolites also shapes immune responses and cellular interactions. Metabolite transporters indeed largely dictate immune cell activity by providing, or restricting, access to nutrients, and thereby determining the cellular metabolic profile [1]. For example, while glucose and amino acids (AAs) are largely imported as part of pro-inflammatory responses, fatty acid (FA) uptake has been found to drive pro-resolving, anti-inflammatory phenotypes [2]. Importantly, expression of the respective transporters is tightly linked with metabolic reprogramming in immune cells, as evident by direct involvement in the activation of metabolic master regulators, such as the mammalian target of rapamycin complex (mTORC) [3]. Furthermore, metabolites are actively released into or scavenged from the extracellular space by some cells to drive metabolic changes in their environment. A prime example is the Warburg effect, where cancer cells switch away from aerobic respiration towards fermentation of glucose to quickly generate biomass [4,5]. At the same time, release of "leftover" metabolites such as lactate hugely affects the metabolism and fate of surrounding immune cells [6].

As cellular metabolism itself, metabolite transporters have been well studied for decades, with their main function mostly being attributed to providing energy sources and building bricks for cells. Being polar molecules, many metabolites require active transport across the cell membrane, as they are unable to readily diffuse into the cell [7]. Hence, regulation and expression of dedicated transporters is critical to meet cell metabolic needs and initiate alternative pathways to adapt to changes in the cellular environment. As rate-limiting providers of nutrients, metabolite transporters have also gained interest as putative drug targets in recent years, with many potential drugs with immunomodulatory function being currently in development.

In mammals, metabolites are mostly transported across the plasma membrane by members of the solute carrier (SLC) family of membrane transport proteins, many of which are expressed in

immune cells. More than 400 individual SLCs have been discovered, grouped into 52 subfamilies [8]. SLCs transport substrates through one of three modes: (i) cotransporters need to translocate their substrate together with an ion, which travels along a concentration gradient, thus providing the energy required; (ii) exchangers use the same mechanism, but here, the ion and substrate travel in opposite directions; and (iii) facilitated transporters translocate a single substrate passively along a concentration gradient. However, as there are still many orphan transporters, i.e., transporters of unknown function and with unknown substrates, additional modes of transport might exist in the SLC family [9,10]. Other than metabolites, SLCs also transport metals, vitamins and neurotransmitters, as well as inorganic ions, confirming their crucial role in maintaining cell survival and regulating cell functionality [8].

In immune cells, expression of SLCs is tightly regulated. Many different SLCs have been shown to control sugar, lipid and amino acid flux in and out of immune cells, thus determining cell fate and function. In this review, we summarize the importance of such transporters in the activation, function and polarization of adaptive and innate immune cells, with a particular focus on T cells and macrophages.

2. Expression and Importance of Metabolite Transporters in T Cells

During differentiation and activation, T cells undergo distinct metabolic changes that cater to their respective needs. While naïve T cells mostly rely on the tricarboxylic acid (TCA) cycle and oxidative phosphorylation (OXPHOS), activated T cells switch to glycolysis, glutaminolysis and FA synthesis to accommodate an increased demand for energy [11]. There are also metabolic differences in different T cell subsets. As an example, regulatory T cells (Tregs) utilize FA oxidation (FAO) to generate energy when proliferating, while conventional $CD4^+$ T cells mostly use glucose as fuel [12]. Abundance of these resources is thus crucial for T cell fate decision making, and expression of the respective transporter molecules is closely linked to T cell activity (Figure 1).

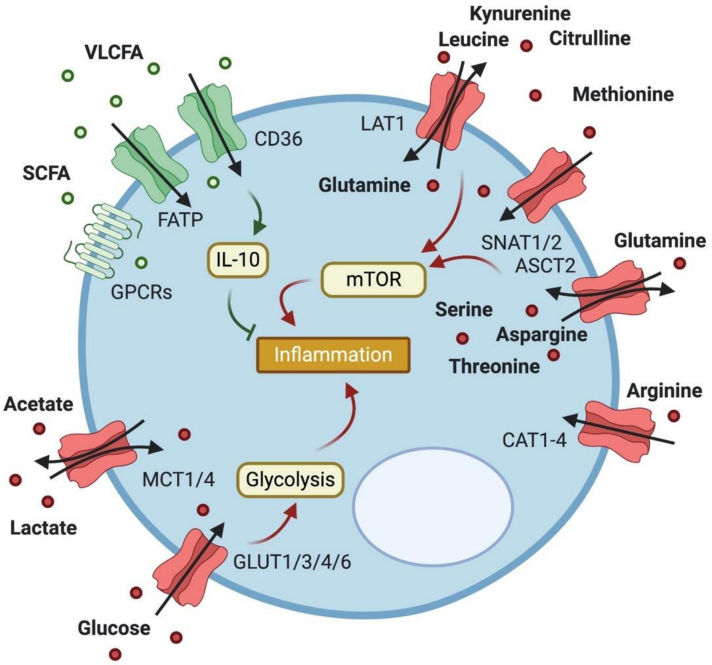


Figure 1. Expression of metabolite transporters on T cells and their impact on T cell function. T cells express a variety of transporters to facilitate their metabolic needs. Import of fatty acids (FAs) of various sizes reduces inflammation through FA oxidation and IL-10 production, while import of lactate and acetate boosts inflammation. Transporters of the GLUT family take up glucose to increase glycolysis in activated T cells, while amino acid (AA) transport drives inflammation mainly via mTOR activation.

2.1. Glucose Transport

Surface expression of the glucose transporter GLUT1 (also known as solute carrier family 2, facilitated glucose transporter member 1, SLC2A1) is induced upon T cell receptor (TCR) engagement [13], as well as signaling through CD28 [14]. Upregulation of GLUT1 is a crucial step in T cell activation, importing glucose to be metabolized through aerobic glycolysis, and restriction of glucose uptake has been found to largely impair T cell activation [14]. In addition to activated T cells, GLUT1 surface expression is also increased in naïve T cells upon interleukin 7 (IL-7) stimulation, and in memory $CD4^+$ T cells after insulin treatment [15]. It is suggested that GLUT1 expression is crucial for development and maintenance of both $CD4^+$ and $CD8^+$ T cell memory [15,16]. Furthermore, $CD4^+$ T cells require GLUT1 expression to differentiate into T helper type 1 (T_H1), T_H2 and T_H17 cells [17], while overexpression of GLUT1 does not affect their development [14]. Other glucose transporters have been found to be expressed in the context of T cell activation. In addition to GLUT1, the glucose transporters GLUT3, GLUT4 and GLUT6 (SLC2A3, SLC2A4 and SLC2A6) have also been found to be upregulated in activated $CD4^+$ T cells to varying degrees [18,19]. As GLUT1 is the most prominent and well-studied glucose transporter, it is believed that the other GLUT variants have mostly supporting or compensatory functions in most T cells [17]. As an exception, renal cell carcinoma (RCC) $CD8^+$ tumor-infiltrating lymphocytes (TILs) specifically upregulate GLUT3 in response to CD28 co-stimulation [20].

Of note, besides providing nutrients, glucose import and metabolism have other distinct impacts on T cell functionality. The glycolytic enzyme glyceraldehyde 3-phosphate dehydrogenase (GAPDH) has been found to have a moonlighting function as a negative regulator of interferon gamma (IFN-γ) production in the absence of glycolysis [21]. Moreover, some products of glycolysis are involved in epigenetic modifications: pyruvate is processed into acetyl-coenzyme A (acetyl-CoA), which is not only oxidized for adenosine triphosphate (ATP) production in the mitochondria, but also involved in histone acetylation [22]. Furthermore, products of glycolysis can glycosylate proteins, modifying their function and localization and ultimately impacting T cell differentiation and activation [23]. Overall, regulation of glucose import and processing by GLUTs represents an essential step for T cell activation and engagement of effector functions.

2.2. Lactate Transport

Lactate often builds up in hypoxic conditions and at sites of inflammation [24]. A by-product of glycolysis, lactate, is generated from pyruvate by lactate dehydrogenase (LDH) as part of aerobic glycolysis [25], and can be further metabolized through the TCA cycle for energy generation [26]. Transport of lactate is facilitated by several transporters: proton-linked monocarboxylic acid transporters (MCTs) 1-4 are all bidirectional, however MCT1 (SLC16A1) is mostly relevant for lactate uptake, whereas MCT4 (SLC16A3) mostly exports excess lactate into the extracellular space [27]. Additionally, two other members of the SLC5 family, SLC5A12 and SLC5A8, can transport lactate [28]. In T cells, MCT1 expression is upregulated upon TCR activation, and its blockage results in impaired cytotoxic T cell (CTL) function in the tumor microenvironment [29]. Excess lactate import into T cells has also been shown to restrict proliferation and cytokine production of CTLs. This is possibly due to their reliance on glycolysis [30], as lactate import goes along with consumption of reduced nicotinamide adenine dinucleotide (NADH) and inhibition of glycolysis [31]. On the other hand, Tregs are able to change their metabolism to function in a lactate-high environment, and are therefore unaffected [32]. Recently, it has been found that lactate uptake via SLC5A12 results in pyruvate kinase M2/signal transducer and activator of transcription 3 (PKM2/STAT3)-mediated production of IL-17 in $CD4^+$ T cells in rheumatoid arthritis (RA) [33]. Imported lactate fuels FA synthesis in these cells, which is indeed increased while they are retained at the site of inflammation, and blockage of SLC5A12 ameliorated the severity of the disease [33]. Similar observations were made previously in the tumor microenvironment, where lactate is imported into $CD4^+$ T cells by SLC5A12, decreasing $CD4^+$ T cell motility while

inducing IL-17 production [34]. These works suggest a complex role for extracellular lactate uptake in controlling T cell fate and function, which may be particularly relevant at the site of inflammation [35].

2.3. Fatty Acid Transport

FAO is halted in activated T cells, and FA synthesis is initiated to provide growing and dividing cells with lipids [11]. Additionally, FAs are transported into activated T cells either by active diffusion [36], or through dedicated transporters. One is the FA translocase CD36 [37] that is also involved in uptake of other molecules, such as lipoproteins [38], oxidized phospholipids [39] and collagen [40]. CD36 is notably upregulated in Tregs, especially in those found in the tumor microenvironment [41]. A more specific uptake of FAs in T cells is through members of the FA transport protein (FATP) family. These transporters take up very long-chain FAs (VLCFAs) and simultaneously esterificate them to trap them inside the cell [42]. The roles of FATP1 and CD36 in T cell function are yet to be clearly determined, as it has proven difficult to separate imported FAs from those produced in metabolic pathways [1]. Shorter FAs can also be imported by a number of G protein-coupled receptors (GPCRs): GPCR40, 41, 43, 84 and 120 all have different affinities for certain FA lengths [43], however only GPCR43 and 84 are expressed in T cells. GPCR43 is crucial for maintaining intestinal homeostasis by inducing IL-10 production in intestinal T cells [44], while GPCR84 regulates IL-4 production in response to CD3 crosslinking, importing medium-chain FAs [45,46].

Acetate is another short-chain fatty acid that is imported into T cells through members of the MCT family or aquaporins [47–49]. In $CD8^+$ T cells, acetate influx is required for optimal memory function: upon entry, acetate is converted to acetyl-CoA, subsequently acetylating and activating GAPDH, and thereby boosting memory $CD8^+$ T cell responses [50]. Moreover, acetate-derived acetyl-CoA has been found to promote IFN-γ production in $CD4^+$ T cells [51]. More recently, Qiu et al. found acetate imported through MCTs to restore effector function in glucose-restricted $CD8^+$ T cells in cancer. Acetate effectively promoted histone acetylation via acetyl-CoA, resulting in increased transcription of IFN-γ and increased tumor clearance [52]. Interestingly however, high acetate levels at sites of infection have also been shown to augment glutaminolysis while simultaneously reducing calcium influx and effector function in $CD8^+$ T cells, resulting in decreased immunopathology, yet improved pathogen clearance [53]. FA import thus regulates T cell functionality, but further investigation is needed to clarify the exact role of different FAs in the control of T cell activity.

2.4. Amino Acid Transport

Amino acids (AAs) are another highly valuable energy source for activated T cells, as they are a valuable resource for protein production. While the relevance of AA transport in developing and naïve T cells is postulated to be relatively low [54], T cell activation and differentiation into effector subsets largely depend on the abundance of extracellular AAs. Dedicated AA transporters like the large neutral amino acid transporter 1 (LAT1, also known as SLC7A5) and the sodium-coupled neutral amino acid transporters (SNATs) SNAT-1/SLC38A1 and SNAT-2/SLC38A2, and Alanine, Serine, Cysteine Transporter 2 (ASCT2/SLC1A5) are increased in expression in activated T cells [55–57]. Although leucine is the primary substrate for LAT1, this transporter is also able to translocate other AAs with a lower affinity. Forming a heterodimer with LAT-2/SLC7A8 in a complex with CD98 [58], LAT1 expression is required for a full $CD8^+$ T cell response [59]. LAT1 is upregulated upon TCR stimulation through the extracellular signal-regulated kinase 1/2-mitogen-activated protein kinase (ERK/MAPK) pathway and activation of the nuclear factor of activated T cells (NFAT) [59], while c-Myc also regulates its expression [60]. Leucin is a critical factor in mTORC1 activation, and deletion of LAT1 results in severely impaired T cell activation [59] and cytokine production [61].

Despite its name, ASCT2 is mainly known as a glutamine transporter [62]. Similarly to LAT1, ASCT2-mediated glutamine uptake is required for TCR- and CD28-induced activation of mTORC1 in $CD4^+$, but not $CD8^+$ activated T cells [57]. Besides being metabolized for ATP generation in the TCA cycle, glutamine can be used as a substrate for production of other AAs, as well as polyamines and

glutathione. The latter is an antioxidant and metabolic regulator, priming T cells for activation and enrolling them in a glycolytic metabolic program [63]. Furthermore, glutamine directly fuels LAT1 activity, because, as an antiporter, LAT1 requires glutamine as an efflux substrate [64]. ASCT2 is an antiporter itself, exporting the small AAs serine, asparagine or threonine [62]. However, how this ASCT2-mediated efflux of important immunomodulatory AAs such as serine [65] affects T cell biology is not known. Extracellular serine has also been found to enter T cells and modulate proliferation [65], but the transporter relevant for serine uptake remains to be identified. AA uptake through both LAT1 and ASCT2 has also been shown to be crucial for differentiation of $CD4^+$ T cells into T_H1 and T_H17 cells, while T_H2 cells and Tregs develop independently of these transporters [59] [57]. Furthermore, it has been suggested that follicular T cells (Tfh cells) require LAT1 for full differentiation, as indicated by impaired T cell mitogen-activated protein kinase-dependent immunoglobulin G (IgG)1 responses in *Slc7a5*$^{fl/fl}$CD4-Cre mice [59]. Finally, there is evidence that depletion of ASCT2 results in impaired $CD4^+$ memory T cell compartments [57]. T cells also express a number of alternative glutamine transporters (SLC3A2, SLC7A5 and SLC38A1) [60], but their role in T cell biology remains to be determined.

Another substrate for LAT1, as well as SNAT2, is the essential AA methionine. Other methionine transporters expressed in T cells include SLC1A5, SLC7A8 and SLC38A1 [66,67]. Methionine metabolism is required for T cell activation and differentiation, and blocking LAT1-mediated methionine import has been shown to largely impair protein synthesis and RNA and histone methylation [68]. Of note, the tryptophan-derived metabolite kynurenine can also be transported via LAT1 [69]. Kynurenine is a potent immunomodulatory metabolite that acts as a ligand for the aryl hydrocarbon receptor (AHR) transcription factor complex, promoting $CD4^+$ T cell differentiation into anti-inflammatory Tregs [70,71]. AHR itself can initiate increased uptake of kynurenine by upregulating alternative kynurenine transporters SLC7A8 and SLC36A4 [72], resulting in a positive feedback loop. Kynurenine has also been found to accumulate and activate mTORC1 in T cells in systemic lupus erythematosus (SLE), markedly enhancing T cell activity and skewing lineage development [73,74]. Conversely, SLE T cells diminish cysteine generation because of an impaired pentose phosphate pathway (PPP), resulting in decreased glutathione synthesis and accumulation of cystine. Glutathione generation can be rescued by PPP-independent treatment with the glutathione precursor N-acetylcysteine (NAC), which can also potently inhibit NADPH-dependent kynurenine synthesis, substantially replenishing intracellular reduced nicotinamide adenine dinucleotide phosphate NADPH levels. As an mTORC inhibitor [75], NAC could ultimately be used as a therapeutic in SLE [76]. NAC is transported across the plasma membrane via the glutamate transporter 1 (GLT-1/SLC1A2) [77], however not much is known about GLT-1 expression in T cells. Of note, recently it has been found that the kynurenine pathway also contributes to tumor-associated $CD4^+$ T cell exhaustion [78].

Differently from the essential AA methionine, arginine is only conditionally essential, as it can be synthesized from citrulline [79]. In addition to synthesis inside the cell, arginine is imported by cationic amino acid transporters 1-4 (CAT1-4/SLC7A1-4) [80] and subsequently metabolized into a variety of downstream products with multiple functions. In activated T cells, imported arginine is primarily metabolized into ornithine, putrescine, agmatine and, to a lower extent, into spermidine and proline [81]. L-arginine metabolism is required for T cell survival, proliferation and anti-tumor effector function, and expression of CAT1 is upregulated upon T cell activation and if arginine levels inside the cell are low [81]. Accordingly, depletion of L-arginine results in arrest of the cell cycle in activated T cells [82], but T cells can escape arginine depletion by increasing citrulline uptake through LAT1, if available, and subsequently recycling arginine from citrulline utilizing the enzymes argininosuccinate synthase (ASS) and argininosuccinate lyase (ASL) [83]. The exact mechanisms involved in CAT1 upregulation, and its direct impact on T cell biology, remain, however, to be identified.

The relevance of most AA transporters in T cell biology relies on their involvement in mTORC1 signaling, but other pathways, like a partly anti-inflammatory kynurenine pathway, are also emerging. As autophagy has been shown to be associated with AA transport, it might be another candidate for an AA-mediated mechanism relevant in T cell activation and differentiation [84,85]. Together, these results

show that the function of AA transporters in T cells is not only to provide them with nutrients, but also to dictate T cell fate and function.

3. Expression and Importance of Metabolite Transporters in Macrophages

As T cells, macrophages undergo drastic metabolic changes throughout activation, and metabolic needs of these cells depend on their polarization and function. While classically activated pro-inflammatory M1 macrophages have a broken TCA cycle and generate ATP through glycolysis and the PPP, anti-inflammatory M2 macrophages upregulate OXPHOS and FAO to meet their energetic needs [86]. As for T cells, expression of metabolite transporters has been suggested to regulate macrophage activation and polarization and is controlled by activation stimuli. However, the importance of metabolite transporters in macrophage functionality has been studied in less detail (Figure 2).

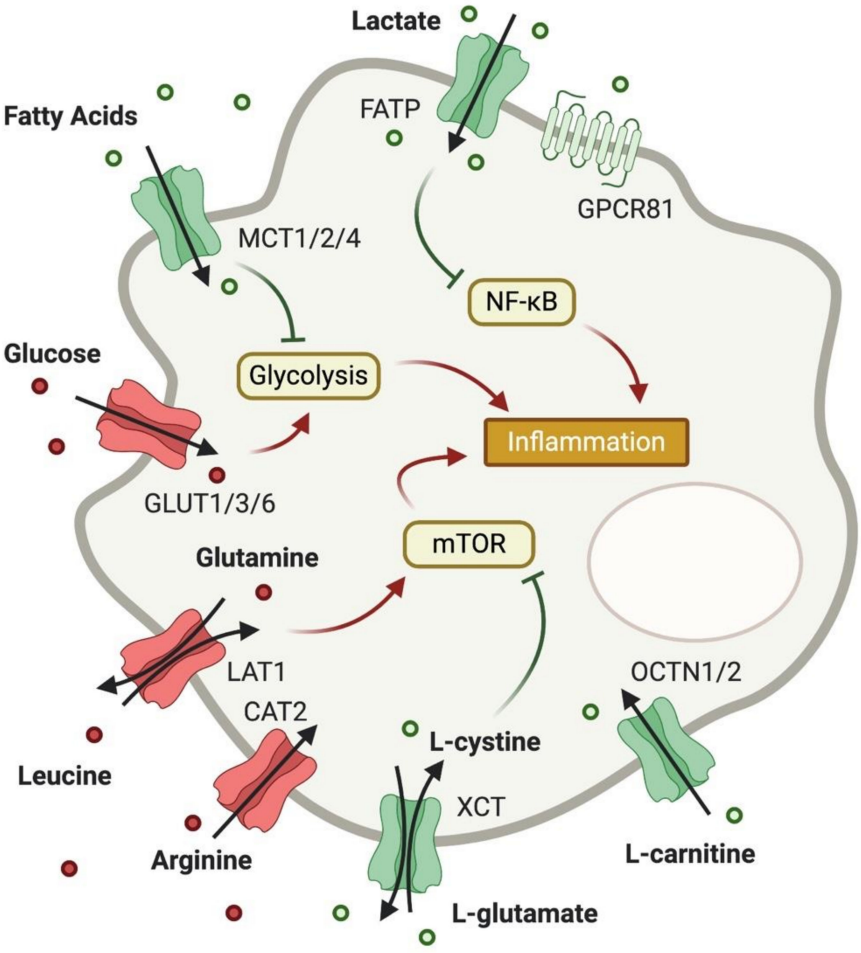


Figure 2. Expression of metabolite transporters on macrophages and their impact on macrophage function. As in T cells, glucose uptake is increased in pro-inflammatory macrophages, and AA uptake boosts mTOR activity. Cystine and glutamate, however, can limit mTOR activation through generation of cysteine and glutathione. Carnitine also exhibits anti-inflammatory potential, while FA uptake can limit glycolysis. Unlike in T cells, lactate uptake into macrophages is considered to be anti-inflammatory through inhibition of NF-κB.

3.1. Glucose Transport

As glycolysis and PPP are energetically not very efficient, M1 macrophages increase their glucose consumption by upregulation of GLUT1 upon lipopolysaccharide (LPS) stimulation [87]. GLUT1 is the rate-limiting protein for glucose uptake, and its overexpression results in a hyper-inflammatory

phenotype in macrophages [87]. On the other hand, deletion of GLUT1 leaves pro-inflammatory macrophages functionally impaired, while boosting M2-associated markers. GLUT1 deficiency also impaired phagocytosis and resulted in a larger abundance of anti-inflammatory metabolites ornithine and polyamines, while accumulation of pro-inflammatory metabolites, such as succinate, is reduced in macrophages lacking GLUT1 [88]. Interestingly, while downregulated in classically activated macrophages [87], expression of the glucose transporter GLUT3 is induced in macrophages in hypoxic conditions in atherosclerotic lesions, increasing lipid synthesis from the imported glucose, and possibly supporting foam cell formation [89]. Another glucose transporter, GLUT6, is expressed in macrophages. However, despite its upregulation upon LPS stimulation, it is believed that GLUT6 merely supports GLUT1-mediated glucose uptake [90]. GLUT1 thus represents the most important glucose transporter controlling macrophage activation and effector functions.

3.2. Lactate Transport

In innate immune cells, lactate is produced and exported in large amounts during pro-inflammatory responses [6]. Lactate export is facilitated by MCT4, whose expression is upregulated in classically activated macrophages in a myeloid differentiation primary response 88 (MYD88)- and NF-κB-dependent manner [91]. MCT4 upregulation is crucial for full macrophage activation, as its deletion results in intracellular accumulation of lactate and decreased glycolysis [91]. Macrophages also express SLC5A12, however blocking this lactate transporter does not affect macrophage metabolism or activation, suggesting SLC5A12 does not play an important role in macrophages [33].

Macrophages also express MCT1, MCT2 [92] and GPR81 to facilitate transport of lactate. Lactate uptake via GPR81 has been shown to reduce LPS-induced IL-1β in murine macrophages, through inhibition of NF-κB and the inflammasome [93]. Similarly, GPR81-independent lactate uptake through MCT1 inhibits pro-inflammatory signaling in bone marrow-derived macrophages and decreases macrophage activation and cytokine production [94]. Mechanistically, lactate uptake in macrophages has been shown to stabilize hypoxia-inducible factor 1α (HIF1α), and to induce the production of vascular endothelial cell growth factor (VEGF) [95]. This is especially remarkable and somehow surprising, as HIF1α is usually considered a pro-inflammatory mediator [96]. Importantly, studies with primary human monocytes and peripheral blood mononuclear cells have confirmed these observations to be relevant for human macrophages biology as well [97]. Overall, lactate import in macrophages seems to limit their pro-inflammatory potential.

3.3. Fatty Acid Transport

The FA transporter FATP1 is downregulated in classically activated macrophages, and its deletion results in increased glucose metabolism and a pro-inflammatory phenotype in adipose tissue macrophages [98]. In accordance, FA uptake through FATP1 is crucial for alternative macrophage activation, and overexpression of FATP1 limited macrophage-induced inflammation through a reduction in glycolysis and PPP [98]. Importantly, *Fatp1* expression in macrophages is largely controlled by peroxisome proliferator-activated receptor (PPAR)α and PPARγ [99]. In contrast, LPS-stimulated macrophages increase expression of the medium-chain FA transporter GPR84, initiating FA uptake and increasing IL-12 p40 expression [46]. More recently, GPR84-mediated FA uptake has been found to induce an inflammatory CD11b^{hi} status in alveolar macrophages during lung injury [100], highlighting the complex functions of FA in macrophage activity.

3.4. Amino Acid Transport

Like T cells, classically activated macrophages have an increased demand for AAs to synthesize proteins and feed into metabolic pathways, however transport of AAs in macrophages has been less studied than in T cells. Classically activated macrophages increase expression of LAT1 to increase leucine uptake, contributing to mTORC1-induced metabolic reprogramming and increased cytokine production. Blockage or downregulation of LAT1 in macrophages results in decreased

mTORC1-induced IL-1β production [101]. Expression of arginine transporter CAT2 is induced in both classically and alternatively activated macrophages, and L-arginine is subsequently imported. Deletion of CAT2 notably reduced arginine metabolism, resulting in decreased amount of nitrites, polyamines and proline, while arginase and nitric-oxide synthase 2 (NOS2) activity remained unchanged [102]. This directly contradicts a previous study, claiming NOS2 activity to depend on CAT2 expression [103].

Mouse peritoneal macrophages upregulate expression of cystine/glutamate transporter (XCT/SLC7A11) upon LPS stimulation [104] to import cystine, which is subsequently converted to cysteine for glutathione and protein synthesis [105]. The same system, as well as the X_{AG} system, was found to import glutamate in human monocyte-derived macrophages for production of glutathione [106]. Glutathione is particularly important in macrophages for maintaining the thiol redox state and protecting from oxidative stress [107].

Human macrophages also import L-carnitine via organic cation transporter, novel and type 1 and 2 (OCTN1/SLC22A4 and OCTN2/SLC22A5). L-carnitine is known to mediate differentiation of monocytes into macrophages [108], and it has been suggested that deficiencies in carnitine transport are associated with increased pathogenicity in Crohn's disease [109].

4. Expression and Importance of Metabolite Transporters in Other Immune Cells

T cells and macrophages are by far the most investigated immune cells in the field of immunometabolism. However, the role of metabolic reprogramming in the fate and function of other cells of the immune system cannot be denied. Nonetheless, very little is known about the role of metabolite transporters in these cells, but it can generally be assumed that expression of glucose importers correlates with cellular activation. Accordingly, B cells upregulate GLUT1, 3 and 4 when activated [18], and restriction of glucose uptake results in attenuated activation and impaired antibody production [110]. Upregulation of GLUTs is also critical for functional activation of dendritic cells (DCs) [111], neutrophils [112] and NK cells [113].

Regarding FAs and AAs, butyrate and propionate uptake from commensal gut bacteria via SLC5A8 has been shown to induce a tolerogenic phenotype in DCs in the gut, protecting against intestinal inflammation [114]. Moreover, some inflammatory neutrophils in cystic fibrosis airways have been found to upregulate ASCT2 to facilitate AA uptake [112], confirming an important role for metabolite transporters in other immune cell subsets. Although metabolite uptake undoubtedly occurs in these cells, information about the expression and function of metabolite transporters in immune cells other than T cells and macrophages is still limited.

5. Metabolite Transport as Intercellular Communication

Metabolites function as signaling molecules both inside and outside cells. While many metabolite-induced signaling events are receptor-mediated, active metabolite transport is used by certain cell types to change their environment and manipulate the behavior of surrounding cells. In addition to immune regulation in T cells and macrophages, non-immune cells use active metabolite transport to shape immune responses by exporting or scavenging metabolites. By creating a favorable milieu, some cells can use metabolites to signal to immune cells and influence their activity.

Prostaglandin E2 (PGE2) can be translocated by SLCO2A1, a transporter expressed in murine macrophages. SLCO2A1 exports PGE2 from the cell in inflammatory conditions [115], potentially to maintain removal of neutrophils from inflamed tissue and promote inflammation resolution [116]. How PGE2 export is initiated and what mechanisms are involved remain to be investigated.

Short-chain FAs (SCFAs) are produced by commensal microbiota in the gut and contribute to intestinal homeostasis. T cells take up SCFAs produced by the microbiome via GPR43 and promote microbiota antigen-specific IL-10 production, ultimately suppressing immune responses against commensal bacteria [44]. Furthermore, microbial butyrate, an SCFA, has been found to have a similar effect on macrophages in the gut by inducing a homeostatic, M2-like phenotype [117].

Classically activated macrophages produce and release succinate, a pro-inflammatory metabolite that induces IL-1β production through stabilization of HIF-1α [118] and reactive oxygen species (ROS) production [119]. Succinate binds the succinate receptor SUCNR1, and in neural stem cells (NSCs), binding of SUCNR1 triggers an anti-inflammatory program, characterized by release of the immune modulator PGE2, and expression of the succinate transporters SLC13A3 and SLC13A5. These transporters subsequently take up the extracellular succinate, effectively scavenging it from the extracellular space and thereby reducing succinate-mediated inflammation. Through this mechanism, NSCs are able to actively reduce neuroinflammation in the central nervous system, and might protect from chronic inflammation and degenerative neurological diseases [120].

Another example for metabolite-induced reprogramming of immune cells is the reversed Warburg effect. The Warburg effect describes a metabolic state in cancer cells that is characterized by aerobic glycolysis and results in production of lactate and pyruvate [4]. In the reversed Warburg effect, cancer cells induce the Warburg effect in neighboring fibroblasts. These "corrupted" cells then produce large amounts of lactate and pyruvate and export them to the extracellular space through mono-carboxylate transporters MCT1 and MCT4 [121]. Cancer cells subsequently express MCT1 and MCT4 to take up these energy-rich metabolites and feed them into their TCA cycle to generate ATP [122]. At the same time, the exported lactate also diminishes CTL responses in the tumor microenvironment due to the inhibitory effects of lactate on glycolysis and subsequently CTL activation [29], and initiates the generation of tumor-tolerating, anti-inflammatory Tregs [32]. This is mediated by reduced T-box expressed in T cells (T-bet) and increased forkhead box protein P3 FoxP3 expression in tumor-associated $CD4^+$ T cells [123]. A similar effect can be observed in macrophages, where lactate produced by cancer cells and fibroblasts induces expression of VEGF in tumor-associated macrophages, polarizing them into a homeostatic, M2-like phenotype in a HIF1α-dependent manner [95]. A great example for lactate as a communicator among cells in a non-cancerous context was recently described by Zhang and colleagues: in the ischemic muscle, endothelial cells export lactate through MCT4. Macrophages then import the lactate via MCT1, subsequently acquiring an M2-like, anti-inflammatory phenotype, promoting muscle regeneration [124].

Interestingly, extracellular lactate can also induce autoimmunity. In RA, synovial fibroblasts upregulate MCT4, much like in the tumor environment, and export large amounts of lactate, enriching the synovial fluid and acidifying it [125]. As discussed before, lactate import into $CD4^+$ T cells can induce production of IL-17. In RA, this increased cytokine production widely contributes to the pathology in this disease. Furthermore, as T cell motility is impaired by lactate as well, these T cells are retained at the site, further promoting inflammation [33]. These works thus highlighted the potential of extracellular metabolites to act as signaling molecules, affecting both tissue and immune cell functionality.

6. Metabolite Transport as Therapeutic Target

As described above, regulation of metabolite transport in immune cells is highly correlated with cell fate and activity, and many pathologies can be linked to transporter malfunctions. Furthermore, many new diseases, mostly of monogenetic origin, keep being discovered and linked to transporter malfunctions or mutations, and the demand for drugs impacting such pathologies is high. Notably, approximately 20% of known SLC transporters are associated with human disease through mutation [7]. As the scientific and clinical relevance of metabolite transporters is increasing, new therapeutic strategies are under development that specifically target these essential proteins.

It has been shown that monocytes from RA patients overexpress LAT1, alongside increased cytokine production, suggesting increased AA influx to be linked to chronic inflammation [101]. Recently, blocking LAT1 expressed on T cells has been found to successfully reduce inflammation in psoriasis [126]. Drugs targeting LAT1 are currently undergoing clinical trials as cancer therapeutics [127]. If successful, these LAT1 inhibitors could potentially be used to treat autoinflammatory diseases. As mentioned before, tumor-associated Tregs upregulate expression of CD36, an FA translocase. CD36 has been

found to be crucial for lipid metabolism in these cells and enables them to suppress immune responses in the tumor microenvironment [41]. Targeting CD36 with antibodies successfully depleted pro-tumor Tregs and improved tumor clearance without inducing autoimmunity [41]. CD36 might therefore be an interesting target for new cancer immunotherapies. Another FA transporter, GPR84, is currently being investigated as a potential therapeutic target in fibrotic diseases. The GPR84-blocking compound PBI-4050 has been shown to not only decrease FA-induced activation of fibroblasts to profibrotic myofibroblasts, but also to reduce macrophage activation [128]. Notably, PBI-4050 has recently undergone phase 2 clinical trials for the treatment of idiopathic pulmonary fibrosis [129]. Finally, as previously described, blocking of lactate transporter SLC5A12 may prove successful in the treatment of RA by limiting T_H17-induced inflammation. Pucino and colleagues have committed to developing potent monoclonal antibodies and advancing to pre-clinical studies [33].

Another potential target for metabolite transporter-modulating drugs are cancer cells. Inhibiting transporters of glucose, AAs or lactate may indeed represent a powerful tool to decrease tumor growth, as these metabolites are usually in high demand in cancer cells, and their respective transporters are often overexpressed [130–132]. Inhibitors of MCT1 in tumor cells have been shown to effectively inhibit lipid synthesis in cancer cells and increase influx of tumor immune cells, and some of these inhibitors are currently being tested in clinical trials [133]. On the other hand, block or downregulation of the lactate exporter MCT4 could potentially decrease lactate build-up in the tumor microenvironment, thus reducing immunosuppression. Studies in multiple types of cancers have shown that this approach not only inhibits tumor growth [134] and prolongs relapse time [135], but also induces apoptotic programs in the cancer cells themselves [136]. Another interesting example is the anti-inflammatory RA drug Sulfasalazine. Sulfasalazine blocks the cystine–glutamate exchange transporter XCT that has also been found to be overexpressed in tumor cells [137]. Sulfasalazine is currently being tested in various tumor models, showing promising results in enhancing tumor clearance in prostate cancer [138,139]. Combined blockage of metabolite transporters in tumor cells may thus offer a new strategy for cancer therapy. Overall, these findings highlight the potential of metabolite transporters as novel drug targets for immunomodulation and cancer therapy.

7. Conclusions

Metabolic pathways shape every aspect of immune cell fate and function. This is becoming more evident with every new publication in the field of immunometabolism. Metabolite transporters, as metabolites themselves, have acquired novel functions as regulators of immunity, some of which we have presented in this review.

As evident form the literature presented, active metabolite transport is key in organizing immune cell functionality. Regulation of metabolite transporter expression is also an important tool in intercellular communication, a system that is susceptible to manipulation and can thus easily promote disease or cancer. Conversely, targeting metabolite transporters bears a large potential for drug development, and has been shown to reduce pathologies in many diseases. While functions of the transporters highlighted in this review are well documented, many metabolite transporters are still categorized as orphan transporters without known function or substrates. Due to a lack of crystallographic data for many SLCs, specificity of many potential and known transporters is hard to determine [140]. On the other hand, many immunomodulatory metabolites, especially from the TCA cycle [141], are known to be actively transported among cells with transporters yet to be identified. It is highly plausible that future research will reveal many more SLCs to be involved in metabolite transport, further diversifying their relevance as regulators of immunity.

Author Contributions: Writing—original draft preparation, H.J.W.; writing—review and editing, S.A. All authors have read and agreed to the published version of the manuscript.

Funding: This project received no external funding.

Acknowledgments: Figures were created with BioRender.com. H.J.W. is supported by the European Union's Horizon 2020 research and innovation programme under the Marie Skłodowska-Curie grant agreement No 813343.

Conflicts of Interest: The authors declare no conflict of interest.

References

1. Hsu, C.-L.; Dzhagalov, I.L. Metabolite Transporters—The Gatekeepers for T Cell Metabolism. *Immunometabolism* **2019**. [CrossRef]
2. O'Neill, L.A.J.; Kishton, R.J.; Rathmell, J. A guide to immunometabolism for immunologists. *Nat. Rev. Immunol.* **2016**, *16*, 553–565. [CrossRef]
3. Chi, H. Regulation and function of mTOR signalling in T cell fate decisions. *Nat. Rev. Immunol.* **2012**, *12*, 325–338. [CrossRef]
4. Warburg, O. On the origin of cancer cells. *Science* **1956**, *123*, 309–314. [CrossRef]
5. Vander Heiden, M.G.; Cantley, L.C.; Thompson, C.B. Understanding the Warburg Effect: The Metabolic Requirements of Cell Proliferation. *Science* **2009**, *324*, 1029–1033. [CrossRef]
6. Palsson-McDermott, E.M.; O'Neill, L.A.J. The Warburg effect then and now: From cancer to inflammatory diseases. *BioEssays* **2013**, *35*, 965–973. [CrossRef]
7. Lin, L.; Yee, S.W.; Kim, R.B.; Giacomini, K.M. SLC transporters as therapeutic targets: Emerging opportunities. *Nat. Rev. Drug Discov.* **2015**, *14*, 543–560. [CrossRef]
8. Perland, E.; Fredriksson, R. Classification Systems of Secondary Active Transporters. *Trends Pharmacol. Sci.* **2017**, *38*, 305–315. [CrossRef]
9. Hediger, M.A.; Romero, M.F.; Peng, J.-B.; Rolfs, A.; Takanaga, H.; Bruford, E.A. The ABCs of solute carriers: Physiological, pathological and therapeutic implications of human membrane transport proteinsIntroduction. *Pflugers Arch.* **2004**, *447*, 465–468. [CrossRef]
10. Zhang, Y.; Zhang, Y.; Sun, K.; Meng, Z.; Chen, L. The SLC transporter in nutrient and metabolic sensing, regulation, and drug development. *J. Mol. Cell Biol.* **2019**, *11*, 1–13. [CrossRef]
11. Chapman, N.M.; Boothby, M.R.; Chi, H. Metabolic coordination of T cell quiescence and activation. *Nat. Rev. Immunol.* **2020**, *20*, 55–70. [CrossRef] [PubMed]
12. Procaccini, C.; Carbone, F.; Di Silvestre, D.; Brambilla, F.; De Rosa, V.; Galgani, M.; Faicchia, D.; Marone, G.; Tramontano, D.; Corona, M.; et al. The Proteomic Landscape of Human Ex Vivo Regulatory and Conventional T Cells Reveals Specific Metabolic Requirements. *Immunity* **2016**, *44*, 406–421. [CrossRef] [PubMed]
13. Rathmell, J.C.; Heiden, M.G.V.; Harris, M.H.; Frauwirth, K.A.; Thompson, C.B. In the absence of extrinsic signals, nutrient utilization by lymphocytes is insufficient to maintain either cell size or viability. *Mol. Cell* **2000**, *6*, 683–692. [CrossRef]
14. Jacobs, S.R.; Herman, C.E.; MacIver, N.J.; Wofford, J.A.; Wieman, H.L.; Hammen, J.J.; Rathmell, J.C. Glucose Uptake Is Limiting in T Cell Activation and Requires CD28-Mediated Akt-Dependent and Independent Pathways. *J. Immunol.* **2008**, *180*, 4476–4486. [CrossRef] [PubMed]
15. Maekawa, Y.; Ishifune, C.; Tsukumo, S.; Hozumi, K.; Yagita, H.; Yasutomo, K. Notch controls the survival of memory CD4+ T cells by regulating glucose uptake. *Nat. Med.* **2015**, *21*, 55–61. [CrossRef]
16. Phan, A.T.; Doedens, A.L.; Palazon, A.; Tyrakis, P.A.; Cheung, K.P.; Johnson, R.S.; Goldrath, A.W. Constitutive Glycolytic Metabolism Supports CD8+ T Cell Effector Memory Differentiation during Viral Infection. *Immunity* **2016**, *45*, 1024–1037. [CrossRef]
17. Macintyre, A.N.; Gerriets, V.A.; Nichols, A.G.; Michalek, R.D.; Rudolph, M.C.; Deoliveira, D.; Anderson, S.M.; Abel, E.D.; Chen, B.J.; Hale, L.P.; et al. The Glucose Transporter Glut1 Is Selectively Essential for CD4 T Cell Activation and Effector Function. *Cell Metab.* **2014**, *20*, 61–72. [CrossRef]
18. Maratou, E.; Dimitriadis, G.; Kollias, A.; Boutati, E.; Lambadiari, V.; Mitrou, P.; Raptis, S.A. Glucose transporter expression on the plasma membrane of resting and activated white blood cells. *Eur. J. Clin. Investig.* **2007**, *37*, 282–290. [CrossRef]
19. Kavanagh Williamson, M.; Coombes, N.; Juszczak, F.; Athanasopoulos, M.; Khan, M.; Eykyn, T.; Srenathan, U.; Taams, L.; Dias Zeidler, J.; Da Poian, A.; et al. Upregulation of Glucose Uptake and Hexokinase Activity of Primary Human CD4+ T Cells in Response to Infection with HIV-1. *Viruses* **2018**, *10*, 114. [CrossRef]
20. Beckermann, K.E.; Hongo, R.; Ye, X.; Young, K.; Carbonell, K.; Healey, D.C.C.; Siska, P.J.; Barone, S.; Roe, C.E.; Smith, C.C.; et al. CD28 costimulation drives tumor-infiltrating T cell glycolysis to promote inflammation. *JCI Insight* **2020**, *5*. [CrossRef]

21. Chang, C.-H.; Curtis, J.D.; Maggi, L.B.; Faubert, B.; Villarino, A.V.; O'Sullivan, D.; Huang, S.C.-C.; van der Windt, G.J.W.; Blagih, J.; Qiu, J.; et al. Posttranscriptional control of T cell effector function by aerobic glycolysis. *Cell* **2013**, *153*, 1239–1251. [CrossRef]
22. Pietrocola, F.; Galluzzi, L.; Bravo-San Pedro, J.M.; Madeo, F.; Kroemer, G. Acetyl coenzyme A: A central metabolite and second messenger. *Cell Metab.* **2015**, *21*, 805–821. [CrossRef] [PubMed]
23. Araujo, L.; Khim, P.; Mkhikian, H.; Mortales, C.-L.; Demetriou, M. Glycolysis and glutaminolysis cooperatively control T cell function by limiting metabolite supply to N-glycosylation. *Elife* **2017**, *6*. [CrossRef] [PubMed]
24. Goetzi, E.J.; Falchuk, K.H.; Zeiger, L.S.; Sullivan, A.L.; Hebert, C.L.; Adams, J.P.; Decker, J.L. A physiological approach to the assessment of disease activity in rheumatoid arthritis. *J. Clin. Investig.* **1971**, *50*, 1167–1180. [CrossRef]
25. Holbrook, J.J.; Liljas, A.; Steindel, S.J.; Rossmann, M.G. 4 Lactate Dehydrogenase. In *The Enzymes*; Academic Press: Cambridge, MA, USA, 1975; pp. 191–292.
26. Hui, S.; Ghergurovich, J.M.; Morscher, R.J.; Jang, C.; Teng, X.; Lu, W.; Esparza, L.A.; Reya, T.; Zhan, L.; Yanxiang Guo, J.; et al. Glucose feeds the TCA cycle via circulating lactate. *Nature* **2017**, *551*, 115–118. [CrossRef] [PubMed]
27. Park, S.J.; Smith, C.P.; Wilbur, R.R.; Cain, C.P.; Kallu, S.R.; Valasapalli, S.; Sahoo, A.; Guda, M.R.; Tsung, A.J.; Velpula, K.K. An overview of MCT1 and MCT4 in GBM: Small molecule transporters with large implications. *Am. J. Cancer Res.* **2018**, *8*, 1967–1976. [PubMed]
28. Halestrap, A.P. The monocarboxylate transporter family-Structure and functional characterization. *IUBMB Life* **2012**, *64*, 1–9. [CrossRef] [PubMed]
29. Fischer, K.; Hoffmann, P.; Voelkl, S.; Meidenbauer, N.; Ammer, J.; Edinger, M.; Gottfried, E.; Schwarz, S.; Rothe, G.; Hoves, S.; et al. Inhibitory effect of tumor cell–derived lactic acid on human T cells. *Blood* **2007**, *109*, 3812–3819. [CrossRef]
30. Brand, A.; Singer, K.; Koehl, G.E.; Kolitzus, M.; Schoenhammer, G.; Thiel, A.; Matos, C.; Bruss, C.; Klobuch, S.; Peter, K.; et al. LDHA-Associated Lactic Acid Production Blunts Tumor Immunosurveillance by T and NK Cells. *Cell Metab.* **2016**, *24*, 657–671. [CrossRef] [PubMed]
31. Degauque, N.; Brosseau, C.; Brouard, S. Regulation of the Immune Response by the Inflammatory Metabolic Microenvironment in the Context of Allotransplantation. *Front. Immunol.* **2018**, *9*. [CrossRef]
32. Angelin, A.; Gil-de-Gómez, L.; Dahiya, S.; Jiao, J.; Guo, L.; Levine, M.H.; Wang, Z.; Quinn, W.J.; Kopinski, P.K.; Wang, L.; et al. Foxp3 Reprograms T Cell Metabolism to Function in Low-Glucose, High-Lactate Environments. *Cell Metab.* **2017**, *25*, 1282–1293. [CrossRef] [PubMed]
33. Pucino, V.; Certo, M.; Bulusu, V.; Cucchi, D.; Goldmann, K.; Pontarini, E.; Haas, R.; Smith, J.; Headland, S.E.; Blighe, K.; et al. Lactate Buildup at the Site of Chronic Inflammation Promotes Disease by Inducing CD4+ T Cell Metabolic Rewiring. *Cell Metab.* **2019**, *30*, 1055–1074. [CrossRef] [PubMed]
34. Haas, R.; Smith, J.; Rocher-Ros, V.; Nadkarni, S.; Montero-Melendez, T.; D'Acquisto, F.; Bland, E.J.; Bombardieri, M.; Pitzalis, C.; Perretti, M.; et al. Lactate Regulates Metabolic and Pro-inflammatory Circuits in Control of T Cell Migration and Effector Functions. *PLoS Biol.* **2015**, *13*, e1002202. [CrossRef]
35. Certo, M.; Tsai, C.-H.; Pucino, V.; Ho, P.-C.; Mauro, C. Lactate modulation of immune responses in inflammatory versus tumour microenvironments. *Nat. Rev. Immunol.* **2020**. [CrossRef] [PubMed]
36. Szamel, M.; Rehermann, B.; Krebs, B.; Kurrle, R.; Resch, K. Activation signals in human lymphocytes. Incorporation of polyunsaturated fatty acids into plasma membrane phospholipids regulates IL-2 synthesis via sustained activation of protein kinase C. *J. Immunol.* **1989**, *143*, 2806–2813. [PubMed]
37. Baillie, A.G.S.; Coburn, C.T.; Abumrad, N.A. Reversible Binding of Long-chain Fatty Acids to Purified FAT, the Adipose CD36 Homolog. *J. Membr. Biol.* **1996**, *153*, 75–81. [CrossRef]
38. Calvo, D.; Gómez-Coronado, D.; Suárez, Y.; Lasunción, M.A.; Vega, M.A. Human CD36 is a high affinity receptor for the native lipoproteins HDL, LDL, and VLDL. *J. Lipid Res.* **1998**, *39*, 777–788.
39. Podrez, E.A.; Poliakov, E.; Shen, Z.; Zhang, R.; Deng, Y.; Sun, M.; Finton, P.J.; Shan, L.; Gugiu, B.; Fox, P.L.; et al. Identification of a Novel Family of Oxidized Phospholipids That Serve as Ligands for the Macrophage Scavenger Receptor CD36. *J. Biol. Chem.* **2002**, *277*, 38503–38516. [CrossRef]
40. Tandon, N.N.; Kralisz, U.; Jamieson, G.A. Identification of glycoprotein IV (CD36) as a primary receptor for platelet-collagen adhesion. *J. Biol. Chem.* **1989**, *264*, 7576–7583.

41. Wang, H.; Franco, F.; Tsui, Y.-C.; Xie, X.; Trefny, M.P.; Zappasodi, R.; Mohmood, S.R.; Fernández-García, J.; Tsai, C.-H.; Schulze, I.; et al. CD36-mediated metabolic adaptation supports regulatory T cell survival and function in tumors. *Nat. Immunol.* **2020**, *21*, 298–308. [CrossRef]
42. Kazantzis, M.; Stahl, A. Fatty acid transport proteins, implications in physiology and disease. *Biochim. Biophys. Acta Mol. Cell Biol. Lipids* **2012**, *1821*, 852–857. [CrossRef]
43. Howie, D.; Ten Bokum, A.; Necula, A.S.; Cobbold, S.P.; Waldmann, H. The Role of Lipid Metabolism in T Lymphocyte Differentiation and Survival. *Front. Immunol.* **2017**, *8*, 1949. [CrossRef]
44. Sun, M.; Wu, W.; Chen, L.; Yang, W.; Huang, X.; Ma, C.; Chen, F.; Xiao, Y.; Zhao, Y.; Ma, C.; et al. Microbiota-derived short-chain fatty acids promote Th1 cell IL-10 production to maintain intestinal homeostasis. *Nat. Commun.* **2018**, *9*, 3555. [CrossRef]
45. Venkataraman, C.; Kuo, F. The G-protein coupled receptor, GPR84 regulates IL-4 production by T lymphocytes in response to CD3 crosslinking. *Immunol. Lett.* **2005**, *101*, 144–153. [CrossRef] [PubMed]
46. Wang, J.; Wu, X.; Simonavicius, N.; Tian, H.; Ling, L. Medium-chain fatty acids as ligands for orphan G protein-coupled receptor GPR84. *J. Biol. Chem.* **2006**, *281*, 34457–34464. [CrossRef] [PubMed]
47. Halestrap, A.P.; Wilson, M.C. The monocarboxylate transporter family—Role and regulation. *IUBMB Life* **2012**, *64*, 109–119. [CrossRef] [PubMed]
48. Kirat, D.; Kato, S. Monocarboxylate transporter 1 (MCT1) mediates transport of short-chain fatty acids in bovine caecum. *Exp. Physiol.* **2006**, *91*, 835–844. [CrossRef]
49. Rae, C.; Fekete, A.D.; Kashem, M.A.; Nasrallah, F.A.; Bröer, S. Metabolism, compartmentation, transport and production of acetate in the cortical brain tissue slice. *Neurochem. Res.* **2012**, *37*, 2541–2553. [CrossRef]
50. Balmer, M.L.; Ma, E.H.; Bantug, G.R.; Grählert, J.; Pfister, S.; Glatter, T.; Jauch, A.; Dimeloe, S.; Slack, E.; Dehio, P.; et al. Memory CD8 + T Cells Require Increased Concentrations of Acetate Induced by Stress for Optimal Function. *Immunity* **2016**, *44*, 1312–1324. [CrossRef]
51. Peng, M.; Yin, N.; Chhangawala, S.; Xu, K.; Leslie, C.S.; Li, M.O. Aerobic glycolysis promotes T helper 1 cell differentiation through an epigenetic mechanism. *Science* **2016**, *354*, 481–484. [CrossRef]
52. Qiu, J.; Villa, M.; Sanin, D.E.; Buck, M.D.; O'Sullivan, D.; Ching, R.; Matsushita, M.; Grzes, K.M.; Winkler, F.; Chang, C.-H.; et al. Acetate Promotes T Cell Effector Function during Glucose Restriction. *Cell Rep.* **2019**, *27*, 2063–2074. [CrossRef] [PubMed]
53. Balmer, M.L.; Ma, E.H.; Thompson, A.J.; Epple, R.; Unterstab, G.; Lötscher, J.; Dehio, P.; Schürch, C.M.; Warncke, J.D.; Perrin, G.; et al. Memory CD8+ T Cells Balance Pro- and Anti-inflammatory Activity by Reprogramming Cellular Acetate Handling at Sites of Infection. *Cell Metab.* **2020**, *32*, 457–467. [CrossRef] [PubMed]
54. Ren, W.; Liu, G.; Yin, J.; Tan, B.; Wu, G.; Bazer, F.W.; Peng, Y.; Yin, Y. Amino-acid transporters in T-cell activation and differentiation. *Cell Death Dis.* **2017**, *8*, 1–9. [CrossRef]
55. Nii, T.; Segawa, H.; Taketani, Y.; Tani, Y.; Ohkido, M.; Kishida, S.; Ito, M.; Endou, H.; Kanai, Y.; Takeda, E.; et al. Molecular events involved in up-regulating human Na+-independent neutral amino acid transporter LAT1 during T-cell activation. *Biochem. J.* **2001**, *358*, 693–704. [CrossRef] [PubMed]
56. Carr, E.L.; Kelman, A.; Wu, G.S.; Gopaul, R.; Senkevitch, E.; Aghvanyan, A.; Turay, A.M.; Frauwirth, K.A. Glutamine uptake and metabolism are coordinately regulated by ERK/MAPK during T lymphocyte activation. *J. Immunol.* **2010**, *185*, 1037–1044. [CrossRef]
57. Nakaya, M.; Xiao, Y.; Zhou, X.; Chang, J.-H.; Chang, M.; Cheng, X.; Blonska, M.; Lin, X.; Sun, S.-C. Inflammatory T Cell Responses Rely on Amino Acid Transporter ASCT2 Facilitation of Glutamine Uptake and mTORC1 Kinase Activation. *Immunity* **2014**, *40*, 692–705. [CrossRef]
58. Yan, R.; Zhao, X.; Lei, J.; Zhou, Q. Structure of the human LAT1-4F2hc heteromeric amino acid transporter complex. *Nature* **2019**, *568*, 127–130. [CrossRef] [PubMed]
59. Sinclair, L.V.; Rolf, J.; Emslie, E.; Shi, Y.B.; Taylor, P.M.; Cantrell, D.A. Control of amino-acid transport by antigen receptors coordinates the metabolic reprogramming essential for T cell differentiation. *Nat. Immunol.* **2013**, *14*, 500–508. [CrossRef]
60. Wang, R.; Dillon, C.P.; Shi, L.Z.; Milasta, S.; Carter, R.; Finkelstein, D.; McCormick, L.L.; Fitzgerald, P.; Chi, H.; Munger, J.; et al. The Transcription Factor Myc Controls Metabolic Reprogramming upon T Lymphocyte Activation. *Immunity* **2011**, *35*, 871–882. [CrossRef]
61. Hayashi, K.; Jutabha, P.; Endou, H.; Sagara, H.; Anzai, N. LAT1 is a critical transporter of essential amino acids for immune reactions in activated human T cells. *J. Immunol.* **2013**, *191*, 4080–4085. [CrossRef]

62. Scalise, M.; Pochini, L.; Console, L.; Losso, M.A.; Indiveri, C. The Human SLC1A5 (ASCT2) Amino Acid Transporter: From Function to Structure and Role in Cell Biology. *Front. Cell Dev. Biol.* **2018**, *6*. [CrossRef]
63. Mak, T.W.; Grusdat, M.; Duncan, G.S.; Dostert, C.; Nonnenmacher, Y.; Cox, M.; Binsfeld, C.; Hao, Z.; Brüstle, A.; Itsumi, M.; et al. Glutathione Primes T Cell Metabolism for Inflammation. *Immunity* **2017**, *46*, 675–689. [CrossRef] [PubMed]
64. Meier, C.; Ristic, Z.; Klauser, S.; Verrey, F. Activation of system L heterodimeric amino acid exchangers by intracellular substrates. *EMBO J.* **2002**, *21*, 580–589. [CrossRef] [PubMed]
65. Ma, E.H.; Bantug, G.; Griss, T.; Condotta, S.; Johnson, R.M.; Samborska, B.; Mainolfi, N.; Suri, V.; Guak, H.; Balmer, M.L.; et al. Serine Is an Essential Metabolite for Effector T Cell Expansion. *Cell Metab.* **2017**, *25*, 345–357. [CrossRef] [PubMed]
66. Fotiadis, D.; Kanai, Y.; Palacín, M. The SLC3 and SLC7 families of amino acid transporters. *Mol. Aspects Med.* **2013**, *34*, 139–158. [CrossRef] [PubMed]
67. Bröer, S. The SLC38 family of sodium–amino acid co-transporters. *Pflügers Arch. Eur. J. Physiol.* **2014**, *466*, 155–172. [CrossRef] [PubMed]
68. Sinclair, L.V.; Howden, A.J.; Brenes, A.; Spinelli, L.; Hukelmann, J.L.; Macintyre, A.N.; Liu, X.; Thomson, S.; Taylor, P.M.; Rathmell, J.C.; et al. Antigen receptor control of methionine metabolism in T cells. *Elife* **2019**, *8*. [CrossRef] [PubMed]
69. Sinclair, L.V.; Neyens, D.; Ramsay, G.; Taylor, P.M.; Cantrell, D.A. Single cell analysis of kynurenine and System L amino acid transport in T cells. *Nat. Commun.* **2018**, *9*, 1981. [CrossRef]
70. Quintana, F.J.; Basso, A.S.; Iglesias, A.H.; Korn, T.; Farez, M.F.; Bettelli, E.; Caccamo, M.; Oukka, M.; Weiner, H.L. Control of T(reg) and T(H)17 cell differentiation by the aryl hydrocarbon receptor. *Nature* **2008**, *453*, 65–71. [CrossRef]
71. Mezrich, J.D.; Fechner, J.H.; Zhang, X.; Johnson, B.P.; Burlingham, W.J.; Bradfield, C.A. An interaction between kynurenine and the aryl hydrocarbon receptor can generate regulatory T cells. *J. Immunol.* **2010**, *185*, 3190–3198. [CrossRef]
72. Liu, Y.; Liang, X.; Dong, W.; Fang, Y.; Lv, J.; Zhang, T.; Fiskesund, R.; Xie, J.; Liu, J.; Yin, X.; et al. Tumor-Repopulating Cells Induce PD-1 Expression in CD8+ T Cells by Transferring Kynurenine and AhR Activation. *Cancer Cell* **2018**, *33*, 480–494. [CrossRef]
73. Perl, A.; Hanczko, R.; Lai, Z.-W.; Oaks, Z.; Kelly, R.; Borsuk, R.; Asara, J.M.; Phillips, P.E. Comprehensive metabolome analyses reveal N-acetylcysteine-responsive accumulation of kynurenine in systemic lupus erythematosus: Implications for activation of the mechanistic target of rapamycin. *Metabolomics* **2015**, *11*, 1157–1174. [CrossRef]
74. Bengtsson, A.A.; Trygg, J.; Wuttge, D.M.; Sturfelt, G.; Theander, E.; Donten, M.; Moritz, T.; Sennbro, C.-J.; Torell, F.; Lood, C.; et al. Metabolic Profiling of Systemic Lupus Erythematosus and Comparison with Primary Sjögren's Syndrome and Systemic Sclerosis. *PLoS ONE* **2016**, *11*, e0159384. [CrossRef] [PubMed]
75. Lai, Z.-W.; Kelly, R.; Winans, T.; Marchena, I.; Shadakshari, A.; Yu, J.; Dawood, M.; Garcia, R.; Tily, H.; Francis, L.; et al. Sirolimus in patients with clinically active systemic lupus erythematosus resistant to, or intolerant of, conventional medications: A single-arm, open-label, phase 1/2 trial. *Lancet* **2018**, *391*, 1186–1196. [CrossRef]
76. Lai, Z.-W.; Hanczko, R.; Bonilla, E.; Caza, T.N.; Clair, B.; Bartos, A.; Miklossy, G.; Jimah, J.; Doherty, E.; Tily, H.; et al. N-acetylcysteine reduces disease activity by blocking mammalian target of rapamycin in T cells from systemic lupus erythematosus patients: A randomized, double-blind, placebo-controlled trial. *Arthritis Rheum.* **2012**, *64*, 2937–2946. [CrossRef]
77. Reissner, K.J.; Gipson, C.D.; Tran, P.K.; Knackstedt, L.A.; Scofield, M.D.; Kalivas, P.W. Glutamate transporter GLT-1 mediates N-acetylcysteine inhibition of cocaine reinstatement. *Addict. Biol.* **2015**, *20*, 316–323. [CrossRef] [PubMed]
78. Rad Pour, S.; Morikawa, H.; Kiani, N.A.; Yang, M.; Azimi, A.; Shafi, G.; Shang, M.; Baumgartner, R.; Ketelhuth, D.F.J.; Kamleh, M.A.; et al. Exhaustion of CD4+ T-cells mediated by the Kynurenine Pathway in Melanoma. *Sci. Rep.* **2019**, *9*, 12150. [CrossRef]
79. Husson, A.; Brasse-Lagnel, C.; Fairand, A.; Renouf, S.; Lavoinne, A. Argininosuccinate synthetase from the urea cycle to the citrulline-NO cycle. *Eur. J. Biochem.* **2003**, *270*, 1887–1899. [CrossRef]
80. Bronte, V.; Zanovello, P. Regulation of immune responses by L-arginine metabolism. *Nat. Rev. Immunol.* **2005**, *5*, 641–654. [CrossRef]

81. Geiger, R.; Rieckmann, J.C.; Wolf, T.; Basso, C.; Feng, Y.; Fuhrer, T.; Kogadeeva, M.; Picotti, P.; Meissner, F.; Mann, M.; et al. L-Arginine Modulates T Cell Metabolism and Enhances Survival and Anti-tumor Activity. *Cell* **2016**, *167*, 829–842. [CrossRef]
82. Rodriguez, P.C.; Quiceno, D.G.; Ochoa, A.C. l-arginine availability regulates T-lymphocyte cell-cycle progression. *Blood* **2007**, *109*, 1568–1573. [CrossRef] [PubMed]
83. Werner, A.; Koschke, M.; Leuchtner, N.; Luckner-Minden, C.; Habermeier, A.; Rupp, J.; Heinrich, C.; Conradi, R.; Closs, E.I.; Munder, M. Reconstitution of T Cell Proliferation under Arginine Limitation: Activated Human T Cells Take Up Citrulline via L-Type Amino Acid Transporter 1 and Use It to Regenerate Arginine after Induction of Argininosuccinate Synthase Expression. *Front. Immunol.* **2017**, *8*. [CrossRef]
84. Jin, M.; Klionsky, D.J. The amino acid transporter SLC38A9 regulates MTORC1 and autophagy. *Autophagy* **2015**, *11*, 1709–1710. [CrossRef] [PubMed]
85. Oral, O.; Yedier, O.; Kilic, S.; Gozuacik, D. Involvement of autophagy in T cell biology. *Histol. Histopathol.* **2017**, *32*, 11–20. [CrossRef] [PubMed]
86. Viola, A.; Munari, F.; Sánchez-Rodríguez, R.; Scolaro, T.; Castegna, A. The Metabolic Signature of Macrophage Responses. *Front. Immunol.* **2019**, *10*. [CrossRef] [PubMed]
87. Freemerman, A.J.; Johnson, A.R.; Sacks, G.N.; Milner, J.J.; Kirk, E.L.; Troester, M.A.; Macintyre, A.N.; Goraksha-Hicks, P.; Rathmell, J.C.; Makowski, L. Metabolic reprogramming of macrophages: Glucose transporter 1 (GLUT1)-mediated glucose metabolism drives a proinflammatory phenotype. *J. Biol. Chem.* **2014**, *289*, 7884–7896. [CrossRef]
88. Freemerman, A.J.; Zhao, L.; Pingili, A.K.; Teng, B.; Cozzo, A.J.; Fuller, A.M.; Johnson, A.R.; Milner, J.J.; Lim, M.F.; Galanko, J.A.; et al. Myeloid Slc2a1 -Deficient Murine Model Revealed Macrophage Activation and Metabolic Phenotype Are Fueled by GLUT1. *J. Immunol.* **2019**, *202*, 1265–1286. [CrossRef]
89. Li, L.; Liu, B.; Håversen, L.; Lu, E.; Magnusson, L.U.; Ståhlman, M.; Borén, J.; Bergström, G.; Levin, M.C.; Hultén, L.M. The Importance of GLUT3 for De Novo Lipogenesis in Hypoxia-Induced Lipid Loading of Human Macrophages. *PLoS ONE* **2012**, *7*, e42360. [CrossRef]
90. Maedera, S.; Mizuno, T.; Ishiguro, H.; Ito, T.; Soga, T.; Kusuhara, H. GLUT6 is a lysosomal transporter that is regulated by inflammatory stimuli and modulates glycolysis in macrophages. *FEBS Lett.* **2019**, *593*, 195–208. [CrossRef]
91. Tan, Z.; Xie, N.; Banerjee, S.; Cui, H.; Fu, M.; Thannickal, V.J.; Liu, G. The Monocarboxylate Transporter 4 Is Required for Glycolytic Reprogramming and Inflammatory Response in Macrophages. *J. Biol. Chem.* **2015**, *290*, 46–55. [CrossRef]
92. Imai, H.; Yoshimura, K.; Miyamoto, Y.; Sasa, K.; Sugano, M.; Chatani, M.; Takami, M.; Yamamoto, M.; Kamijo, R. Roles of monocarboxylate transporter subtypes in promotion and suppression of osteoclast differentiation and survival on bone. *Sci. Rep.* **2019**, *9*, 15608. [CrossRef] [PubMed]
93. Hoque, R.; Farooq, A.; Ghani, A.; Gorelick, F.; Mehal, W.Z. Lactate Reduces Liver and Pancreatic Injury in Toll-Like Receptor– and Inflammasome-Mediated Inflammation via GPR81-Mediated Suppression of Innate Immunity. *Gastroenterology* **2014**, *146*, 1763–1774. [CrossRef] [PubMed]
94. Errea, A.; Cayet, D.; Marchetti, P.; Tang, C.; Kluza, J.; Offermanns, S.; Sirard, J.-C.; Rumbo, M. Lactate Inhibits the Pro-Inflammatory Response and Metabolic Reprogramming in Murine Macrophages in a GPR81-Independent Manner. *PLoS ONE* **2016**, *11*, e0163694. [CrossRef] [PubMed]
95. Colegio, O.R.; Chu, N.-Q.; Szabo, A.L.; Chu, T.; Rhebergen, A.M.; Jairam, V.; Cyrus, N.; Brokowski, C.E.; Eisenbarth, S.C.; Phillips, G.M.; et al. Functional polarization of tumour-associated macrophages by tumour-derived lactic acid. *Nature* **2014**, *513*, 559–563. [CrossRef]
96. Wang, T.; Liu, H.; Lian, G.; Zhang, S.-Y.; Wang, X.; Jiang, C. HIF1 α -Induced Glycolysis Metabolism Is Essential to the Activation of Inflammatory Macrophages. *Mediat. Inflamm.* **2017**, *2017*, 1–10. [CrossRef]
97. Ratter, J.M.; Rooijackers, H.M.M.; Hooiveld, G.J.; Hijmans, A.G.M.; de Galan, B.E.; Tack, C.J.; Stienstra, R. In vitro and in vivo Effects of Lactate on Metabolism and Cytokine Production of Human Primary PBMCs and Monocytes. *Front. Immunol.* **2018**, *9*. [CrossRef]
98. Johnson, A.R.; Qin, Y.; Cozzo, A.J.; Freemerman, A.J.; Huang, M.J.; Zhao, L.; Sampey, B.P.; Milner, J.J.; Beck, M.A.; Damania, B.; et al. Metabolic reprogramming through fatty acid transport protein 1 (FATP1) regulates macrophage inflammatory potential and adipose inflammation. *Mol. Metab.* **2016**, *5*, 506–526. [CrossRef]

99. Ye, G.; Gao, H.; Wang, Z.; Lin, Y.; Liao, X.; Zhang, H.; Chi, Y.; Zhu, H.; Dong, S. PPARα and PPARγ activation attenuates total free fatty acid and triglyceride accumulation in macrophages via the inhibition of Fatp1 expression. *Cell Death Dis.* **2019**, *10*, 39. [CrossRef] [PubMed]
100. Yin, C.; Cheng, L.; Pan, J.; Chen, L.; Xue, Q.; Qin, J.; Wang, S.; Du, B.; Liu, M.; Zhang, Y.; et al. Regulatory role of Gpr84 in the switch of alveolar macrophages from CD11blo to CD11bhi status during lung injury process. *Mucosal Immunol.* **2020**. [CrossRef]
101. Yoon, B.R.; Oh, Y.J.; Kang, S.W.; Lee, E.B.; Lee, W.W. Role of SLC7A5 in metabolic reprogramming of human monocyte/macrophage immune responses. *Front. Immunol.* **2018**, *9*. [CrossRef]
102. Yeramian, A.; Martin, L.; Serrat, N.; Arpa, L.; Soler, C.; Bertran, J.; McLeod, C.; Palacín, M.; Modolell, M.; Lloberas, J.; et al. Arginine Transport via Cationic Amino Acid Transporter 2 Plays a Critical Regulatory Role in Classical or Alternative Activation of Macrophages. *J. Immunol.* **2006**, *176*, 5918–5924. [CrossRef]
103. Nicholson, B.; Manner, C.K.; Kleeman, J.; MacLeod, C.L. Sustained Nitric Oxide Production in Macrophages Requires the Arginine Transporter CAT2. *J. Biol. Chem.* **2001**, *276*, 15881–15885. [CrossRef]
104. Sato, H.; Fujiwara, K.; Sagara, J.; Bannai, S. Induction of cystine transport activity in mouse peritoneal macrophages by bacterial lipopolysaccharide. *Biochem. J.* **1995**, *310*, 547–551. [CrossRef]
105. Sato, H.; Tamba, M.; Ishii, T.; Bannai, S. Cloning and Expression of a Plasma Membrane Cystine/Glutamate Exchange Transporter Composed of Two Distinct Proteins. *J. Biol. Chem.* **1999**, *274*, 11455–11458. [CrossRef] [PubMed]
106. Rimaniol, A.-C.; Mialocq, P.; Clayette, P.; Dormont, D.; Gras, G. Role of glutamate transporters in the regulation of glutathione levels in human macrophages. *Am. J. Physiol. Physiol.* **2001**, *281*, C1964–C1970. [CrossRef]
107. Deneke, S.M.; Fanburg, B.L. Regulation of cellular glutathione. *Am. J. Physiol. Cell. Mol. Physiol.* **1989**, *257*, L163–L173. [CrossRef] [PubMed]
108. Ingoglia, F.; Visigalli, R.; Rotoli, B.M.; Barilli, A.; Riccardi, B.; Puccini, P.; Milioli, M.; Di Lascia, M.; Bernuzzi, G.; Dall'Asta, V. Human macrophage differentiation induces OCTN2–mediated L-carnitine transport through stimulation of mTOR–STAT3 axis. *J. Leukoc. Biol.* **2017**, *101*, 665–674. [CrossRef]
109. Leung, E.; Hong, J.; Fraser, A.G.; Merriman, T.R.; Vishnu, P.; Krissansen, G.W. Polymorphisms in the organic cation transporter genes SLC22A4 and SLC22A5 and Crohn's disease in a New Zealand Caucasian cohort. *Immunol. Cell Biol.* **2006**, *84*, 233–236. [CrossRef]
110. Caro-Maldonado, A.; Wang, R.; Nichols, A.G.; Kuraoka, M.; Milasta, S.; Sun, L.D.; Gavin, A.L.; Abel, E.D.; Kelsoe, G.; Green, D.R.; et al. Metabolic Reprogramming Is Required for Antibody Production That Is Suppressed in Anergic but Exaggerated in Chronically BAFF-Exposed B Cells. *J. Immunol.* **2014**, *192*, 3626–3636. [CrossRef]
111. Thwe, P.M.; Pelgrom, L.R.; Cooper, R.; Beauchamp, S.; Reisz, J.A.; D'Alessandro, A.; Everts, B.; Amiel, E. Cell-Intrinsic Glycogen Metabolism Supports Early Glycolytic Reprogramming Required for Dendritic Cell Immune Responses. *Cell Metab.* **2017**, *26*, 558–567. [CrossRef] [PubMed]
112. Laval, J.; Touhami, J.; Herzenberg, L.A.; Conrad, C.; Taylor, N.; Battini, J.-L.; Sitbon, M.; Tirouvanziam, R. Metabolic Adaptation of Neutrophils in Cystic Fibrosis Airways Involves Distinct Shifts in Nutrient Transporter Expression. *J. Immunol.* **2013**, *190*, 6043–6050. [CrossRef] [PubMed]
113. Pfeifer, C.; Highton, A.J.; Peine, S.; Sauter, J.; Schmidt, A.H.; Bunders, M.J.; Altfeld, M.; Körner, C. Natural Killer Cell Education Is Associated With a Distinct Glycolytic Profile. *Front. Immunol.* **2018**, *9*. [CrossRef] [PubMed]
114. Singh, N.; Thangaraju, M.; Prasad, P.D.; Martin, P.M.; Lambert, N.A.; Boettger, T.; Offermanns, S.; Ganapathy, V. Blockade of Dendritic Cell Development by Bacterial Fermentation Products Butyrate and Propionate through a Transporter (Slc5a8)-dependent Inhibition of Histone Deacetylases. *J. Biol. Chem.* **2010**, *285*, 27601–27608. [CrossRef]
115. Shimada, H.; Nakamura, Y.; Nakanishi, T.; Tamai, I. OATP2A1/SLCO2A1-mediated prostaglandin E2 loading into intracellular acidic compartments of macrophages contributes to exocytotic secretion. *Biochem. Pharmacol.* **2015**, *98*, 629–638. [CrossRef] [PubMed]
116. Loynes, C.A.; Lee, J.A.; Robertson, A.L.; Steel, M.J.; Ellett, F.; Feng, Y.; Levy, B.D.; Whyte, M.K.B.; Renshaw, S.A. PGE 2 production at sites of tissue injury promotes an anti-inflammatory neutrophil phenotype and determines the outcome of inflammation resolution in vivo. *Sci. Adv.* **2018**, *4*, eaar8320. [CrossRef]

117. Ji, J.; Shu, D.; Zheng, M.; Wang, J.; Luo, C.; Wang, Y.; Guo, F.; Zou, X.; Lv, X.; Li, Y.; et al. Microbial metabolite butyrate facilitates M2 macrophage polarization and function. *Sci. Rep.* **2016**, *6*, 24838. [CrossRef]
118. Tannahill, G.M.; Curtis, A.M.; Adamik, J.; Palsson-McDermott, E.M.; McGettrick, A.F.; Goel, G.; Frezza, C.; Bernard, N.J.; Kelly, B.; Foley, N.H.; et al. Succinate is an inflammatory signal that induces IL-1β through HIF-1α. *Nature* **2013**, *496*, 238–242. [CrossRef]
119. Mills, E.L.; Kelly, B.; Logan, A.; Costa, A.S.H.; Varma, M.; Bryant, C.E.; Tourlomousis, P.; Däbritz, J.H.M.; Gottlieb, E.; Latorre, I.; et al. Succinate Dehydrogenase Supports Metabolic Repurposing of Mitochondria to Drive Inflammatory Macrophages. *Cell* **2016**, *167*, 457–470. [CrossRef]
120. Peruzzotti-Jametti, L.; Bernstock, J.D.; Vicario, N.; Costa, A.S.H.; Kwok, C.K.; Leonardi, T.; Booty, L.M.; Bicci, I.; Balzarotti, B.; Volpe, G.; et al. Macrophage-Derived Extracellular Succinate Licenses Neural Stem Cells to Suppress Chronic Neuroinflammation. *Cell Stem Cell* **2018**, *22*, 355–368. [CrossRef]
121. Schneiderhan, W.; Scheler, M.; Holzmann, K.-H.; Marx, M.; Gschwend, J.E.; Bucholz, M.; Gress, T.M.; Seufferlein, T.; Adler, G.; Oswald, F. CD147 silencing inhibits lactate transport and reduces malignant potential of pancreatic cancer cells in in vivo and in vitro models. *Gut* **2009**, *58*, 1391–1398. [CrossRef]
122. Pavlides, S.; Whitaker-Menezes, D.; Castello-Cros, R.; Flomenberg, N.; Witkiewicz, A.K.; Frank, P.G.; Casimiro, M.C.; Wang, C.; Fortina, P.; Addya, S.; et al. The reverse Warburg effect: Aerobic glycolysis in cancer associated fibroblasts and the tumor stroma. *Cell Cycle* **2009**. [CrossRef] [PubMed]
123. Comito, G.; Iscaro, A.; Bacci, M.; Morandi, A.; Ippolito, L.; Parri, M.; Montagnani, I.; Raspollini, M.R.; Serni, S.; Simeoni, L.; et al. Lactate modulates CD4+ T-cell polarization and induces an immunosuppressive environment, which sustains prostate carcinoma progression via TLR8/miR21 axis. *Oncogene* **2019**, *38*, 3681–3695. [CrossRef]
124. Zhang, J.; Muri, J.; Fitzgerald, G.; Gorski, T.; Gianni-Barrera, R.; Masschelein, E.; D'Hulst, G.; Gilardoni, P.; Turiel, G.; Fan, Z.; et al. Endothelial Lactate Controls Muscle Regeneration from Ischemia by Inducing M2-like Macrophage Polarization. *Cell Metab.* **2020**, *31*, 1136–1153. [CrossRef] [PubMed]
125. Fujii, W.; Kawahito, Y.; Nagahara, H.; Kukida, Y.; Seno, T.; Yamamoto, A.; Kohno, M.; Oda, R.; Taniguchi, D.; Fujiwara, H.; et al. Monocarboxylate Transporter 4, Associated With the Acidification of Synovial Fluid, Is a Novel Therapeutic Target for Inflammatory Arthritis. *Arthritis Rheumatol.* **2015**, *67*, 2888–2896. [CrossRef] [PubMed]
126. Cibrian, D.; Castillo-González, R.; Fernández-Gallego, N.; de la Fuente, H.; Jorge, I.; Saiz, M.L.; Punzón, C.; Ramírez-Huesca, M.; Vicente-Manzanares, M.; Fresno, M.; et al. Targeting L-type amino acid transporter 1 in innate and adaptive T cells efficiently controls skin inflammation. *J. Allergy Clin. Immunol.* **2020**, *145*, 199–214. [CrossRef] [PubMed]
127. Okunushi, K.; Furihata, T.; Morio, H.; Muto, Y.; Higuchi, K.; Kaneko, M.; Otsuka, Y.; Ohno, Y.; Watanabe, Y.; Reien, Y.; et al. JPH203, a newly developed anti-cancer drug, shows a preincubation inhibitory effect on L-type amino acid transporter 1 function. *J. Pharmacol. Sci.* **2020**, *144*, 16–22. [CrossRef]
128. Gagnon, L.; Leduc, M.; Thibodeau, J.-F.; Zhang, M.-Z.; Grouix, B.; Sarra-Bournet, F.; Gagnon, W.; Hince, K.; Tremblay, M.; Geerts, L.; et al. A Newly Discovered Antifibrotic Pathway Regulated by Two Fatty Acid Receptors. *Am. J. Pathol.* **2018**, *188*, 1132–1148. [CrossRef]
129. Khalil, N.; Manganas, H.; Ryerson, C.J.; Shapera, S.; Cantin, A.M.; Hernandez, P.; Turcotte, E.E.; Parker, J.M.; Moran, J.E.; Albert, G.R.; et al. Phase 2 clinical trial of PBI-4050 in patients with idiopathic pulmonary fibrosis. *Eur. Respir. J.* **2019**, *53*, 1800663. [CrossRef]
130. Ganapathy, V.; Thangaraju, M.; Prasad, P.D. Nutrient transporters in cancer: Relevance to Warburg hypothesis and beyond. *Pharmacol. Ther.* **2009**, *121*, 29–40. [CrossRef]
131. Airley, R.E.; Mobasheri, A. Hypoxic regulation of glucose transport, anaerobic metabolism and angiogenesis in cancer: Novel pathways and targets for anticancer therapeutics. *Chemotherapy* **2007**, *53*, 233–256. [CrossRef]
132. Miranda-Gonçalves, V.; Honavar, M.; Pinheiro, C.; Martinho, O.; Pires, M.M.; Pinheiro, C.; Cordeiro, M.; Bebiano, G.; Costa, P.; Palmeirim, I.; et al. Monocarboxylate transporters (MCTs) in gliomas: Expression and exploitation as therapeutic targets. *Neuro. Oncol.* **2013**, *15*, 172–188. [CrossRef]
133. Beloueche-Babari, M.; Casals Galobart, T.; Delgado-Goni, T.; Wantuch, S.; Parkes, H.G.; Tandy, D.; Harker, J.A.; Leach, M.O. Monocarboxylate transporter 1 blockade with AZD3965 inhibits lipid biosynthesis and increases tumour immune cell infiltration. *Br. J. Cancer* **2020**, *122*, 895–903. [CrossRef] [PubMed]

134. Choi, S.Y.C.; Xue, H.; Wu, R.; Fazli, L.; Lin, D.; Collins, C.C.; Gleave, M.E.; Gout, P.W.; Wang, Y. The MCT4 Gene: A Novel, Potential Target for Therapy of Advanced Prostate Cancer. *Clin. Cancer Res.* **2016**, *22*, 2721–2733. [CrossRef]
135. Kim, H.K.; Lee, I.; Bang, H.; Kim, H.C.; Lee, W.Y.; Yun, S.H.; Lee, J.; Lee, S.J.; Park, Y.S.; Kim, K.-M.; et al. MCT4 Expression Is a Potential Therapeutic Target in Colorectal Cancer with Peritoneal Carcinomatosis. *Mol. Cancer Ther.* **2018**, *17*, 838–848. [CrossRef] [PubMed]
136. Kuo, T.-C.; Huang, K.-Y.; Yang, S.-C.; Wu, S.; Chung, W.-C.; Chang, Y.-L.; Hong, T.-M.; Wang, S.-P.; Chen, H.-Y.; Hsiao, T.-H.; et al. Monocarboxylate Transporter 4 Is a Therapeutic Target in Non-small Cell Lung Cancer with Aerobic Glycolysis Preference. *Mol. Ther. Oncolytics* **2020**, *18*, 189–201. [CrossRef] [PubMed]
137. Gout, P.; Buckley, A.; Simms, C.; Bruchovsky, N. Sulfasalazine, a potent suppressor of lymphoma growth by inhibition of the xc − cystine transporter: A new action for an old drug. *Leukemia* **2001**, *15*, 1633–1640. [CrossRef]
138. Nashed, M.G.; Ungard, R.G.; Young, K.; Zacal, N.J.; Seidlitz, E.P.; Fazzari, J.; Frey, B.N.; Singh, G. Behavioural Effects of Using Sulfasalazine to Inhibit Glutamate Released by Cancer Cells: A Novel target for Cancer-Induced Depression. *Sci. Rep.* **2017**, *7*, 41382. [CrossRef]
139. Zheng, Z.; Luo, G.; Shi, X.; Long, Y.; Shen, W.; Li, Z.; Zhang, X. The Xc− inhibitor sulfasalazine improves the anti-cancer effect of pharmacological vitamin C in prostate cancer cells via a glutathione-dependent mechanism. *Cell. Oncol.* **2020**, *43*, 95–106. [CrossRef]
140. Bai, X.; Moraes, T.F.; Reithmeier, R.A.F. Structural biology of solute carrier (SLC) membrane transport proteins. *Mol. Membr. Biol.* **2017**, *34*, 1–32. [CrossRef]
141. Ryan, D.G.; Murphy, M.P.; Frezza, C.; Prag, H.A.; Chouchani, E.T.; O'Neill, L.A.; Mills, E.L. Coupling Krebs cycle metabolites to signalling in immunity and cancer. *Nat. Metab.* **2019**, *1*, 16–33. [CrossRef]

Publisher's Note: MDPI stays neutral with regard to jurisdictional claims in published maps and institutional affiliations.

© 2020 by the authors. Licensee MDPI, Basel, Switzerland. This article is an open access article distributed under the terms and conditions of the Creative Commons Attribution (CC BY) license (http://creativecommons.org/licenses/by/4.0/).

Check for updates

Immunology & Cell Biology 2021; **99**: 122–125
www.wileyonlinelibrary.com/journal/icb

NEWS AND COMMENTARY

Bridging the gap – a new role for STAT3 in TLR4-mediated metabolic reprogramming

Hauke J Weiss & Luke AJ O'Neill

School of Biochemistry and Immunology, Trinity College Dublin, Trinity Biomedical Sciences Institute, Dublin 2, Ireland

Immunology & Cell Biology 2021; **99**: 122–125; doi: 10.1111/imcb.12414

In this article, we discuss a new study from the laboratory of Ashley Mansell that successfully links innate immune receptor signaling to metabolic changes in macrophages, establishing for the first time an uninterrupted pathway from ligand binding to mitochondrial reprogramming and subsequential effector function modulation in this cell type.[1]

Macrophages were first described by Ilya Metchnikoff as early as 1882 and have since been identified as critical players in innate immunity. The main function of macrophages is the clearance of microbes, cancer cells, cellular debris and other foreign components in a process called phagocytosis, in which the macrophage engulfs and digests its target. Macrophages detect foreign substances through an array of pattern-recognition receptors (PRRs), one of which is the lipopolysaccharide (LPS) sensing receptor Toll-like receptor 4 (TLR4). Activation of TLR4 on macrophages induces distinct metabolic changes, characterized by increased glycolysis, accumulation of the tricarboxylic acid (TCA) cycle metabolite succinate[2] and decreased oxidative phosphorylation (OXPHOS).[3] These changes facilitate the increased demand for energy and biomaterials and are crucial for macrophage cytokine production and effector function.[4] A direct result of succinate accumulation in macrophages is the stabilization of hypoxia-inducible factor-1α (HIF-1α), a key mediator in the expression of pro-glycolytic genes and the production of pro-inflammatory cytokines such as interleukin-1β (IL-1β).[5] Precise mechanistic details on how TLR4 shapes metabolic reprogramming, however, are lacking. TLR4 drives phosphorylation of the well-known TLR activated kinases TANK-binding kinase 1 (TBK-1) and IκB kinase-ε (IKKε)[6] and promotes glycolysis.[7] In an elegant study reported in this issue, Balic *et al.* link these kinases to the signal transducer and activator of transcription 3 (STAT3), which was known to impact mitochondrial metabolism[8] and to induce the generation of reactive oxygen species (ROS).[9] The study proposes a new non-canonical role for STAT3 in TLR-mediated signaling.

Tumor necrosis factor receptor (TNFR)-associated factor 6 (TRAF6) is a well-known mediator of signaling events downstream of TLR activation.[10] Due to its structure, Balic *et al.* expected TRAF6 to be a binding partner of activated STAT3, a hypothesis they were able to confirm by identifying TRAF6 binding motifs on STAT3, and subsequently pulling down STAT3 together with TRAF6 in LPS-activated macrophages, thus presenting the first link between STAT3 activation and TLR signaling. STAT3 phosphorylation on Tyr705 is known to induce translocation to the nucleus and to activate the expression of several genes; however, TLR4 stimulation induced phosphorylation at a different site, Ser727, rapidly enough to be considered part of direct downstream signaling events, rather than an autocrine secondary effect. The group and others had previously shown that phosphorylation at this particular site translocates STAT3 to the mitochondria. Here, STAT3 alters mitochondrial metabolism by driving the activity of complex I and II of the electron transport chain, ultimately enhancing mitochondrial respiration.[8] STAT3 phosphorylation was not detected in the myeloid differentiation primary response 88 (MyD88) deficient cells. As MyD88 is a well-known adaptor protein downstream of TLR signaling, these results integrate STAT3 into TLR signaling for the first time (Figure 1).

At this point, the relationship between Ser727 and Tyr705 phosphorylation of STAT3 should be mentioned, as these events are not subject to two completely independent functioning pathways. Both phosphorylation events seem to influence each other under certain conditions; however, details are

Correspondence
Hauke J Weiss, School of Biochemistry and Immunology, Trinity College Dublin, Trinity Biomedical Sciences Institute, Dublin 2, Ireland.
E-mail: weissh@tcd.ie

14401711, 2021, 2, Downloaded from https://onlinelibrary.wiley.com/doi/10.1111/imcb.12414 by Trinity College Dublin, Wiley Online Library on [21/01/2023]. See the Terms and Conditions (https://onlinelibrary.wiley.com/terms-and-conditions) on Wiley Online Library for rules of use; OA articles are governed by the applicable Creative Commons License

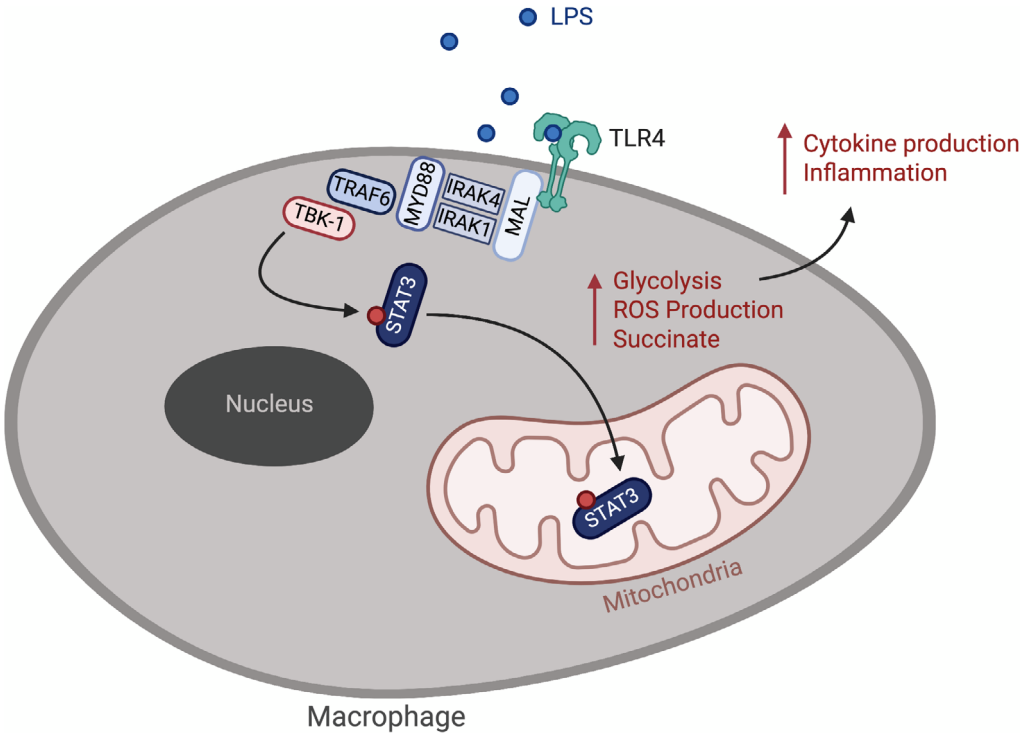


Figure 1. Lipopolysaccharide-induced activation of TLR4 results in TRAF6-mediated recruitment of the serine kinase TBK-1. TBK-1 subsequently phosphorylates STAT3 at Ser727, which is then translocated to the mitochondria. Here, STAT3 induces drastic metabolic reprogramming, resulting in increased glycolytic activity, succinate accumulation and cytokine production, driving a pro-inflammatory phenotype.

subject to debate. Regardless, the authors next aimed to investigate whether STAT3 Ser727 phosphorylation was indeed critical for TLR-induced metabolic reprogramming. Mutating the relevant serine in mouse peritoneal macrophages decreased both resting glycolysis and the glycolytic burst upon TLR4 stimulation, confirming phosphorylation of Ser727 to be a critical step in the pathway. The mutant cells exhibited a drastically reduced oxygen consumption rate (OCR) and maximal respiratory capacity compared with wild type cells. These cells were viable, but unable to respond to LPS stimulation, as respiratory capacity could not be upregulated above basal levels. Other than changes in the respiratory chain, LPS-stimulated macrophages also exhibit characteristic breaks in the TCA cycle, leading to accumulation of the pro-inflammatory metabolite succinate. Succinate production not only deprives the respiratory chain of its substrate, it is also required for ROS pro-inflammatory IL-1 production.[5] The authors found that in the above mentioned STAT3 mutants, LPS-induced succinate production was reduced compared with wild type cells. Conversely, the mutants exhibited increased the production of lactate, suggesting that due to defective mitochondrial metabolism, they rely more on aerobic glycolysis than wild type macrophages. These data suggest that Ser727 phosphorylation of STAT3 is not only required for induction of OXPHOS, but also for LPS-induced accumulation of succinate.

The authors now asked what kinases might phosphorylate STAT3? As the group had previously shown mitochondrial STAT3 to be responsible for the generation of ROS,[11] mitochondrial ROS concentrations were used as a readout while screening a large library of kinase inhibitors. They pointed to TBK-1, which was then shown to interact with both TRAF6 and STAT3 upon LPS stimulation. Deletion of TBK-1 confirmed this kinase to be responsible for Ser727 phosphorylation of STAT3. The related kinase IKKε was subsequently shown to be required for full STAT3 phosphorylation as well. Both kinases were previously mainly known for being involved in TLR-induced IRF3 phosphorylation and induction of IFNβ, another pro-inflammatory cytokine.[12] TBK-1 dysregulation has been found to be involved in multiple inflammatory diseases such as colitis, rheumatoid arthritis, hepatitis, and atherosclerosis,[13] while an interesting study published this year has

14401711, 2021, 2, Downloaded from https://onlinelibrary.wiley.com/doi/10.1111/imcb.12414 by Trinity College Dublin, Wiley Online Library on [21/01/2023]. See the Terms and Conditions (https://onlinelibrary.wiley.com/terms-and-conditions) on Wiley Online Library for rules of use; OA articles are governed by the applicable Creative Commons License

implicated IKKε in tumor formation in breast cancer.[14] These data elegantly explain the immunomodulatory properties of these kinases by revealing a new substrate and completing the signaling pathway below. Furthermore, this discovery reveals differences between metabolic reprogramming in myeloid cell lines. While dendritic cells for example rely on phosphoinositide 3-kinase (PI3K) and Akt activity for TBK-1/IKKε induced glycolysis, macrophages increase glycolytic activity independent of these mediators.

Lastly, it only remained to be investigated whether the metabolic changes associated with TLR4-induced STAT3 signaling result in actual functional consequences in macrophages. A key effector function in LPS-stimulated macrophages is the production of IL-1β. Generation of this pro-inflammatory cytokine is critically dependent on TCA cycle remodeling and the subsequent succinate accumulation and should therefore be mediated by the pathway described in this study. When stimulated with LPS, macrophages with mutated STAT3 were impaired in IL-1β mRNA generation and protein production compared with wild type cells. The production of IL-6, IL-10 and tumor necrosis factor (TNF) upon LPS challenge was also reduced in the mutants, while basal IL-10 expression was slightly increased. STAT3 mutant mice were also analyzed *in vivo* in a model of LPS-induced sepsis, and, in line with the *in vitro* experiments, the production of IL-1β and IL-6, as well as chemokine (C-C motif) ligand 2 (Ccl2) were decreased in the serum of mutant mice following LPS challenge, while TNF production was unchanged. This is surprising as TNF dependent macrophage functions have been postulated to require mitochondrial STAT3,[15] suggesting the possibility of surrogate pathways in physiologically relevant conditions. The roles of TNF and also of the anti-inflammatory cytokine IL-10 in this pathway could indeed be a subject for further investigation.

Together, these findings demonstrate a critical role of STAT3 Ser727 phosphorylation in LPS-induced cytokine production in macrophages and therefore effector function. The authors have unraveled a new process in LPS-induced metabolic reprogramming in macrophages. LPS induces TRAF6-mediated phosphorylation of STAT3 by TBK-1, resulting in localization of STAT3 to the mitochondria, shaping metabolic remodelling and subsequently effector functions. One interesting question for further exploration is precisely how STAT3 regulates mitochondrial functions. It is well established that mitochondrial STAT3 can regulate ATP synthesis, increase mitochondrial Ca^{2+} influx and decrease ROS release in T and B lymphocytes. Here, STAT3 associates with various components of the electron transport chain (ETC), enhancing ETC complex activity.[16] Interestingly, a recent study has found that mitochondrial STAT3 phosphorylated at Ser727 induced autophagy in human gastric epithelial cells when infected with *Helicobacter pylori*,[17] expanding the list of the potential functions of mitochondrial STAT3. As a well-described transcription factor, STAT3 could possibly also directly regulate mitochondrial gene expression. The study presented in this article elegantly pieces together established pathways to increase our understanding of immune cells to explain cell fate and effector function. It is a great example of how expanding one's horizon and interpreting previous observations can lead to important new discoveries.

CONFLICT OF INTEREST

The authors declare no conflict of interest.

AUTHOR CONTRIBUTION

Hauke J Weiss: Conceptualization; Writing-original draft; Writing-review & editing. **Luke O'Neill:** Conceptualization; Writing-original draft; Writing-review & editing.

REFERENCES

1. Balic JJ, Albargy H, Luu K, *et al*. STAT3 serine phosphorylation is required for TLR4 metabolic reprogramming and IL-1β expression. *Nat Commun* 2020; **11**: 3816.
2. Mills EL, Kelly B, Logan A, *et al*. Succinate dehydrogenase supports metabolic repurposing of mitochondria to drive inflammatory macrophages. *Cell* 2016; **167**: 457–470.
3. Garaude J. Reprogramming of mitochondrial metabolism by innate immunity. *Curr Opin Immunol* 2019; **56**: 17–23.
4. O'Neill LAJ, Kishton RJ, Rathmell J. A guide to immunometabolism for immunologists. *Nat Rev Immunol* 2016; **16**: 553–565.
5. Tannahill GM, Curtis AM, Adamik J, *et al*. Succinate is an inflammatory signal that induces IL-1β through HIF-1α. *Nature* 2013; **496**: 238–242.
6. Everts B, Amiel E, Huang SC-C, *et al*. TLR-driven early glycolytic reprogramming via the kinases TBK1-IKKε supports the anabolic demands of dendritic cell activation. *Nat Immunol* 2014; **15**: 323–332.
7. Tan Y, Kagan JC. Innate immune signaling organelles display natural and programmable signaling flexibility. *Cell* 2019; **177**: 384–398.
8. Wegrzyn J, Potla R, Chwae Y-J, *et al*. Function of mitochondrial Stat3 in cellular respiration. *Science* 2009; **323**: 793–797.

14401711, 2021, 2, Downloaded from https://onlinelibrary.wiley.com/doi/10.1111/imcb.12414 by Trinity College Dublin, Wiley Online Library on [21/01/2023]. See the Terms and Conditions (https://onlinelibrary.wiley.com/terms-and-conditions) on Wiley Online Library for rules of use; OA articles are governed by the applicable Creative Commons License

9. Mantel C, Messina-Graham S, Moh A, *et al*. Mouse hematopoietic cell–targeted STAT3 deletion: stem/progenitor cell defects, mitochondrial dysfunction, ROS overproduction, and a rapid aging–like phenotype. *Blood* 2012; **120**: 2589–2599.
10. Verstak B, Stack J, Ve T, *et al*. The TLR signaling adaptor TRAM interacts with TRAF6 to mediate activation of the inflammatory response by TLR4. *J Leukoc Biol* 2014; **96**: 427–436.
11. Garama DJ, Harris TJ, White CL, *et al*. A synthetic lethal interaction between glutathione synthesis and mitochondrial reactive oxygen species provides a tumor-specific vulnerability dependent on STAT3. *Mol Cell Biol* 2015; **35**: 3646–3656.
12. Fitzgerald KA, McWhirter SM, Faia KL, *et al*. IKKε and TBK1 are essential components of the IRF3 signaling pathway. *Nat Immunol* 2003; **4**: 491–496.
13. Yu T, Yi Y-S, Yang Y, Oh J, Jeong D, Cho JY. The pivotal role of TBK1 in inflammatory responses mediated by macrophages. *Mediators Inflamm* 2012; **2012**: 1–8.
14. Wilcz-Villega E, Carter E, Ironside A, *et al*. Macrophages induce malignant traits in mammary epithelium via IKKε/TBK1 kinases and the serine biosynthesis pathway. *EMBO Mol Med* 2020; **12**: e10491.
15. Shulga N, Pastorino JG. GRIM-19-mediated translocation of STAT3 to mitochondria is necessary for TNF-induced necroptosis. *J Cell Sci* 2012; **125**: 2995–3003.
16. Rincon M, Pereira F. A new perspective: mitochondrial Stat3 as a regulator for lymphocyte function. *Int J Mol Sci* 2018; **19**: 1656.
17. Piao J-Y, Kim S-J, Kim D-H, *et al*. *Helicobacter pylori* infection induces STAT3 phosphorylation on Ser727 and autophagy in human gastric epithelial cells and mouse stomach. *Sci Rep* 2020; **10**: 15711.

© 2020 Australian and New Zealand Society for Immunology Inc.

14401711, 2021, 2, Downloaded from https://onlinelibrary.wiley.com/doi/10.1111/imcb.12414 by Trinity College Dublin, Wiley Online Library on [21/01/2023]. See the Terms and Conditions (https://onlinelibrary.wiley.com/terms-and-conditions) on Wiley Online Library for rules of use; OA articles are governed by the applicable Creative Commons License

cells

MDPI

Review

Of Flies and Men—The Discovery of TLRs

Hauke Johannes Weiss * and Luke Anthony John O'Neill

School of Biochemistry and Immunology, Trinity Biomedical Sciences Institute, Trinity College Dublin, D02 R590 Dublin, Ireland

* Correspondence: weissh@tcd.ie

Abstract: In 2011, the Nobel Prize in Physiology or Medicine was awarded to three immunologists: Bruce A. Beutler, Jules A. Hoffmann, and Ralph M. Steinman. While Steinman was honored for his work on dendritic cells and adaptive immunity, Beutler and Hoffman received the prize for their contributions to discoveries in innate immunity. In 1996, Hoffmann found the *toll* gene to be crucial for mounting antimicrobial responses in fruit flies, first implicating this developmental gene in immune signaling. Two years later, Beutler built on this observation by describing a Toll-like gene, *tlr4*, as the receptor for the bacterial product LPS, representing a crucial step in innate immune activation and protection from bacterial infections in mammals. These publications spearheaded research in innate immune sensing and sparked a huge interest regarding innate defense mechanisms in the following years and decades. Today, Beutler and Hoffmann's research has not only resulted in the discovery of the role of multiple TLRs in innate immunity but also in a much broader understanding of the molecular components of the innate immune system. In this review, we aim to collect the discoveries leading up to the publications of Beutler and Hoffmann, taking a close look at how early advances in both developmental biology and immunology converged into the research awarded with the Nobel Prize. We will also discuss how these discoveries influenced future research and highlight the importance they hold today.

Keywords: Toll-like receptors (TLRs); innate immunity; immunology; Drosophila; LPS; innate immune signaling; Nobel Prize; TIR domain

check for updates

Citation: Weiss, H.J.; O'Neill, L.A.J. Of Flies and Men—The Discovery of TLRs. *Cells* **2022**, *11*, 3127. https://doi.org/10.3390/cells11193127

Academic Editor: Dieter Kabelitz

Received: 26 August 2022
Accepted: 2 October 2022
Published: 5 October 2022

Publisher's Note: MDPI stays neutral with regard to jurisdictional claims in published maps and institutional affiliations.

Copyright: © 2022 by the authors. Licensee MDPI, Basel, Switzerland. This article is an open access article distributed under the terms and conditions of the Creative Commons Attribution (CC BY) license (https://creativecommons.org/licenses/by/4.0/).

1. Introduction

The 2011 Nobel Prize to Hoffmann, Beutler, and Steinmann was a testament to the advances in research on innate immunity made in the 1990s and early 2000s. While concepts of adaptive immunity were already well described at the time, the function of innate immune cells was mostly thought to be reduced to the activation of the adaptive immune system, the nonspecific elimination of microbes and materials by phagocytosis, and inflammation. While Steinmann bridged the gap between the two with his work on dendritic cells [1–3], it was the work of Hoffmann and Beutler that elevated the field of innate immune recognition. Hoffmann published on the antimicrobial function of the developmental gene *toll* in *Drosophila melanogaster* in 1996 [4], and Beutler built on these data by identifying the Toll-like receptor TLR4 as the receptor for bacterial lipopolysaccharide (LPS) in mammals in 1998 [5], sparking a revolution in the field. These publications gave rise to the identification of the TLR family of receptors and allowed for the discovery of many other pattern recognition receptors (PRRs) as well. While ground-breaking, the findings of Hoffmann and Beutler were built on decades worth of discoveries in the fields of immunology and developmental biology, the most important of which we will discuss in this review.

2. Toll and Pathways in *Drosophila*

The origin of Toll in immunity can be traced to development biology research. The fruit fly *Drosophila melanogaster* has been a key model organism in studying developmental

biology and genetics for over a century, and, besides Hoffmann, four more Nobel Prizes have been awarded to scientists for their work with this animal. The first experiments involving *Drosophila* were conducted as early as 1901 by William Castle at Harvard University [6]; however, it was Thomas Hunt Morgan who achieved the first breakthrough results with *Drosophila*, confirming Mendel's theory of inheritance and establishing the concepts of genes and chromosomes [7]. This discovery earned him the 1933 Nobel Prize in Physiology or Medicine. Morgan's student, Hermann Muller, later found that radiation mutates genes and that the offspring of irradiated *Drosophila* have mutated genes too [8], earning him a Nobel Prize in physiology or medicine as well. Easy to breed and inexpensive to house, *Drosophila* quickly became the gold standard animal model in genetic research.

Modern *Drosophila* research emerged in the 1970s, when new techniques allowed for the genetic mapping of embryonic development. It emerged that larvae contain predetermined groups of cells—so-called imaginal discs—that would give rise to the various features and body parts of the adult *Drosophila* yet hold no function in the larvae themselves [9,10]. These imaginal discs could be transplanted [11,12], allowing for the investigation of their individual functions. Clonal analysis of these discs and the resulting labelling techniques [10,13] helped in understanding the fate of these individual cell clusters, resulting in the discovery of anterior (A) and posterior (P) compartments within various structures of the adult fly, being based on different imaginal discs [14–16]. Several morphogens that organize the development of distinct compartments were discovered during this time [17]; among them is *dorsal*, a mutation which caused a fully dorsalized phenotype [18]. Other mutants displaying similar phenotypes, including *pelle*, *tube*, *toll*, *spätzle*, and *cactus* [19,20], which soon emerged one after the other, revealed the genetic blueprint of the animal. A key factor in the discovery of these genes was the utilization of new molecular techniques in DNA cloning [21], and these findings were later awarded with another Nobel Prize to Edward B. Lewis, Christiane Nüsslein-Volhard, and Eric F. Wieschaus in 1995 for their discoveries regarding "the genetic control of early embryonic development" [22].

Toll was identified as one of the most important genes in embryonic development and the establishment of embryonic polarity. While most mutations of genes from the *dorsal* group retain some residual polarization, *toll* mutants lack any organization, and dorsoventral polarization by the reintroduction of wildtype (WT) cytoplasm is fully dependent on where the cytoplasm is injected [23]. It was suggested that the *toll* protein product is constantly expressed but would exist in an activated or an inactivated state and that members of the *dorsal* group, including *toll*, might be part of a signaling pathway [24], hypotheses that should later be confirmed on a biochemical level. The *toll* gene product Toll was soon identified as a membrane-bound receptor [25], capable of signal transduction through an extracellular stimulus [26]. This ligand was then identified as Spätzle, another member of the *dorsal* group [27], and Dorsal itself was shown to be a transcription factor recruited to the nucleus upon Spätzle binding to Toll. As stated above, Toll was then shown to be homologous to the mammalian type 1 IL-1 receptor (IL1R1) [28], while Dorsal was closely related to the IL-1-induced transcription factor NF-κB [29]. More similarities between the Toll pathway and the inflammation-inducing anti-microbial IL-1 receptor-induced signaling cascades soon became apparent, laying the groundwork for the discoveries of Hoffmann. Most notably, cactus was shown to be a homologue of the inhibitor of NF-κB (I-κB) in its function to retain Dorsal or NF-κB, respectively, in the cytoplasm [30,31], and both pathways involve structurally related protein kinases, such as the *pelle* gene product (pll) in the Toll pathway [32] and the interleukin-receptor associated kinase (IRAK) in the IL-1 pathway, respectively [33]. In addition, both *dorsal* itself as well as the closely related *Dorsal-related immunity factor* (*dif*) had been shown to exert antimicrobial functions in fat body cells from *Drosophila* [34,35].

Interestingly, a protein structurally related to both Toll and IL1R1 was discovered in a different kingdom of life. The N protein from the tobacco plant shared a cytoplasmic domain with Toll and IL1R1, a domain termed the Toll-IL-1 receptor resistance (TIR) domain

by Barbara Baker, who uncovered the role of the N protein in the antiviral responses against *Tobacco mosaic virus* [36]. The developmental role of Toll and its homology to both IL1R1 and the N protein were therefore important precursors to the discovery of the role of Toll in *Drosophila* innate immunity.

3. *Toll* Has Antimicrobial Functions

In 1996, Jules Hoffmann published on the antimicrobial function of three different genes, *spätzle*, *cactus*, and *toll* (*tl*), in the fruit fly *Drosophila melanogaster* [4]. Jules Hoffmann was born in Luxembourg on 2 August 1942. From an early age, he had a fascination for insects, an interest that would carry over into his research career. He obtained his doctoral degree in biology in 1969 from the University of Strasbourg, becoming a research associate in the same year. He went on to pursue postdoctoral training at the Philipps University of Marburg, Germany in the area of biochemistry before returning to Strasburg in 1974 to set up his own lab and establish a research unit on the immune response in insects in 1978. Here, he laid the groundwork for the research that would result in him being awarded the Nobel Prize decades later. After initial success working on grasshoppers [37], he turned towards *Drosophila melanogaster* later, identifying antimicrobial polypeptides such as diptericin [38] or defensin [39] as being part of the immune system of these insects. His groundbreaking and Nobel Prize-awarded work, however, was for the 1996 paper on Toll in *Drosophila* immunity, where he and Bruno Lemaitre were the first to describe the Toll pathway as being responsible for the production of the antifungal peptide dorsomycin [4], a discovery sparking a huge interest in similar proteins in mammals and ultimately leading to the discovery of the role of TLRs in innate immunity.

Spätzle, *cactus*, and *toll* are part of the dorsoventral signaling pathway and, curiously, the activation of the pathway had first been shown to lead to the activation of the dorsoventral morphogen *dorsal*, which is key to the establishment of dorsoventral polarity in the developing *Drosophila* embryo [40]. Hoffmann found that all three of these genes are involved in mounting an antifungal response, showing a decreased induction of the antifungal peptide gene *drosomycin* in animals with mutations in *spätzle*, *cactus*, or *toll*. *Dorsal*, however, was not involved. Drawing parallels to the components of the NF-κB pathway, Hoffmann described how the activation of the Toll receptor by its ligand spätzle leads to a similar signaling cascade as the activation of IL1R1 by IL-1 [41]. As stated above, IL1R1 had been shown to be a homologue to Toll, as well as the N protein in tobacco [36], which led to the concept of the 'TIR' domain. The N protein had been shown to be required for resistance to *Tobacco mosaic virus*. That Toll had been shown to be involved in host defense made biological sense, since IL1R1 and the N protein were already known to be similarly involved in immunity in mammals and plants, respectively. The TIR domain was therefore a very ancient signaling domain for innate immunity stretching back billions of years to the common ancestor of plants and animals.

Toll drove an antifungal response but not antibacterial response. Antibacterial responses are facilitated by the *immune deficiency* (*imd*) gene [42], with the antibacterial peptides cecropin, attacin, and defensin being partly dependent on Toll and diptericin and drosocin being independent of Toll. These results were achieved by the mutation of components of either the *imd* or *tl* pathways and the subsequent investigation of the downstream activation of components of these antimicrobial pathways or the challenge of the mutated flies with bacterial or fungal infections. This paper was therefore the first to describe the Toll pathway as a component of the innate immune system, a finding that will later be expanded to mammals and lead to the discovery of a multitude of receptors and pathways in innate immunity common to plants and animals.

4. Innate Immune Signaling and LPS

The idea of innate immune sensing by so-called pattern recognition receptors was proposed by Charles Janeway in 1989 [43]. TLR4 emerged as a prototypical PRR. It is worth going back a bit further in time to fully understand the motivations that drove Beutler

in his pursuit of the LPS receptor. LPS was first described as an "endotoxin" derived from *Vibrio cholerae*, the bacterium responsible for cholera, by Richard Pfeiffer in 1892, inducing fever and death even when the bacterium was killed [44]. Soon after, Eugenio Centanni isolated the substance and proposed it to be non-proteinous due to its remarkable heat stability [45]. Around the same time, physician William B. Coley started treating his cancer patients at the Memorial Hospital in New York with heat-inactivated bacteria, observing tumor remission in some cases [46], which, today, we know was due to the strong activation of the immune system by the bacterial LPS [47]. The endotoxin was identified as lipopolysaccharide in 1943 [48] but was not fully structurally identified until the 1980s [49], and while the detailed composition and the strength of the response may vary depending on the bacteria in question, they all induced the same inflammatory symptoms [50]—that is, until the 1960s. Suddenly a mouse strain was mentioned that was resistant to LPS-induced inflammation [51], indicating how this susceptibility to endotoxin may be down to very distinct cellular processes. It was later discovered that the resistance stemmed from a mutation in a distinct locus, appropriately named *lps* [52,53]. These mice, as well as another resistant strain identified in 1977 [54], termed C57BL/10ScCr, were important pillars for Beutler's work, as the genetic analysis of the *lps* locus would provide the key for the discovery of the LPS receptor.

With emerging knowledge about the individual cells acting within inflammation and the immune system, it became clear that macrophages were the main cell type responsible for LPS-induced inflammation [55], raising the question of whether such an intense reaction to LPS was a good thing or a bad thing. As a strong inducer of sepsis, it might be viewed as a purely toxic substance; however, Coley's work showed how LPS responses could keep malignancies at bay. In addition, by the end of the 1960s, it was clear that LPS could be beneficial in pathogen clearance, acting as an adjuvant [56–58]. In the 1980s, it was also shown that mice of the above-mentioned strains that lack an LPS response are more susceptible to infection with gram-negative bacteria [59,60], the very organisms that carry LPS on their surface. It was therefore clear that a sensing mechanism for LPS must exist to detect and respond to LPS-bearing bacteria. One of these responses included the production of cytokines such as tumor necrosis factor (TNF) [61], the induction of which was found to be at least partly responsible for LPS-induced toxicity [62], and TNF seemed to be beneficial in resolving the same type of microbial infections as LPS [63,64].

The work on cytokines such as IL-1 and TNF, which overlap in many of their pro-inflammatory effects, in turn provided the first ideas as to how the signal transduction from LPS to the nucleus might work. In the years before the discovery of TLR4, it had already been established that IL-1 binds IL1R1, resulting in the activation of the transcription factor NF-κB, as does LPS [65]. Two LPS-binding proteins could be identified prior to the discovery of TLR4. The LPS-binding protein (LBP) was first described in 1986 [66] and was found to enhance LPS-induced signaling events [67,68]. This protein, however, was not membrane-bound and could thus not act as a signal transducer. The second receptor, CD14, is a membrane-bound protein [69,70], but it lacks cytoplasmic domains [71]. Then, in 1996, Hoffmann published his work on the antimicrobial role of Toll in *Drosophila* [4], and, suddenly, the relevance of this receptor family in immunity became apparent and gave Beutler a reason to pursue TLR4 once it came up as a candidate in the unravelling of the *lps* locus. Importantly, Charles Janeway and Ruslan Medzhitov had shown in 1997 that TLR4, described as human Toll in their paper, could activate immune cells [72]. While other TLR members had been described before TLR4, their function and ligands remained unknown until after the identification of TLR4 as the LPS receptor [73,74], further highlighting the significance of Beutler's discovery. The most important milestones leading up to Beutler and Hoffmann's discoveries are listed in a timeline in Figure 1.

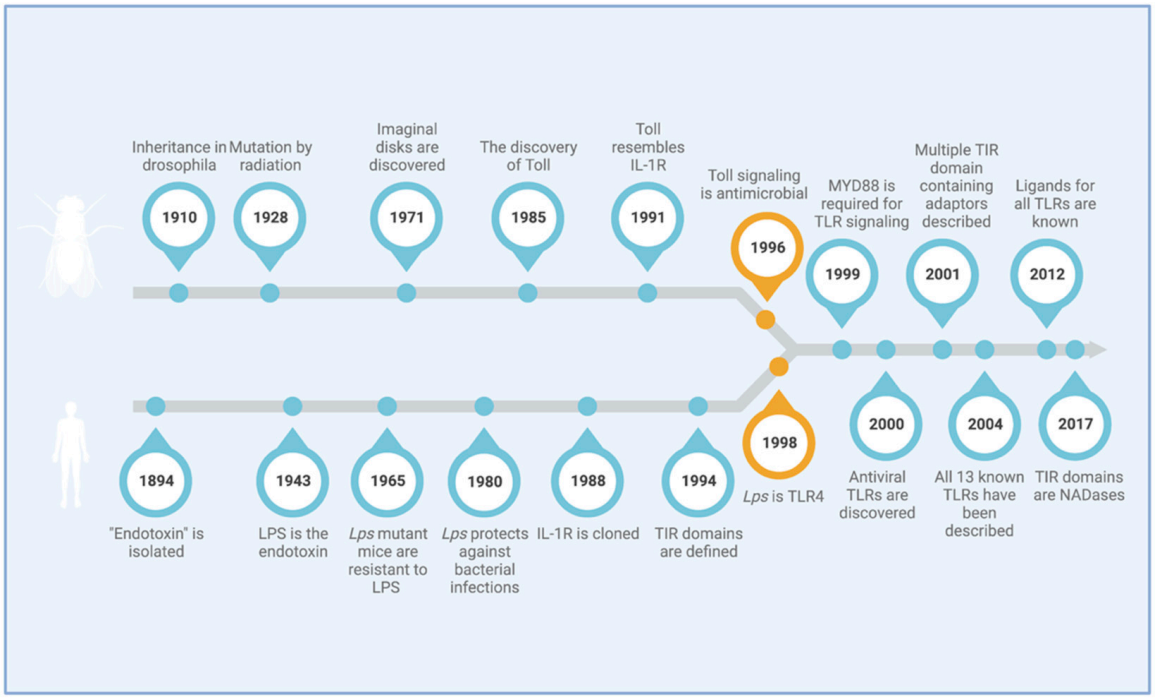


Figure 1. Milestones along the way to TLR discovery. The highlighted publications contributed significantly to today's knowledge on TLRs and innate immunity.

5. TLR4 Is the Receptor for Bacterial LPS

The search for the LPS receptor started with a thorough investigation of the so-called *lps* locus after it was reported decades previously that C3H/HeJ mice, a strain with mutated *lps*, are unresponsive to LPS [75,76]. LPS resistance was also shown in mice of the C57BL/10ScCr strain [54,77]. While an LPS-binding protein termed cluster of differentiation 14 (CD14) had already been identified on the surface of macrophages, this protein is not able to transduce a signal due to a lack of a cytoplasmic domain, as described above [70]. CD14 augments LPS-induced signaling [71]; however, it was likely to act as a co-receptor for the then-unknown TLR4. Utilizing genetic and physical mapping data, Beutler characterized the *lps* locus and identified *tlr4* in the area mapped. Bruce A. Beutler was born on 29 December 1957 in Chicago, Illinois. Growing up in California, he graduated from the University of California, San Diego in 1976 at only 18 years old with a degree in biology. Beutler then pursued an M.D. degree at the University of Chicago, which he obtained in 1981. After postdoctoral training at Rockefeller University in New York, he became Assistant Professor in 1985 before moving to Dallas a year later. It was in New York where he made one of his first important discoveries: isolating tumor necrosis factor-alpha (TNF-α) in mice [61]. At the University of Texas (UT) Southwestern Medical Center in Dallas, he obtained an associate professorship in 1990 and, finally, a full professorship in 1996. Here, he continued working on TNF, generating Immunoglobulin G (IgG) heavy chain-based TNF antagonists [78], eventually leading him to become interested in one particular TNF-inducing agent, LPS. Setting out to explain the induction of TNF and other cytokines by LPS, together with Alexander Poltorak, he was able to identify Toll-like receptor 4 (TLR4) as the receptor for LPS in 1998 [5], earning him his Nobel Prize.

Tlr4 was a promising target, as it was by then known to be part of the IL1R/TLR family. Comparing the macrophage mRNA and genomic DNA from an LPS-responsive vs. C3H/HeJ mouse strain, Beutler and collogues identified a mutation in the *tlr4* gene, resulting in a proline to histidine substitution in the *tlr4* gene from the LPS-unresponsive mice. In the C57BL/10ScCr strain, *tlr4* mRNA was entirely absent, further supporting the importance of this gene in LPS-induced signaling. Finally, TLR4 was shown to be downregulated in response to LPS treatment, possibly to facilitate tolerance to LPS, a well-known

phenomenon. In the context of the discoveries made by Hoffmann two years prior [37], Beutler therefore concluded that TLR4, like the *Drosophila* homologue Toll, launched a response to microbial infection. In the case of TLR4, however, this pathway has evolved to detect gram-negative bacteria, with developmental aspects that had been described for Toll in insects being lost. The homologies between Toll and TLR4 are highlighted in Figure 2. In this work, Beutler expands the discovery made by Hoffmann in insects to mammals, revealing one of the most important antimicrobial receptors in mammals in the process.

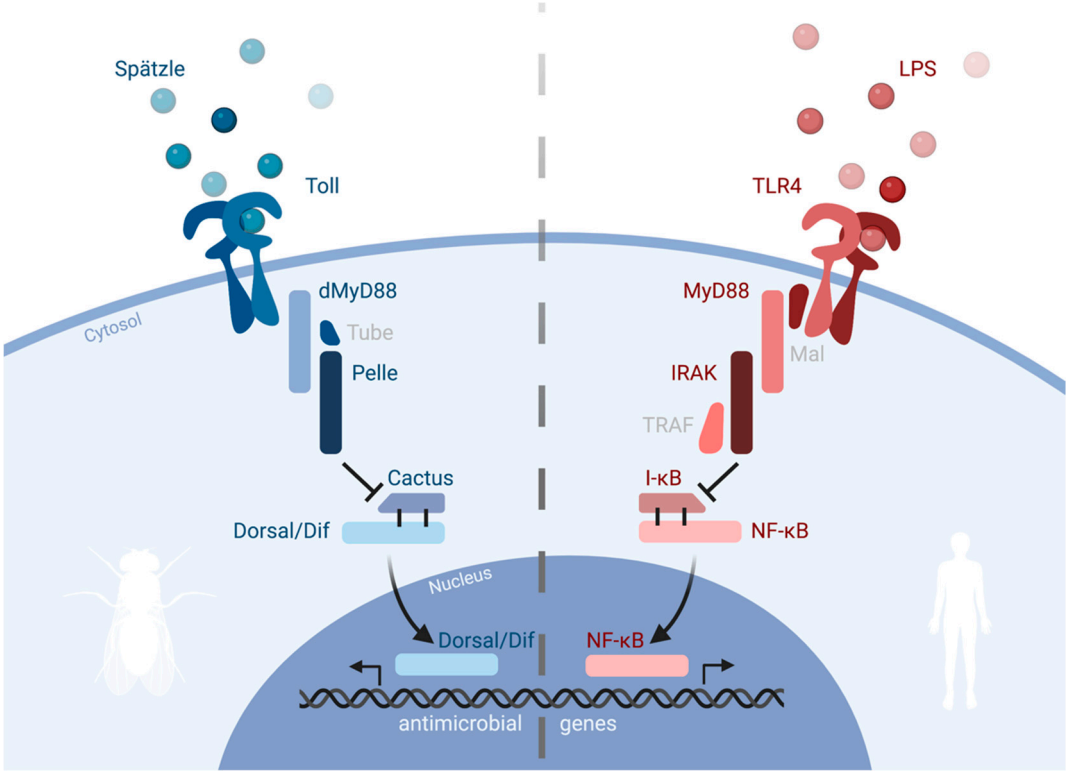


Figure 2. Simplified illustration of the Toll and TLR4 signaling pathways. Homologue components of both pathways are depicted in blue and red, respectively.

The Nobel Prize was awarded to Hoffmann and Beutler in recognition of their contribution to the discovery of Toll and TLRs in innate immunity. While years of research are represented in this award, these two papers are particularly important.

6. Scientific Impact

After the function of TLR4 was determined, the field of innate immune recognition exploded. Suddenly, the innate immune system was no longer seen as a crude, unspecific system with the simple task of activating adaptive immunity. It proved to be a sophisticated detection system capable of responding to and selecting between distinct microbial threats.

Soon after TLR4, the functions of many other TLRs were defined, each with another specific microbial ligand. Shizuo Akira found that TLR2 and TLR6 recognize gram-positive bacteria by binding to lipid structures [79,80], and TLR9 was shown to bind to bacterial DNA [81]. TLR3 was found to bind to double-stranded RNA (dsRNA), as found after viral infection [82], TLR5 was found to bind bacterial flagellin [83], and TLR7 and 8 were found to recognize viral single-stranded RNA (ssRNA) [84]. TLR10 binds triacylated lipopeptides [85] and is expressed in humans but not in mice. Conversely, mice express TLR11, which binds bacterial profilin and flagellin [86,87], TLR12, which binds profilin [86], and TLR13, which binds bacterial ribosomal RNA [88], which are all missing in humans. In addition, TLR2 was found to heterodimerize with TLR1 or TLR6 [89], while TLR11

dimerizes with TLR12 [90]. In Figure 3, all currently known TLRs are displayed, with their ligands and primary adaptors.

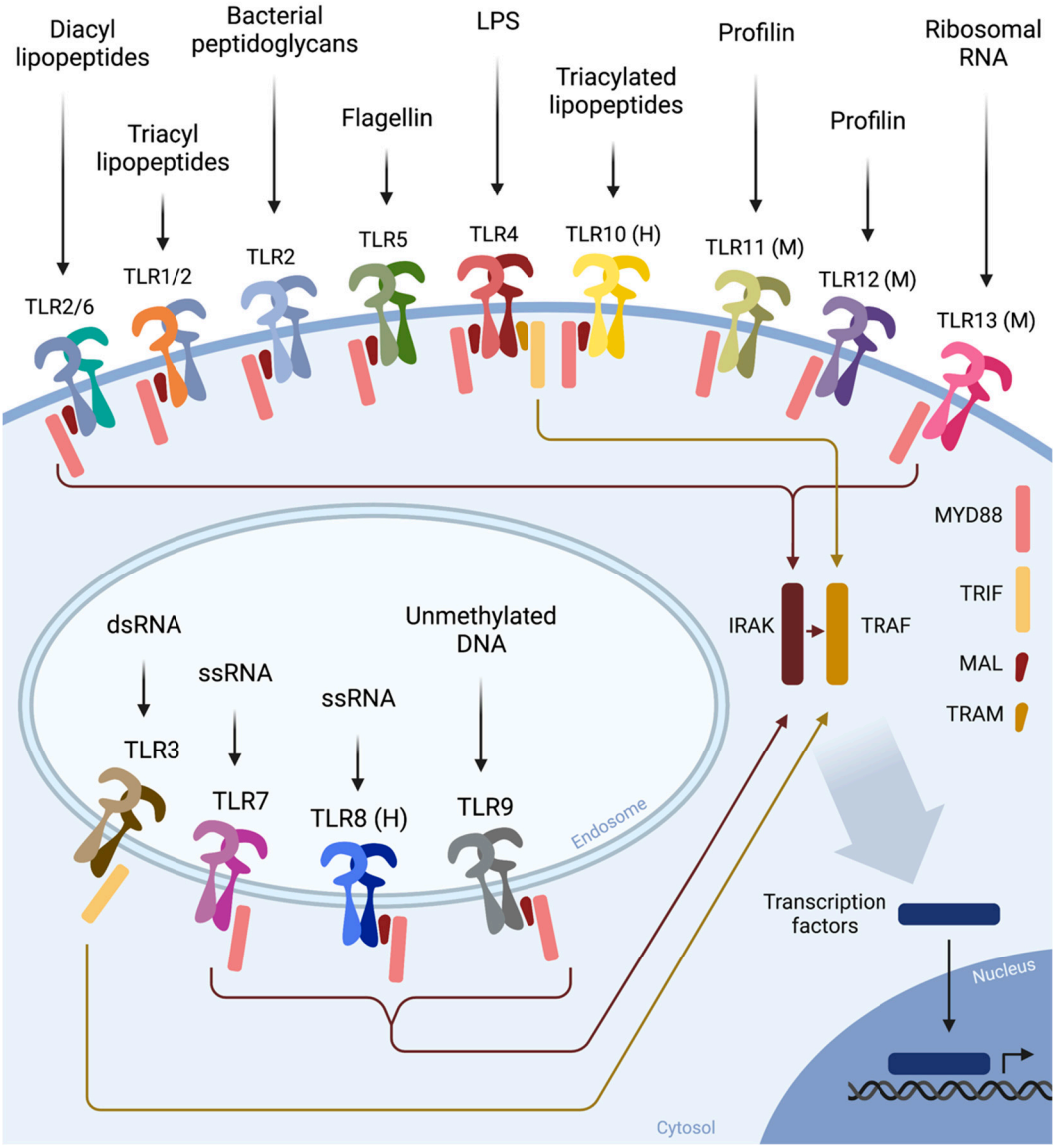


Figure 3. Illustration of all known TLRs and their ligands and adaptors, including those exclusive to mice (M) and humans (H).

Besides TLRs, other PRRs were also discovered in the following years—most notably, NOD-like receptors (NLRs) [91], the first of which was discovered in 1999 [92], RIG-like receptors (RLRs) [93], first described in 2004 [94], and C-type lectin receptors (CLRs) [95], which, although being considered part of the immune system for a long time, were shown to bind microbial products in 2000 [96].

There were also remarkable advances in determining the signaling pathways initiated by TLRs. Adaptor proteins involved in signaling were shown to have TIR domains. The first to be described was Myeloid differentiation primary-response protein 88 (MYD88). Discovered before the TLRs, it was found to bind to IL1R1, facilitating downstream signaling events [97], and, subsequently, it was found to mediate TLR signaling in TLRs as well [98]. Signaling was therefore initiated by TIR–TIR interactions from the receptor to adaptors. An exception was TLR3, which signals through TIR domain-containing adaptor protein inducing IFNβ (TRIF) [99,100]. TLR4 is also able to signal independently of MYD88

through TRIF when endocytosed [101,102]. TRIF-related adaptor molecule (TRAM) recruits TRIF to the TLR signaling complex [103,104], while MYD88-adaptor-like protein (MAL) recruits MYD88 to TLR4 and all other TLRs that use MYD88 [105]. From here on, TLR signaling gets more complex (described in more depth elsewhere) [106,107]. Even today, new aspects of TLR signaling are still being uncovered, especially revolving around the functionality of TIR domains. The TIR domain containing protein sterile alpha and the TIR motif containing 1 (SARM1), for example, were found to have enzymatic activity, depleting nicotinamide adenine dinucleotide (NAD^+) [108]. Indeed, several TIR domains have been found to have NADase activities, across various species as well [109]. While TIR domains from TLR signaling components other than SARM1 in animals do not seem to have NADase activity, the discovery of the enzymatic activity of this domain gives this aspect of TLR-signaling molecules a whole new angle and contributes to the burgeoning field of immunometabolism.

7. Concluding Remarks

Overall, it cannot be denied that the discoveries that resulted in the Nobel Prize being awarded to Hoffmann and Beutler are among the most important immunological milestones of the outgoing 20th century and are a testament to the tenacity of both scientists, along with the members of their research groups. They reshaped the way innate immunity was perceived and our understanding of how the first line of defense in our body actually works. While the Nobel Prize was well deserved, other pioneers in the field deserve recognition too. Without the groundbreaking discoveries of Nüsslein-Volhard in the field of Toll signaling or the emphasis placed on the innate immune system by Charles Janeway, these discoveries would not have been possible. Additionally, other brilliant scientists, such as Ruslan Medzhitov and Shizuo Akira, should be mentioned alongside Hoffmann and Beutler for their many contributions. The two key publications described here truly elevated the field, the consequences of which are still being extensively explored by many scientists.

Author Contributions: Conceptualization, H.J.W. and L.A.J.O.; investigation, H.J.W.; resources, H.J.W.; writing—original draft preparation, H.J.W.; writing—review and editing, L.A.J.O.; visualization, H.J.W.; supervision, L.A.J.O.; funding acquisition, L.A.J.O. All authors have read and agreed to the published version of the manuscript.

Funding: The O'Neill laboratory acknowledges grant support from the European Research Council Metabinate (834370), the Wellcome Trust (205455) and Science Foundation Ireland (19/FFP/6507). H.J.W. is supported by the European Union's Horizon 2020 research and innovation program under the Marie Skłodowska-Curie grant agreement No 813343.

Institutional Review Board Statement: Not applicable.

Informed Consent Statement: Not applicable.

Data Availability Statement: Not applicable.

Acknowledgments: Figures were created with BioRender.com.

Conflicts of Interest: The authors declare no conflict of interest.

References

1. Steinman, R.M.; Cohn, Z.A. Identification of a Novel Cell Type in Peripheral Lymphoid Organs of Mice. *J. Exp. Med.* **1973**, *137*, 1142–1162. [CrossRef] [PubMed]
2. Steinman, R.M.; Witmer, M.D. Lymphoid dendritic cells are potent stimulators of the primary mixed leukocyte reaction in mice. *Proc. Natl. Acad. Sci. USA* **1978**, *75*, 5132–5136. [CrossRef] [PubMed]
3. Schuler, G.; Steinman, R.M. Murine epidermal Langerhans cells mature into potent immunostimulatory dendritic cells in vitro. *J. Exp. Med.* **1985**, *161*, 526–546. [CrossRef] [PubMed]
4. Lemaitre, B.; Nicolas, E.; Michaut, L.; Reichhart, J.-M.; Hoffmann, J.A. The Dorsoventral Regulatory Gene Cassette spätzle/Toll/cactus Controls the Potent Antifungal Response in Drosophila Adults. *Cell* **1996**, *86*, 973–983. [CrossRef]
5. Poltorak, A.; He, X.; Smirnova, I.; Liu, M.-Y.; Huffel, C.V.; Du, X.; Birdwell, D.; Alejos, E.; Silva, M.; Galanos, C.; et al. Defective LPS Signaling in C3H/HeJ and C57BL/10ScCr Mice: Mutations in Tlr4 Gene. *Science* **1998**, *282*, 2085–2088. [CrossRef]

6. Jennings, B.H. Drosophila—A versatile model in biology & medicine. *Mater. Today* **2011**, *14*, 190–195. [CrossRef]
7. Morgan, T.H. Sex Limited Inheritance in Drosophila. *Science* **1910**, *32*, 120–122. [CrossRef]
8. Muller, H.J. The Production of Mutations by X-Rays. *Proc. Natl. Acad. Sci. USA* **1928**, *14*, 714–726. [CrossRef]
9. Mandaravally Madhavan, M.; Schneiderman, H.A. Histological analysis of the dynamics of growth of imaginal discs and histoblast nests during the larval development ofDrosophila melanogaster. *Wilhelm Roux's Arch. Dev. Biol.* **1977**, *183*, 269–305. [CrossRef]
10. Garcia-Bellido, A.; Merriam, J.R. Parameters of the wing imaginal disc development ofDrosophila melanogaster. *Dev. Biol.* **1971**, *24*, 61–87. [CrossRef]
11. Gehring, W. The Stability of the Determined State in Cultures of Imaginal Disks in Drosophila. *Develop. Biol.* **1967**, *16*, 438–456. [CrossRef]
12. Beadle, G.W.; Ephrussi, B. The differentiation of eye pigments in drosophila as studied by transplantation. *Genetics* **1936**, *21*, 225–247. [CrossRef] [PubMed]
13. Bryant, P.J. Cell lineage relationships in the imaginal wing disc of Drosophila melanogaster. *Dev. Biol.* **1970**, *22*, 389–411. [CrossRef]
14. Steiner, E. Establishment of compartments in the developing leg imaginal discs ofDrosophila melanogaster. *Wilhelm Roux's Arch. Dev. Biol.* **1976**, *180*, 9–30. [CrossRef]
15. MORATA, G.; LAWRENCE, P.A. Anterior and posterior compartments in the head of Drosophila. *Nature* **1978**, *274*, 473–474. [CrossRef]
16. Lawrence, P.A.; Morata, G. Compartments in the wing of Drosophila: A study of the engrailed gene. *Dev. Biol.* **1976**, *50*, 321–337. [CrossRef]
17. Nüsslein-Volhard, C.; Wieschaus, E. Mutations affecting segment number and polarity in Drosophila. *Nature* **1980**, *287*, 795–801. [CrossRef]
18. Santamaria, P.; Nüsslein-Volhard, C. Partial rescue of dorsal, a maternal effect mutation affecting the dorso-ventral pattern of the Drosophila embryo, by the injection of wild-type cytoplasm. *EMBO J.* **1983**, *2*, 1695–1699. [CrossRef]
19. Anderson, K.V.; Nüsslein-Volhard, C. Information for the dorsal–ventral pattern of the Drosophila embryo is stored as maternal mRNA. *Nature* **1984**, *311*, 223–227. [CrossRef]
20. Schüpbach, T.; Wieschaus, E. Female sterile mutations on the second chromosome of Drosophila melanogaster. I. Maternal effect mutations. *Genetics* **1989**, *121*, 101–117. [CrossRef]
21. Morata, G.; Lawrence, P. An exciting period of Drosophila developmental biology: Of imaginal discs, clones, compartments, parasegments and homeotic genes. *Dev. Biol.* **2022**, *484*, 12–21. [CrossRef]
22. Press Release: The Nobel Prize in Physiology or Medicine. 1995. Available online: https://www.nobelprize.org/prizes/medicine/1995/press-release/ (accessed on 10 September 2022).
23. Anderson, K.V.; Bokla, L.; Nüsslein-Volhard, C. Establishment of dorsal-ventral polarity in the drosophila embryo: The induction of polarity by the Toll gene product. *Cell* **1985**, *42*, 791–798. [CrossRef]
24. Nüsslein-Volhard, C. The Toll gene in Drosophila pattern formation. *Trends Genet.* **2022**, *38*, 231–245. [CrossRef]
25. Hashimoto, C.; Hudson, K.L.; Anderson, K.V. The Toll gene of drosophila, required for dorsal-ventral embryonic polarity, appears to encode a transmembrane protein. *Cell* **1988**, *52*, 269–279. [CrossRef]
26. Stein, D.; Roth, S.; Vogelsang, E.; Nu¨sslein-Volhard, C. The polarity of the dorsoventral axis in the drosophila embryo is defined by an extracellular signal. *Cell* **1991**, *65*, 725–735. [CrossRef]
27. Schneider, D.S.; Jin, Y.; Morisato, D.; Anderson, K.V. A processed form of the Spatzle protein defines dorsal-ventral polarity in the Drosophila embryo. *Development* **1994**, *120*, 1243–1250. [CrossRef]
28. Schneider, D.S.; Hudson, K.L.; Lin, T.Y.; Anderson, K.V. Dominant and recessive mutations define functional domains of Toll, a transmembrane protein required for dorsal-ventral polarity in the Drosophila embryo. *Genes Dev.* **1991**, *5*, 797–807. [CrossRef]
29. Steward, R. Dorsal, an Embryonic Polarity Gene in Drosophila, Is Homologous to the Vertebrate Proto-Oncogene, c- rel. *Science* **1987**, *238*, 692–694. [CrossRef]
30. Kidd, S. Characterization of the Drosophila cactus locus and analysis of interactions between cactus and dorsal proteins. *Cell* **1992**, *71*, 623–635. [CrossRef]
31. Geisler, R.; Bergmann, A.; Hiromi, Y.; Nüsslein-Volhard, C. cactus, a gene involved in dorsoventral pattern formation of Drosophila, is related to the IκB gene family of vertebrates. *Cell* **1992**, *71*, 613–621. [CrossRef]
32. Shelton, C.A.; Wasserman, S.A. pelle encodes a protein kinase required to establish dorsoventral polarity in the Drosophila embryo. *Cell* **1993**, *72*, 515–525. [CrossRef]
33. Cao, Z.; Henzel, W.J.; Gao, X. IRAK: A Kinase Associated with the Interleukin-1 Receptor. *Science* **1996**, *271*, 1128–1131. [CrossRef]
34. Reichhart, J.M.; Georgel, P.; Meister, M.; Lemaitre, B.; Kappler, C.; Hoffmann, J.A. Expression and nuclear translocation of the rel/NF-kappa B-related morphogen dorsal during the immune response of Drosophila. *C. R. Acad. Sci. III.* **1993**, *316*, 1218–1224.
35. Ip, Y.T.; Reach, M.; Engstrom, Y.; Kadalayil, L.; Cai, H.; González-Crespo, S.; Tatei, K.; Levine, M. Dif, a dorsal-related gene that mediates an immune response in Drosophila. *Cell* **1993**, *75*, 753–763. [CrossRef]
36. Whitham, S.; Dinesh-Kumar, S.P.; Choi, D.; Hehl, R.; Corr, C.; Baker, B. The product of the tobacco mosaic virus resistance gene N: Similarity to toll and the interleukin-1 receptor. *Cell* **1994**, *78*, 1101–1115. [CrossRef]

37. Hoffmann, D.; Brehelin, M.; Hoffmann, J.A. Modifications of the hemogram and of the hemocytopoietic tissue of male adults of Locusta migratoria (Orthoptera) after injection of Bacillus thuringiensis. *J. Invertebr. Pathol.* **1974**, *24*, 238–247. [CrossRef]
38. Dimarcq, J.-L.; Keppi, E.; Dunbar, B.; Lambert, J.; Reichart, J.-M.; Hoffmann, D.; Rankine, S.M.; Fothergill, J.E.; Hoffmann, J.A. Insect immunity. Purification and characterization of a family of novel inducible antibacterial proteins from immunized larvae of the dipteran Phormia terranovae and complete amino-acid sequence of the predominant member, diptericin A. *Eur. J. Biochem.* **1988**, *171*, 17–22. [CrossRef]
39. Dimarcq, J.-L.; Hoffmann, D.; Meister, M.; Bulet, P.; Lanot, R.; Reichhart, J.-M.; Hoffmann, J.A. Characterization and transcriptional profiles of a Drosophila gene encoding an insect defensin. A study in insect immunity. *Eur. J. Biochem.* **1994**, *221*, 201–209. [CrossRef]
40. Morisalo, D.; Anderson, K.V. Signaling pathways that establish the dorsal-ventral pattern of the drosophila embryo. *Annu. Rev. Genet.* **1995**, *29*, 371–399. [CrossRef]
41. GAY, N.J.; KEITH, F.J. Drosophila Toll and IL-1 receptor. *Nature* **1991**, *351*, 355–356. [CrossRef]
42. Lemaitre, B.; Kromer-Metzger, E.; Michaut, L.; Nicolas, E.; Meister, M.; Georgel, P.; Reichhart, J.M.; Hoffmann, J.A. A recessive mutation, immune deficiency (imd), defines two distinct control pathways in the Drosophila host defense. *Proc. Natl. Acad. Sci. USA* **1995**, *92*, 9465–9469. [CrossRef]
43. Janeway, C.A. Approaching the Asymptote? Evolution and Revolution in Immunology. *Cold Spring Harb. Symp. Quant. Biol.* **1989**, *54*, 1–13. [CrossRef]
44. Pfeiffer, R. Untersuchungen über das Choleragift. *Z. Hyg. Infekt.* **1892**, *11*, 393–412. [CrossRef]
45. Centanni, E.; Bruschettini, A. Untersuchungen über das Infectionsfieber. *DMW-Dtsch. Med. Wochenschr.* **1894**, *20*, 270–272. [CrossRef]
46. Coley, W.B. The Treatment of Inoperable Sarcoma by Bacterial Toxins (the Mixed Toxins of the Streptococcus erysipelas and the Bacillus prodigiosus). *Proc. R. Soc. Med.* **1910**, *3*, 1–48. [CrossRef]
47. Starnes, C.O. Coley's toxins in perspective. *Nature* **1992**, *357*, 11–12. [CrossRef]
48. Shear, M.J.; Turner, F.C.; Perrault, A.; Shovelton, T. Chemical Treatment of Tumors. V. Isolation of the Hemorrhage-Producing Fraction from Serratia marcescens (Bacillus prodigiosus) Culture Filtrate. *JNCI J. Natl. Cancer Inst.* **1943**, *4*, 81–97. [CrossRef]
49. Strain, S.M.; Fesik, S.W.; Armitage, I.M. Characterization of lipopolysaccharide from a heptoseless mutant of Escherichia coli by carbon 13 nuclear magnetic resonance. *J. Biol. Chem.* **1983**, *258*, 2906–2910. [CrossRef]
50. Beutler, B.; Rietschel, E.T. Innate immune sensing and its roots: The story of endotoxin. *Nat. Rev. Immunol.* **2003**, *3*, 169–176. [CrossRef]
51. Heppner, G.; Weiss, D.W. High Susceptibility of Strain A Mice to Endotoxin and Endotoxin-Red Blood Cell Mixtures. *J. Bacteriol.* **1965**, *90*, 696–703. [CrossRef]
52. Watson, J.; Riblet, R. Genetic control of responses to bacterial lipopolysaccharides in mice. *J. Exp. Med.* **1974**, *140*, 1147–1161. [CrossRef] [PubMed]
53. Watson, J.; Riblet, R. Genetic control of responses to bacterial lipopolysaccharides in mice. II. A gene that influences a membrane component involved in the activation of bone marrow-derived lymphocytes by lipipolysaccharides. *J. Immunol.* **1975**, *114*, 1462–1468. [PubMed]
54. Coutinho, A.; Forni, L.; Melchers, F.; Watanabe, T. Genetic defect in responsiveness to the B cell mitogen lipopolysaccharide. *Eur. J. Immunol.* **1977**, *7*, 325–328. [CrossRef] [PubMed]
55. Moore, R.N.; Goodrum, K.J.; Berry, L.J. Mediation of an endotoxic effect by macrophages. *J. Reticuloendothel. Soc.* **1976**, *19*, 187–197.
56. SIBAL, L.R. Effect of endotoxin on antibody production by chicken spleen cells transferred to chick chorioallantois. *J. Immunol.* **1961**, *87*, 362–366.
57. Davies, A.M.; Gery, I.; Rosenmann, E.; Laufer, A. Endotoxin as Adjuvant in Autoimmunity to Cardiac Tissue. *Exp. Biol. Med.* **1963**, *114*, 520–523. [CrossRef]
58. Neter, E. Endotoxins and the Immune Response. In *Current Topics in Microbiology and Immunology*; Springer: Berlin/Heidelberg, Germany, 1969; pp. 82–124.
59. O'Brien, A.D.; Rosenstreich, D.L.; Scher, I.; Campbell, G.H.; MacDermott, R.P.; Formal, S.B. Genetic control of susceptibility to Salmonella typhimurium in mice: Role of the LPS gene. *J. Immunol.* **1980**, *124*, 20–24.
60. Hagberg, L.; Hull, R.; Hull, S.; McGhee, J.R.; Michalek, S.M.; Svanborg Edén, C. Difference in susceptibility to gram-negative urinary tract infection between C3H/HeJ and C3H/HeN mice. *Infect. Immun.* **1984**, *46*, 839–844. [CrossRef]
61. Beutler, B.; Greenwald, D.; Hulmes, J.D.; Chang, M.; Pan, Y.-C.E.; Mathison, J.; Ulevitch, R.; Cerami, A. Identity of tumour necrosis factor and the macrophage-secreted factor cachectin. *Nature* **1985**, *316*, 552–554. [CrossRef]
62. Beutler, B.; Milsark, I.W.; Cerami, A.C. Passive Immunization Against Cachectin/Tumor Necrosis Factor Protects Mice from Lethal Effect of Endotoxin. *Science* **1985**, *229*, 869–871. [CrossRef]
63. Havell, E.A. Production of tumor necrosis factor during murine listeriosis. *J. Immunol.* **1987**, *139*, 4225–4231. [PubMed]
64. Kindler, V.; Sappino, A.-P.; Grau, G.E.; Piguet, P.-F.; Vassalli, P. The inducing role of tumor necrosis factor in the development of bactericidal granulomas during BCG infection. *Cell* **1989**, *56*, 731–740. [CrossRef]

65. Shakhov, A.N.; Collart, M.A.; Vassalli, P.; Nedospasov, S.A.; Jongeneel, C. V Kappa B-type enhancers are involved in lipopolysaccharide-mediated transcriptional activation of the tumor necrosis factor alpha gene in primary macrophages. *J. Exp. Med.* **1990**, *171*, 35–47. [CrossRef] [PubMed]
66. Tobias, P.S.; Soldau, K.; Ulevitch, R.J. Isolation of a lipopolysaccharide-binding acute phase reactant from rabbit serum. *J. Exp. Med.* **1986**, *164*, 777–793. [CrossRef] [PubMed]
67. Wright, S.D.; Tobias, P.S.; Ulevitch, R.J.; Ramos, R.A. Lipopolysaccharide (LPS) binding protein opsonizes LPS-bearing particles for recognition by a novel receptor on macrophages. *J. Exp. Med.* **1989**, *170*, 1231–1241. [CrossRef] [PubMed]
68. Schumann, R.R.; Leong, S.R.; Flaggs, G.W.; Gray, P.W.; Wright, S.D.; Mathison, J.C.; Tobias, P.S.; Ulevitch, R.J. Structure and Function of Lipopolysaccharide Binding Protein. *Science* **1990**, *249*, 1429–1431. [CrossRef]
69. Wright, S.D.; Ramos, R.A.; Tobias, P.S.; Ulevitch, R.J.; Mathison, J.C. CD14, a Receptor for Complexes of Lipopolysaccharide (LPS) and LPS Binding Protein. *Science* **1990**, *249*, 1431–1433. [CrossRef]
70. Tobias, P.S.; Soldau, K.; Ulevitch, R.J. Identification of a Lipid A Binding Site in the Acute Phase Reactant Lipopolysaccharide Binding Protein. *J. Biol. Chem.* **1989**, *264*, 10867–10871. [CrossRef]
71. Haziot, A.; Ferrero, E.; Köntgen, F.; Hijiya, N.; Yamamoto, S.; Silver, J.; Stewart, C.L.; Goyert, S.M. Resistance to Endotoxin Shock and Reduced Dissemination of Gram-Negative Bacteria in CD14-Deficient Mice. *Immunity* **1996**, *4*, 407–414. [CrossRef]
72. Medzhitov, R.; Preston-Hurlburt, P.; Janeway, C.A. A human homologue of the Drosophila Toll protein signals activation of adaptive immunity. *Nature* **1997**, *388*, 394–397. [CrossRef]
73. Nomura, N.; Miyajima, N.; Sazuka, T.; Tanaka, A.; Kawarabayasi, Y.; Sato, S.; Nagase, T.; Seki, N.; Ishikawa, K.-i.; Tabata, S. Prediction of the Coding Sequences of Unidentified Human Genes. I. The Coding Sequences of 40 New Genes (KIAA0001-KIAA0040) Deduced by Analysis of Randomly Sampled cDNA Clones from Human Immature Myeloid Cell Line KG-1. *DNA Res.* **1994**, *1*, 27–35. [CrossRef]
74. Rock, F.L.; Hardiman, G.; Timans, J.C.; Kastelein, R.A.; Bazan, J.F. A family of human receptors structurally related to Drosophila Toll. *Proc. Natl. Acad. Sci. USA* **1998**, *95*, 588–593. [CrossRef] [PubMed]
75. SULTZER, B.M. Genetic Control of Leucocyte Responses to Endotoxin. *Nature* **1968**, *219*, 1253–1254. [CrossRef] [PubMed]
76. Rosenstreich, D.L.; Michael Glade, L.; Mergenhagen, S.E. Action of Endotoxin on Lymphoid Cells. *J. Infect. Dis.* **1977**, *136*, S239–S245. [CrossRef] [PubMed]
77. Coutinho, A.; Meo, T. Genetic basis for unresponsiveness to lipopolysaccharide in C57BL/10Cr mice. *Immunogenetics* **1978**, *7*, 17–24. [CrossRef]
78. Peppel, K.; Crawford, D.; Beutler, B. A tumor necrosis factor (TNF) receptor-IgG heavy chain chimeric protein as a bivalent antagonist of TNF activity. *J. Exp. Med.* **1991**, *174*, 1483–1489. [CrossRef]
79. Takeuchi, O.; Hoshino, K.; Kawai, T.; Sanjo, H.; Takada, H.; Ogawa, T.; Takeda, K.; Akira, S. Differential Roles of TLR2 and TLR4 in Recognition of Gram-Negative and Gram-Positive Bacterial Cell Wall Components. *Immunity* **1999**, *11*, 443–451. [CrossRef]
80. Takeuchi, O.; Kawai, T.; Mühlradt, P.F.; Morr, M.; Radolf, J.D.; Zychlinsky, A.; Takeda, K.; Akira, S. Discrimination of bacterial lipoproteins by Toll-like receptor 6. *Int. Immunol.* **2001**, *13*, 933–940. [CrossRef]
81. Hemmi, H.; Takeuchi, O.; Kawai, T.; Kaisho, T.; Sato, S.; Sanjo, H.; Matsumoto, M.; Hoshino, K.; Wagner, H.; Takeda, K.; et al. A Toll-like receptor recognizes bacterial DNA. *Nature* **2000**, *408*, 740–745. [CrossRef]
82. Alexopoulou, L.; Holt, A.C.; Medzhitov, R.; Flavell, R.A. Recognition of double-stranded RNA and activation of NF-κB by Toll-like receptor 3. *Nature* **2001**, *413*, 732–738. [CrossRef]
83. Hayashi, F.; Smith, K.D.; Ozinsky, A.; Hawn, T.R.; Yi, E.C.; Goodlett, D.R.; Eng, J.K.; Akira, S.; Underhill, D.M.; Aderem, A. The innate immune response to bacterial flagellin is mediated by Toll-like receptor 5. *Nature* **2001**, *410*, 1099–1103. [CrossRef] [PubMed]
84. Heil, F.; Hemmi, H.; Hochrein, H.; Ampenberger, F.; Kirschning, C.; Akira, S.; Lipford, G.; Wagner, H.; Bauer, S. Species-Specific Recognition of Single-Stranded RNA via Toll-like Receptor 7 and 8. *Science* **2004**, *303*, 1526–1529. [CrossRef] [PubMed]
85. Guan, Y.; Ranoa, D.R.E.; Jiang, S.; Mutha, S.K.; Li, X.; Baudry, J.; Tapping, R.I. Human TLRs 10 and 1 Share Common Mechanisms of Innate Immune Sensing but Not Signaling. *J. Immunol.* **2010**, *184*, 5094–5103. [CrossRef] [PubMed]
86. Yarovinsky, F.; Zhang, D.; Andersen, J.F.; Bannenberg, G.L.; Serhan, C.N.; Hayden, M.S.; Hieny, S.; Sutterwala, F.S.; Flavell, R.A.; Ghosh, S.; et al. TLR11 activation of dendritic cells by a protozoan profilin-like protein. *Science* **2005**, *308*, 1626–1629. [CrossRef]
87. Hatai, H.; Lepelley, A.; Zeng, W.; Hayden, M.S.; Ghosh, S. Toll-Like Receptor 11 (TLR11) Interacts with Flagellin and Profilin through Disparate Mechanisms. *PLoS ONE* **2016**, *11*, e0148987. [CrossRef]
88. Oldenburg, M.; Krüger, A.; Ferstl, R.; Kaufmann, A.; Nees, G.; Sigmund, A.; Bathke, B.; Lauterbach, H.; Suter, M.; Dreher, S.; et al. TLR13 Recognizes Bacterial 23 S rRNA Devoid of Erythromycin Resistance–Forming Modification. *Science* **2012**, *337*, 1111–1115. [CrossRef]
89. Jin, M.S.; Kim, S.E.; Heo, J.Y.; Lee, M.E.; Kim, H.M.; Paik, S.-G.; Lee, H.; Lee, J.-O. Crystal Structure of the TLR1-TLR2 Heterodimer Induced by Binding of a Tri-Acylated Lipopeptide. *Cell* **2007**, *130*, 1071–1082. [CrossRef]
90. Andrade, W.A.; do Carmo Souza, M.; Ramos-Martinez, E.; Nagpal, K.; Dutra, M.S.; Melo, M.B.; Bartholomeu, D.C.; Ghosh, S.; Golenbock, D.T.; Gazzinelli, R.T. Combined Action of Nucleic Acid-Sensing Toll-like Receptors and TLR11/TLR12 Heterodimers Imparts Resistance to Toxoplasma gondii in Mice. *Cell Host Microbe* **2013**, *13*, 42–53. [CrossRef]
91. Rosenstiel, P.; Till, A.; Schreiber, S. NOD-like receptors and human diseases. *Microbes Infect.* **2007**, *9*, 648–657. [CrossRef]

92. Inohara, N.; Koseki, T.; del Peso, L.; Hu, Y.; Yee, C.; Chen, S.; Carrio, R.; Merino, J.; Liu, D.; Ni, J.; et al. Nod1, an Apaf-1-like Activator of Caspase-9 and Nuclear Factor-κB. *J. Biol. Chem.* **1999**, *274*, 14560–14567. [CrossRef]
93. Rehwinkel, J.; Gack, M.U. RIG-I-like receptors: Their regulation and roles in RNA sensing. *Nat. Rev. Immunol.* **2020**, *20*, 537–551. [CrossRef] [PubMed]
94. Yoneyama, M.; Kikuchi, M.; Natsukawa, T.; Shinobu, N.; Imaizumi, T.; Miyagishi, M.; Taira, K.; Akira, S.; Fujita, T. The RNA helicase RIG-I has an essential function in double-stranded RNA-induced innate antiviral responses. *Nat. Immunol.* **2004**, *5*, 730–737. [CrossRef] [PubMed]
95. Kutikhin, A.; Yuzhalin, A. C-type lectin receptors and RIG-I-like receptors: New points on the oncogenomics map. *Cancer Manag. Res.* **2012**, *4*, 39–53. [CrossRef] [PubMed]
96. Neth, O.; Jack, D.L.; Dodds, A.W.; Holzel, H.; Klein, N.J.; Turner, M.W. Mannose-Binding Lectin Binds to a Range of Clinically Relevant Microorganisms and Promotes Complement Deposition. *Infect. Immun.* **2000**, *68*, 688–693. [CrossRef]
97. Wesche, H.; Henzel, W.J.; Shillinglaw, W.; Li, S.; Cao, Z. MyD88: An Adapter That Recruits IRAK to the IL-1 Receptor Complex. *Immunity* **1997**, *7*, 837–847. [CrossRef]
98. O'Neill, L.A.J.; Bowie, A.G. The family of five: TIR-domain-containing adaptors in Toll-like receptor signalling. *Nat. Rev. Immunol.* **2007**, *7*, 353–364. [CrossRef]
99. Yamamoto, M.; Sato, S.; Mori, K.; Hoshino, K.; Takeuchi, O.; Takeda, K.; Akira, S. Cutting Edge: A Novel Toll/IL-1 Receptor Domain-Containing Adapter That Preferentially Activates the IFN-β Promoter in the Toll-Like Receptor Signaling. *J. Immunol.* **2002**, *169*, 6668–6672. [CrossRef]
100. Oshiumi, H.; Matsumoto, M.; Funami, K.; Akazawa, T.; Seya, T. TICAM-1, an adaptor molecule that participates in Toll-like receptor 3–mediated interferon-β induction. *Nat. Immunol.* **2003**, *4*, 161–167. [CrossRef]
101. Hoebe, K.; Du, X.; Georgel, P.; Janssen, E.; Tabeta, K.; Kim, S.O.; Goode, J.; Lin, P.; Mann, N.; Mudd, S.; et al. Identification of Lps2 as a key transducer of MyD88-independent TIR signalling. *Nature* **2003**, *424*, 743–748. [CrossRef]
102. Yamamoto, M.; Sato, S.; Hemmi, H.; Hoshino, K.; Kaisho, T.; Sanjo, H.; Takeuchi, O.; Sugiyama, M.; Okabe, M.; Takeda, K.; et al. Role of Adaptor TRIF in the MyD88-Independent Toll-Like Receptor Signaling Pathway. *Science* **2003**, *301*, 640–643. [CrossRef]
103. Fitzgerald, K.A.; Rowe, D.C.; Barnes, B.J.; Caffrey, D.R.; Visintin, A.; Latz, E.; Monks, B.; Pitha, P.M.; Golenbock, D.T. LPS-TLR4 Signaling to IRF-3/7 and NF-κB Involves the Toll Adapters TRAM and TRIF. *J. Exp. Med.* **2003**, *198*, 1043–1055. [CrossRef] [PubMed]
104. Yamamoto, M.; Sato, S.; Hemmi, H.; Uematsu, S.; Hoshino, K.; Kaisho, T.; Takeuchi, O.; Takeda, K.; Akira, S. TRAM is specifically involved in the Toll-like receptor 4–mediated MyD88-independent signaling pathway. *Nat. Immunol.* **2003**, *4*, 1144–1150. [CrossRef] [PubMed]
105. Fitzgerald, K.A.; Palsson-McDermott, E.M.; Bowie, A.G.; Jefferies, C.A.; Mansell, A.S.; Brady, G.; Brint, E.; Dunne, A.; Gray, P.; Harte, M.T.; et al. Mal (MyD88-adapter-like) is required for Toll-like receptor-4 signal transduction. *Nature* **2001**, *413*, 78–83. [CrossRef] [PubMed]
106. Kawasaki, T.; Kawai, T. Toll-Like Receptor Signaling Pathways. *Front. Immunol.* **2014**, *5*, 461. [CrossRef] [PubMed]
107. O'Neill, L.A.J.; Golenbock, D.; Bowie, A.G. The history of Toll-like receptors—Redefining innate immunity. *Nat. Rev. Immunol.* **2013**, *13*, 453–460. [CrossRef] [PubMed]
108. Essuman, K.; Summers, D.W.; Sasaki, Y.; Mao, X.; DiAntonio, A.; Milbrandt, J. The SARM1 Toll/Interleukin-1 Receptor Domain Possesses Intrinsic NAD + Cleavage Activity that Promotes Pathological Axonal Degeneration. *Neuron* **2017**, *93*, 1334–1343.e5. [CrossRef]
109. Essuman, K.; Milbrandt, J.; Dangl, J.L.; Nishimura, M.T. Shared TIR enzymatic functions regulate cell death and immunity across the tree of life. *Science* **2022**, *377*, 6614. [CrossRef]